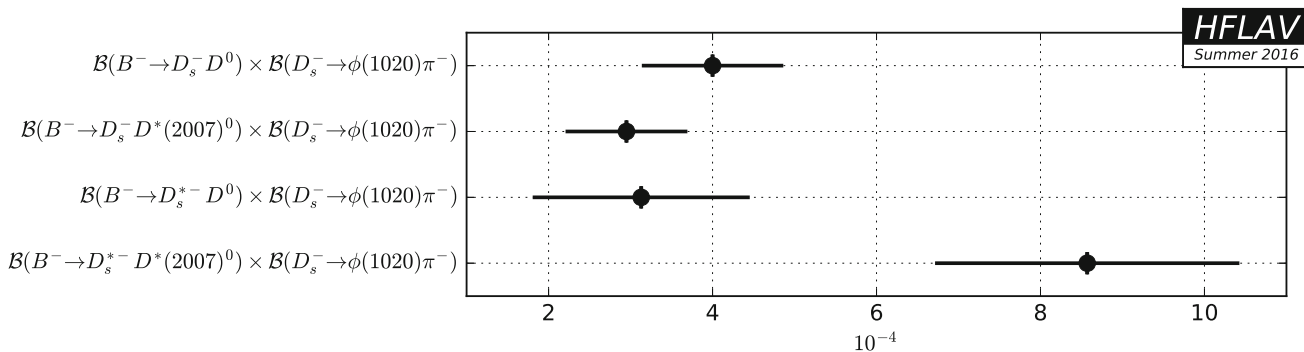
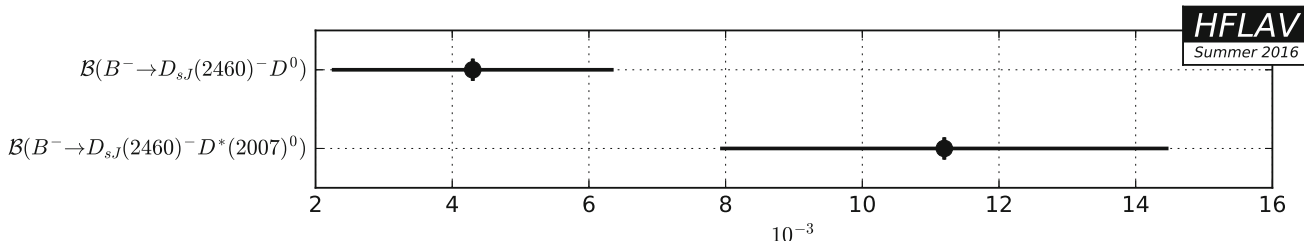
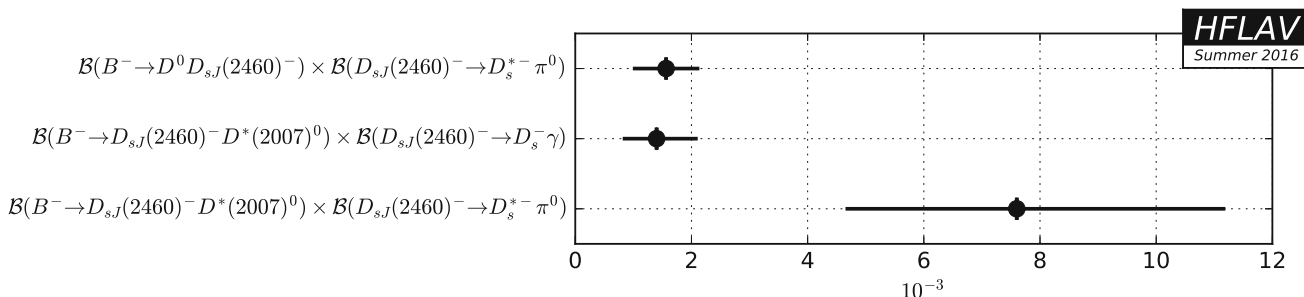
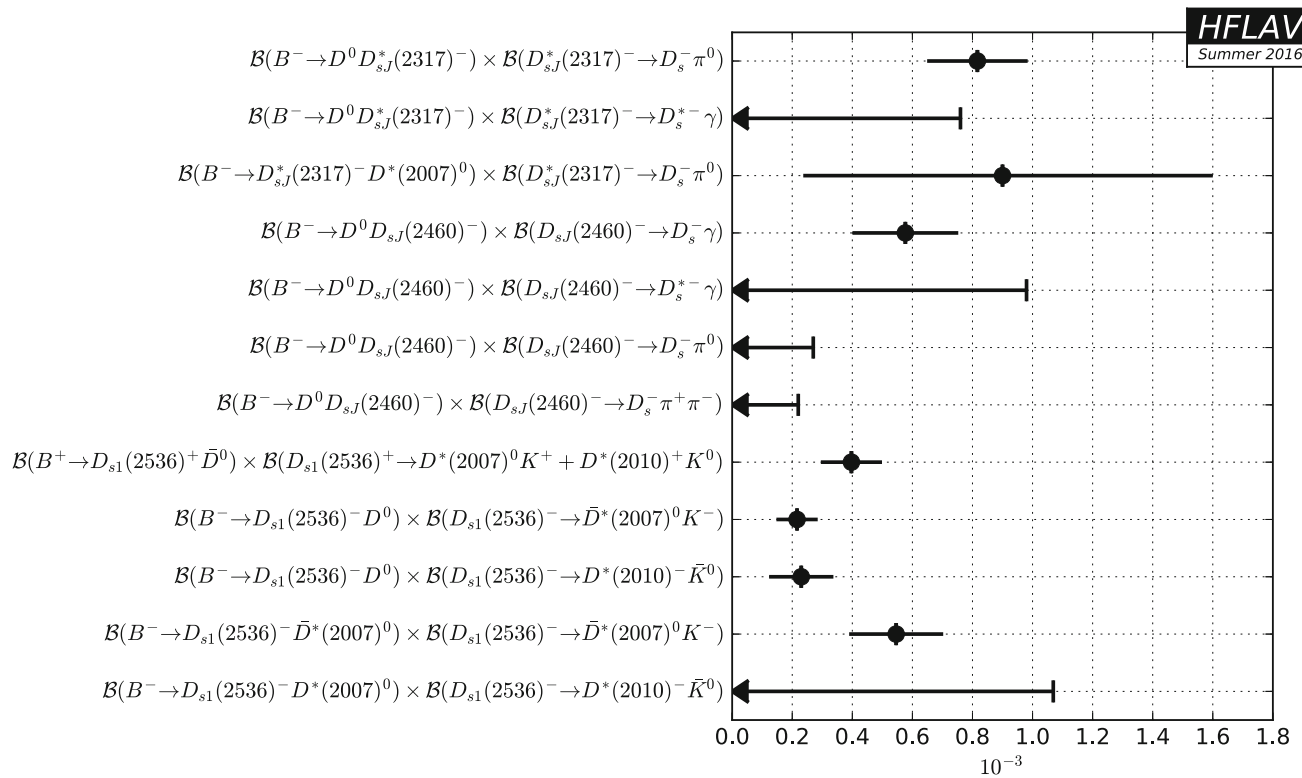
**Fig. 123** Summary of the averages from Table 153**Fig. 124** Summary of the averages from Table 154**Fig. 125** Summary of the averages from Table 156**Fig. 126** Summary of the averages from Table 157



**Fig. 127** Summary of the averages from Table 158

### 6.2.3 Decays to charmonium states

Averages of  $B^-$  decays to charmonium states are shown in Tables 159, 160, 161, 162, 163, 164, 165, 166, 167, 168, 169 and Figs. 128, 129, 130, 131, 132, 133, 134, 135, 136, 137, 138.

**Table 159** Decays to  $J/\psi$  and one kaon I [ $10^{-3}$ ]

Parameter	Measurements	Average
$\mathcal{B}(B^- \rightarrow J/\psi K^-)$	Belle [646]: $1.01 \pm 0.02 \pm 0.07$ BABAR [706]: $0.81 \pm 0.13 \pm 0.07$ BABAR [10]: $1.061 \pm 0.015 \pm 0.048$	$1.028 \pm 0.040$
$\mathcal{B}(B^- \rightarrow J/\psi K^*(892)^-)$	CDF [645]: $1.58 \pm 0.47 \pm 0.27$ Belle [733]: $1.28 \pm 0.07 \pm 0.14$ BABAR [10]: $1.454 \pm 0.047 \pm 0.097$	$1.404 \pm 0.089$
$\mathcal{B}(B^- \rightarrow J/\psi K_1(1270)^-)$	Belle [653]: $1.80 \pm 0.34 \pm 0.39$	$1.80 \pm 0.52$
$\mathcal{B}(B^- \rightarrow J/\psi K^- \pi^+ \pi^-)$	CDF [734]: $0.69 \pm 0.18 \pm 0.12$ Belle [735]: $0.716 \pm 0.010 \pm 0.060$ BABAR [736]: $1.16 \pm 0.07 \pm 0.09$	$0.807 \pm 0.052$ CL = $2.3\%$

**Table 160** Decays to  $J/\psi$  and one kaon II [ $10^{-4}$ ]

Parameter	Measurements	Average
$\mathcal{B}(B^- \rightarrow J/\psi \eta K^-)$	Belle [654]: $1.27 \pm 0.11 \pm 0.11$ BABAR [655]: $1.08 \pm 0.23 \pm 0.24$	$1.24 \pm 0.14$
$\mathcal{B}(B^- \rightarrow J/\psi \omega(782) K^-)$	BABAR [651]: $3.2 \pm 0.1^{+0.6}_{-0.3}$	$3.2^{+0.6}_{-0.3}$
$\mathcal{B}(B^- \rightarrow J/\psi \phi(1020) K^-)$	BABAR [652]: $0.44 \pm 0.14 \pm 0.05$	$0.44 \pm 0.15$

**Table 161** Decays to charmonium other than  $J/\psi$  and one kaon I [ $10^{-3}$ ]

Parameter	Measurements	Average
$\mathcal{B}(B^- \rightarrow \psi(2S)K^-)$	CDF [648]: $0.55 \pm 0.10 \pm 0.06$ Belle [646]: $0.69 \pm 0.06$ BABAR [706]: $0.49 \pm 0.16 \pm 0.04$ BABAR [10]: $0.617 \pm 0.032 \pm 0.044$ Belle [657]: $0.77 \pm 0.08 \pm 0.09$ Belle [657]: $0.63 \pm 0.09 \pm 0.06$ BABAR [10]: $0.592 \pm 0.085 \pm 0.089$ Belle [735]: $0.431 \pm 0.020 \pm 0.050$ Belle [732]: $0.48 \pm 0.11 \pm 0.07$ BABAR [706]: $0.35 \pm 0.25 \pm 0.03$ BABAR [643]: $0.084 \pm 0.032 \pm 0.021$ BABAR [643]: $0.141 \pm 0.030 \pm 0.022$ Belle [737]: $0.60^{+0.21}_{-0.18} \pm 0.11$ BABAR [706]: $<0.18$ BABAR [273]: $0.184 \pm 0.032 \pm 0.031$ BABAR [658]: $<2.86$ BABAR [659]: $0.14 \pm 0.05 \pm 0.02$ CDF [734]: $1.55 \pm 0.54 \pm 0.20$ Belle [660]: $0.494 \pm 0.011 \pm 0.033$ BABAR [706]: $0.80 \pm 0.14 \pm 0.07$ BABAR [661]: $0.45 \pm 0.01 \pm 0.03$ Belle [664]: $0.41 \pm 0.06 \pm 0.09$ BABAR [661]: $0.26 \pm 0.05 \pm 0.04$ Belle [662]: $0.329 \pm 0.029 \pm 0.019$ Belle [662]: $0.575 \pm 0.026 \pm 0.032$ BABAR [663]: $0.552 \pm 0.026 \pm 0.061$ Belle [662]: $0.374 \pm 0.018 \pm 0.024$ Belle [662]: $0.116 \pm 0.022 \pm 0.012$ Belle [662]: $0.134 \pm 0.017 \pm 0.009$ Belle [665]: $1.25 \pm 0.14^{+0.39}_{-0.40}$ BABAR [706]: $0.87 \pm 0.15$ BABAR [667]: $1.29 \pm 0.09 \pm 0.38$ $\mathcal{B}(B^- \rightarrow \eta_c K^-(892)^-)$ BABAR [666]: $1.21^{+0.43}_{-0.35}{}^{+0.64}_{-0.40}$ $\mathcal{B}(B^- \rightarrow \eta_c(2S)K^-)$ BABAR [706]: $0.34 \pm 0.18 \pm 0.03$	$0.632 \pm 0.037$ $0.77 \pm 0.12$ $0.63 \pm 0.11$ $0.592 \pm 0.123$ $0.431 \pm 0.054$ $0.45 \pm 0.12$ $0.084 \pm 0.038$ $0.141 \pm 0.037$ $0.200 \pm 0.044$ $0.14 \pm 0.05$ $0.479 \pm 0.023$ $0.30 \pm 0.06$ $0.329 \pm 0.035$ $0.569 \pm 0.035$ $0.374 \pm 0.030$ $0.116 \pm 0.025$ $0.134 \pm 0.019$ $0.92 \pm 0.14$ $1.21^{+0.77}_{-0.53}$ $0.34 \pm 0.18$

**Table 162** Decays to charmonium other than  $J/\psi$  and one kaon II [ $10^{-5}$ ]

Parameter	Measurements	Average
$\mathcal{B}(B^- \rightarrow \chi_{c2}K^-)$	Belle [660]: $1.11^{+0.36}_{-0.34} \pm 0.09$ BABAR [661]: $1 \pm 1 \pm 0$	$1.08 \pm 0.31$
$\mathcal{B}(B^- \rightarrow \chi_{c2}K^*(892)^-)$	BABAR [661]: $1.1 \pm 4.3 \pm 5.5$	$1.1 \pm 7.0$
$\mathcal{B}(B^- \rightarrow h_c(1P)K^-) \times \mathcal{B}(h_c(1P) \rightarrow \eta_c\gamma)$	BABAR [668]: $<4.8$	$<4.8$

**Table 163** Decays to charmonium other than  $J/\psi$  and one kaon III [ $10^{-6}$ ]

Parameter	Measurements	Average
$\mathcal{B}(B^- \rightarrow K^-\eta_c) \times \mathcal{B}(\eta_c \rightarrow K^0K^+\pi^+)$	Belle [738]: $0.267 \pm 0.014^{+0.057}_{-0.055}$	$0.267^{+0.059}_{-0.057}$
$\mathcal{B}(B^- \rightarrow \eta_c K^-) \times \mathcal{B}(\eta_c \rightarrow p\bar{p})$	Belle [739]: $1.42 \pm 0.11^{+0.16}_{-0.20}$	$1.53 \pm 0.18$
$\mathcal{B}(B^- \rightarrow \eta_c K^-) \times \mathcal{B}(\eta_c \rightarrow \Lambda\bar{\Lambda})$	Belle [739]: $0.95^{+0.25}_{-0.22}{}^{+0.08}_{-0.11}$	$0.95^{+0.26}_{-0.25}$
$\mathcal{B}(B^- \rightarrow K^-\eta_c(2S)) \times \mathcal{B}(\eta_c(2S) \rightarrow K^0K^-\pi^+)$	Belle [738]: $0.034^{+0.022}_{-0.015}{}^{+0.005}_{-0.004}$	$0.034^{+0.023}_{-0.016}$
$\mathcal{B}(B^- \rightarrow h_c(1P)K^-)$	Belle [741]: $<3.8$	$<3.8$
$\mathcal{B}(B^- \rightarrow h_c(1P)K^-) \times \mathcal{B}(h_c(1P) \rightarrow J/\psi\pi^+\pi^-)$	BABAR [736]: $<3.4$	$<3.4$

**Table 164** Decays to charmonium and light mesons [ $10^{-5}$ ]

Parameter	Measurements	Average
$\mathcal{B}(B^- \rightarrow J/\psi\pi^-)$	LHCb [742]: $3.88 \pm 0.11 \pm 0.15$ Belle [646]: $3.8 \pm 0.6 \pm 0.3$ BABAR [743]: $5.37 \pm 0.45 \pm 0.24$	$4.04 \pm 0.17$
$\mathcal{B}(B^- \rightarrow J/\psi\pi^-\pi^0)$	BABAR [669]: $<0.73$	$<0.73$
$\mathcal{B}(B^- \rightarrow J/\psi\rho^-(770))$	BABAR [669]: $5 \pm 1 \pm 0$	$5 \pm 1$
$\mathcal{B}(B^- \rightarrow \psi(2S)\pi^-)$	LHCb [742]: $2.52 \pm 0.26 \pm 0.15$	$2.52 \pm 0.30$
$\mathcal{B}(B^- \rightarrow \chi_{c0}\pi^-)$	BABAR [744]: $<6.1$	$<6.1$
$\mathcal{B}(B^- \rightarrow \chi_{c1}\pi^-)$	Belle [745]: $2.2 \pm 0.4 \pm 0.3$	$2.2 \pm 0.5$

**Table 165** Decays to  $J/\psi$  and a heavy mesons [ $10^{-4}$ ]

Parameter	Measurements	Average
$\mathcal{B}(B^- \rightarrow J/\psi D^-)$	BABAR [682]: $<1.2$	$<1.2$
$\mathcal{B}(B^- \rightarrow J/\psi D^0\pi^-)$	Belle [681]: $<0.25$ BABAR [736]: $<0.52$	$<0.25$

**Table 166** Decays with baryons I [ $10^{-5}$ ]

Parameter	Measurements	Average
$\mathcal{B}(B^- \rightarrow J/\psi\Lambda\bar{p})$	Belle [679]: $1.16 \pm 0.28^{+0.18}_{-0.23}$ BABAR [680]: $1.16^{+0.74}_{-0.53}{}^{+0.42}_{-0.18}$	$1.16 \pm 0.31$
$\mathcal{B}(B^- \rightarrow J/\psi\Sigma^0\bar{p})$	Belle [679]: $<1.1$	$<1.1$

**Table 167** Decays with baryons II [ $10^{-6}$ ]

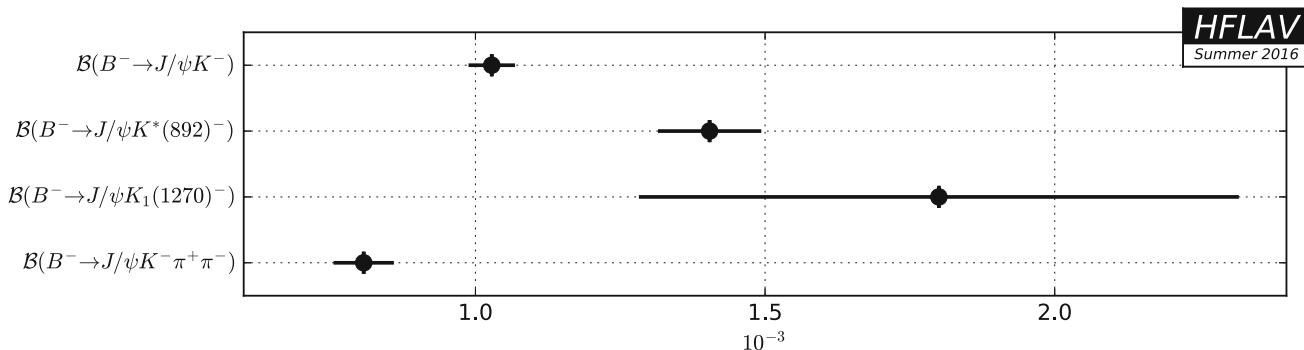
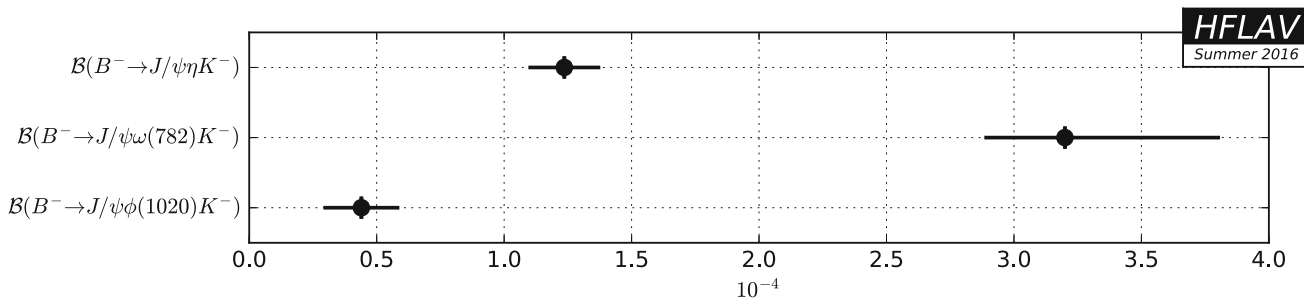
Parameter	Measurements	Average
$\mathcal{B}(B^- \rightarrow J/\psi p\bar{p}\pi^-)$	LHCb [678]: $<0.50$	$<0.50$
$\mathcal{B}(B^- \rightarrow J/\psi K^-) \times \mathcal{B}(J/\psi \rightarrow \Lambda\bar{\Lambda})$	Belle [739]: $2.0^{+0.3}_{-0.3} \pm 0.3$	$2.0^{+0.5}_{-0.4}$
$\mathcal{B}(B^- \rightarrow J/\psi K^-) \times \mathcal{B}(J/\psi \rightarrow p\bar{p})$	Belle [739]: $2.21 \pm 0.13 \pm 0.10$ BABAR [740]: $2.2 \pm 0.2 \pm 0.1$	$2.21 \pm 0.13$

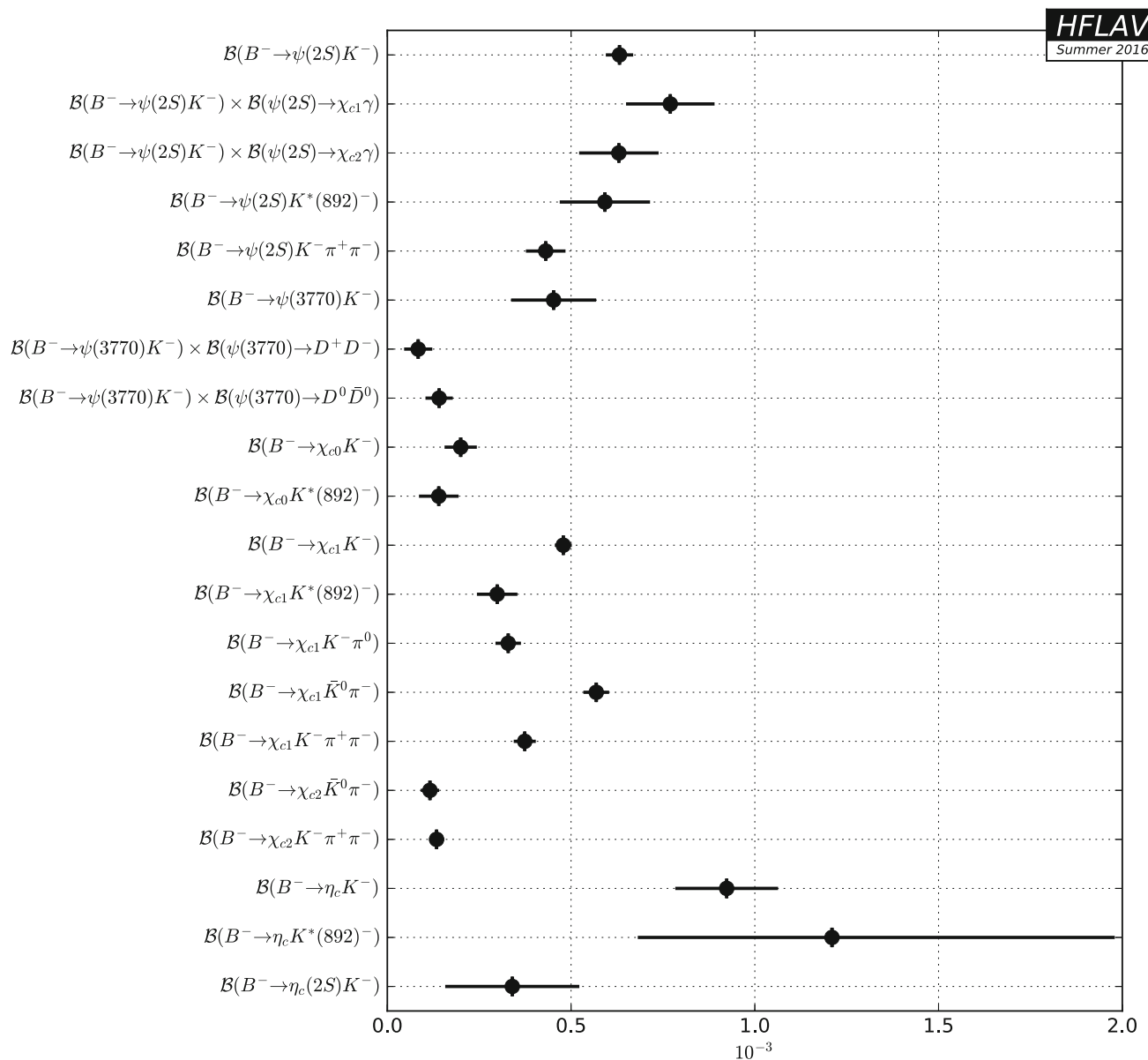
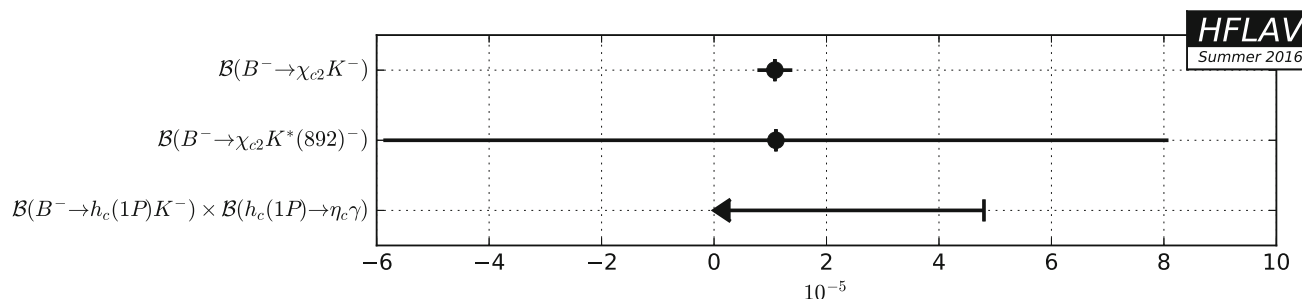
**Table 168** Relative decay rates I

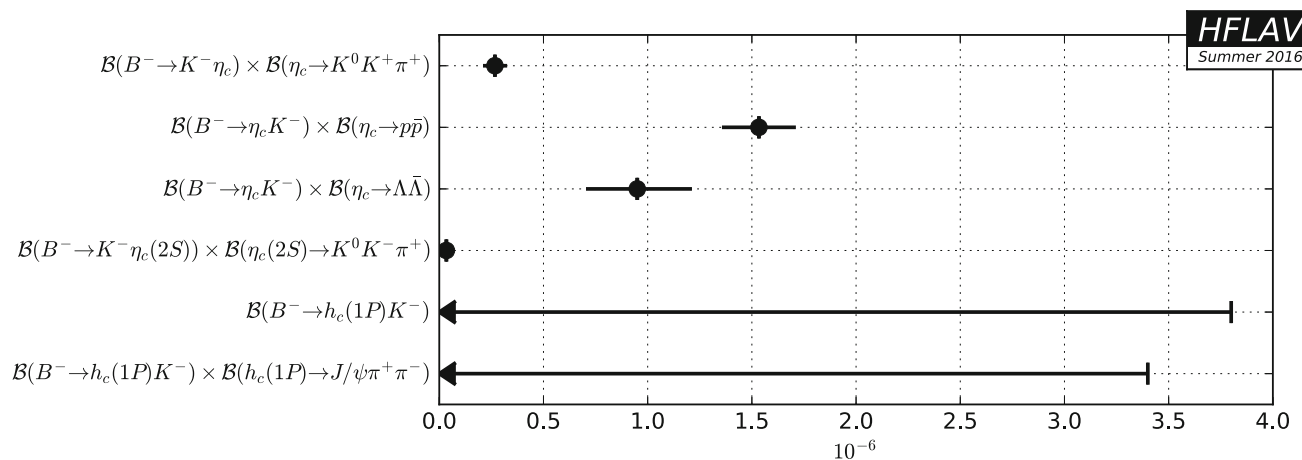
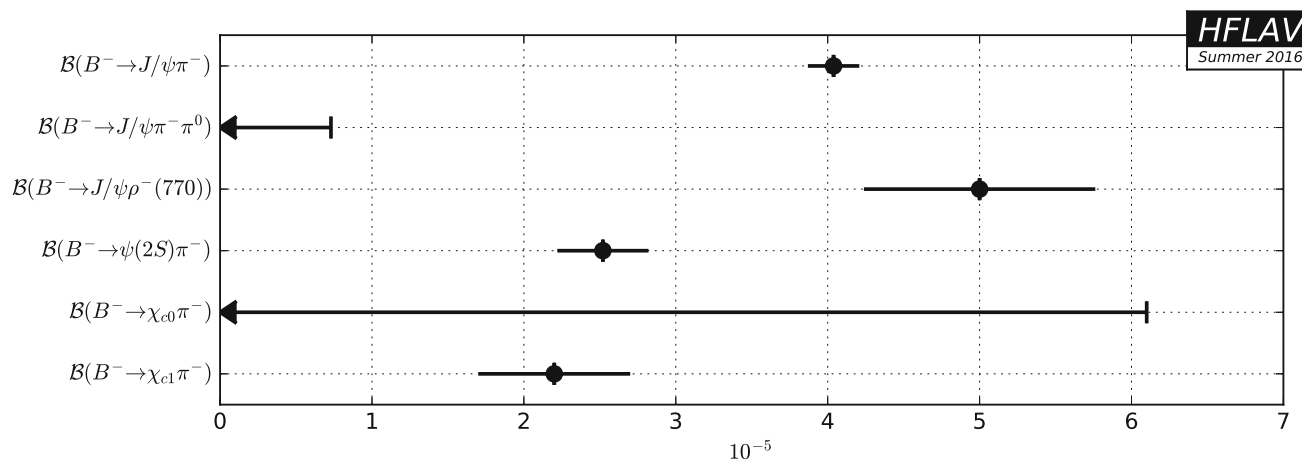
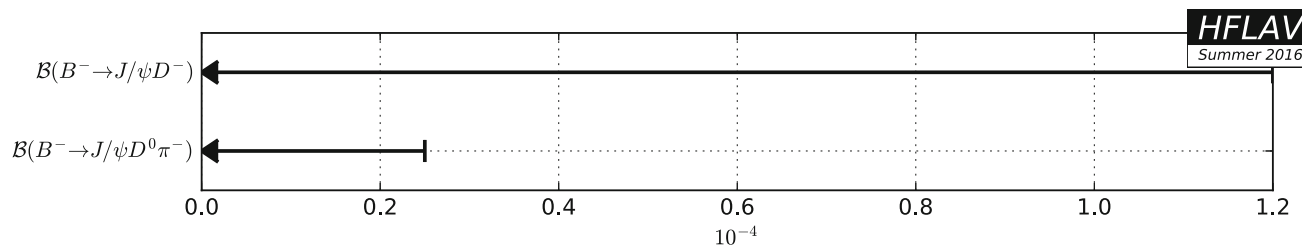
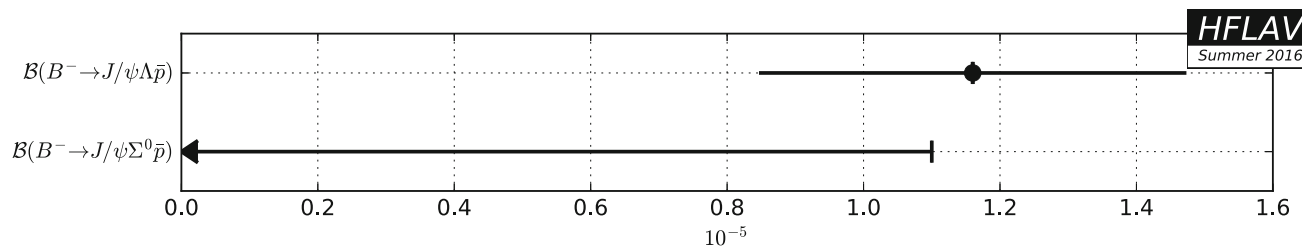
Parameter	Measurements	Average
$\mathcal{B}(B^- \rightarrow J/\psi K^*(892)^-) / \mathcal{B}(B^- \rightarrow J/\psi K^-)$	CDF [683]: $1.92 \pm 0.60 \pm 0.17$ BABAR [10]: $1.37 \pm 0.05 \pm 0.08$	$1.38 \pm 0.09$
$\mathcal{B}(B^- \rightarrow J/\psi K_1(1270)^-) / \mathcal{B}(B^- \rightarrow J/\psi K^-)$	Belle [653]: $1.80 \pm 0.34 \pm 0.34$	$1.80 \pm 0.48$
$\mathcal{B}(B^- \rightarrow J/\psi K_1^-(1400)) / \mathcal{B}(B^- \rightarrow J/\psi K_1(1270)^-)$	Belle [653]: $<0.30$	$<0.30$
$\mathcal{B}(B^- \rightarrow \psi(2S)K^-) / \mathcal{B}(B^- \rightarrow J/\psi K^-)$	LHCb [685]: $0.594 \pm 0.006 \pm 0.022$ D0 [746]: $0.65 \pm 0.04 \pm 0.08$	$0.598 \pm 0.022$
$\mathcal{B}(B^- \rightarrow \psi(2S)K^*(892)^-) / \mathcal{B}(B^- \rightarrow \psi(2S)K^-)$	BABAR [10]: $0.96 \pm 0.15 \pm 0.09$	$0.96 \pm 0.17$
$\mathcal{B}(B^- \rightarrow \chi_{c0}K^-) / \mathcal{B}(B^- \rightarrow J/\psi K^-)$	Belle [737]: $0.60^{+0.21}_{-0.18} \pm 0.09$	$0.60^{+0.23}_{-0.20}$
$\mathcal{B}(B^- \rightarrow \chi_{c1}K^*(892)^-) / \mathcal{B}(B^- \rightarrow \chi_{c1}K^-)$	BABAR [10]: $0.51 \pm 0.17 \pm 0.16$	$0.51 \pm 0.23$
$\mathcal{B}(B^- \rightarrow \chi_{c1}\bar{K}^0\pi^-) / \mathcal{B}(B^- \rightarrow J/\psi \bar{K}^0\pi^-)$	BABAR [663]: $0.501 \pm 0.024 \pm 0.055$	$0.501 \pm 0.060$
$\mathcal{B}(B^- \rightarrow \eta_c K^-) / \mathcal{B}(B^- \rightarrow J/\psi K^-)$	BABAR [706]: $1.06 \pm 0.23 \pm 0.04$ BABAR [667]: $1.28 \pm 0.10 \pm 0.38$	$1.12 \pm 0.20$
$[\mathcal{B}(B^- \rightarrow \eta_c K^-) \times \mathcal{B}(\eta_c \rightarrow p\bar{p})] / [\mathcal{B}(B^- \rightarrow J/\psi K^-) \times \mathcal{B}(J/\psi \rightarrow p\bar{p})]$	LHCb [747]: $0.578 \pm 0.035 \pm 0.027$	$0.578 \pm 0.044$

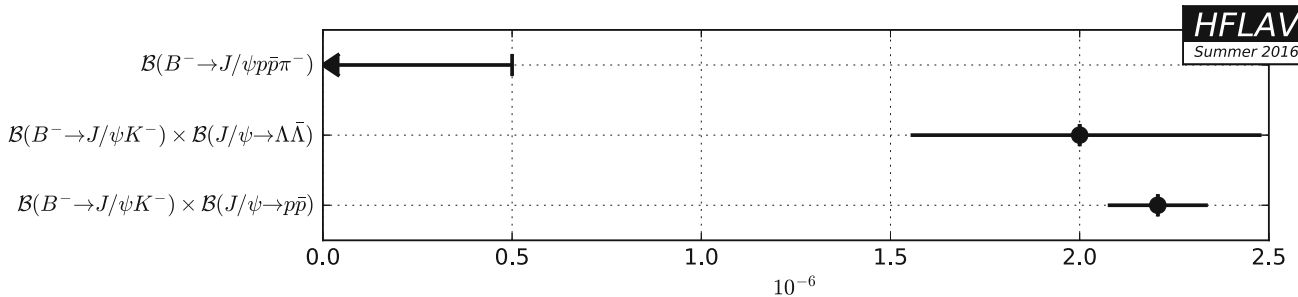
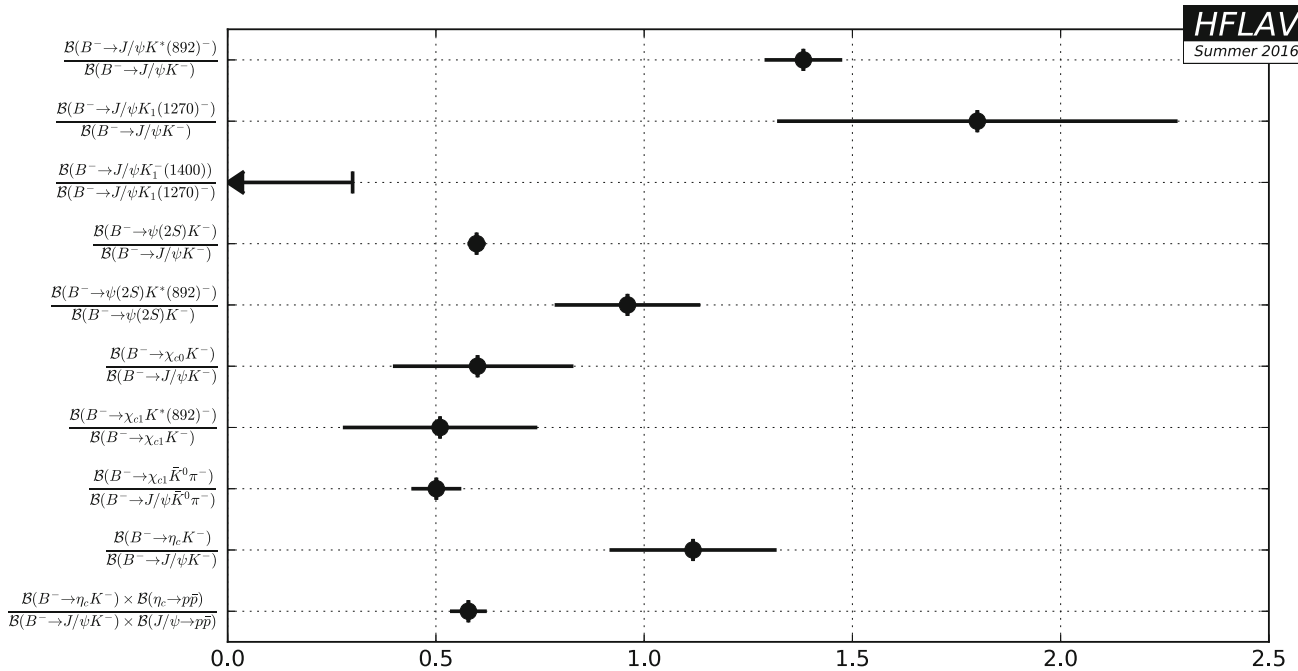
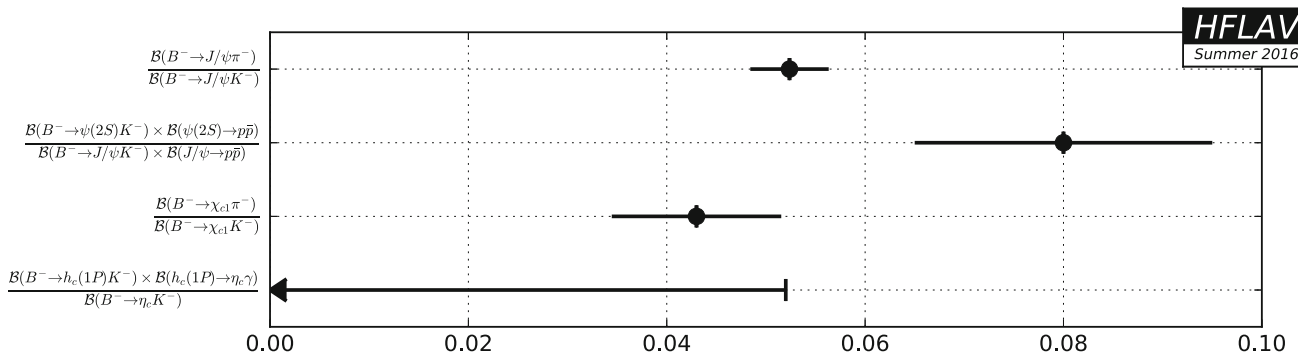
**Table 169** Relative decay rates II

Parameter	Measurements	Average
$\mathcal{B}(B^- \rightarrow J/\psi \pi^-) / \mathcal{B}(B^- \rightarrow J/\psi K^-)$	CDF [748]: $0.050^{+0.019}_{-0.017} \pm 0.001$ CDF [749]: $0.0486 \pm 0.0082 \pm 0.0015$ BABAR [743]: $0.0537 \pm 0.0045 \pm 0.0011$	$0.0524 \pm 0.0040$
$[\mathcal{B}(B^- \rightarrow \psi(2S)K^-) \times \mathcal{B}(\psi(2S) \rightarrow p\bar{p})] / [\mathcal{B}(B^- \rightarrow J/\psi K^-) \times \mathcal{B}(J/\psi \rightarrow p\bar{p})]$	LHCb [747]: $0.080 \pm 0.012 \pm 0.009$	$0.080 \pm 0.015$
$\mathcal{B}(B^- \rightarrow \chi_{c1}\pi^-) / \mathcal{B}(B^- \rightarrow \chi_{c1}K^-)$	Belle [745]: $0.043 \pm 0.008 \pm 0.003$	$0.043 \pm 0.009$
$[\mathcal{B}(B^- \rightarrow h_c(1P)K^-) \times \mathcal{B}(h_c(1P) \rightarrow \eta_c\gamma)] / \mathcal{B}(B^- \rightarrow \eta_c K^-)$	BABAR [668]: $<0.052$	$<0.052$

**Fig. 128** Summary of the averages from Table 159**Fig. 129** Summary of the averages from Table 160

**Fig. 130** Summary of the averages from Table 161**Fig. 131** Summary of the averages from Table 162

**Fig. 132** Summary of the averages from Table 163**Fig. 133** Summary of the averages from Table 164**Fig. 134** Summary of the averages from Table 165**Fig. 135** Summary of the averages from Table 166

**Fig. 136** Summary of the averages from Table 167**Fig. 137** Summary of the averages from Table 168**Fig. 138** Summary of the averages from Table 169

#### 6.2.4 Decays to charm baryons

Averages of  $B^-$  decays to charm baryons are shown in Tables 170, 171, 172 and Figs. 139, 140.

**Table 170** Absolute (product) decay rates [ $10^{-4}$ ]

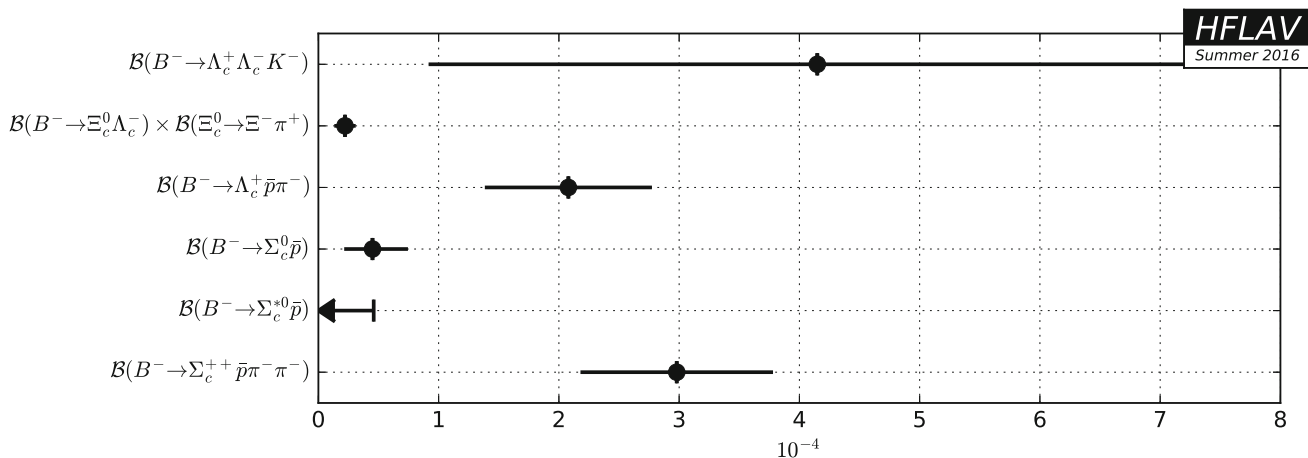
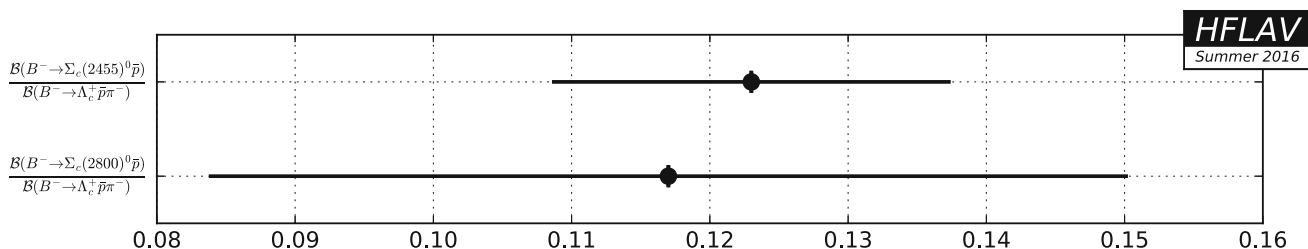
Parameter	Measurements	Average
$\mathcal{B}(B^- \rightarrow \Lambda_c^+ \Lambda_c^- K^-)$	Belle [693]: $6.5^{+1.0}_{-0.9} \pm 3.6$ BABAR [694]: $11.4 \pm 1.5 \pm 6.2$	$4.1 \pm 3.2$
$\mathcal{B}(B^- \rightarrow \Xi_c^0 \Lambda_c^-) \times \mathcal{B}(\Xi_c^0 \rightarrow \Xi^- \pi^+)$	Belle [699]: $0.48^{+0.10}_{-0.09} \pm 0.16$ BABAR [694]: $0.208 \pm 0.065 \pm 0.061$	$0.221 \pm 0.089$
$\mathcal{B}(B^- \rightarrow \Lambda_c^+ \bar{p} \pi^-)$	Belle [690]: $1.87^{+0.43}_{-0.40} \pm 0.56$ BABAR [697]: $3.38 \pm 0.12 \pm 0.89$	$2.08 \pm 0.69$
$\mathcal{B}(B^- \rightarrow \Sigma_c^0 \bar{p})$	Belle [690]: $0.45^{+0.26}_{-0.19} \pm 0.14$	$0.45^{+0.29}_{-0.24}$
$\mathcal{B}(B^- \rightarrow \Sigma_c^{*0} \bar{p})$	Belle [690]: $<0.46$	$<0.46$
$\mathcal{B}(B^- \rightarrow \Sigma_c^{++} \bar{p} \pi^- \pi^-)$	BABAR [750]: $2.98 \pm 0.16 \pm 0.78$	$2.98 \pm 0.80$

**Table 171** Relative decay rates I

Parameter	Measurements	Average
$\mathcal{B}(B^- \rightarrow \Lambda_c^+ \bar{p} \pi^-) / \mathcal{B}(\bar{B}^0 \rightarrow \Lambda_c^+ \bar{p})$	BABAR [697]: $15.4 \pm 1.8 \pm 0.3$	$15.4 \pm 1.8$

**Table 172** Relative decay rates II

Parameter	Measurements	Average
$\mathcal{B}(B^- \rightarrow \Sigma_c(2455)^0 \bar{p}) / \mathcal{B}(B^- \rightarrow \Lambda_c^+ \bar{p} \pi^-)$	BABAR [697]: $0.123 \pm 0.012 \pm 0.008$	$0.123 \pm 0.014$
$\mathcal{B}(B^- \rightarrow \Sigma_c(2800)^0 \bar{p}) / \mathcal{B}(B^- \rightarrow \Lambda_c^+ \bar{p} \pi^-)$	BABAR [697]: $0.117 \pm 0.023 \pm 0.024$	$0.117 \pm 0.033$

**Fig. 139** Summary of the averages from Table 170**Fig. 140** Summary of the averages from Table 172

### 6.2.5 Decays to other (XYZ) states

Averages of  $B^-$  decays to other (XYZ) states are shown in Tables 173, 174, 175, 176, 177, 178 and Figs. 141, 142, 143, 144, 145.

**Table 173** Absolute decay rates [ $10^{-4}$ ]

Parameter	Measurements	Average
$\mathcal{B}(B^- \rightarrow X(3872)K^-)$	BABAR [706]: <3.2	<3.2

**Table 174** Product decay rates to  $X(3872)$  I [ $10^{-4}$ ]

Parameter	Measurements	Average
$\mathcal{B}(B^- \rightarrow X(3872)K^-) \times \mathcal{B}(X(3872) \rightarrow \bar{D}^*(2007)^0 D^0)$	BABAR [643]: $1.67 \pm 0.36 \pm 0.47$	$1.67 \pm 0.59$
$\mathcal{B}(B^- \rightarrow X(3872)K^-) \times \mathcal{B}(X(3872) \rightarrow D^0 \bar{D}^0 \pi^0)$	Belle [732]: <0.6	<0.6
$\mathcal{B}(B^- \rightarrow X(3872)K^-) \times \mathcal{B}(X(3872) \rightarrow D^0 \bar{D}^0)$	Belle [732]: <0.6	<0.6
$\mathcal{B}(B^- \rightarrow X(3872)K^-) \times \mathcal{B}(X(3872) \rightarrow D^+ D^-)$	Belle [732]: <0.4	<0.4

**Table 175** Product decay rates to  $X(3872)$  II [ $10^{-5}$ ]

Parameter	Measurements	Average
$\mathcal{B}(B^- \rightarrow K^- X(3872)) \times \mathcal{B}(X(3872) \rightarrow J/\psi \pi^+ \pi^-)$	Belle [751]: $0.861 \pm 0.062 \pm 0.052$ BABAR [704]: $0.84 \pm 0.15 \pm 0.07$	$0.857 \pm 0.073$
$\mathcal{B}(B^- \rightarrow X(3872)K^-) \times \mathcal{B}(X(3872) \rightarrow J/\psi \omega(782))$	BABAR [651]: $0.6 \pm 0.2 \pm 0.1$	$0.6 \pm 0.2$
$\mathcal{B}(B^- \rightarrow X(3872)K^-) \times \mathcal{B}(X(3872) \rightarrow J/\psi \eta)$	BABAR [655]: <0.77	<0.77
$\mathcal{B}(B^- \rightarrow X(3872)K^-) \times \mathcal{B}(X(3872) \rightarrow J/\psi \gamma)$	Belle [660]: $0.178^{+0.048}_{-0.044} \pm 0.012$ BABAR [661]: $0.28 \pm 0.08 \pm 0.01$	$0.204 \pm 0.041$
$\mathcal{B}(B^- \rightarrow X(3872)K^*(892)^-) \times \mathcal{B}(X(3872) \rightarrow J/\psi \gamma)$	BABAR [661]: $0.07 \pm 0.26 \pm 0.01$	$0.07 \pm 0.26$
$\mathcal{B}(B^- \rightarrow X(3872)K^*(892)^-) \times \mathcal{B}(X(3872) \rightarrow \psi(2S)\gamma)$	Belle [660]: <0.345 BABAR [661]: $0.95 \pm 0.27 \pm 0.06$	$0.95 \pm 0.28$
$\mathcal{B}(B^- \rightarrow X(3872)K^*(892)^-) \times \mathcal{B}(X(3872) \rightarrow \psi(2S)\gamma)$	BABAR [661]: $0.64 \pm 0.98 \pm 0.96$	$0.64 \pm 1.37$
$\mathcal{B}(B^- \rightarrow X(3872)K^-) \times \mathcal{B}(X(3872) \rightarrow \chi_{c1}\gamma)$	Belle [657]: <0.19	<0.19
$\mathcal{B}(B^- \rightarrow X(3872)K^-) \times \mathcal{B}(X(3872) \rightarrow \chi_{c2}\gamma)$	Belle [657]: <0.67	<0.67

**Table 176** Product decay rates to neutral states other than  $X(3872)$  [ $10^{-5}$ ]

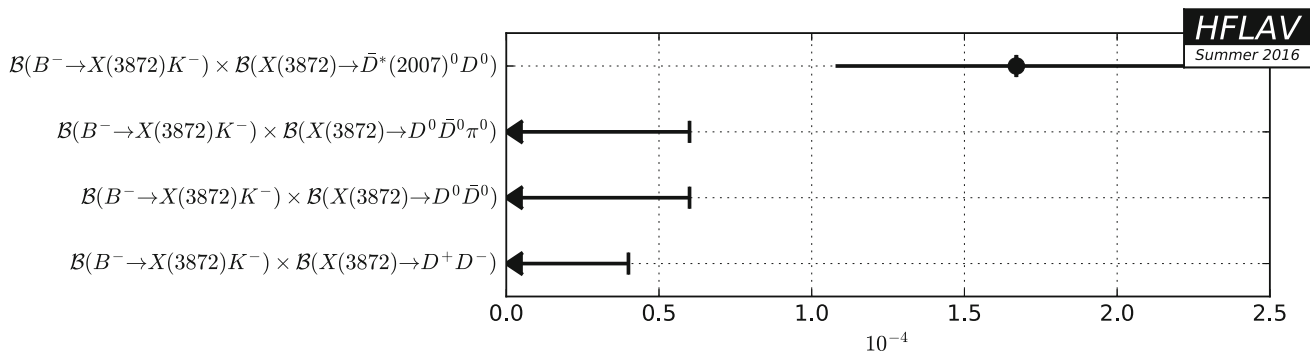
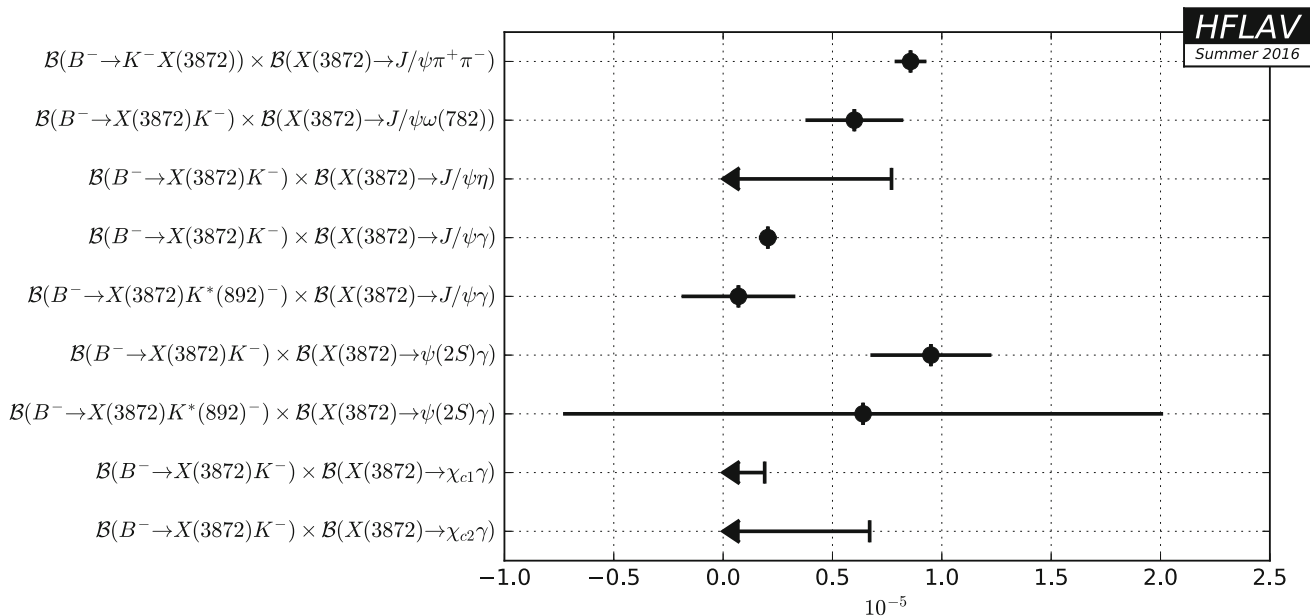
Parameter	Measurements	Average
$\mathcal{B}(B^- \rightarrow X(3823)K^-) \times \mathcal{B}(X(3823) \rightarrow \chi_{c1}\gamma)$	Belle [657]: $0.97 \pm 0.28 \pm 0.11$	$0.97 \pm 0.30$
$\mathcal{B}(B^- \rightarrow X(3823)K^-) \times \mathcal{B}(X(3823) \rightarrow \chi_{c2}\gamma)$	Belle [657]: <0.36	<0.36
$\mathcal{B}(B^- \rightarrow Y(3940)K^-) \times \mathcal{B}(Y(3940) \rightarrow J/\psi \gamma)$	BABAR [752]: <1.4	<1.4
$\mathcal{B}(B^- \rightarrow Y(3940)K^-) \times \mathcal{B}(Y(3940) \rightarrow J/\psi \omega(782))$	BABAR [651]: $3.0^{+0.7}_{-0.6}{}^{+0.5}_{-0.3}$	$3.0^{+0.9}_{-0.7}$
$\mathcal{B}(B^- \rightarrow Y(4260)K^-) \times \mathcal{B}(Y(4260) \rightarrow J/\psi \pi^+ \pi^-)$	BABAR [753]: $2.0 \pm 0.7 \pm 0.2$	$2.0 \pm 0.7$

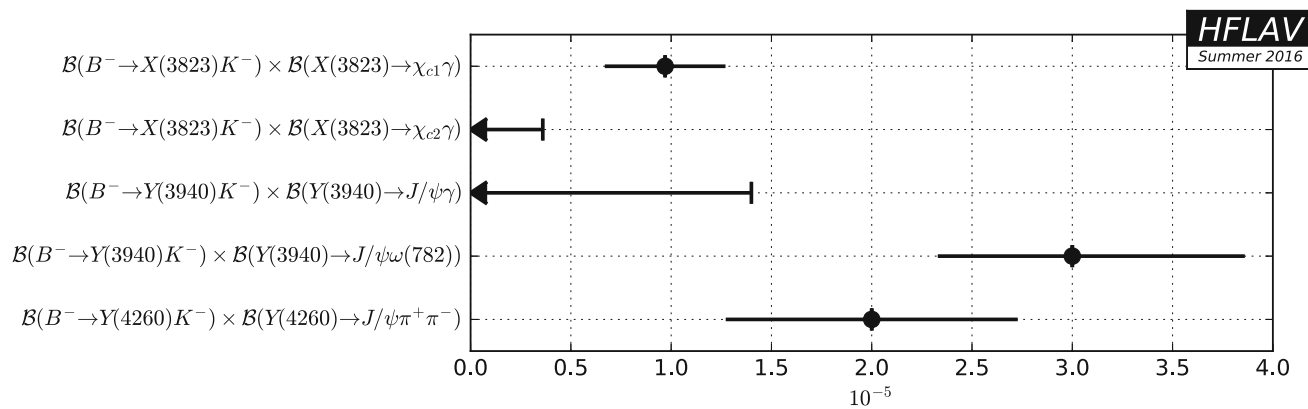
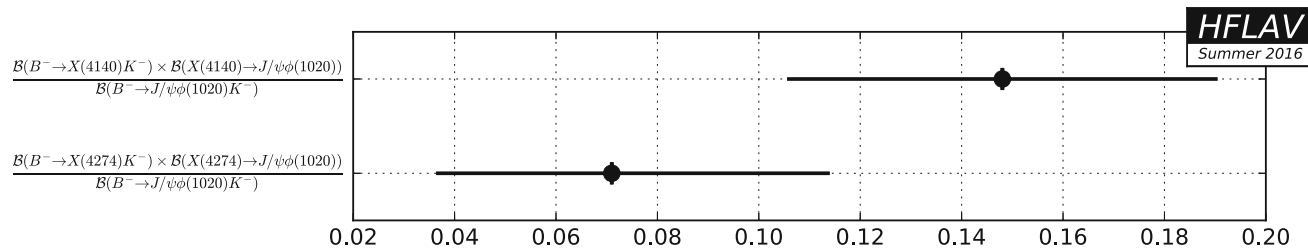
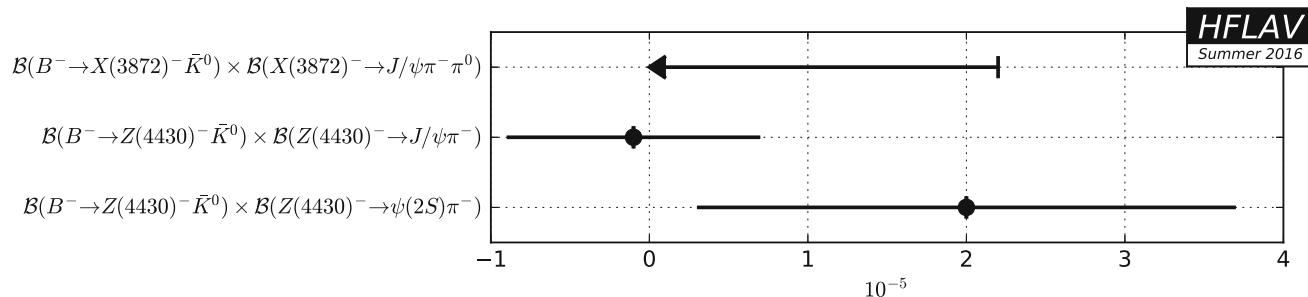
**Table 177** Relative product decay rates to states with  $s\bar{s}$  component

Parameter	Measurements	Average
$[\mathcal{B}(B^- \rightarrow X(4140)K^-) \times \mathcal{B}(X(4140) \rightarrow J/\psi \phi(1020))] / \mathcal{B}(B^- \rightarrow J/\psi \phi(1020)K^-)$	LHCb [754]: $0.130 \pm 0.032^{+0.047}_{-0.020}$ D0 [755]: $0.21 \pm 0.08 \pm 0.04$	$0.148 \pm 0.042$
$[\mathcal{B}(B^- \rightarrow X(4274)K^-) \times \mathcal{B}(X(4274) \rightarrow J/\psi \phi(1020))] / \mathcal{B}(B^- \rightarrow J/\psi \phi(1020)K^-)$	LHCb [754]: $0.071 \pm 0.025^{+0.035}_{-0.024}$	$0.071^{+0.043}_{-0.035}$

**Table 178** Product decay rates to charged states [ $10^{-5}$ ]

Parameter	Measurements	Average
$\mathcal{B}(B^- \rightarrow X(3872)^- \bar{K}^0) \times \mathcal{B}(X(3872)^- \rightarrow J/\psi \pi^- \pi^0)$	BABAR [707]: <2.2	<2.2
$\mathcal{B}(B^- \rightarrow Z(4430)^- \bar{K}^0) \times \mathcal{B}(Z(4430)^- \rightarrow J/\psi \pi^-)$	BABAR [708]: $-0.1 \pm 0.8 \pm 0.0$	$-0.1 \pm 0.8$
$\mathcal{B}(B^- \rightarrow Z(4430)^- \bar{K}^0) \times \mathcal{B}(Z(4430)^- \rightarrow \psi(2S) \pi^-)$	BABAR [708]: $2.0 \pm 1.7 \pm 0.0$	$2.0 \pm 1.7$

**Fig. 141** Summary of the averages from Table 174**Fig. 142** Summary of the averages from Table 175

**Fig. 143** Summary of the averages from Table 176**Fig. 144** Summary of the averages from Table 177**Fig. 145** Summary of the averages from Table 178

### 6.3 Decays of admixtures of $\bar{B}^0 / B^-$ mesons

Measurements of  $\bar{B}^0 / B^-$  decays to charmed hadrons are summarized in Sects. 6.3.1–6.3.3.

#### 6.3.1 Decays to two open charm mesons

Averages of  $\bar{B}^0 / B^-$  decays to two open charm mesons are shown in Table 179.

**Table 179** B decays to double charm [ $10^{-4}$ ]

Parameter	Measurements	Average
$\mathcal{B}(B \rightarrow D^0\bar{D}^0\pi^0K)$	Belle [633]: $1.27 \pm 0.31^{+0.22}_{-0.39}$	$1.27^{+0.38}_{-0.50}$

### 6.3.2 Decays to charmonium states

Averages of  $\bar{B}^0 / B^-$  decays to charmonium states are shown in Tables 180, 181, 182, 183, 184 and Figs. 146, 147, 148, 149, 150.

**Table 180** Decay amplitudes for parallel transverse polarization

Parameter	Measurements	Average
$ \mathcal{A}_\parallel ^2(B \rightarrow J/\psi K^*)$	Belle [324]: $0.231 \pm 0.012 \pm 0.008$ BABAR [323]: $0.211 \pm 0.010 \pm 0.006$	$0.219 \pm 0.009$
$ \mathcal{A}_\parallel ^2(B \rightarrow \chi_{c1} K^*)$	BABAR [323]: $0.20 \pm 0.07 \pm 0.04$	$0.20 \pm 0.08$
$ \mathcal{A}_\parallel ^2(B \rightarrow \psi(2S) K^*)$	BABAR [323]: $0.22 \pm 0.06 \pm 0.02$	$0.22 \pm 0.06$

**Table 181** Decay amplitudes for perpendicular transverse polarization

Parameter	Measurements	Average
$ \mathcal{A}_\perp ^2(B \rightarrow J/\psi K^*)$	Belle [324]: $0.195 \pm 0.012 \pm 0.008$ BABAR [323]: $0.233 \pm 0.010 \pm 0.005$	$0.219 \pm 0.009$
$ \mathcal{A}_\perp ^2(B \rightarrow \chi_{c1} K^*)$	BABAR [323]: $0.03 \pm 0.04 \pm 0.02$	$0.03 \pm 0.04$
$ \mathcal{A}_\perp ^2(B \rightarrow \psi(2S) K^*)$	BABAR [323]: $0.30 \pm 0.06 \pm 0.02$	$0.30 \pm 0.06$

**Table 182** Decay amplitudes for longitudinal polarization

Parameter	Measurements	Average
$ \mathcal{A}_0 ^2(B \rightarrow J/\psi K^*)$	Belle [324]: $0.574 \pm 0.012 \pm 0.009$ BABAR [323]: $0.556 \pm 0.009 \pm 0.010$	$0.564 \pm 0.010$
$ \mathcal{A}_0 ^2(B \rightarrow \chi_{c1} K^*)$	BABAR [323]: $0.77 \pm 0.07 \pm 0.04$	$0.77 \pm 0.08$
$ \mathcal{A}_0 ^2(B \rightarrow \psi(2S) K^*)$	BABAR [323]: $0.48 \pm 0.05 \pm 0.02$	$0.48 \pm 0.05$

**Table 183** Relative phases of parallel transverse polarization decay amplitudes

Parameter	Measurements	Average
$\delta_\parallel(B \rightarrow J/\psi K^*)$	Belle [324]: $-2.887 \pm 0.090 \pm 0.008$ BABAR [323]: $-2.93 \pm 0.08 \pm 0.04$	$-2.909 \pm 0.064$
$\delta_\parallel(B \rightarrow \chi_{c1} K^*)$	BABAR [323]: $0.0 \pm 0.3 \pm 0.1$	$0.0 \pm 0.3$
$\delta_\parallel(B \rightarrow \psi(2S) K^*)$	BABAR [323]: $-2.8 \pm 0.4 \pm 0.1$	$-2.8 \pm 0.4$

**Table 184** Relative phases of perpendicular transverse polarization decay amplitudes

Parameter	Measurements	Average
$\delta_\perp(B \rightarrow J/\psi K^*)$	Belle [324]: $2.938 \pm 0.064 \pm 0.010$ BABAR [323]: $2.91 \pm 0.05 \pm 0.03$	$2.923 \pm 0.043$
$\delta_\perp(B \rightarrow \psi(2S) K^*)$	BABAR [323]: $2.8 \pm 0.3 \pm 0.1$	$2.8 \pm 0.3$

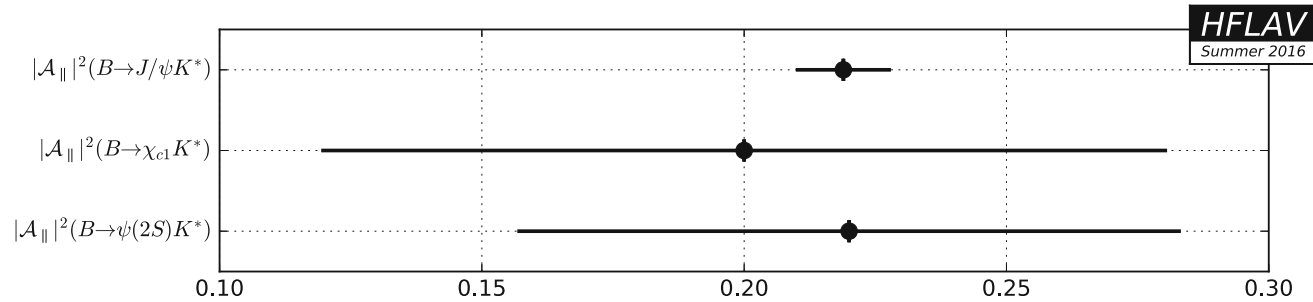


**Fig. 146** Summary of the averages from Table 180

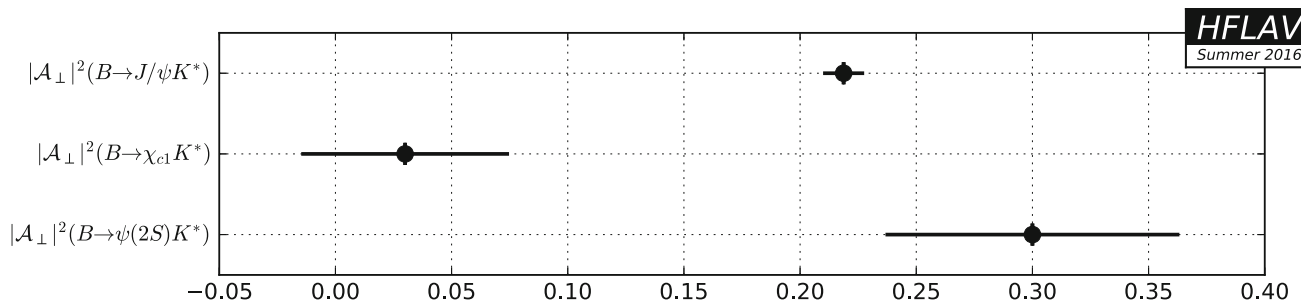


**Fig. 147** Summary of the averages from Table 181

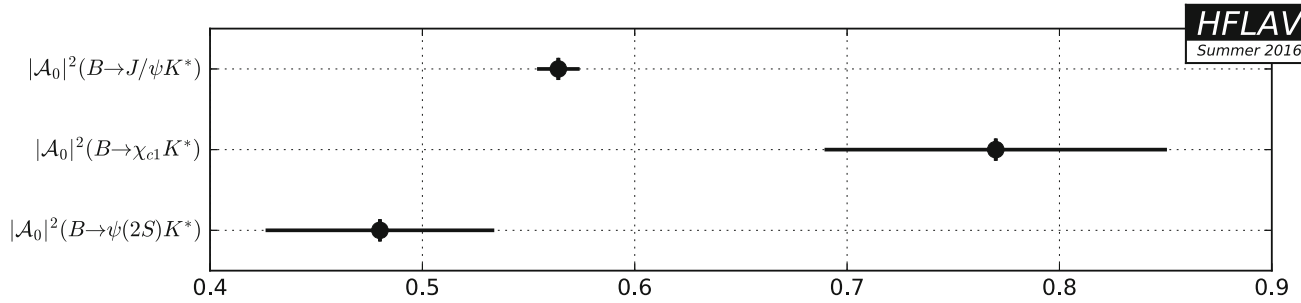


**Fig. 148** Summary of the averages from Table 182

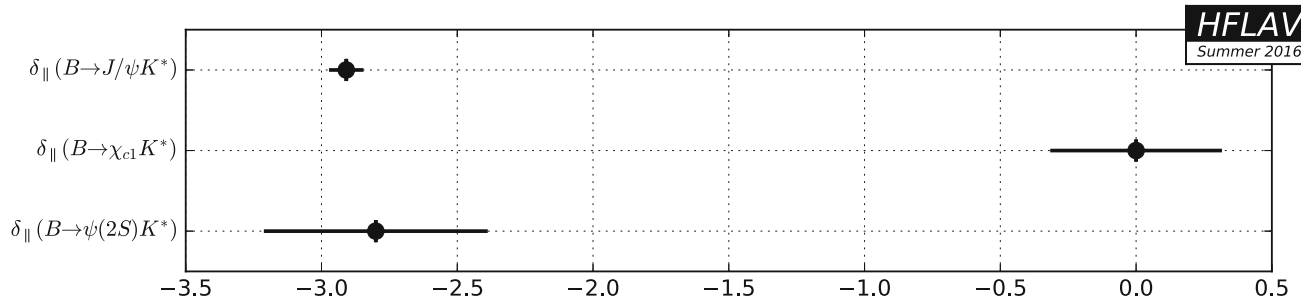


**Fig. 149** Summary of the averages from Table 183

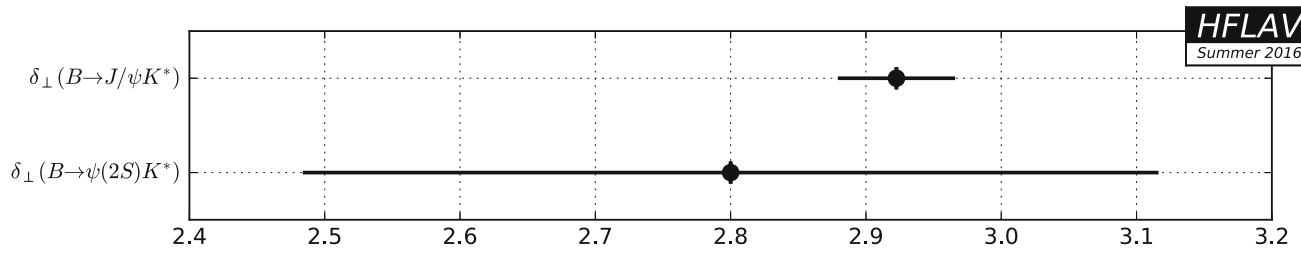


**Fig. 150** Summary of the averages from Table 184

### 6.3.3 Decays to other (XYZ) states

Averages of  $\bar{B}_s^0 / B^-$  decays to other (XYZ) states are shown in Table 185 and Fig. 151.

### 6.4 Decays of $\bar{B}_s^0$ mesons

Measurements of  $\bar{B}_s^0$  decays to charmed hadrons are summarized in Sects. 6.4.1–6.4.4. These measurements require knowledge of the production rates of  $\bar{B}_s^0$  mesons, usually measured relative to those of  $\bar{B}^0$  and  $B^-$  mesons, in the appropriate experimental environment. Since these production fractions are reasonably well known, see Sect. 3.1, they can be corrected for allowing the results to be presented in

terms of the absolute  $\bar{B}_s^0$  branching fraction, or the relative branching fraction to a lighter  $B$  meson decay mode. This is usually done in the publications; we do not make any attempt to rescale results according to more recent determinations of the relative production fractions. Ratios of branching fractions of two decays of the same hadron do not require any such correction.

### 6.4.1 Decays to a single open charm meson

Averages of  $\bar{B}_s^0$  decays to a single open charm meson are shown in Tables 186, 187, 188, 189, 190, 191 and Figs. 152, 153, 154, 155, 156, 157.

**Table 185** Absolute decay rates to  $X/Y$  states [ $10^{-4}$ ]

Parameter	Measurements	Average
$\mathcal{B}(B \rightarrow X(3872)K) \times \mathcal{B}(X(3872) \rightarrow D^*(2007)^0 \bar{D}^0)$	Belle [756]: $0.80 \pm 0.20 \pm 0.10$	$0.80 \pm 0.22$
$\mathcal{B}(B \rightarrow Y(3940)K) \times \mathcal{B}(Y(3940) \rightarrow D^*(2007)^0 \bar{D}^0)$	Belle [756]: $<0.67$	$<0.67$
$\mathcal{B}(B \rightarrow KY(3940)) \times \mathcal{B}(Y(3940) \rightarrow J/\psi\omega(782))$	Belle [757]: $0.71 \pm 0.13 \pm 0.31$	$0.71 \pm 0.34$

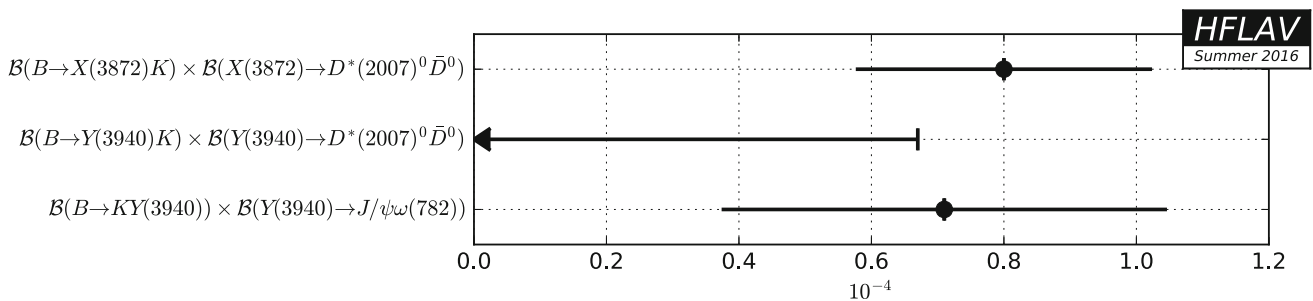


**Fig. 151** Summary of the averages from Table 185

**Table 186** Decays to a  $D_s^{(*)}$  and a light meson I [ $10^{-3}$ ]

Parameter	Measurements	Average
$\mathcal{B}(\bar{B}_s^0 \rightarrow D_s^+ \pi^-)$	LHCb [758]: $2.95 \pm 0.05^{+0.25}_{-0.28}$ Belle [29]: $3.67^{+0.35}_{-0.33}{}^{+0.65}_{-0.65}$	$3.03 \pm 0.25$
$\mathcal{B}(\bar{B}_s^0 \rightarrow D_s^{*+} \pi^-)$	Belle [759]: $2.4^{+0.5}_{-0.4} \pm 0.4$	$2.4^{+0.7}_{-0.6}$
$\mathcal{B}(\bar{B}_s^0 \rightarrow D_s^+ \rho^-(770))$	Belle [759]: $8.5^{+1.3}_{-1.2} \pm 1.7$	$8.5^{+2.1}_{-2.1}$
$\mathcal{B}(\bar{B}_s^0 \rightarrow D_s^{*+} \rho^-(770))$	Belle [759]: $11.8^{+2.2}_{-2.0} \pm 2.5$	$11.8^{+3.3}_{-3.2}$

**Table 187** Decays to a  $D_s^{(*)}$  and a light meson II [ $10^{-4}$ ]

Parameter	Measurements	Average
$\mathcal{B}(\bar{B}_s^0 \rightarrow D_s^+ K^-)$	LHCb [758]: $1.90 \pm 0.12^{+0.18}_{-0.19}$ Belle [29]: $2.4^{+1.2}_{-1.0} \pm 0.4$	$1.92 \pm 0.22$
$\mathcal{B}(\bar{B}_s^0 \rightarrow D_s^{*+} K^-)$	LHCb [760]: $1.63 \pm 0.12^{+0.49}_{-0.48}$	$1.63^{+0.50}_{-0.50}$

**Table 188** Decays to a  $D^{(*)}$  and a light meson I [ $10^{-4}$ ]

Parameter	Measurements	Average
$\mathcal{B}(\bar{B}_s^0 \rightarrow D^0 K^0)$	LHCb [761]: $4.3 \pm 0.5 \pm 0.8$	$4.3 \pm 0.9$
$\mathcal{B}(\bar{B}_s^0 \rightarrow D^{*0} K^0)$	LHCb [761]: $2.8 \pm 1.0 \pm 0.5$	$2.8 \pm 1.1$
$\mathcal{B}(\bar{B}_s^0 \rightarrow D^0 K^{*0})$	LHCb [762]: $4.72 \pm 1.07 \pm 0.96$	$4.72 \pm 1.44$

**Table 189** Decays to a  $D^{(*)}$  and a light meson II [ $10^{-6}$ ]

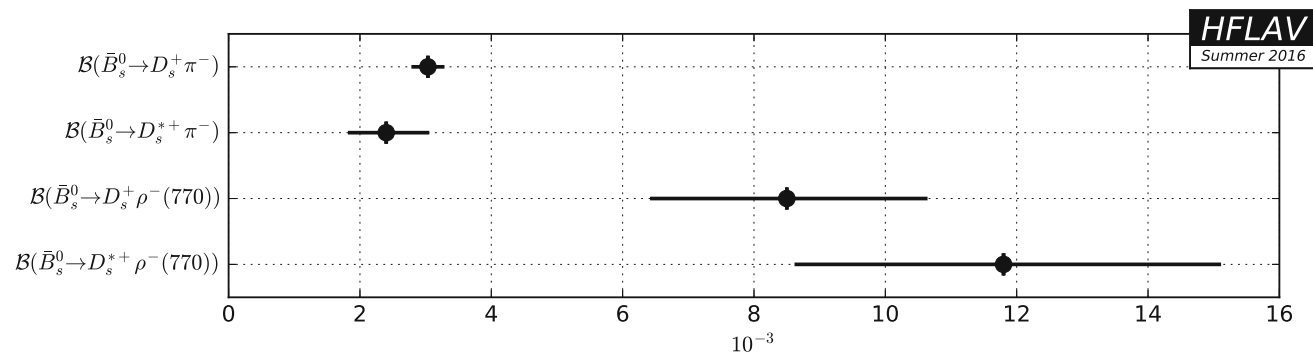
Parameter	Measurements	Average
$\mathcal{B}(\bar{B}_s^0 \rightarrow D^*(2010)^{\pm} \pi^{\mp})$	LHCb [763]: $<6.1$	$<6.1$
$\mathcal{B}(\bar{B}_s^0 \rightarrow D^0 f_0(980))$	LHCb [764]: $<3.1$	$<3.1$

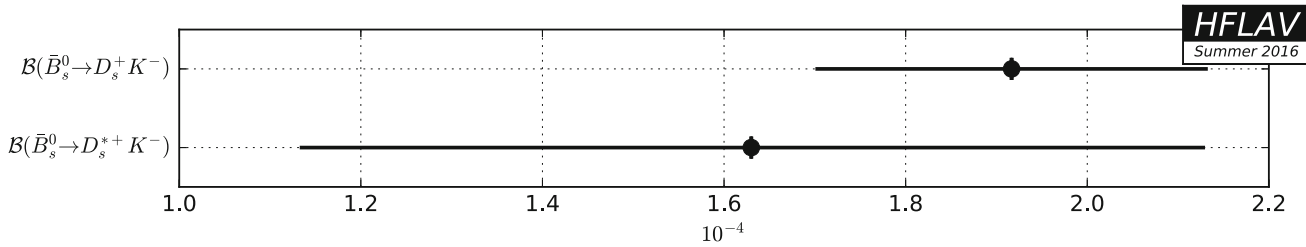
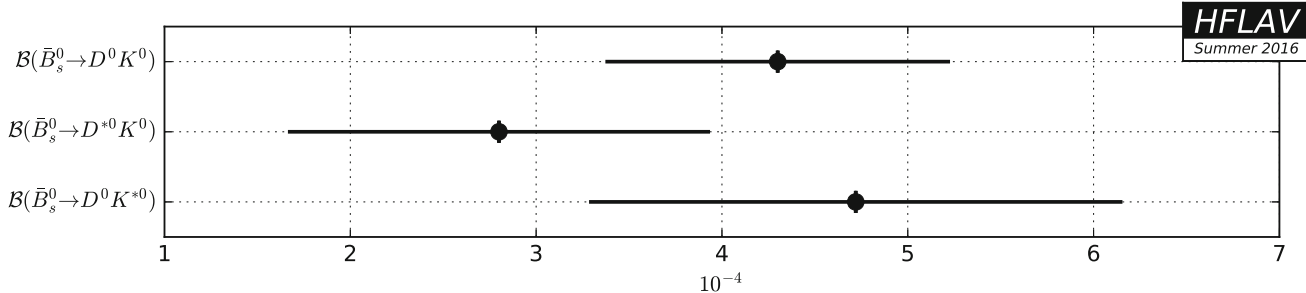
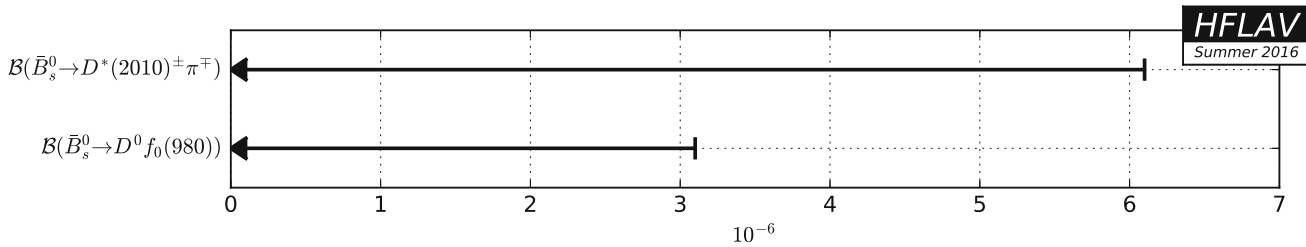
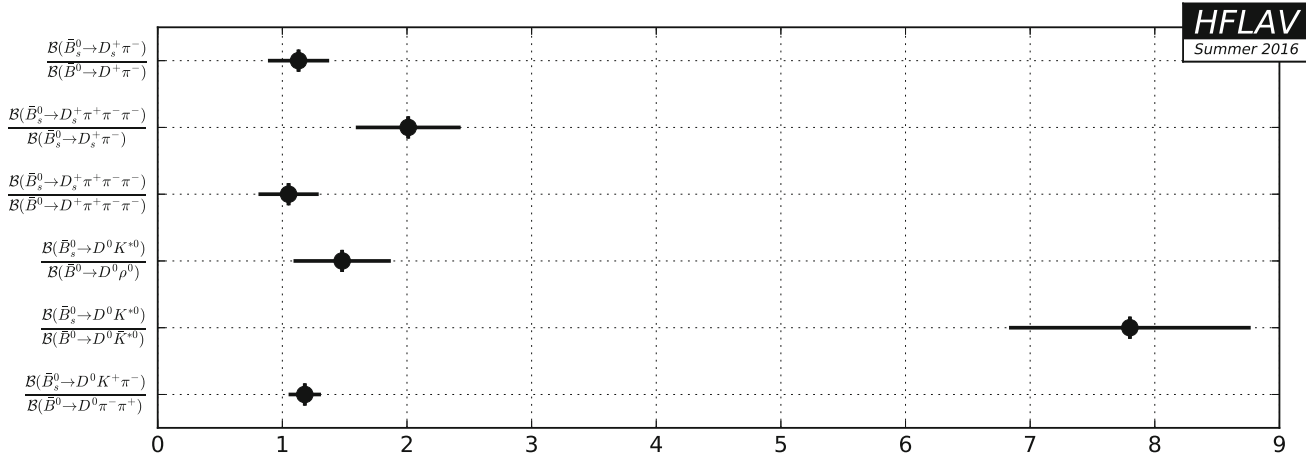
**Table 190** Relative decay rates I

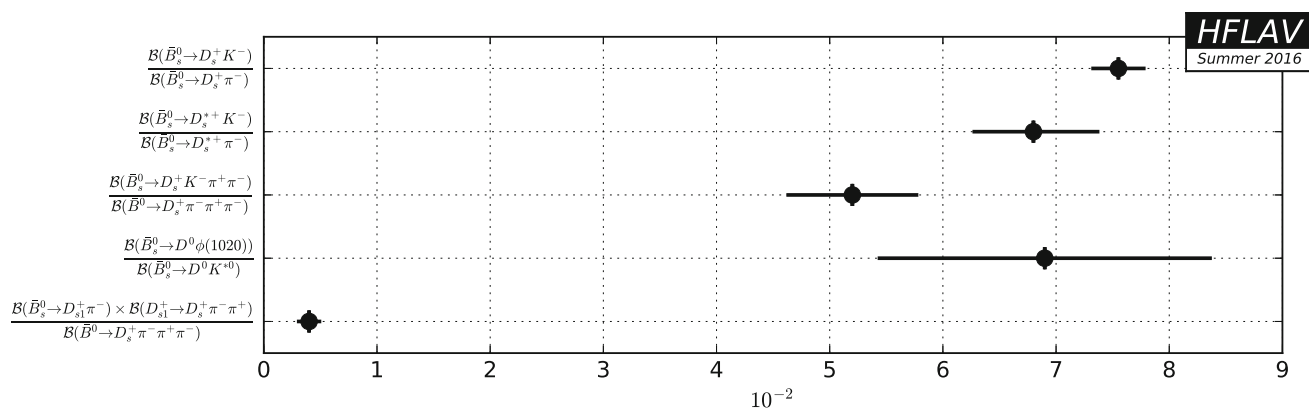
Parameter	Measurements	Average
$\mathcal{B}(\bar{B}_s^0 \rightarrow D_s^+ \pi^-)/\mathcal{B}(\bar{B}_s^0 \rightarrow D^+ \pi^-)$	CDF [765]: $1.13 \pm 0.08 \pm 0.23$	$1.13 \pm 0.25$
$\mathcal{B}(\bar{B}_s^0 \rightarrow D_s^+ \pi^+ \pi^- \pi^-)/\mathcal{B}(\bar{B}_s^0 \rightarrow D_s^+ \pi^-)$	LHCb [616]: $2.01 \pm 0.37 \pm 0.20$	$2.01 \pm 0.42$
$\mathcal{B}(\bar{B}_s^0 \rightarrow D_s^+ \pi^+ \pi^- \pi^-)/\mathcal{B}(\bar{B}_s^0 \rightarrow D^+ \pi^+ \pi^- \pi^-)$	CDF [765]: $1.05 \pm 0.10 \pm 0.22$	$1.05 \pm 0.24$
$\mathcal{B}(\bar{B}_s^0 \rightarrow D^0 K^{*0})/\mathcal{B}(\bar{B}_s^0 \rightarrow D^0 \rho^0)$	LHCb [762]: $1.48 \pm 0.34 \pm 0.19$	$1.48 \pm 0.39$
$\mathcal{B}(\bar{B}_s^0 \rightarrow D^0 K^{*0})/\mathcal{B}(\bar{B}_s^0 \rightarrow D^0 \bar{K}^{*0})$	LHCb [766]: $7.8 \pm 0.7 \pm 0.7$	$7.8 \pm 1.0$
$\mathcal{B}(\bar{B}_s^0 \rightarrow D^0 K^+ \pi^-)/\mathcal{B}(\bar{B}_s^0 \rightarrow D^0 \pi^- \pi^+)$	LHCb [618]: $1.18 \pm 0.05 \pm 0.12$	$1.18 \pm 0.13$

**Table 191** Relative decay rates II [ $10^{-2}$ ]

Parameter	Measurements	Average
$\mathcal{B}(\bar{B}_s^0 \rightarrow D_s^+ K^-)/\mathcal{B}(\bar{B}_s^0 \rightarrow D_s^+ \pi^-)$	LHCb [621]: $7.52 \pm 0.15 \pm 0.19$ CDF [767]: $9.7 \pm 1.8 \pm 0.9$	$7.55 \pm 0.24$
$\mathcal{B}(\bar{B}_s^0 \rightarrow D_s^{*+} K^-)/\mathcal{B}(\bar{B}_s^0 \rightarrow D_s^{*+} \pi^-)$	LHCb [760]: $6.8 \pm 0.5^{+0.3}_{-0.2}$	$6.8^{+0.6}_{-0.5}$
$\mathcal{B}(\bar{B}_s^0 \rightarrow D_s^+ K^- \pi^+ \pi^-)/\mathcal{B}(\bar{B}_s^0 \rightarrow D_s^+ \pi^- \pi^+ \pi^-)$	LHCb [617]: $5.2 \pm 0.5 \pm 0.3$	$5.2 \pm 0.6$
$\mathcal{B}(\bar{B}_s^0 \rightarrow D^0 \phi(1020))/\mathcal{B}(\bar{B}_s^0 \rightarrow D^0 K^{*0})$	LHCb [766]: $6.9 \pm 1.3 \pm 0.7$	$6.9 \pm 1.5$
$[\mathcal{B}(\bar{B}_s^0 \rightarrow D_s^+ \pi^-) \times \mathcal{B}(D_{s1}^+ \rightarrow D_s^+ \pi^- \pi^+)]/\mathcal{B}(\bar{B}_s^0 \rightarrow D_s^+ \pi^- \pi^+ \pi^-)$	LHCb [617]: $0.40 \pm 0.10 \pm 0.04$	$0.40 \pm 0.11$

**Fig. 152** Summary of the averages from Table 188

**Fig. 153** Summary of the averages from Table 187**Fig. 154** Summary of the averages from Table 188**Fig. 155** Summary of the averages from Table 189**Fig. 156** Summary of the averages from Table 190

**Fig. 157** Summary of the averages from Table 191

#### 6.4.2 Decays to two open charm mesons

Averages of  $\bar{B}_s^0$  decays to two open charm mesons are shown in Tables 192, 193, 194 and Figs. 158, 159, 160.

**Table 192** Absolute decay rates [ $10^{-2}$ ]

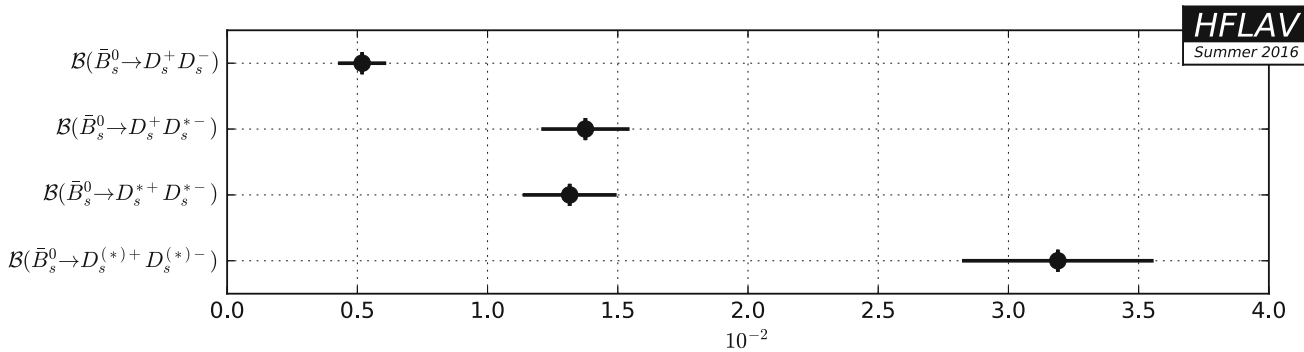
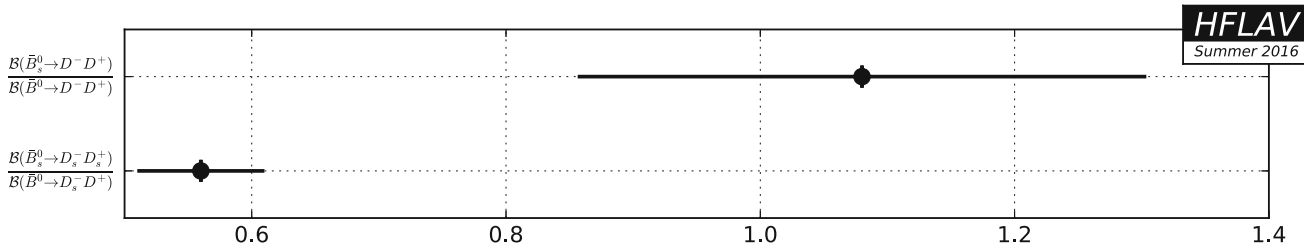
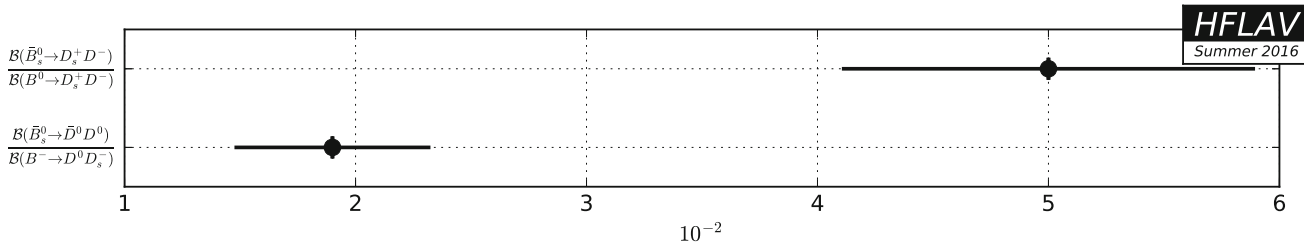
Parameter	Measurements	Average
$\mathcal{B}(\bar{B}_s^0 \rightarrow D_s^+ D_s^-)$	CDF [768]: $0.49 \pm 0.06 \pm 0.09$ Belle [20]: $0.58^{+0.11}_{-0.09} \pm 0.13$	$0.52 \pm 0.09$
$\mathcal{B}(\bar{B}_s^0 \rightarrow D_s^+ D_s^{*-})$	LHCb [769]: $1.35 \pm 0.06 \pm 0.17$ CDF [768]: $1.13 \pm 0.12 \pm 0.21$ Belle [20]: $1.76^{+0.23}_{-0.22} \pm 0.40$	$1.38 \pm 0.17$
$\mathcal{B}(\bar{B}_s^0 \rightarrow D_s^{*+} D_s^{*-})$	LHCb [769]: $1.27 \pm 0.08 \pm 0.17$ CDF [768]: $1.75 \pm 0.19 \pm 0.34$ Belle [20]: $1.98^{+0.33}_{-0.31}{}^{+0.51}_{-0.50}$	$1.32 \pm 0.18$
$\mathcal{B}(\bar{B}_s^0 \rightarrow D_s^{(*)+} D_s^{(*)-})$	LHCb [769]: $3.05 \pm 0.10 \pm 0.39$ D0 [206]: $3.5 \pm 1.0 \pm 1.1$ CDF [768]: $3.38 \pm 0.25 \pm 0.64$ Belle [20]: $4.32^{+0.42}_{-0.39}{}^{+1.04}_{-1.03}$	$3.19 \pm 0.37$

**Table 193** Relative decay rates I

Parameter	Measurements	Average
$\mathcal{B}(\bar{B}_s^0 \rightarrow D^- D^+)/\mathcal{B}(\bar{B}^0 \rightarrow D^- D^+)$	LHCb [639]: $1.08 \pm 0.20 \pm 0.10$	$1.08 \pm 0.22$
$\mathcal{B}(\bar{B}_s^0 \rightarrow D_s^- D_s^+)/\mathcal{B}(\bar{B}^0 \rightarrow D_s^- D_s^+)$	LHCb [639]: $0.56 \pm 0.03 \pm 0.04$	$0.56 \pm 0.05$

**Table 194** Relative decay rates II [ $10^{-2}$ ]

Parameter	Measurements	Average
$\mathcal{B}(\bar{B}_s^0 \rightarrow D_s^+ D^-)/\mathcal{B}(B^0 \rightarrow D_s^+ D^-)$	LHCb [639]: $5.0 \pm 0.8 \pm 0.4$	$5.0 \pm 0.9$
$\mathcal{B}(\bar{B}_s^0 \rightarrow \bar{D}^0 D^0)/\mathcal{B}(B^- \rightarrow D^0 D_s^-)$	LHCb [639]: $1.9 \pm 0.3 \pm 0.3$	$1.9 \pm 0.4$

**Fig. 158** Summary of the averages from Table 192**Fig. 159** Summary of the averages from Table 193**Fig. 160** Summary of the averages from Table 194

#### 6.4.3 Decays to charmonium states

Averages of  $\bar{B}_s^0$  decays to charmonium states are shown in Tables 195, 196, 197, 198, 199 and Figs. 161, 162, 163, 164, 165.

**Table 195** Absolute decay rates I [ $10^{-4}$ ]

Parameter	Measurements	Average
$\mathcal{B}(\bar{B}_s^0 \rightarrow J/\psi \eta)$	Belle [770]: $5.10 \pm 0.50^{+1.17}_{-0.83}$	$5.10^{+1.27}_{-0.97}$
$\mathcal{B}(\bar{B}_s^0 \rightarrow J/\psi \eta')$	Belle [770]: $3.71 \pm 0.61^{+0.85}_{-0.60}$	$3.71^{+1.05}_{-0.85}$
$\mathcal{B}(\bar{B}_s^0 \rightarrow J/\psi \phi(1020))$	LHCb [771]: $10.5 \pm 0.1 \pm 1.0$ CDF [683]: $9.3 \pm 2.8 \pm 1.7$ Belle [772]: $12.5 \pm 0.7 \pm 2.3$	$10.0 \pm 0.9$
$\mathcal{B}(\bar{B}_s^0 \rightarrow J/\psi K^0 K^\pm \pi^\mp)$	LHCb [649]: $9.1 \pm 0.6 \pm 0.7$	$9.1 \pm 0.9$
$\mathcal{B}(\bar{B}_s^0 \rightarrow J/\psi f_0(980)) \times \mathcal{B}(f_0(980) \rightarrow \pi^+\pi^-)$	Belle [28]: $1.16^{+0.31}_{-0.19}{}^{+0.30}_{-0.25}$	$1.16^{+0.43}_{-0.32}$

**Table 196** Absolute decay rates II [ $10^{-5}$ ]

Parameter	Measurements	Average
$\mathcal{B}(\bar{B}_s^0 \rightarrow J/\psi \bar{K}^0)$	LHCb [773]: $3.66 \pm 0.42 \pm 0.37$ CDF [774]: $3.5 \pm 0.6 \pm 0.6$	$3.61 \pm 0.46$
$\mathcal{B}(\bar{B}_s^0 \rightarrow J/\psi K^{*0})$	LHCb [775]: $4.17 \pm 0.18 \pm 0.35$ CDF [774]: $8.3 \pm 1.2 \pm 3.6$	$4.15 \pm 0.40$
$\mathcal{B}(\bar{B}_s^0 \rightarrow J/\psi p \bar{p})$	LHCb [678]: $<0.48$	$<0.48$
$\mathcal{B}(\bar{B}_s^0 \rightarrow J/\psi f_1(1285))$	LHCb [671]: $7.14 \pm 0.99 {}^{+0.93}_{-1.00}$	$7.14 {}^{+1.36}_{-1.41}$
$\mathcal{B}(\bar{B}_s^0 \rightarrow J/\psi K^0 \pi^+ \pi^-)$	LHCb [649]: $<4.4$	$<4.4$
$\mathcal{B}(\bar{B}_s^0 \rightarrow J/\psi K^0 K^+ K^-)$	LHCb [649]: $<1.2$	$<1.2$
$\mathcal{B}(\bar{B}_s^0 \rightarrow J/\psi f_0(1370)) \times \mathcal{B}(f_0(1370) \rightarrow \pi^+ \pi^-)$	Belle [28]: $3.4 {}^{+1.1}_{-1.4} {}^{+0.9}_{-0.5}$	$3.4 {}^{+1.4}_{-1.5}$
$\mathcal{B}(\bar{B}_s^0 \rightarrow J/\psi f_1(1285)) \times \mathcal{B}(f_1(1285) \rightarrow \pi^+ \pi^- \pi^+ \pi^-)$	LHCb [671]: $0.785 \pm 0.109 {}^{+0.089}_{-0.101}$	$0.785 {}^{+0.141}_{-0.149}$
$\mathcal{B}(\bar{B}_s^0 \rightarrow J/\psi \gamma)$	LHCb [676]: $<0.73$	$<0.73$

**Table 197** Relative decay rates I

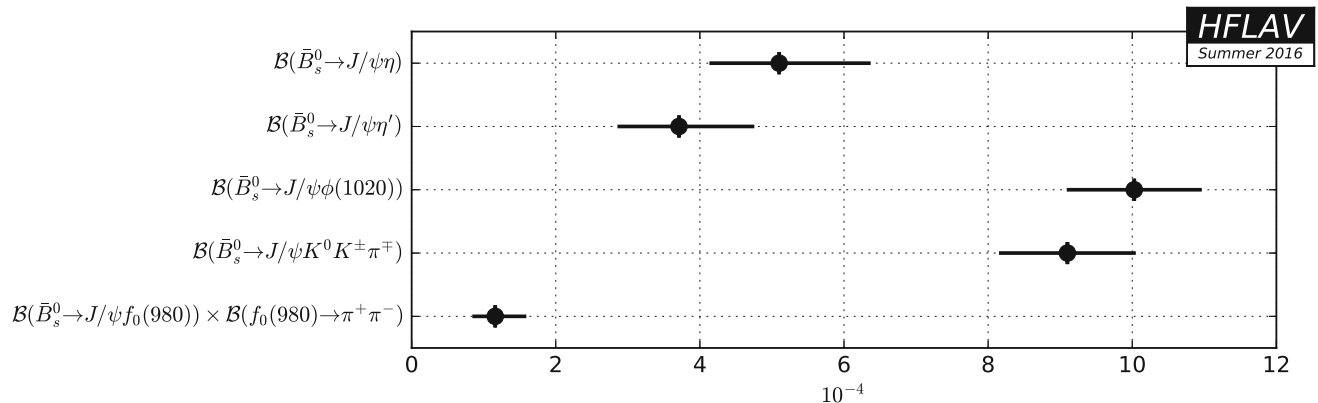
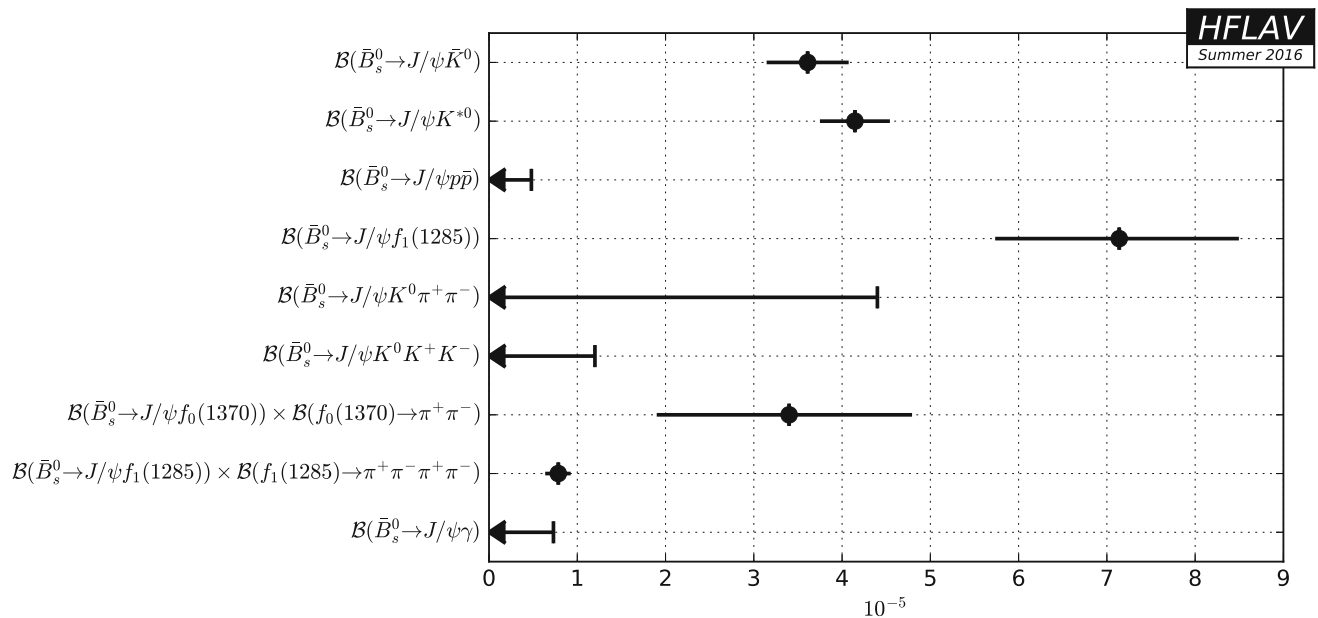
Parameter	Measurements	Average
$\mathcal{B}(\bar{B}_s^0 \rightarrow J/\psi \eta)/\mathcal{B}(\bar{B}_s^0 \rightarrow J/\psi \rho)$	LHCb [684]: $14.0 \pm 1.2 {}^{+1.6}_{-1.8}$	$14.0 {}^{+2.0}_{-2.2}$
$\mathcal{B}(\bar{B}_s^0 \rightarrow J/\psi \eta')/\mathcal{B}(\bar{B}_s^0 \rightarrow J/\psi \rho)$	LHCb [684]: $12.7 \pm 1.1 {}^{+1.1}_{-0.9}$	$12.7 {}^{+1.6}_{-1.4}$
$\mathcal{B}(\bar{B}_s^0 \rightarrow J/\psi K_S^0 K^\pm \pi^\mp)/\mathcal{B}(\bar{B}_s^0 \rightarrow J/\psi \pi^+ \pi^-)$	LHCb [649]: $2.12 \pm 0.15 \pm 0.18$	$2.12 \pm 0.23$

**Table 198** Relative decay rates II

Parameter	Measurements	Average
$\mathcal{B}(\bar{B}_s^0 \rightarrow J/\psi \eta)/\mathcal{B}(\bar{B}_s^0 \rightarrow J/\psi \eta')$	Belle [770]: $0.73 \pm 0.14 \pm 0.02$	$0.73 \pm 0.14$
$\mathcal{B}(\bar{B}_s^0 \rightarrow J/\psi \eta')/\mathcal{B}(\bar{B}_s^0 \rightarrow J/\psi \eta)$	LHCb [684]: $0.90 \pm 0.09 {}^{+0.06}_{-0.02}$	$0.90 {}^{+0.11}_{-0.09}$
$\mathcal{B}(\bar{B}_s^0 \rightarrow J/\psi f'_2)/\mathcal{B}(\bar{B}_s^0 \rightarrow J/\psi \phi(1020))$	LHCb [776]: $0.264 \pm 0.027 \pm 0.024$ D0 [777]: $0.19 \pm 0.05 \pm 0.04$	$0.246 \pm 0.031$
$\mathcal{B}(\bar{B}_s^0 \rightarrow J/\psi \pi^+ \pi^-)/\mathcal{B}(\bar{B}_s^0 \rightarrow J/\psi \phi(1020))$	LHCb [778]: $0.162 \pm 0.022 \pm 0.016$	$0.162 \pm 0.027$
$\mathcal{B}(\bar{B}_s^0 \rightarrow \psi(2S) \pi^+ \pi^-)/\mathcal{B}(\bar{B}_s^0 \rightarrow J/\psi \pi^+ \pi^-)$	LHCb [686]: $0.34 \pm 0.04 \pm 0.03$	$0.34 \pm 0.05$
$\mathcal{B}(\bar{B}_s^0 \rightarrow \psi(2S) \phi(1020))/\mathcal{B}(\bar{B}_s^0 \rightarrow J/\psi \phi(1020))$	LHCb [685]: $0.489 \pm 0.026 \pm 0.024$ D0 [746]: $0.55 \pm 0.11 \pm 0.09$ CDF [779]: $0.52 \pm 0.13 \pm 0.07$	$0.494 \pm 0.034$
$\mathcal{B}(\bar{B}_s^0 \rightarrow J/\psi K_S^0 \pi^+ \pi^-)/\mathcal{B}(\bar{B}_s^0 \rightarrow J/\psi \pi^+ \pi^-)$	LHCb [649]: $<0.10$	$<0.10$
$[\mathcal{B}(\bar{B}_s^0 \rightarrow J/\psi f_0(980)) \times \mathcal{B}(f_0(980) \rightarrow \pi^+ \pi^-)]/[\mathcal{B}(\bar{B}_s^0 \rightarrow J/\psi \phi(1020)) \times \mathcal{B}(\phi \rightarrow K^+ K^-)]$	LHCb [778]: $0.252 {}^{+0.046}_{-0.032} {}^{+0.027}_{-0.033}$ D0 [780]: $0.275 \pm 0.041 \pm 0.061$ CMS [781]: $0.140 \pm 0.008 \pm 0.023$ CDF [128]: $0.257 \pm 0.020 \pm 0.014$	$0.207 \pm 0.016$ CL = 3.8 %

**Table 199** Relative decay rates III [ $10^{-2}$ ]

Parameter	Measurements	Average
$\mathcal{B}(\bar{B}_s^0 \rightarrow J/\psi K_S^0)/\mathcal{B}(\bar{B}^0 \rightarrow J/\psi K_S^0)$	LHCb [773]: $4.20 \pm 0.49 \pm 0.40$	$4.20 \pm 0.63$
$\mathcal{B}(\bar{B}_s^0 \rightarrow J/\psi\phi(1020)\phi(1020))/\mathcal{B}(\bar{B}_s^0 \rightarrow J/\psi\phi(1020))$	LHCb [782]: $1.15 \pm 0.12^{+0.05}_{-0.09}$	$1.15^{+0.13}_{-0.15}$
$\mathcal{B}(\bar{B}_s^0 \rightarrow \psi(2S)K^+\pi^-)/\mathcal{B}(\bar{B}^0 \rightarrow \psi(2S)K^+\pi^-)$	LHCb [783]: $5.38 \pm 0.36 \pm 0.38$	$5.38 \pm 0.52$
$\mathcal{B}(\bar{B}_s^0 \rightarrow \psi(2S)K^{*0})/\mathcal{B}(\bar{B}^0 \rightarrow \psi(2S)K^{*0})$	LHCb [783]: $5.38 \pm 0.57 \pm 0.51$	$5.38 \pm 0.77$
$\mathcal{B}(\bar{B}_s^0 \rightarrow J/\psi K_S^0 K^+ K^-)/\mathcal{B}(\bar{B}^0 \rightarrow J/\psi\pi^+\pi^-)$	LHCb [649]: $<2.7$	$<2.7$
$[\mathcal{B}(\bar{B}_s^0 \rightarrow J/\psi f_0(500)) \times \mathcal{B}(f_0(500) \rightarrow \pi^+\pi^-)]/[\mathcal{B}(\bar{B}_s^0 \rightarrow J/\psi f_0(980)) \times \mathcal{B}(f_0(980) \rightarrow \pi^+\pi^-)]$	LHCb [784]: $<3.4$	$<3.4$

**Fig. 161** Summary of the averages from Table 195**Fig. 162** Summary of the averages from Table 196

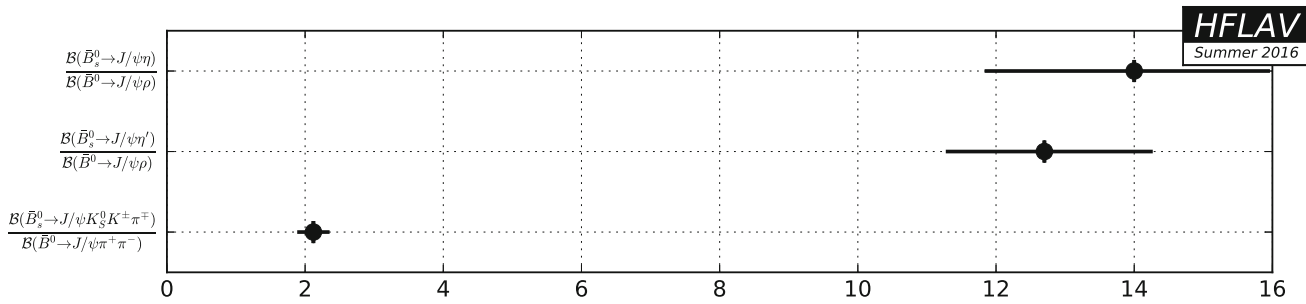


Fig. 163 Summary of the averages from Table 197

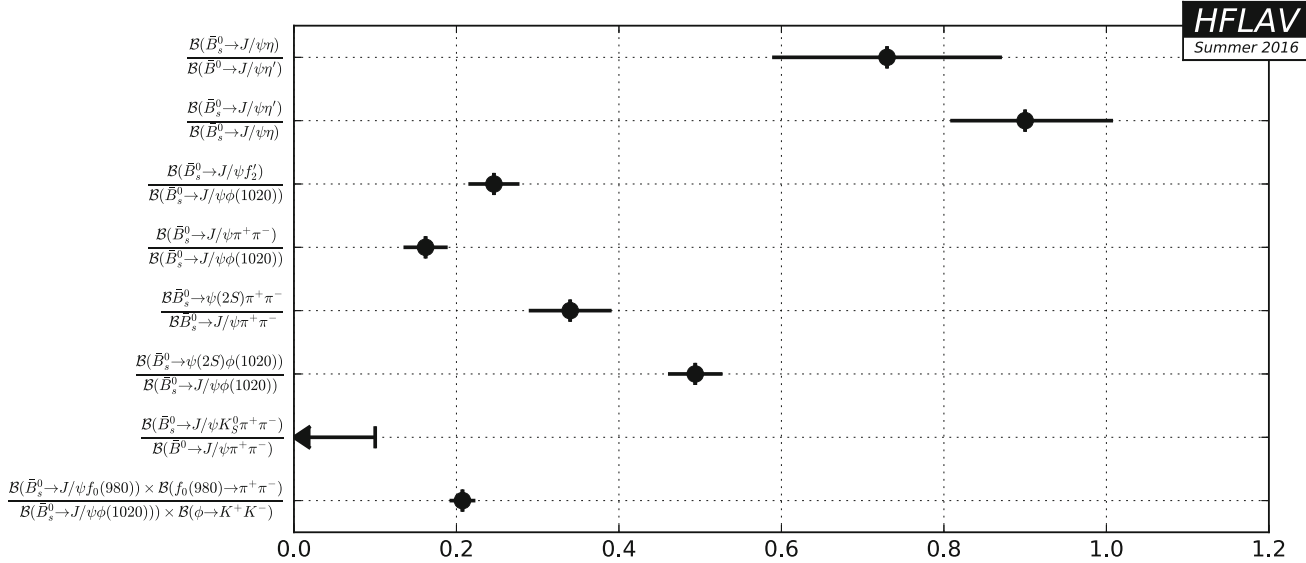


Fig. 164 Summary of the averages from Table 198

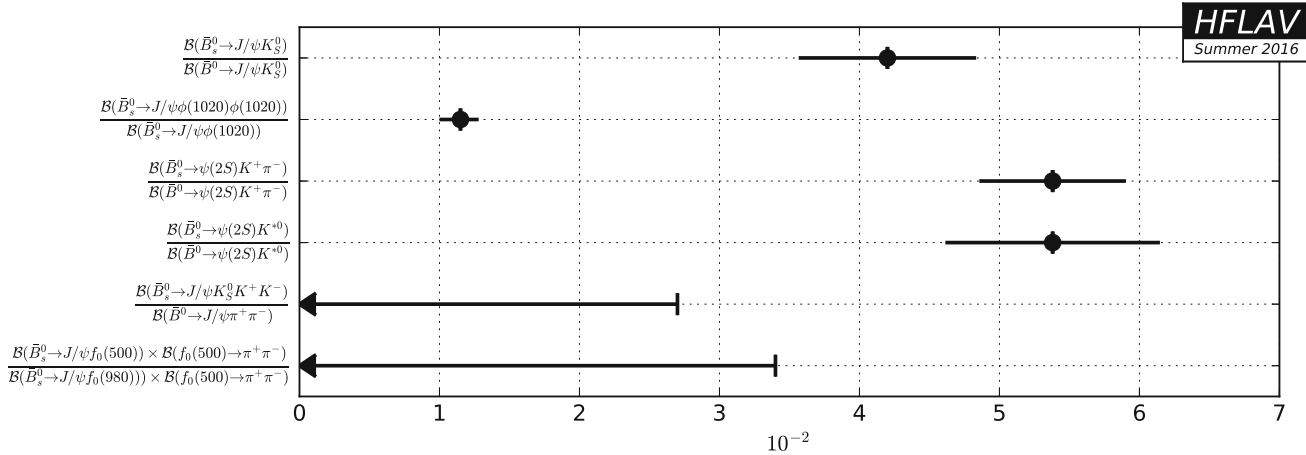


Fig. 165 Summary of the averages from Table 199

**Table 200** Decays to one charm baryon [ $10^{-4}$ ]

Parameter	Measurements	Average
$\mathcal{B}(\bar{B}_s^0 \rightarrow \Lambda_c^+ \bar{\Lambda} \pi^-)$	Belle [785]: $3.6 \pm 1.1^{+1.2}_{-1.2}$	$3.6^{+1.6}_{-1.7}$

**Table 201** Decays to two charm baryons

Parameter	Measurements	Average
$\mathcal{B}(\bar{B}_s^0 \rightarrow \Lambda_c^- \Lambda_c^+)/\mathcal{B}(\bar{B}_s^0 \rightarrow D^- D_s^+)$	LHCb [703]: $<0.30$	$<0.30$

#### 6.4.4 Decays to charm baryons

Averages of  $\bar{B}_s^0$  decays to charm baryons are shown in Tables 200 and 201.

#### 6.5 Decays of $B_c^-$ mesons

Measurements of  $B_c^-$  decays to charmed hadrons are summarized in Sects. 6.5.1–6.5.2. Since the absolute cross-section for  $B_c^-$  meson production in any production environment is currently not known, it is not possible to determine absolute branching fractions. Instead, results are presented either as ratios of branching fractions of different  $B_c^-$  decays, or are normalised to the branching fraction of the decay of a lighter  $B$  meson (usually  $B^-$ ). In the latter case the mea-

sured quantity is the absolute or relative  $B_c^-$  branching fraction multiplied by the ratio of cross-sections (or, equivalently, production fractions) of the  $B_c^-$  and the lighter  $B$  meson.

It should be noted that the ratio of cross-sections for different  $b$  hadron species can depend on production environment, and on the fiducial region accessed by each experiment. While this has been studied for certain  $b$  hadron species (see Sect. 3.1), there is currently little published data that would allow to investigate the effect for  $B_c^-$  mesons. Therefore, we do not attempt to apply any correction for this effect.

#### 6.5.1 Decays to charmonium states

Averages of  $B_c^-$  decays to charmonium states are shown in Tables 202, 203, 204, 205 and Figs. 166, 167.

#### 6.5.2 Decays to a $B$ meson

Averages of  $B_c^-$  decays to a  $B$  meson are shown in Table 206.

#### 6.6 Decays of $b$ baryons

Measurements of  $b$  baryons decays to charmed hadrons are summarized in Sects. 6.6.1–6.6.3. Comments regarding the production rates of  $\bar{B}_s^0$  and  $B_c^-$  mesons relative to lighter  $B$  mesons, in Sects. 6.4 and 6.5 respectively, are also appropriate here. Specifically, since the cross-

**Table 202** Relative decay rates I

Parameter	Measurements	Average
$\mathcal{B}(B_c^- \rightarrow J/\psi D_s^-)/\mathcal{B}(B_c^- \rightarrow J/\psi \pi^-)$	LHCb [786]: $2.90 \pm 0.57 \pm 0.24$ ATLAS [787]: $3.8 \pm 1.1 \pm 0.4$	$3.09 \pm 0.55$
$\mathcal{B}(B_c^- \rightarrow J/\psi D_s^{*-})/\mathcal{B}(B_c^- \rightarrow J/\psi D_s^-)$	ATLAS [787]: $2.8^{+1.2}_{-0.8} \pm 0.3$	$2.8^{+1.2}_{-0.9}$
$\mathcal{B}(B_c^- \rightarrow J/\psi D_s^-)/\mathcal{B}(B_c^- \rightarrow J/\psi \pi^-)$	ATLAS [787]: $10.4 \pm 3.1 \pm 1.6$	$10.4 \pm 3.5$
$\mathcal{B}(B_c^- \rightarrow J/\psi \pi^+ \pi^- \pi^-)/\mathcal{B}(B_c^- \rightarrow J/\psi \pi^-)$	LHCb [788]: $2.41 \pm 0.30 \pm 0.33$ CMS [789]: $2.55 \pm 0.80^{+0.33}_{-0.33}$	$2.44 \pm 0.40$

**Table 203** Relative decay rates II

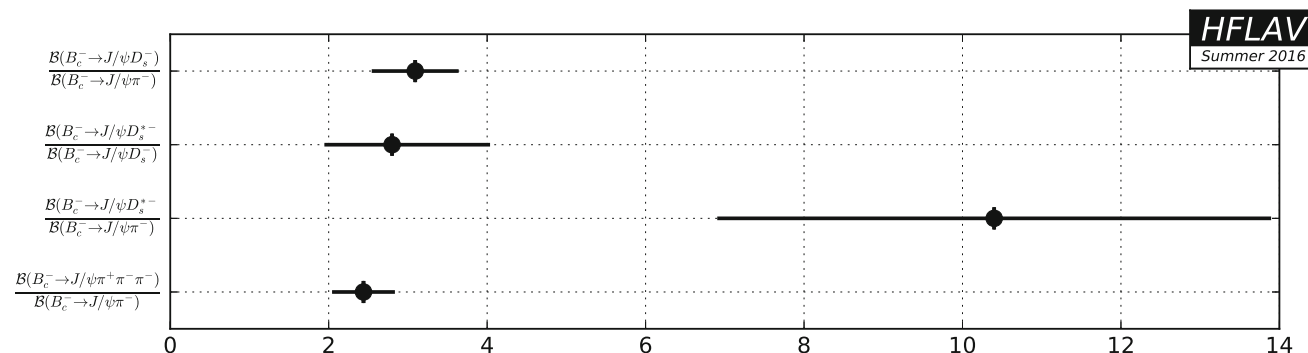
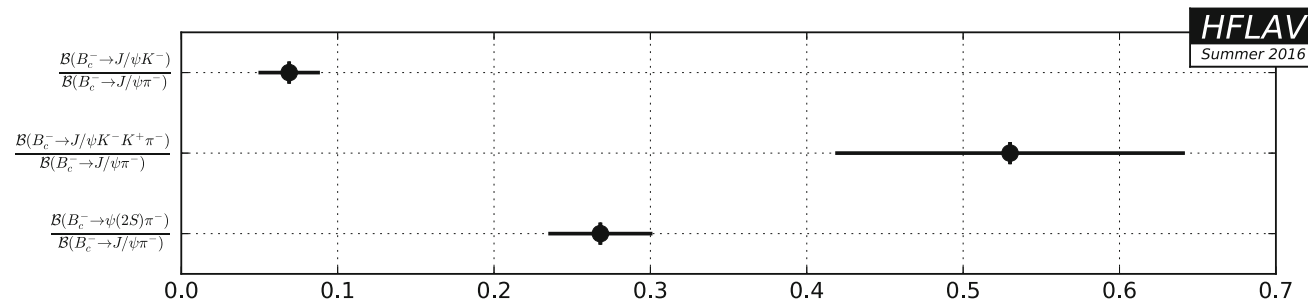
Parameter	Measurements	Average
$\mathcal{B}(B_c^- \rightarrow J/\psi K^-)/\mathcal{B}(B_c^- \rightarrow J/\psi \pi^-)$	LHCb [790]: $0.069 \pm 0.019 \pm 0.005$	$0.069 \pm 0.020$
$\mathcal{B}(B_c^- \rightarrow J/\psi K^- K^+ \pi^-)/\mathcal{B}(B_c^- \rightarrow J/\psi \pi^-)$	LHCb [791]: $0.53 \pm 0.10 \pm 0.05$	$0.53 \pm 0.11$
$\mathcal{B}(B_c^- \rightarrow \psi(2S) \pi^-)/\mathcal{B}(B_c^- \rightarrow J/\psi \pi^-)$	LHCb [792]: $0.268 \pm 0.032 \pm 0.009$	$0.268 \pm 0.033$

**Table 204** Relative production times decay rates [ $10^{-3}$ ]

Parameter	Measurements	Average
$[\sigma(B_c^-) \times \mathcal{B}(B_c^- \rightarrow J/\psi \pi^-)]/[\sigma(B^-) \times \mathcal{B}(B^- \rightarrow J/\psi K^-)]$	LHCb [793]: $6.83 \pm 0.18 \pm 0.09$ LHCb [794]: $6.8 \pm 1.0 \pm 0.6$ CMS [789]: $4.8 \pm 0.5 \pm 0.6$	$6.72 \pm 0.19$

**Table 205** Decay rates times relative production rates [ $10^{-6}$ ]

Parameter	Measurements	Average
$[\sigma(B_c^-)/\sigma(B^-)] \times \mathcal{B}(B_c^- \rightarrow \chi_{c0}\pi^-)$	LHCb [795]: $9.8^{+3.4}_{-3.0} \pm 0.8$	$9.8^{+3.5}_{-3.1}$

**Fig. 166** Summary of the averages from Table 202**Fig. 167** Summary of the averages from Table 203**Table 206** Decays to  $B_s^0$  meson [ $10^{-3}$ ]

Parameter	Measurements	Average
$[\sigma(B_c^+)/\sigma(B_s^0)] \times \mathcal{B}(B_c^+ \rightarrow B_s^0 \pi^+)$	LHCb [796]: $2.37 \pm 0.31^{+0.20}_{-0.17}$	$2.37^{+0.37}_{-0.35}$

**Table 207** Relative decay rates to  $D^0$  mesons

Parameter	Measurements	Average
$\mathcal{B}(\Lambda_b^0 \rightarrow D^0 p K^-) / \mathcal{B}(\Lambda_b^0 \rightarrow D^0 p \pi^-)$	LHCb [797]: $0.073 \pm 0.008^{+0.005}_{-0.006}$	$0.073^{+0.009}_{-0.010}$
$[\mathcal{B}(\Lambda_b^0 \rightarrow D^0 p \pi^-) \times \mathcal{B}(D^0 \rightarrow K^+ \pi^-)] / [\mathcal{B}(\Lambda_b^0 \rightarrow \Lambda_c^+ \pi^-) \times \mathcal{B}(\Lambda_c^+ \rightarrow p K^- \pi^+)]$	LHCb [797]: $0.0806 \pm 0.0023 \pm 0.0035$	$0.0806 \pm 0.0042$
$[\mathcal{f}_{\Xi_b^0} \times \mathcal{B}(\Xi_b^0 \rightarrow D^0 p K^-)] / [\mathcal{f}_{\Lambda_b^0} \times \mathcal{B}(\Lambda_b^0 \rightarrow D^0 p K^-)]$	LHCb [797]: $0.44 \pm 0.09 \pm 0.06$	$0.44 \pm 0.11$

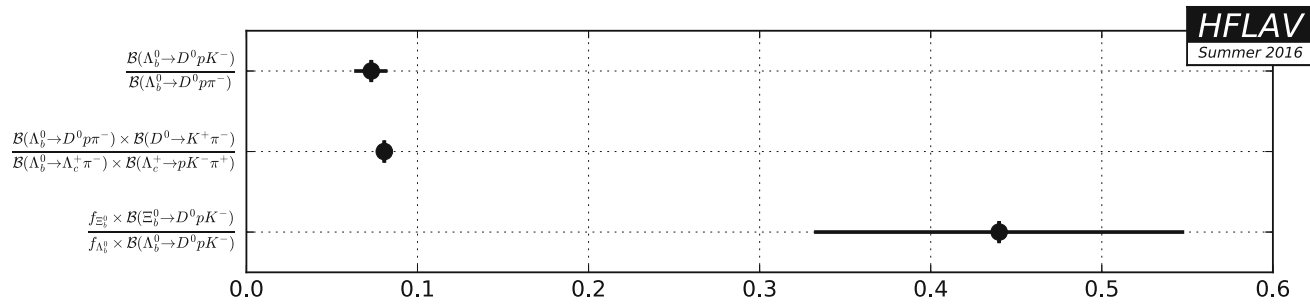
section for production of  $\Lambda_b^0$  baryons is reasonably well-known, it is possible to determine absolute or relative branching fractions for its decays (although some older measurements are presented as products involving the cross-section). The cross-sections for production of heavier  $b$  baryons are not known, and therefore measured quantities are presented as absolute or relative branching fraction multiplied by a ratio of cross-sections (or, equivalently, production fractions).

### 6.6.1 Decays to a single open charm meson

Averages of  $b$  baryons decays to a single open charm meson are shown in Table 207 and Fig. 168.

### 6.6.2 Decays to charmonium states

Averages of  $b$  baryons decays to charmonium states are shown in Tables 208, 209, 210, 211, 212 and Figs. 169, 170, 171.

**Fig. 168** Summary of the averages from Table 207**Table 208**  $\Lambda_b^0$  decays to charmonium [ $10^{-4}$ ]

Parameter	Measurements	Average
$\mathcal{B}(\Lambda_b^0 \rightarrow J/\psi p K^-)$	LHCb [798]: $3.17 \pm 0.04^{+0.46}_{-0.29}$	$3.17^{+0.46}_{-0.29}$
$\mathcal{B}(\Lambda_b^0 \rightarrow J/\psi \Lambda)$	CDF [799]: $4.7 \pm 2.1 \pm 1.9$	$4.7 \pm 2.8$

**Table 209**  $f_b$  times  $\Lambda_b^0$  decay to charmonium [ $10^{-5}$ ]

Parameter	Measurements	Average
$f_{\Lambda_b} \times \mathcal{B}(\Lambda_b^0 \rightarrow J/\psi \Lambda)$	D0 [800]: $6.01 \pm 0.60 \pm 0.64$	$6.01 \pm 0.88$

**Table 210** Relative  $\Lambda_b^0$  decay rates

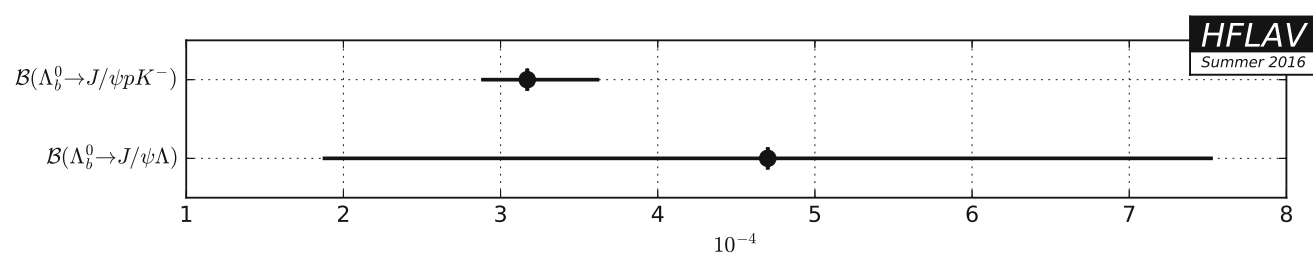
Parameter	Measurements	Average
$\mathcal{B}(\Lambda_b^0 \rightarrow \psi(2S)\Lambda)/\mathcal{B}(\Lambda_b^0 \rightarrow J/\psi \Lambda)$	ATLAS [801]: $0.501 \pm 0.033 \pm 0.019$	$0.501 \pm 0.038$
$\mathcal{B}(\Lambda_b^0 \rightarrow J/\psi p \pi^-)/\mathcal{B}(\Lambda_b^0 \rightarrow J/\psi p K^-)$	LHCb [802]: $0.0824 \pm 0.0025 \pm 0.0042$	$0.0824 \pm 0.0049$
$\mathcal{B}(\Lambda_b^0 \rightarrow J/\psi \pi^+ \pi^- p K^-)/\mathcal{B}(\Lambda_b^0 \rightarrow J/\psi p K^-)$	LHCb [803]: $0.2086 \pm 0.0096 \pm 0.0134$	$0.2086 \pm 0.0165$
$\mathcal{B}(\Lambda_b^0 \rightarrow \psi(2S)p K^-)/\mathcal{B}(\Lambda_b^0 \rightarrow J/\psi p K^-)$	LHCb [803]: $0.2070 \pm 0.0076 \pm 0.0059$	$0.2070 \pm 0.0096$

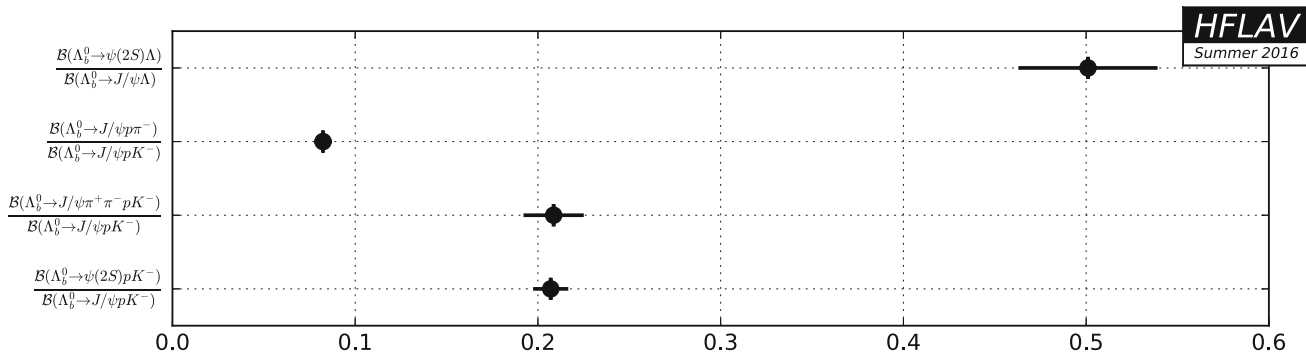
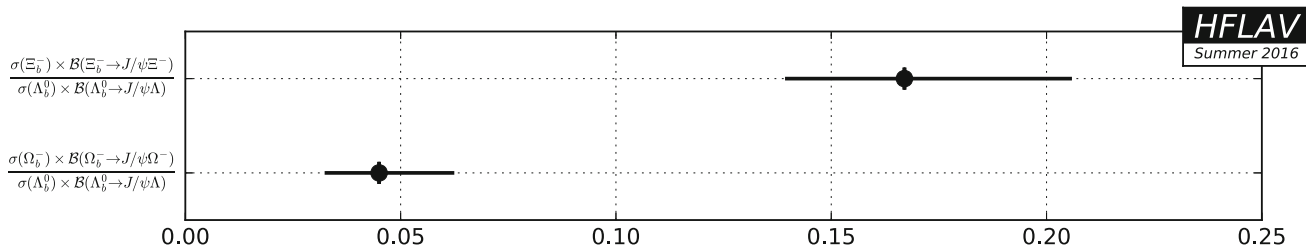
**Table 211**  $\Xi_b^-$  and  $\Omega_b^-$  decays to charmonium

Parameter	Measurements	Average
$[\sigma(\Xi_b^-) \times \mathcal{B}(\Xi_b^- \rightarrow J/\psi \Xi^-)]/[\sigma(\Lambda_b^0) \times \mathcal{B}(\Lambda_b^0 \rightarrow J/\psi \Lambda)]$	CDF [45]: $0.167^{+0.037}_{-0.025} \pm 0.012$	$0.167^{+0.039}_{-0.028}$
$[\sigma(\Omega_b^-) \times \mathcal{B}(\Omega_b^- \rightarrow J/\psi \Omega^-)]/[\sigma(\Lambda_b^0) \times \mathcal{B}(\Lambda_b^0 \rightarrow J/\psi \Lambda)]$	CDF [45]: $0.045^{+0.017}_{-0.012} \pm 0.004$	$0.045^{+0.017}_{-0.013}$

**Table 212** Parity violation in  $\Lambda_b^0$  decays to charmonium

Parameter	Measurements	Average
$\alpha_b(\Lambda_b^0 \rightarrow J/\psi \Lambda)$	ATLAS [804]: $0.30 \pm 0.16 \pm 0.06$	$0.30 \pm 0.17$

**Fig. 169** Summary of the averages from Table 208

**Fig. 170** Summary of the averages from Table 210**Fig. 171** Summary of the averages from Table 211

### 6.6.3 Decays to charm baryons

Averages of  $b$  baryons decays to charm baryons are shown in Tables 213, 214, 215, 216, 217 and Figs. 172, 173, 174, 175.

**Table 213** Absolute decay rates [ $10^{-2}$ ]

Parameter	Measurements	Average
$\mathcal{B}(\Lambda_b^0 \rightarrow \Lambda_c^+ \pi^-)$	LHCb [48]: $0.430 \pm 0.003^{+0.036}_{-0.035}$	$0.430^{+0.036}_{-0.035}$
$\mathcal{B}(\Lambda_b^0 \rightarrow \Lambda_c^+ \pi^+ \pi^- \pi^-)$	CDF [805]: $2.68 \pm 0.29^{+1.15}_{-1.09}$	$2.68^{+1.19}_{-1.12}$

**Table 214** Relative decay rates to  $\Lambda_c$  I

Parameter	Measurements	Average
$\mathcal{B}(\Lambda_b^0 \rightarrow \Lambda_c^+ \pi^-) / \mathcal{B}(\bar{B}^0 \rightarrow D^+ \pi^-)$	CDF [806]: $3.3 \pm 0.3 \pm 1.2$	$3.3 \pm 1.2$
$\mathcal{B}(\Lambda_b^0 \rightarrow \Lambda_c^+ \pi^+ \pi^- \pi^-) / \mathcal{B}(\Lambda_b^0 \rightarrow \Lambda_c^+ \pi^-)$	LHCb [616]: $1.43 \pm 0.16 \pm 0.13$ CDF [805]: $3.04 \pm 0.33^{+0.70}_{-0.55}$	$1.55 \pm 0.20$
$[\mathcal{B}(\Xi_b^0 \rightarrow \Lambda_c^+ K^-) \times \mathcal{B}(\Lambda_c^+ \rightarrow p K^- \pi^+)] / [\mathcal{B}(\Xi_b^0 \rightarrow D^0 p K^-) \times \mathcal{B}(D^0 \rightarrow K^+ \pi^-)]$	LHCb [797]: $0.57 \pm 0.22 \pm 0.21$	$0.57 \pm 0.30$

**Table 215** Relative decay rates to  $\Lambda_c$  II [ $10^{-2}$ ]

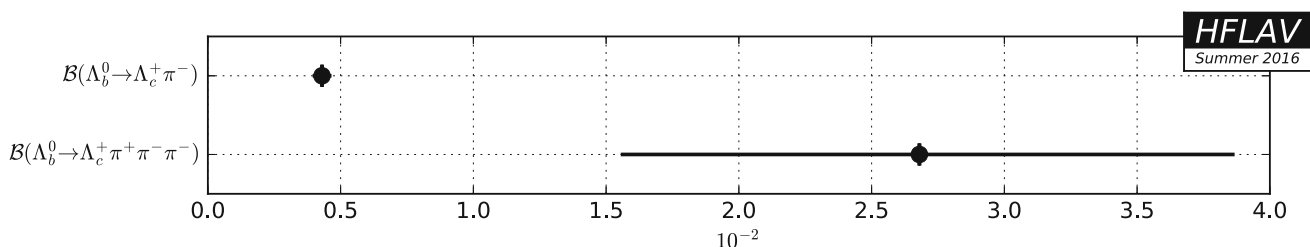
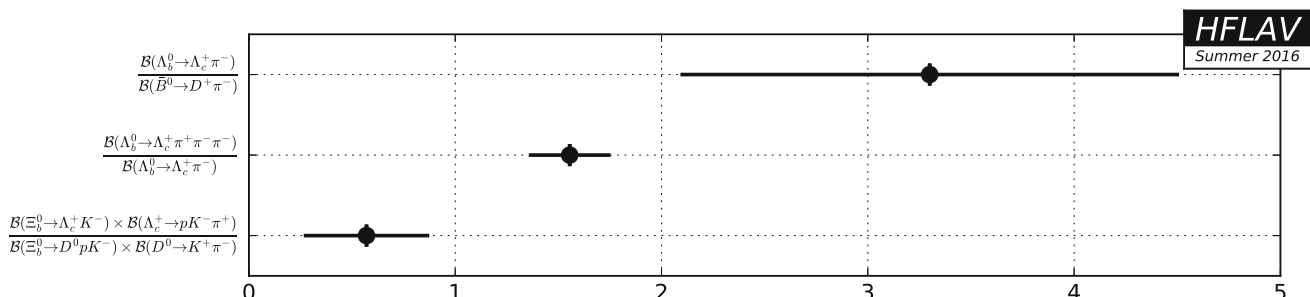
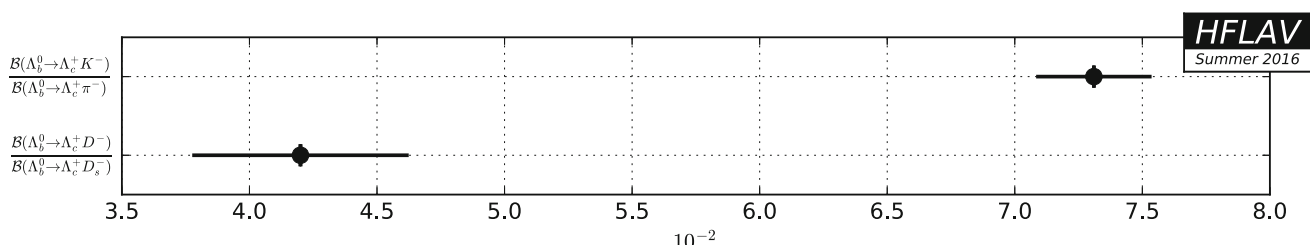
Parameter	Measurements	Average
$\mathcal{B}(\Lambda_b^0 \rightarrow \Lambda_c^+ K^-) / \mathcal{B}(\Lambda_b^0 \rightarrow \Lambda_c^+ \pi^-)$	LHCb [797]: $7.31 \pm 0.16 \pm 0.16$	$7.31 \pm 0.23$
$\mathcal{B}(\Lambda_b^0 \rightarrow \Lambda_c^+ D^-) / \mathcal{B}(\Lambda_b^0 \rightarrow \Lambda_c^+ D_s^-)$	LHCb [703]: $4.2 \pm 0.3 \pm 0.3$	$4.2 \pm 0.4$

**Table 216** Relative decay rates to excited or  $\Sigma_c$  states

Parameter	Measurements	Average
$[\mathcal{B}(\Lambda_b^0 \rightarrow \Lambda_c(2595)^+ \pi^-) \times \mathcal{B}(\Lambda_c(2595)^+ \rightarrow \Lambda_c^+ \pi^+ \pi^-)] / \mathcal{B}(\Lambda_b^0 \rightarrow \Lambda_c^+ \pi^+ \pi^- \pi^-)$	LHCb [616]: $0.044 \pm 0.017^{+0.006}_{-0.004}$	$0.044^{+0.018}_{-0.017}$
$[\mathcal{B}(\Lambda_b^0 \rightarrow \Lambda_c(2625)^+ \pi^-) \times \mathcal{B}(\Lambda_c(2625)^+ \rightarrow \Lambda_c^+ \pi^+ \pi^-)] / \mathcal{B}(\Lambda_b^0 \rightarrow \Lambda_c^+ \pi^+ \pi^- \pi^-)$	LHCb [616]: $0.043 \pm 0.015 \pm 0.004$	$0.043 \pm 0.016$
$[\mathcal{B}(\Lambda_b^0 \rightarrow \Sigma_c^0 \pi^+ \pi^-) \times \mathcal{B}(\Sigma_c^0 \rightarrow \Lambda_c^+ \pi^-)] / \mathcal{B}(\Lambda_b^0 \rightarrow \Lambda_c^+ \pi^+ \pi^- \pi^-)$	LHCb [616]: $0.074 \pm 0.024 \pm 0.012$	$0.074 \pm 0.027$
$[\mathcal{B}(\Lambda_b^0 \rightarrow \Sigma_c^{++} \pi^- \pi^-) \times \mathcal{B}(\Sigma_c^{++} \rightarrow \Lambda_c^+ \pi^+)] / \mathcal{B}(\Lambda_b^0 \rightarrow \Lambda_c^+ \pi^+ \pi^- \pi^-)$	LHCb [616]: $0.042 \pm 0.018 \pm 0.007$	$0.042 \pm 0.019$

**Table 217**  $\Xi_b$  decay rates [ $10^{-4}$ ]

Parameter	Measurements	Average
$[f_{\Xi_b^-} / f_{A_b^0}] \times \mathcal{B}(\Xi_b^- \rightarrow A_b^0 \pi^-)$	LHCb [807]: $5.7 \pm 1.8^{+0.8}_{-0.9}$	$5.7^{+2.0}_{-2.0}$

**Fig. 172** Summary of the averages from Table 213**Fig. 173** Summary of the averages from Table 214**Fig. 174** Summary of the averages from Table 215

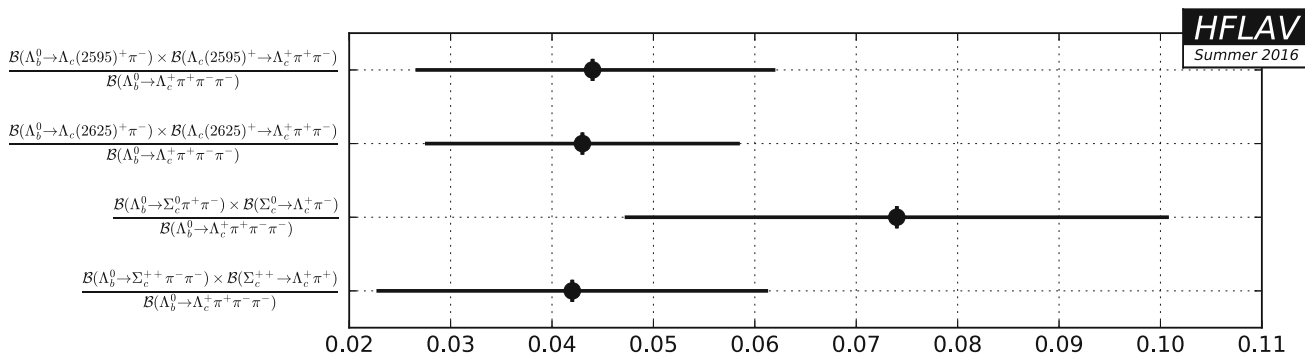


**Fig. 175** Summary of the averages from Table 216

## 7 $B$ decays to charmless final states

This section provides branching fractions (BF), polarization fractions, partial rate asymmetries ( $A_{CP}$ ) and other observables of  $B$  decays to final states that do not contain charm hadrons or charmonia mesons. The order of entries in the tables corresponds to that in PDG2014 [327], and the quoted RPP numbers are the PDG numbers of the corresponding branching fractions. The asymmetry is defined as

$$A_{CP} = \frac{N_b - N_{\bar{b}}}{N_b + N_{\bar{b}}}, \quad (220)$$

where  $N_b$  ( $N_{\bar{b}}$ ) is the number of hadrons containing a  $b$  ( $\bar{b}$ ) quark decaying into a specific final state. This definition is consistent with that of Eq. (104) in Sect. 4.2.1. Four different  $B^0$  and  $B^+$  decay categories are considered: charmless mesonic (i.e., final states containing only mesons), baryonic (only hadrons, but including a baryon-antibaryon pair), radiative (including a photon or a lepton-antilepton pair) and semileptonic/leptonic (including/only leptons). We also include measurements of  $B_s^0$ ,  $B_c^+$  and  $b$ -baryon decays. Measurements supported with written documents are accepted in the averages; written documents include journal papers, conference contributed papers, preprints or conference proceedings. In all the tables of this section, values in red (blue) are new published (preliminary) results since PDG2014. Results from  $A_{CP}$  measurements obtained from time-dependent analyses are listed and described in Sect. 4.

Most of the branching fractions from BABAR and Belle assume equal production of charged and neutral  $B$  pairs. The best measurements to date show that this is still a reasonable approximation (see Sect. 3). For branching fractions, we provide either averages or the most stringent upper limits. If one or more experiments have measurements with  $> 4\sigma$  for a decay channel, all available central values for that channel are used in the averaging. We also give central values and errors for cases where the significance of the average value is at least  $3\sigma$ , even if no single measurement is above  $4\sigma$ . For  $A_{CP}$  we provide averages in all cases. At the end of some of the tables we give a list of results that were not included. Typical cases are the measurements of distributions, such

as differential branching fractions or longitudinal polarizations, which are measured in different binning schemes by the different collaborations, and thus cannot be directly used to obtain averages.

Our averaging is performed by maximizing the likelihood,  $\mathcal{L} = \prod_i \mathcal{P}_i(x)$ , where  $\mathcal{P}_i$  is the probability density function (PDF) of the  $i$ th measurement, and  $x$  is, e.g., the branching fraction or  $A_{CP}$ . The PDF is modelled by an asymmetric Gaussian function with the measured central value as its most probable value and the quadratic sum of the statistical and systematic errors as the standard deviation. The experimental uncertainties are considered to be uncorrelated with each other when the averaging is performed. As mentioned in Sect. 2, no error scaling is applied when the fit  $\chi^2$  is greater than 1, except for cases of extreme disagreement (at present we have no such cases).

The largest improvement since the last report has come from the inclusion of a variety of new measurements from the LHC, especially LHCb. The measurements of  $B_s^0$  decays are particularly noteworthy.

Sects. 7.1 and 7.2 provide compilations of branching fractions of  $B^0$  and  $B^+$  to mesonic and baryonic charmless final states, respectively, while Sect. 7.3 gives branching fractions of  $b$ -baryon decays. In Sects. 7.4 and 7.5 various observables of interest are given in addition to branching fractions: in the former, branching fractions of  $B_s^0$ -meson charmless decays, and in the latter observables related to leptonic and radiative  $B^0$  and  $B^+$  meson decays, including processes in which the photon yields a pair of charged or neutral leptons. Section 7.5 also reports limits from searches for lepton-flavor/number-violating decays. Sects. 7.6 and 7.7 give  $CP$  asymmetries and results of polarization measurements, respectively, in various  $b$ -hadron charmless decays. Finally, Sect. 7.8 gives branching fractions of  $B_c^+$  meson decays to charmless final states.

### 7.1 Mesonic decays of $B^0$ and $B^+$ mesons

This section provides branching fractions of charmless mesonic decays: Tables 218, 219 and 220 for  $B^+$  and

**Table 218** Branching fractions of charmless mesonic  $B^+$  decays with kaons (part 1) in units of  $\times 10^{-6}$ . Upper limits are at 90% CL. Where values are shown in red (blue), this indicates that they are new published (preliminary) results since PDG2014

RPP#	Mode	PDG2014 Avg.	BaBar	Belle	CLEO	CDF	LHCb	Our Avg.
262	$K^0\pi^+$	23.7 $\pm$ 0.8	23.9 $\pm$ 1.1 $\pm$ 1.0	[398]	23.97 $\pm$ 0.53 $\pm$ 0.71	[808]	18.8 $^{+3.7+2.1}_{-3.3-1.8}$	[809]
263	$K^+\pi^0$	12.9 $\pm$ 0.5	13.6 $\pm$ 0.6 $\pm$ 0.7	[810]	12.62 $\pm$ 0.31 $\pm$ 0.56	[808]	12.9 $^{+2.4+1.2}_{-2.2-1.1}$	[809]
264	$\eta'K^+$	70.6 $\pm$ 2.5	71.5 $\pm$ 1.3 $\pm$ 3.2	[811]	69.2 $\pm$ 2.2 $\pm$ 3.7	[812]	70.6 $\pm$ 2.7	
265	$\eta K^{*+}$	4.8 $^{+1.8}_{-1.6}$	4.8 $^{+1.6}_{-1.4}\pm$ 0.8	[813]	< 2.9	[814]	4.8 $^{+1.8}_{-1.6}$	
266	$\eta'K_0^*(1430)^+$	5.2 $\pm$ 2.1	5.2 $\pm$ 1.9 $\pm$ 1.0	[813]			5.2 $\pm$ 2.1	
267	$\eta'K_2^*(1430)^+$	28 $\pm$ 5	28.0 $^{+4.6}_{-4.3}\pm$ 2.6	[813]			28.0 $^{+5.3}_{-5.0}$	
268	$\eta K^+$	2.4 $\pm$ 0.4	2.94 $^{+0.39}_{-0.34}\pm$ 0.21	[811]	2.12 $\pm$ 0.23 $\pm$ 0.11	[815]	2.2 $^{+2.8}_{-2.2}$	[816]
269	$\eta K^{*+}$	19.3 $\pm$ 1.6	18.9 $\pm$ 1.8 $\pm$ 1.3	[817]	19.3 $^{+2.0}_{-1.9}\pm$ 1.5	[818]	26.4 $^{+9.6}_{-8.2}\pm$ 3.3	[816]
270	$\eta K_0^*(1430)^+$	18 $\pm$ 4	18.2 $\pm$ 2.6 $\pm$ 2.6	[817]			19.3 $\pm$ 1.6	
271	$\eta K_2^*(1430)^+$	9.1 $\pm$ 3.0	9.1 $\pm$ 2.7 $\pm$ 1.4	[817]			18.2 $\pm$ 3.7	
272	$\eta(1295)K^+\dagger$	2.9 $^{+0.8}_{-0.7}$	2.9 $^{+0.8}_{-0.7}\pm$ 0.2 $^\ddagger$	[819]	< 1.2	[819]	9.1 $\pm$ 3.0	
274	$\eta(1405)K^+\dagger$	< 1.2	< 1.2	[819]			2.9 $^{+0.8}_{-0.7}$	
275	$\eta(1475)K^+\dagger$	13.8 $^{+2.1}_{-1.8}$	13.8 $^{+1.8+1.0}_{-1.7-0.6}$	[819]			< 1.2	
276	$f_1(1285)K^+$	< 2.0	< 2.0	[819]			13.8 $^{+2.1}_{-1.8}$	
277	$f_1(1420)K^+\dagger$	< 2.9	< 2.9	[819]			< 2.0	
279	$\phi(1680)K^+\dagger$	< 3.4	< 3.4	[819]			< 2.9	
280	$f_0(1500)K^+$	3.7 $\pm$ 2.2	3.7 $\pm$ 2.2 $^\S$	[271, 278]			< 3.4	
281	$\omega K^+$	6.7 $\pm$ 0.8	6.3 $\pm$ 0.5 $\pm$ 0.3	[820]	<b>6.8<math>\pm</math>0.4<math>\pm</math>0.4</b>	[389]	3.2 $^{+2.4}_{-1.9}\pm$ 0.8	[821]
282	$\omega K^{*+}$	< 7.4	< 7.4	[822]			6.5 $\pm$ 0.4	
283	$\omega(K\pi)_0^{*+}$	28 $\pm$ 4	27.5 $^{+3.0}_{-2.6}$	[822]			< 7.4	
284	$\omega K_0^*(1430)^+$	24 $\pm$ 5	24.0 $\pm$ 2.6 $\pm$ 4.4	[822]			27.5 $^{+3.0}_{-2.6}$	
285	$\omega K_2^*(1430)^+$	21 $\pm$ 4	21.5 $\pm$ 3.6 $\pm$ 2.4	[822]			24.0 $\pm$ 5.1	
286	$a_0(980)^+K^0\dagger$	< 3.9	< 3.9	[823]			21.5 $\pm$ 4.3	
287	$a_0(980)^0K^+\dagger$	< 2.5	< 2.5	[823]			< 3.9	
288	$K^{*0}\pi^+$	10.1 $\pm$ 0.9	10.8 $\pm$ 0.6 $^{+1.2}_{-1.4}$	[278]	9.7 $\pm$ 0.6 $^{+0.8}_{-0.9}$	[276]	< 2.5	
289	$K^{*+}\pi^0$	8.2 $\pm$ 1.9	8.2 $\pm$ 1.5 $\pm$ 1.1	[824]			10.1 $^{+0.8}_{-0.9}$	
290	$K^+\pi^+\pi^-$	51 $\pm$ 2.9	54.4 $\pm$ 1.1 $\pm$ 4.6	[278]	48.8 $\pm$ 1.1 $\pm$ 3.6	[276]	8.2 $\pm$ 1.8	
291	$K^+\pi^+\pi^-(NR)$	16.3 $^{+2.1}_{-1.5}$	9.3 $\pm$ 1.0 $^{+6.9}_{-1.7}$	[278]	16.9 $\pm$ 1.3 $^{+1.7}_{-1.6}$	[276]	51.0 $\pm$ 3.0	
292	$\omega(782)K^+(K^+\pi^+\pi^-)$	6 $\pm$ 9	5.9 $^{+8.8+0.5}_{-9.0-0.4}$	[278]			16.3 $\pm$ 2.0	
293	$f_0(980)K^+(K^+\pi^+\pi^-)^\dagger$	9.4 $^{+1.0}_{-1.2}$	10.3 $\pm$ 0.5 $^{+2.0}_{-1.4}$	[278]	8.8 $\pm$ 0.8 $^{+0.9}_{-1.8}$	[276]	5.9 $^{+8.8}_{-9.0}$	

Table 218 continued

RPP#	Mode	PDG2014 Avg.	BABAR	Belle	CLEO	CDF	LHCb	Our Avg.
294	$f_2(1270)^0 K^+ (K^+ \pi^+ \pi^-)$	$1.07 \pm 0.27$	$0.88^{+0.38+0.01}_{-0.33-0.03}$	[278]	$1.33 \pm 0.30^{+0.23}_{-0.34}$	[276]		$1.07 \pm 0.29$
295	$f_0(1370)^0 K^+ (K^+ \pi^+ \pi^-)^\dagger$	$< 10.7$	$< 10.7$	[277]				$< 10.7$
296	$\rho(1450)^0 K^+ (K^+ \pi^+ \pi^-)$	$< 11.7$	$< 11.7$	[277]				$< 11.7$
297	$f_2'(1525) K^+ (K^+ \pi^+ \pi^-)$	$< 3.4$	$< 3.4$	[277]				$< 3.4$
298	$\rho^0 K^+ (K^+ \pi^+ \pi^-)$	$3.7 \pm 0.5$	$3.56 \pm 0.45^{+0.57}_{-0.46}$	[278]	$3.89 \pm 0.47^{+0.43}_{-0.41}$	[276]		$3.74^{+0.49}_{-0.45}$
299	$K_0^*(1430)^0 \pi^+ (K^+ \pi^+ \pi^-)$	$45^{+9}_{-7}$	$32.0 \pm 1.2^{+10.8}_{-6.0}$	[278]	$51.6 \pm 1.7^{+7.0}_{-7.5}$	[276]		$45.1 \pm 6.3$
300	$K_2^*(1430)^0 \pi^+ (K^+ \pi^+ \pi^-)$	$5.6^{+2.2}_{-1.5}$	$5.6 \pm 1.2^{+1.8}_{-0.8}$	[278]	$< 6.9$	[272]		$5.6^{+2.2}_{-1.4}$
301	$K^*(1410)^0 \pi^+ (K^+ \pi^+ \pi^-)$	$< 45$			$< 45$	[272]		$< 45$
302	$K^*(1680)^0 \pi^+ (K^+ \pi^+ \pi^-)$	$< 12$	$< 15$	[277]	$< 12$	[272]		$< 12$
303	$K^+ \pi^- \pi^0$	$16.2 \pm 1.9$	$16.2 \pm 1.2 \pm 1.5$	[824]				$16.2 \pm 1.9$
304	$f_0(980) K^+ (K^+ \pi^0 \pi^0)$	$2.8 \pm 0.8$	$2.8 \pm 0.6 \pm 0.5$	[824]				$2.8 \pm 0.8$
305	$K^- \pi^+ \pi^+$	$< 0.95$	$< 0.95$	[825]	$< 4.5$	[826]		$< 0.046$
306	$K^- \pi^+ \pi^+ (N^R)$	$< 56$						$< 0.046$
307	$K_1(1270)^0 \pi^+$	$< 40$	$< 40$	[415]				$< 40$
308	$K_1(1400)^0 \pi^+$	$< 39$	$< 39$	[415]				$< 39$
309	$K^0 \pi^+ \pi^0$	$< 66$						$< 66$
310	$\rho^+ K^0 (K^0 \pi^+ \pi^0)$	$8.0 \pm 1.5$	$8.0^{+1.4}_{-1.3} \pm 0.6$	[820]				$8.0^{+1.5}_{-1.4}$
311	$K^{*+} \pi^+ \pi^-$	$75 \pm 10$	$75.3 \pm 6.0 \pm 8.1$	[831]				$75.3 \pm 10.1$
312	$K^{*+} \rho^0$	$4.6 \pm 1.1$	$4.6 \pm 1.0 \pm 0.4$	[822]				$4.6 \pm 1.1$
313	$f_0(980) K^{*+} \dagger$	$4.2 \pm 0.7$	$4.2 \pm 0.6 \pm 0.3$	[822]				$4.2 \pm 0.7$

Results for LHCb are relative BFs converted to absolute BFs.

CLEO upper limits that have been greatly superseded are not shown.

<sup>†</sup> In this product of BFs, all daughter BFs not shown are set to 100%.

<sup>‡</sup> The value quoted is  $B(B^+ \rightarrow \eta(1295) K^+) \times B(\eta(1295) \rightarrow \eta \pi \pi)$ .

<sup>§</sup> Average of results in  $K_S^0 K^+ K^-$ ,  $K_S^0 K^0 K^-$ ,  $K^+ \pi^+ \pi^-$  [278]. Includes an  $f_X$  resonance with parameters that are compatible with  $f_0(1500)$ .

**Table 219** Branching fractions of charmless mesonic  $B^+$  decays with kaons (part 2) in units of  $\times 10^{-6}$ . Upper limits are at 90% CL. Where values are shown in red (blue), this indicates that they are new published (preliminary) results since PDG2014

RPP#	Mode	PDG2014 Avg.	BABAR	Belle	CLEO	CDF	LHCb	Our Avg.
314	$a_1^+ K^0$	35±7	34.9±5.0±4.4	[833]				34.9±6.7
315	$b_1^+ K^0 \dagger$	9.6±1.9	9.6±1.7±0.9	[834]				9.6±1.9
317	$K_1(1400)^+ \rho^0$	< 780	< 780	[835]				< 780
318	$K_2(1430)^+ \rho^0$	< 1500	< 1500	[835]				< 1500
319	$b_1^0 K^{+ \dagger}$	9.1±2.0	9.1±1.7±1.0	[836]				9.1±2.0
320	$b_1^+ K^{*0} \dagger$	< 5.9	< 5.9	[837]				< 5.9
321	$b_1^0 K^{*+ \dagger}$	< 6.7	< 6.7	[837]				< 6.7
322	$K^+ \bar{K}^0$	1.31±0.17	1.61±0.44±0.09	[398]	1.11±0.19±0.05	[808]		<b>1.52±0.21±0.05</b>
323	$\bar{K}^0 K^+ \pi^0$	< 24		[829]				< 24
324	$K^+ K_S K_S$	10.8±0.6	10.6±0.5±0.3	[271]	13.4±1.9±1.5	[826]		10.8±0.6
325	$f_0(980) K^+ (K^+ K_S K_S)$	14.7±3.3	14.7±2.8±1.8	[271]				14.7±3.3
326	$f_0(1710) K^+ (K^+ K_S K_S)$	0.48 <sup>+0.40</sup> <sub>-0.24</sub> ±0.11	0.48 <sup>+0.40</sup> <sub>-0.24</sub> ±0.11	[271]				0.48 <sup>+0.41</sup> <sub>-0.26</sub>
327	$K^+ K_S K_S (NR)$	20±4	19.8±3.7±2.5	[271]				19.8±4.5
328	$K_S K_S \pi^+$	< 0.51	< 0.51	[839]	< 3.2			< 0.51
329	$K^+ K^- \pi^+$	5.0±0.7	5.0±0.5±0.5	[840]	< 13			5.0±0.7
330	$K^+ K^- \pi^+ (NR)$	< 75		[826]				< 75
331	$\bar{K}^{*0} K^+ (K^+ K^- \pi^+)$	< 1.1	< 1.1	[841]				< 1.1
332	$\bar{K}_0^*(1430)^0 K^+ (K^+ K^- \pi^+)$	< 2.2	< 2.2	[841]				< 2.2
333	$K^+ K^+ \pi^-$	< 0.16	< 0.16	[825]	< 2.4			<b>&lt; 0.011</b>
334	$K^+ K^+ \pi^- (NR)$	< 87.9		[826]				[827]
335	$f_2'(1525) K^+$	1.8±0.5	1.8±0.5 <sup>‡</sup>	[271]	< 8			< 87.9
336	$f_J(2220) K^+$	< 1.2		[842]	< 1.2			1.8±0.5
337	$K^{*-} \pi^+ K^-$	< 11.8	< 11.8	[831]				< 1.2
338	$K^{*-} \bar{K}^{*0}$	1.2±0.5	1.2±0.5±0.1	[843]	<b>&lt; 1.31</b>			< 11.8
339	$K^{*-} K^+ \pi^-$	< 6.1	< 6.1	[831]				1.2±0.5
340	$K^+ K^- K^+$	34.0±1.4	34.6±0.6±0.9	[271]	30.6±1.2±2.3	[272]		< 6.1
341	$\phi K^+ (K^+ K^- K^+)$	8.8 <sup>+0.7</sup> <sub>-0.6</sub>	9.2±0.4 <sup>+0.7</sup> <sub>-0.5</sub>	[271]	9.6±0.9 <sup>+1.1</sup> <sub>-0.8</sub>	[272]		34.0±1.0
342	$f_0(980) K^+ (K^+ K^- K^+)$	9.4±3.2	9.4 <sup>+1.6</sup> <sub>-2.8</sub>	[271]				8.8±0.5
343	$a_2(1320) K^+ (K^+ K^- K^+)^\dagger$	< 1.1		[844]	< 1.1			9.4 <sup>+1.6</sup> <sub>-2.8</sub>
344	$X_0(1550) K^+ (K^+ K^- K^+)$	4.3±0.7	4.3±0.60±0.30	[847]				< 1.1
345	$\phi(1680) K^+ (K^+ K^- K^+)^\dagger$	< 0.8		[272]				4.30±0.67
346	$f_0(1710) K^+ (K^+ K^- K^+)^\dagger$	1.1±0.6	1.12±0.25±0.50	[271]	< 0.8			< 0.8
								1.12±0.56

**Table 219** continued

RPP#	MODE	PDG2014 AVG.	BABAR	BELLE	CLEO	CDF	LHCb	OURAVG.
347	$K^+ K^- K^+ (NR)$	$23.8^{+2.8}_{-5.0}$	$22.8 \pm 2.7 \pm 7.6$	[271]	$24.0 \pm 1.5^{+2.6}_{-6.0}$	[272]		$23.8^{+2.9}_{-5.1}$
348	$K^{*+} K^+ K^-$	$36 \pm 5$	$36.2 \pm 3.3 \pm 3.6$	[831]				$36.2 \pm 4.9$
349	$\phi K^{*+}$	$10.0 \pm 2.0$	$11.2 \pm 1.0 \pm 0.9$	[848]	$6.7^{+2.1 \pm 0.7}_{-1.9 - 1.0}$	[849]	$10.6^{+6.4 \pm 1.8}_{-4.9 - 1.6}$	[845]
350	$\phi (K\pi)^{*+}_0$	$8.3 \pm 1.6$	$8.3^{+1.4}_{-0.8}$	[850]				$8.3^{+1.4}_{-0.8}$
351	$\phi K_1(1270)^+$	$6.1 \pm 1.9$	$6.1 \pm 1.6 \pm 1.1$	[850]				$6.1 \pm 1.9$
352	$\phi K_1(1400)^+$	$< 3.2$	$< 3.2$	[850]				$< 3.2$
353	$\phi K^*(1410)^+$	$< 4.3$	$< 4.3$	[850]				$< 4.3$
354	$\phi K_0^*(1430)^+$	$7.0 \pm 1.6$	$7.0 \pm 1.3 \pm 0.9$	[850]				$7.0 \pm 1.6$
355	$\phi K_2^*(1430)^+$	$8.4 \pm 2.1$	$8.4 \pm 1.8 \pm 1.0$	[850]				$8.4 \pm 2.1$
356	$\phi K_2(1770)^+$	$< 15$	$< 15$	[850]				$< 15$
357	$\phi K_2(1820)^+$	$< 16.3$	$< 16.3$	[850]				$< 16.3$
358	$a_1^+ K^{*0}$	$< 3.6$	$< 3.6$	[851]				$< 3.6$
359	$\phi \phi K^+ \S$	$5.0 \pm 1.2$	$5.6 \pm 0.5 \pm 0.3$	[852]	$2.6^{+1.1 \pm 0.3}_{-0.9}$	[842]		$5.0 \pm 0.5$
360	$\eta \eta' K^+$	$< 25$	$< 25$	[853]				$< 25$
361	$K^+ \omega \phi$	$< 1.9$						$< 1.9$
362	$K^+ X(1812)^\dagger$	$< 0.32$			$< 0.32$	[854]		$< 0.32$

Results for CDF and LHCb are relative BFs converted to absolute BFs.

CLEO upper limits that have been greatly superseded are not shown.

<sup>†</sup> In this product of BFs, all daughter BFs not shown are set to 100%.

<sup>‡</sup> Average of results in  $K_S^0 K^+ K^-$ ,  $K_S^0 K_S^0 K^+$  [271].

<sup>§</sup>  $M_{\phi\phi} < 2.85 \text{ GeV}/c^2$ .

<sup>¶</sup> Result from ARGUS. Cited in the BABAR column to avoid adding a column to the table.

**Table 220** Branching fractions of charmless mesonic  $B^+$  decays without kaons in units of  $\times 10^{-6}$ . Upper limits are at 90% CL. Where values are shown in red (blue), this indicates that they are new published (preliminary) results since PDG2014

RPP#	Mode	PDG2014 Avg.	BABAR	Belle	CLEO	CDF	LHCb	Our Avg.
379	$\pi^+\pi^0$	5.5±0.4	5.02±0.46±0.29	[810]	5.86±0.26±0.38	[808]	4.6 <sup>+1.8</sup> <sub>-1.6</sub> <sup>+0.6</sup> <sub>-0.7</sub>	[809]
380	$\pi^+\pi^+\pi^-$	15.2±1.4	15.2±0.6±1.3	[855]	8.0 <sup>+2.3</sup> <sub>-2.0</sub> <sup>±0.7</sup>	[856]	10.4 <sup>+3.3</sup> <sub>-3.4</sub> <sup>±2.1</sup>	[821]
381	$\rho^0\pi^+$	8.3±1.2	8.1±0.7 <sup>+1.3</sup> <sub>-1.6</sub>	[855]				8.3 <sup>+1.2</sup> <sub>-1.3</sub>
382	$f_0(980)\pi^+\pi^{\dagger}$	< 1.5	< 1.5	[855]				< 1.5
383	$f_2(1270)\pi^+$	1.6 <sup>+0.7</sup> <sub>-0.4</sub>	1.57±0.42 <sup>+0.55</sup> <sub>-0.25</sub>	[855]				1.57 <sup>+0.69</sup> <sub>-0.49</sub>
384	$\rho(1450)^0\pi^+\pi^{\dagger}$	1.4 <sup>+0.6</sup> <sub>-0.9</sub>	1.4±0.4 <sup>+0.5</sup> <sub>-0.8</sub>	[855]				1.4 <sup>+0.6</sup> <sub>-0.9</sub>
385	$f_0(1370)\pi^+\pi^{\dagger}$	< 4.0	< 4.0	[855]				< 4.0
387	$\pi^+\pi^-\pi^+(NR)$	5.3 <sup>+1.5</sup> <sub>-1.1</sub>	5.3±0.7 <sup>+1.3</sup> <sub>-0.8</sub>	[855]				5.3 <sup>+1.5</sup> <sub>-1.1</sub>
388	$\pi^+\pi^0\pi^0$	< 890	< 890 <sup>‡</sup>	[857]				< 890 <sup>‡</sup>
389	$\rho^+\pi^0$	10.9±1.4	10.2±1.4±0.9	[858]	13.2±2.3 <sup>+1.4</sup> <sub>-1.9</sub>	[859]	10.9 <sup>+1.4</sup> <sub>-1.5</sub>	
391	$\rho^+\rho^0$	24.0±1.9	23.7±1.4±1.4	[421]	31.7±7.1 <sup>+3.8</sup> <sub>-6.7</sub>	[800]	24.0 <sup>+1.9</sup> <sub>-2.0</sub>	
392	$f_0(980)\rho^+\rho^{\dagger}$	< 2.0	< 2.0	[421]				< 2.0
393	$a_1^+\pi^0$	26±7	26.4±5.4±4.1	[861]				26.4±6.8
394	$a_1^0\pi^+$	20±6	20.4±4.7±3.4	[861]				20.4±5.8
395	$\omega\pi^+$	6.9±0.5	6.7±0.5±0.4	[820]	6.9±0.6±0.5	[862]	6.9±0.5	
396	$\omega\rho^+$	15.9±2.1	15.9±1.6±1.4	[822]				15.9±2.1
397	$\eta\pi^+$	4.02±0.27	4.00±0.40±0.24	[811]	4.07±0.26±0.21	[815]	4.02±0.27	
398	$\eta\rho^+$	7.0±2.9	9.9±1.2±0.8	[863]	4.1 <sup>+1.4</sup> <sub>-1.3</sub> <sup>±0.4</sup>	[818]	6.9±1.0	
399	$\eta'\pi^+$	2.7±0.9	3.5±0.6±0.2	[811]	1.8 <sup>+0.7</sup> <sub>-0.6</sub> <sup>±0.1</sup>	[812]	2.7 <sup>+0.5</sup> <sub>-0.4</sub>	
400	$\eta'\rho^+$	9.7±2.2	9.7 <sup>+1.9</sup> <sub>-1.8</sub> <sup>±1.1</sup>	[813]	< 5.8	[814]	9.7 <sup>+2.2</sup> <sub>-2.1</sub>	
401	$\phi\pi^+$	< 0.15	< 0.24	[864]	< 0.33	[865]	< 0.15	
402	$\phi\rho^+$	< 3.0	< 3.0	[867]			< 3.0	
403	$a_0(980)^0\pi^+\pi^{\dagger}$	< 5.8	< 5.8	[823]				< 5.8
404	$a_0(980)^+\pi^0\pi^{\dagger}$	< 1.4	< 1.4	[868]				< 1.4
405	$\pi^+\pi^+\pi^-\pi^-\pi^-$	< 860	< 860 <sup>‡</sup>	[857]				< 860 <sup>‡</sup>
406	$\rho^0a_1(1260)^+$	< 620						< 620
407	$\rho^0a_2(1320)^+$	< 720						< 720
408	$b_1^0\pi^+\pi^{\dagger}$	6.7±2.0	6.7±1.7±1.0	[836]				6.7±2.0
409	$b_1^+\pi^0\pi^{\dagger}$	< 3.3	< 3.3	[834]				< 3.3

RPP#	Mode	PDG2014 Avg.	BABAR	Belle	CLEO	CDF	LHCb	Our Avg.
410	$\pi^+\pi^+\pi^-\pi^-\pi^0$	< 6300	< 6300 <sup>‡</sup>	[857]				< 6300 <sup>‡</sup>
411	$b_1^+\rho^0$ <sup>†</sup>	< 5.2	< 5.2	[837]				< 5.2
413	$b_1^0\rho^+$ <sup>†</sup>	< 3.3	< 3.3	[837]				< 3.3

Results for LHCb are relative BFs converted to absolute BFs.

CLEO upper limits that have been greatly superseded are not shown.

<sup>†</sup> In this product of BFs, all daughter BFs not shown are set to 100%.

<sup>‡</sup> Result from ARGUS. Cited in the BABAR column to avoid adding a column to the table.

Tables 221, 222, 223 and 224 for  $B^0$  mesons. The tables are separated according to the presence or absence of kaons in the final state. Finally, Table 225 details several relative branching fractions of  $B^0$  decays.

Figure 176 gives a graphic representation of a selection of high-precision branching fractions given in this section. Footnote symbols indicate that the footnote in the corresponding table should be consulted.

## 7.2 Baryonic decays of $B^+$ and $B^0$ mesons

This section provides branching fractions of charmless baryonic decays of  $B^+$  and  $B^0$  mesons in Tables 226 and 227, respectively. Relative branching fractions are given in Table 228.

Figures 177 and 178 show graphic representations of a selection of results given in this section. Footnote symbols indicate that the footnote in the corresponding table should be consulted.

## 7.3 Decays of $b$ baryons

A compilation of branching fractions of  $\Lambda_b^0$  baryon decays is given in Table 229. Table 230 provides the partial branching fractions of  $\Lambda_b^0 \rightarrow \Lambda\mu^+\mu^-$  decays. A compilation of branching fractions of  $\Xi_b^0$  baryon decays is given in Table 231.

Figure 179 shows a graphic representation of branching fractions of  $\Lambda_b^0$  decays. Footnote symbols indicate that the footnote in the corresponding table should be consulted.

List of other measurements that are not included in the tables:

- In Ref. [928], LHCb provides a measurement of the differential  $\Lambda_b^0 \rightarrow \Lambda\mu^+\mu^-$  branching fraction. It is given in bins of  $m^2(\mu^+\mu^-)$  that are different from those used in the past by the LHCb and CDF collaborations (see table of differential branching fractions).
- In the paper [929], LHCb measures the ratios

$$\frac{\sigma(pp \rightarrow \Xi_b^{*-} X) \mathcal{B}(\Xi_b^{*-} \rightarrow \Xi_b^0 \pi^-)}{\sigma(pp \rightarrow \Xi_b^0 X)},$$

$$\frac{\sigma(pp \rightarrow \Xi_b^{*-} X) \mathcal{B}(\Xi_b^{*-} \rightarrow \Xi_b^0 \pi^-)}{\sigma(pp \rightarrow \Xi_b^{*-} X) \mathcal{B}(\Xi_b^{*-} \rightarrow \Xi_b^0 \pi^-)}.$$

- In the paper [930], LHCb measures the ratio

$$\frac{\sigma(pp \rightarrow \Xi_b^{*-} X) \mathcal{B}(\Xi_b^{*-} \rightarrow \Xi_b^0 \pi^-)}{\sigma(pp \rightarrow \Xi_b^0 X)}.$$

**Table 221** Branching fractions of charmless mesonic  $B^0$  decays with kaons (part 1) in units of  $\times 10^{-6}$ . Upper limits are at 90% CL. Where values are shown in red (blue), this indicates that they are new published (preliminary) results since PDG2014

RPD#	Mode	PDG2014 Avg.	BABAR	Belle	CLEO	CDF	LHCb	Our Avg.
227	$K^+\pi^-$	$19.6 \pm 0.5$	$19.1 \pm 0.6 \pm 0.6$	[870]	$20.0 \pm 0.34 \pm 0.60$	[808]	$18.0^{+2.3 \pm 1.2}_{-21.0 \pm 0.9}$	[809]
228	$K^0\pi^0$	$9.9 \pm 0.5$	$10.1 \pm 0.6 \pm 0.4$	[416]	$9.68 \pm 0.46 \pm 0.50$	[808]	$12.8^{+4.0 \pm 1.7}_{-3.3 \pm 1.4}$	[809]
229	$\eta'K^0$	$66 \pm 4$	$68.5 \pm 2.2 \pm 3.1$	[811]	$58.9^{+3.6 \pm 4.3}_{-3.5}$	[812]	$89^{+18}_{-16} \pm 9$	[816]
230	$\eta'K^{*0}$	$3.1 \pm 0.9$	$3.1^{+0.9}_{-0.8} \pm 0.3$	[813]	<b>2.6 <math>\pm</math> 0.7 <math>\pm</math> 0.2</b>	[871]	$7.8^{+7.7}_{-5.7}$	[816]
231	$\eta'K_0^*(1430)^0$	$6.3 \pm 1.6$	$6.3 \pm 1.3 \pm 0.9$	[813]				$6.3 \pm 1.6$
232	$\eta'K_2^*(1430)^0$	$13.7 \pm 3.2$	$13.7^{+3.0}_{-1.9} \pm 1.2$	[813]				$13.7^{+3.2}_{-2.2}$
233	$\eta K^0$	$1.23^{+0.27}_{-0.24}$	$1.15^{+0.43}_{-0.38} \pm 0.09$	[811]	$1.27^{+0.33}_{-0.29} \pm 0.08$	[815]	$0.0^{+3.0}_{-0.0}$	[816]
234	$\eta K^{*0}$	$15.9 \pm 1.0$	$16.5 \pm 1.1 \pm 0.8$	[817]	$15.2 \pm 1.2 \pm 1.0$	[818]	$13.8^{+5.5}_{-4.6} \pm 1.6$	[816]
235	$\eta K_0^*(1430)^0$	$11.0 \pm 2.2$	$11.0 \pm 1.6 \pm 1.5$	[817]				$11.0 \pm 2.2$
236	$\eta K_2^*(1430)^0$	$9.6 \pm 2.1$	$9.6 \pm 1.8 \pm 1.1$	[817]				$9.6 \pm 2.1$
237	$\omega K^0$	$5.0 \pm 0.6$	$5.4 \pm 0.8 \pm 0.3$	[820]	<b>4.5 <math>\pm</math> 0.4 <math>\pm</math> 0.3</b>	[389]	$10.0^{+5.4}_{-4.2} \pm 1.4$	[821]
238	$a_0(980)^0 K^0$ †	$< 7.8$	$< 7.8$	[823]				$< 7.8$
239	$b_1^0 K^0$ †	$< 7.8$	$< 7.8$	[834]				$< 7.8$
240	$a_0(980)^- K^+$ †	$< 1.9$	$< 1.9$	[872]				$< 1.9$
241	$b_1^- K^+$ †	$7.4 \pm 1.4$	$7.4 \pm 1.0 \pm 1.0$	[836]				$7.4 \pm 1.4$
242	$b_1^0 K^{*0}$ †	$< 8.0$	$< 8.0$	[837]				$< 8.0$
243	$b_1^- K^{*+}$ †	$< 5.0$	$< 5.0$	[837]				$< 5.0$
244	$a_0(1450)^- K^+$ †	$< 3.1$	$< 3.1$	[872]				$< 3.1$
245	$K_S X^0$ (Familon) †	$< 53$						$< 53$
246	$\omega K^{*0}$	$2.0 \pm 0.5$	$2.2 \pm 0.6 \pm 0.2$	[822]	$1.8 \pm 0.7^{+0.3}_{-0.2}$	[874]		$2.0 \pm 0.5$
247	$\omega K_0^*(1430)^0$	$18.4 \pm 2.5$	$18.4^{+1.8}_{-1.7}$	[822]				$18.4^{+1.8}_{-1.7}$
248	$\omega K_2^*(1430)^0$	$16.0 \pm 3.4$	$16.0 \pm 1.6 \pm 3.0$	[822]				$16.0 \pm 3.4$
249	$\rho(1450)^- K^+$	$10.1 \pm 2.3$	$10.1 \pm 2.0 \pm 1.1$	[822]				$10.1 \pm 2.3$
250	$\omega K^+ \pi^-$ ( $NR$ ) †	$5.1 \pm 1.0$			$5.1 \pm 0.7 \pm 0.7$	[874]		$5.1 \pm 1.0$
251	$K^+ \pi^- \pi^0$	$37.8 \pm 3.2$	$38.5 \pm 1.0 \pm 3.9$	[875]	$36.6^{+4.2}_{-4.3} \pm 3.0$	[876]		$37.8 \pm 3.2$
252	$\rho^- K^+$	$7.0 \pm 0.9$	$6.6 \pm 0.5 \pm 0.8$	[875]	$15.1^{+3.4}_{-3.3} \pm 2.4$	[876]		$7.0 \pm 0.9$
253	$\rho(1450)^- K^+$	$2.4 \pm 1.2$	$2.4 \pm 1.0 \pm 0.6$	[875]				$2.4 \pm 1.2$
254	$\rho(1700)^- K^+$	$0.6 \pm 0.7$	$0.6 \pm 0.6 \pm 0.4$	[875]				$0.6 \pm 0.7$
255	$K^+ \pi^- \pi^0$ ( $NR$ )	$2.8 \pm 0.6$	$2.8 \pm 0.5 \pm 0.4$	[875]	$< 9.4$	[876]		$2.8 \pm 0.6$
256	$(K\pi)_0^{*+} \pi^-$	$34 \pm 5$	$34.2 \pm 2.4 \pm 4.1$	[875]				$34.2 \pm 4.8$
257	$(K\pi)_0^{*+} \pi^0$	$8.5 \pm 1.7$	$8.6^{+1.1}_{-1.3}$	[875]				$8.6^{+1.1}_{-1.3}$
258	$K_2^*(1430)^0 \pi^0$	$< 4.0$	$< 4.0$	[877]				$< 4.0$

**Table 221** continued

RPP#	Mode	PDG2014 Avg.	BABAR	Belle	CLEO	CDF	LHCb	Our Avg.
259	$K^*(1680)^0\pi^0$	< 7.5	[877]	$6.1^{+1.6+0.5}_{-1.5-0.6}$	[876]			< 7.5
260	$K_x^* \pi^0 \pi^2$	$6.1 \pm 1.6$		$47.5 \pm 2.4 \pm 3.7$	[878]	$50^{+10}_{-9} \pm 7$	[829]	$6.1^{+1.7}_{-1.6}$
261	$K^0 \pi^+ \pi^-$	$65 \pm 8$	[274]	$11.1^{+2.5}_{-1.0} \pm 0.9$	[274]	$19.9 \pm 2.5^{+1.7}_{-2.0}$	[878]	$65.2^{+6.0}_{-5.1} \ddagger$
262	$K^0 \pi^+ \pi^- (NR)$	$14.7^{+4.0}_{-2.6}$		$4.4 \pm 0.7 \pm 0.3$	[274]	$6.1 \pm 1.0^{+1.1}_{-1.2}$	[878]	$14.7 \pm 2.0$
263	$\rho^0 K^0$	$4.7 \pm 0.6$		$8.2 \pm 0.9^3$	[274, 875]	$8.4 \pm 1.1^{+1.0}_{-0.9}$	[878]	$4.7 \pm 0.7$
264	$K^{*+} \pi^-$	$8.4 \pm 0.8$		$29.9^{+2.3}_{-1.7} \pm 3.6$	[274]	$49.7 \pm 3.8^{+6.8}_{-8.2}$	[878]	$8.4 \pm 0.8$
265	$K_0^* (1430)^+ \pi^-$	$33 \pm 7$				$5.1^{+1.5+0.6}_{-1.5-0.7}$	[876]	$33.5^{+3.9}_{-3.8}$
266	$K_x^{*+} \pi^- 2$	$5.1 \pm 1.6$						$5.1^{+1.6}_{-1.7}$
267	$K^* (1410)^+ \pi^- \dagger$	< 3.8				< 3.8	[878]	< 3.8
268	$f_0(980) K^0 \dagger$	$7.0 \pm 0.9$		$6.9 \pm 0.8 \pm 0.6$	[274]	$7.6 \pm 1.7^{+0.9}_{-1.3}$	[878]	$7.0 \pm 0.9$
269	$f_2(1270)^0 K^0$	$2.7^{+1.3}_{-1.2}$		$2.7^{+1.0}_{-0.8} \pm 0.9$	[274]	< 2.5 $\dagger$	[878]	$2.7^{+1.3}_{-1.2}$
270	$f_x(1300)^0 K^0$	$1.8 \pm 0.7$		$1.81^{+0.55}_{-0.45} \pm 0.48$	[274]			$1.81^{+0.73}_{-0.66}$

Results for LHCb are relative BF<sub>s</sub> converted to absolute BF<sub>s</sub>.

CLEO upper limits that have been greatly superseded are not shown.

 $\dagger$  In this product of BF<sub>s</sub>, all daughter BF<sub>s</sub> not shown are set to 100%. $\ddagger$  Obtained from a fit to the ratios of BF<sub>s</sub> measured by LHCb (Ref. [879]) and to the averages of the BF<sub>s</sub> in their numerators, as measured by other experiments (RPP 292 and 298).<sup>1</sup>  $0.755 < M(K\pi) < 1.250$  GeV/ $c^2$ .<sup>2</sup>  $K_x^*$  stands for the possible candidates for  $K^*(1410)$ ,  $K_0^*(1430)$ ,  $K_2^*(1430)$ .<sup>3</sup> Average of BABAR results from  $B^0 \rightarrow K^+ \pi^-$  [875] and  $B^0 \rightarrow K^0 \pi^+ \pi^-$  [274].

**Table 222** Branching fractions of charmless mesonic  $B^0$  decays with kaons (part 2) in units of  $\times 10^{-6}$ . Upper limits are at 90% CL. Where values are shown in red (blue), this indicates that they are new published (preliminary) results since PDG2014

RPP#	Mode	PDG2014 Avg.	BaBar	Belle	CLEO	CDF	LHCb	Our Avg.
271	$K^{*0}\pi^0$	$3.3 \pm 0.6$	$3.3 \pm 0.5 \pm 0.4$	[875] < 3.5	[876]			$3.3 \pm 0.6$
272	$K_2^*(1430)^+\pi^-$	< 6	< 16.2	[877] < 6.3	[878]			< 6.3
273	$K^*(1680)^+\pi^-$	< 10	< 25	[877] < 10.1	[878]			< 10.1
275	$\rho^0 K^+\pi^-$	$2.8 \pm 0.7$		$2.8 \pm 0.5 \pm 0.5^2$	[880]			$2.8 \pm 0.7$
276	$f_0(980)K^+\pi^-$	$1.4_{-0.6}^{+0.5}$		$1.4 \pm 0.4_{-0.4}^{+0.3,2}$	[880]			$1.4_{-0.6}^{+0.5}$
277	$K^+\pi^-\pi^+\pi^-$	< 2.1		< 2.1	[880]			< 2.1
278	$K^{*0}\pi^+\pi^-$	$55 \pm 5$	$54.5 \pm 2.9 \pm 4.3$	[881]				$54.5 \pm 5.2$
279	$K^{*0}\rho^0$	$3.9 \pm 1.3$	$5.1 \pm 0.6_{-0.8}^{+0.6}$	[882] $2.1_{-0.7}^{+0.8 \pm 0.9}$	[880]			$3.9 \pm 0.8$
280	$f_0(980)K^{*0\dagger}$	$3.9_{-1.8}^{+2.1}$	$5.7 \pm 0.6 \pm 0.4$	[882] $1.4_{-0.5}^{+0.6 \pm 0.6}$	[880]			$3.9 \pm 0.5$
281	$K_1(1270)^+\pi^-$	< 30	$17_{-25}^{+6}$	[415]				$17_{-25}^{+6}$
282	$K_1(1400)^+\pi^-$	< 27	$16_{-24}^{+8}$	[415]				$16_{-24}^{+8}$
283	$a_1^-\pi^+$	$16 \pm 4$	$16.3 \pm 2.9 \pm 2.3$	[833]				$16.3 \pm 3.7$
284	$K^{*+}\rho^-$	$10.3 \pm 0.26$	$10.3 \pm 2.3 \pm 1.3$	[882]				$10.3 \pm 2.6$
285	$K_0(1430)^+\rho^-$	$28 \pm 12$	$28 \pm 10 \pm 6$	[882]				$28 \pm 11$
287	$K_0^*(1430)^0\rho^0$	$27 \pm 6$	$27 \pm 4 \pm 4$	[882]				$27 \pm 5$
288	$K_0^*(1430)^0f_0(980)$	$2.7 \pm 0.9$	$2.7 \pm 0.7 \pm 0.6$	[882]				$2.7 \pm 0.9$
289	$K_2^*(1430)^0f_0(980)$	$8.6 \pm 2.0$	$8.6 \pm 1.7 \pm 1.0$	[882]				$8.6 \pm 2.0$
290	$K^+K^-$	$0.13 \pm 0.05$	< 0.5	[870] $0.10 \pm 0.08 \pm 0.04$	[808]			
291	$K^0\bar{K}^0$	$1.21 \pm 0.16$	$1.08 \pm 0.28 \pm 0.11$	[398] $1.26 \pm 0.19 \pm 0.05$	[808]			
292	$K^0K^-\pi^+$	$7.3 \pm 1.1$	$6.4 \pm 1.0 \pm 0.6$	[885] < 18	[826]			$1.21 \pm 0.16$
293	$K^{*0}\bar{K}^0\dagger$	< 1.9	< 1.9	[886]				$6.64 \pm 0.99^1$
	$K^{*\mp}K^\pm$							$< 0.96$
294	$K^+K^-\pi^0$	$2.2 \pm 0.6$	$2.17 \pm 0.60 \pm 0.24$	[889]				$< 0.4$
295	$K_SK_S\pi^0$	< 0.9	< 0.9	[890]				$< 0.9$
296	$K_SK_S\eta$	< 1.0	< 1.0	[890]				$< 1.0$
297	$K_SK_S\eta'$	< 2.0	< 2.0	[890]				$< 2.0$
298	$K^+K^-K^0$	$26.3 \pm 1.5$	$26.5 \pm 0.9 \pm 0.8$	[271] $28.3 \pm 3.3 \pm 4.0$	[826]			$19.1 \pm 1.9^1$
299	$\phi K^0$	$7.3 \pm 0.7$	$7.1 \pm 0.6_{-0.3}^{+0.4}$	[271] $9.0_{-1.8}^{+2.2} \pm 0.7$	[849]	$5.4_{-2.7}^{+3.7} \pm 0.7$	[845]	$7.3_{-0.6}^{+0.7}$
300	$f_0(980)K^0\dagger$	$7.0_{-3.0}^{+3.5}$	$7.0_{-1.8}^{+2.6} \pm 2.4$	[271]				$7.0_{-3.0}^{+3.5}$
301	$f_0(1500)K^0\dagger$	$13_{-5}^{+7}$	$13_{-4.4}^{+5.8} \pm 3.2$	[271]				$13.3_{-5.4}^{+6.6}$

**Table 222** continued

RPP#	Mode	PDG2014 Avg.	BABAR	Belle	CLEO	CDF	LHCb	Our Avg.
302	$J_2'(1525)K^0$	$0.3^{+0.5}_{-0.4}$	$0.29^{+0.27}_{-0.18} \pm 0.36$	[271]				$0.29^{+0.45}_{-0.40}$
303	$f_0(1710)K^0 \dagger$	$4.4 \pm 0.9$	$4.4 \pm 0.7 \pm 0.5$	[271]				$4.4 \pm 0.9$
304	$K^0 K^+ K^- (\text{NR})$	$33 \pm 10$	$33 \pm 5 \pm 9$	[271]				$33 \pm 10$
305	$K_S K_S K_S$	$6.2^{+1.2}_{-1.1}$	$6.19 \pm 0.48 \pm 0.19$	[387]	$4.2^{+1.6}_{-1.3} \pm 0.8$	[826]		$6.04 \pm 0.50$
306	$f_0(980)K_S \dagger$	$2.7 \pm 1.8$	$2.7^{+1.3}_{-1.2} \pm 1.3 \dagger$	[387]				$2.7 \pm 1.8$
307	$f_0(1710)K_S \dagger$	$0.50^{+0.050}_{-0.026}$	$0.50^{+0.46}_{-0.24} \pm 0.11 \dagger$	[387]				$0.50^{+0.47}_{-0.26}$
308	$f_0(2010)K_S \dagger$	$0.5 \pm 0.6$	$0.54^{+0.21}_{-0.20} \pm 0.52 \dagger$	[387]				$0.54 \pm 0.56$
309	$K_S K_S K_S (\text{NR})$	$13.3 \pm 3.1$	$13.3^{+2.2}_{-2.3} \pm 2.2$	[387]				$13.3^{+3.1}_{-3.2}$
310	$K_S K_S K_L$	$< 16$	$< 16^{+2}_{-2}$	[891]				$< 16^{+2}_{-2}$
311	$K^{*0} K^+ K^-$	$27.5 \pm 2.6$	$27.5 \pm 1.3 \pm 2.2$	[881]				$27.5 \pm 2.6$
312	$\phi K^{*0}$	$10.0 \pm 0.5$	$9.7 \pm 0.5 \pm 0.6$	[391]	$10.4 \pm 0.5 \pm 0.6$	[892]		$10.1^{+0.6}_{-0.5}$
313	$K^+ \pi^- \pi^+ K^-$	$< 72$			$< 72^{+3}_{-3}$	[893]		$< 72^{+3}_{-3}$
314	$K^{*0} \pi^+ K^-$	$4.5 \pm 1.3$	$4.6 \pm 1.1 \pm 0.8$	[881]				$4.6 \pm 1.4$
315	$K^{*0} \bar{K}^{*0}$	$0.8 \pm 0.5$	$1.28^{+0.35}_{-0.30} \pm 0.11$	[894]				$0.81 \pm 0.23$
316	$K^+ \pi^- K^+ \pi^- (\text{NR})$	$< 6.0$			$< 6.0^{+3}_{-3}$	[893]		$< 6.0^{+3}_{-3}$
317	$K^{*0} K^+ \pi^-$	$< 2.2$	$< 2.2$	[881]	$< 7.6^{+3}_{-3}$	[893]		$< 2.2$
318	$K^{*0} K^{*0}$	$< 0.2$	$< 0.41$	[894]	$< 0.2$	[893]		$< 0.2$
319	$K^{*+} K^{*-}$	$< 2.0$	$< 2.0$	[895]				$< 2.0$
320	$K_1^*(1400)^0 \phi$	$< 5000$	$< 5000^5$	[835]				$< 5000^5$
321	$(K\pi)_0^{*0} \phi$	$4.3 \pm 0.4$	$4.3 \pm 0.4 \pm 0.4$	[391]	$4.3 \pm 0.4 \pm 0.4$	[892]		$4.3 \pm 0.4$
322	$(K\pi)_0^{*0} \phi^4$	$< 1.7$	$< 1.7$	[896]				$< 1.7$
323	$K_0^*(1430)^0 \pi^+ K^-$	$< 31.8$			$< 31.8^{+3}_{-3}$	[893]		$< 31.8^{+3}_{-3}$
324	$K_0^*(1430)^0 \bar{K}^{*0}$	$< 3.3$			$< 3.3$	[893]		$< 3.3$

Results for CDF and LHCb are relative BFs converted to absolute BFs.

CLEO upper limits that have been greatly superseded are not shown.

$\dagger$  In this product of BFs, all daughter BFs not shown are set to 100%.

<sup>1</sup> Obtained from a fit to the ratios of BFs measured by LHCb (Ref. [879]) and to the averages of the BFs therein, as measured by other experiments (excluding the present line).

<sup>2</sup>  $0.75 < M(K\pi) < 1.20 \text{ GeV}/c^2$ .

<sup>3</sup>  $0.70 < M(K\pi) < 1.70 \text{ GeV}/c^2$ .

<sup>4</sup>  $1.60 < M(K\pi) < 2.15 \text{ GeV}/c^2$ .

<sup>5</sup> Result from ARGUS. Cited in the BABAR column to avoid adding a column to the table.

**Table 223** Branching fractions of charmless mesonic  $B^0$  decays with kaons (part 3) in units of  $\times 10^{-6}$ . Upper limits are at 90% CL. Where values are shown in red (blue), this indicates that they are new published (preliminary) results since PDG2014

RPP#	Mode	PDG2014 Avg.	BABAR	Belle	CLEO	CDF	LHCb	Our Avg.
325	$K_0^*(1430)^0 \bar{K}_0^*(1430)^0$	< 8.4		< 8.4	[893]		< 8.4	
326	$\phi K_0^*(1430)^0$	$3.9 \pm 0.8$	$3.9 \pm 0.5 \pm 0.6$	[391]	<b>4.3 ± 0.4 ± 0.4</b>	[892]	$4.2 \pm 0.5$	
327	$K_0^*(1430)^0 K^{*0}$	< 1.7		< 1.7	[893]		< 1.7	
328	$K_0^*(1430)^0 K_0^*(1430)^0$	< 4.7		< 4.7	[893]		< 4.7	
329	$\phi K^*(1680)^0$	< 3.5		< 3.5	[896]		< 3.5	
330	$\phi K_3^*(1780)^0$	< 2.7		< 2.7	[896]		< 2.7	
331	$\phi K_4^*(2045)^0$	< 15.3		< 15.3	[896]		< 15.3	
332	$\rho^0 K_2^*(1430)^0$	< 1100		< 1100 <sup>‡</sup>	[835]		< 1100 <sup>‡</sup>	
333	$\phi K_2^*(1430)^0$	$6.8 \pm 0.9$	$7.5 \pm 0.9 \pm 0.5$	[391]	$5.5^{+0.5}_{-0.7} \pm 1.0$	[892]	$6.8 \pm 0.8$	
334	$\phi \phi K^0$ <sup>†</sup>	$4.5 \pm 0.9$	$4.5 \pm 0.8 \pm 0.3$	[852]			$4.5 \pm 0.9$	
335	$\eta' \eta' K^0$	< 31	< 31	< 31	[853]		< 31	

<sup>†</sup>  $M_{\phi\phi} < 2.85 \text{ GeV}/c^2$ .

<sup>‡</sup> Result from ARGUS. Cited in the BABAR column to avoid adding a column to the table.

**Table 224** Branching fractions of charmless mesonic  $B^0$  decays without kaons in units of  $\times 10^{-6}$ . Upper limits are at 90% CL. Where values are shown in red (blue), this indicates that they are new published (preliminary) results since PDG2014

RPP#	Mode	PDG2014 Avg.	BABAR	Belle	CLEO	CDF	LHCb	Our Avg.
356	$\pi^+ \pi^-$	5.15 ± 0.19	5.5 ± 0.4 ± 0.3	[870]	5.04 ± 0.21 ± 0.18	[808]	4.5 <sup>+1.4</sup> <sub>-1.2</sub> <sup>+0.5</sup> <sub>-0.4</sub>	[898] 5.10 ± 0.19
357	$\pi^0 \pi^0$	1.91 ± 0.22	1.83 ± 0.21 ± 0.13	[416]	2.3 <sup>+0.4</sup> <sub>-0.5</sub> <sup>+0.2</sup> <sub>-0.3</sub>	[899]		1.91 <sup>+0.22</sup> <sub>-0.23</sub>
358	$\eta \pi^0$	< 1.5	< 1.5	[863]	4.1 <sup>+1.7</sup> <sub>-1.5</sub> <sup>+0.5</sup> <sub>-0.7</sub>	[900]	< 2.9	4.1 <sup>+1.8</sup> <sub>-1.7</sub>
359	$\eta \eta$	< 1.0	< 1.0	[811]	0.76 <sup>+0.27</sup> <sub>-0.23</sub> <sup>+0.4</sup> <sub>-0.6</sub>	[901]		0.76 <sup>+0.30</sup> <sub>-0.28</sub>
360	$\eta' \pi^0$	1.2 ± 0.6	0.9 ± 0.4 ± 0.1	[863]	2.8 ± 1.0 ± 0.3	[812]	0.0 <sup>+1.8</sup> <sub>-0.0</sub>	1.2 ± 0.4
361	$\eta' \eta'$	< 1.7	< 1.7	[811]	< 6.5	[814]		< 1.7
362	$\eta' \eta$	< 1.2	< 1.2	[863]	< 4.5	[814]		< 1.2
363	$\eta' \rho^0$	< 1.3	< 2.8	[813]	< 1.3	[814]		< 1.3
364	$f_0(980) \eta' \dagger$	< 0.9	< 0.9	[813]				< 0.9
365	$\eta \rho^0$	< 1.5	< 1.5	[872]	< 1.9	[818]		< 1.5
366	$f_0(980) \eta \dagger$	< 0.4	< 0.4	[872]				< 0.4
367	$\omega \eta$	0.94 <sup>+0.40</sup> <sub>-0.31</sub>	0.94 <sup>+0.35</sup> <sub>-0.30</sub> <sup>+0.09</sup>	[811]				0.94 <sup>+0.36</sup> <sub>-0.31</sub>
368	$\omega \eta'$	1.0 <sup>+0.5</sup> <sub>-0.4</sub>	1.01 <sup>+0.46</sup> <sub>-0.38</sub> <sup>+0.09</sup>	[811]	< 2.2	[814]		1.01 <sup>+0.47</sup> <sub>-0.39</sub>
369	$\omega \rho^0$	< 1.6	< 1.6	[822]				< 1.6
370	$f_0(980) \omega \dagger$	< 1.5	< 1.5	[822]				< 1.5
371	$\omega \phi \phi$	1.2 ± 0.4	1.2 ± 0.3 <sup>+0.3</sup> <sub>-0.2</sub>	[902]				1.2 ± 0.4
372	$\phi \pi^0$	< 0.15	< 0.28	[864]	< 0.15	[865]		< 0.15
373	$\phi \eta$	< 0.5	< 0.5	[811]				< 0.5
374	$\phi \eta'$	< 0.5	< 1.1	[811]	< 0.5	[814]		< 0.5
375	$\phi \rho^0$	< 0.33	< 0.33	[867]				< 0.33
376	$f_0(980) \phi \dagger$	< 0.38	< 0.38	[867]				< 0.38
377	$\phi \phi$	< 0.7	< 0.7	[902]				< 0.7
378	$\phi \phi$	< 0.2	< 0.2	[867]				< 0.2
379	$a_0^\mp(980) \pi^\pm \dagger$	< 3.1	< 3.1	[872]				< 3.1
380	$a_0^\mp(1450) \pi^\pm \dagger$	< 2.3	< 2.3	[872]				< 2.3
382	$\rho^0 \pi^0$	2.0 ± 0.5	1.4 ± 0.6 ± 0.3	[904]	3.0 ± 0.5 ± 0.7	[284]	1.6 <sup>+2.0</sup> <sub>-1.4</sub> <sup>+0.8</sup> <sub>-0.8</sub>	[821] 2.0 ± 0.5
383	$\rho^\mp \pi^\pm$	23.0 ± 2.3	22.6 ± 1.8 ± 2.2	[288]	22.6 ± 1.1 ± 4.4	[284]	27.6 <sup>+8.4</sup> <sub>-7.4</sub> <sup>+4.2</sup> <sub>-4.2</sub>	[821] 23.0 ± 2.3
384	$\pi^+ \pi^- \pi^+ \pi^-$	< 19.3	< 23.1	[411]	< 11.2	[412]		< 11.2
385	$\rho^0 \pi^+ \pi^- (NR)$	< 8.8	< 8.8	[411]	< 12	[412]		< 8.8
386	$\rho^0 \rho^0$	0.73 ± 0.28	0.92 ± 0.32 ± 0.14	[411]	1.02 ± 0.30 ± 0.15	[412]	0.94 ± 0.17 ± 0.11 <sup>‡</sup>	[413] 0.95 ± 0.16
387	$f_0(980) \pi^+ \pi^- (NR) \dagger$	< 3.8			< 3.0	[412]		< 3.0

Table 224 continued

RPP#	Mode	PDG2014 Avg.	BABAR	Belle	CLEO	CDF	LHCb	Our Avg.
388	$f_0(980)\rho^0$ †	< 0.3	< 0.40	[411]	<b>0.78±0.22±0.11</b>	[412]		0.78 ± 0.25
389	$f_0(980)f_0(980)$ †	< 0.1	< 0.19	[411]	<b>&lt; 0.2</b>	[412]	< 0.19	
391	$a_1^\mp\pi^\pm$	26 ± 5	33.2 ± 3.8 ± 3.0	[905]	22.2 ± 2.0 ± 2.8	[418]	25.9 ± 2.8	
392	$a_2^\mp\pi^\pm$	< 6.3			< 6.3	[418]	< 6.3	
393	$\pi^+\pi^-\pi^0\pi^0$	< 3100	< 3100 ¶	[857]			< 3100 ¶	
394	$\rho^+\rho^-$	24.2 ± 3.1	25.5 ± 2.1 ± 3.6	[409]	22.8 ± 3.8 ± 2.3	[906]	24.2 ± 3.1	
395	$a_1(1260)^0\pi^0$	< 1100	< 1100 ¶	[857]			< 1100 ¶	
396	$\omega\pi^0$	< 0.5	< 0.5	[863]	< 2.0	[862]	< 0.5	
397	$\pi + \pi^+ \pi^- \pi^- \pi^0$	< 9000	< 9000 ¶	[857]			< 9000 ¶	
398	$a_1^\pm\rho^\mp$	< 61	< 61	[907]			< 61	
399	$a_1^\pm\rho^0$	< 600	< 6000 ¶	[857]			< 6000 ¶	
400	$b_1^\mp\pi^\pm$ †	10.9 ± 1.5	10.9 ± 1.2 ± 0.9	[836]	10.9 ± 1.5		10.9 ± 1.5	
401	$b_1^0\pi^0$ †	< 1.9	< 1.9	[834]			< 1.9	
402	$b_1^\pm\rho^\mp$ †	< 1.4	< 1.4	[837]			< 1.4	
403	$b_1^0\rho^0$ †	< 3.4	< 3.4	[837]			< 3.4	
404	$\pi^+\pi^+\pi^+\pi^-\pi^-\pi^-$	< 3000	< 3000 ¶	[857]			< 3000 ¶	
405	$a_1^\pm a_1^\mp$	11.8 ± 2.6	11.8 ± 2.6	[908]			11.8 ± 2.6	
406	$\pi + \pi^+ \pi^+ \pi^- \pi^- \pi^0$	< 11000	< 11000 ¶	[857]			< 11000 ¶	
	$\phi\pi^+\pi^-$				<b>0.182±0.048±0.014</b> §	[909]	0.182 ± 0.050	

Results for CDF and LHCb are relative BFs converted to absolute BFs.

CLEO upper limits that have been greatly superseded are not shown.

† In this product of BFs, all daughter BFs not shown are set to 100%.

‡ Result given as  $0.94 \pm 0.17 \pm 0.09 \pm 0.06$  where last error is from  $\mathcal{B}(B^0 \rightarrow \phi K^{*0})$ .

§ In the mass range  $400 < m(\pi^+\pi^-) < 1600$  GeV/ $c^2$ .

¶ Result from ARGUS. Cited in the BABAR column to avoid adding a column to the table.

**Table 225** Relative branching fractions of charmless mesonic  $B^0$  decays. Upper limits are at 90% CL. Where values are shown in red (blue), this indicates that they are new published (preliminary) results since PDG2014

RPP#	Mode	PDG2014 Avg.	CDF	LHCb	Our Avg.
273	$\mathcal{B}(B^0 \rightarrow K^+ K^-)/\mathcal{B}(B^0 \rightarrow K^+ \pi^-)$	$0.012 \pm 0.005 \pm 0.005$	[883]	<b>0.00398 <math>\pm 0.00065 \pm 0.00042</math></b>	[884] $0.00416 \pm 0.00099$
356	$\mathcal{B}(B^0 \rightarrow \pi^+ \pi^-)/\mathcal{B}(B^0 \rightarrow K^+ \pi^-)$	$0.261 \pm 0.010$	[897]	$0.262 \pm 0.009 \pm 0.017$	[888] $0.261 \pm 0.015$
	$\mathcal{B}(B^0 \rightarrow K^{*\mp} K^\pm)/\mathcal{B}(B^0 \rightarrow K^{*\mp} \pi^\pm)$	$0.259 \pm 0.017 \pm 0.016$		< 0.05	< 0.05
	$\mathcal{B}(B^0 \rightarrow K_S^0 K^{*0})/\mathcal{B}(B^0 \rightarrow K_S^0 \pi^+ \pi^-)$			< 0.020	< 0.020

<sup>†</sup> Numerator includes two distinct decay processes:  $\mathcal{B}(B^0 \rightarrow f) + \mathcal{B}(B^0 \rightarrow \bar{f})$ .

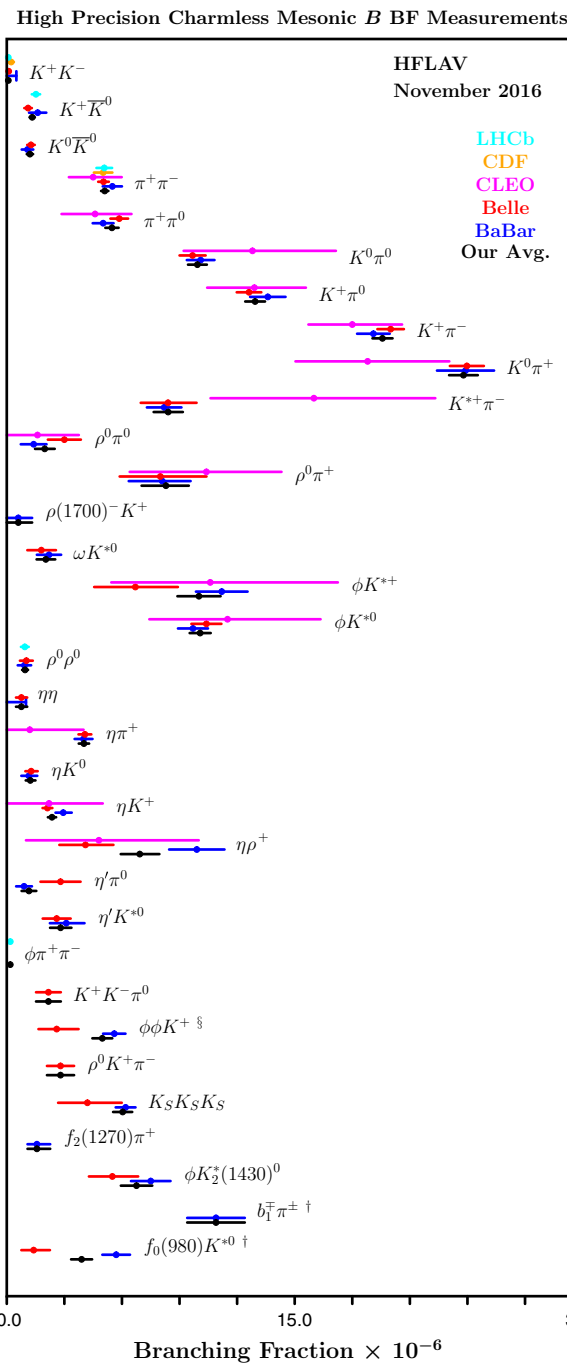


**Fig. 176** Selection of high-precision charmless mesonic  $B$  meson branching fraction measurements

#### 7.4 Decays of $B_s^0$ mesons

Tables 232 and 233 detail branching fractions and relative branching fractions of  $B_s^0$  meson decays, respectively.

Figures 180 and 181 show graphic representations of a selection of results given in this section. Footnote symbols

indicate that the footnote in the corresponding table should be consulted.

List of other measurements that are not included in the tables:

- $B_s^0 \rightarrow \phi\mu^+\mu^-$ : LHCb measures the differential BF in bins of  $m^2(\mu^+\mu^-)$ . It also performs an angular analysis and measures  $F_L, S_3, S_4, S_7, A_5, A_6, A_8$  and  $A_9$  in bins of  $m^2(\mu^+\mu^-)$  [948].
- $B_s^0 \rightarrow \phi\gamma$ : LHCb has measured the photon polarization [407].

### 7.5 Radiative and leptonic decays of $B^0$ and $B^+$ mesons.

This section reports different observables for leptonic and radiative  $B^0$  and  $B^+$  meson decays, including processes in which the photon yields a pair of charged or neutral leptons. Tables 234 and 235 provide compilations of branching fractions of  $B^+$  mesons to radiative, and lepton-flavor/number-violating final states, respectively. Tables 236 and 237 provide compilations of branching fractions of  $B^0$  mesons, and  $B^\pm/B^0$  meson admixture, respectively. Table 238 contains branching fractions of leptonic and radiative-leptonic  $B^+$  and  $B^0$  decays. It is followed by Tables 239 and 240, which give relative branching fractions of  $B^+$  decays and a compilations of inclusive decays, respectively. Table 241 contains isospin asymmetry measurements.

Figures 182, 183, 184, 185, 186 and 187 show graphic representations of a selection of results given in this section. Footnote symbols indicate that the footnote in the corresponding table should be consulted.

List of other measurements that are not included in the tables:

- $B^+ \rightarrow K^+\pi^-\pi^+\gamma$ : LHCb has measured the up-down asymmetries in bins of the  $K\pi\pi\gamma$  mass [1022].
- In Ref. [1023], LHCb has also measured the branching fraction of  $B^+ \rightarrow K^+e^-e^+$  in the  $m^2(\ell\ell)$  bin  $[1, 6] \text{ GeV}^2/c^4$ .
- In the  $B^+ \rightarrow \pi^+\mu^+\mu^-$  paper [966], LHCb has also measured the differential branching fraction in bins of  $m^2(\ell\ell)$ .
- For  $B \rightarrow K\ell^-\ell^+$ , LHCb has measured  $F_H$  and  $A_{FB}$  in 17 (5) bins of  $m^2(\ell\ell)$  for the  $K^+$  ( $K_S^0$ ) final state [1024]. Belle has measured  $F_L$  and  $A_{FB}$  in 6  $m^2(\ell\ell)$  bins [1025].
- For the  $B \rightarrow K^*\ell^-\ell^+$  analyses, partial branching fractions and angular observables in bins of  $m^2(\ell\ell)$  are also available:

- $B^0 \rightarrow K^{*0}e^-e^+$ : LHCb has measured  $F_L, A_T^{(2)}, A_T^{\text{Im}}, A_T^{\text{Re}}$  in the  $[0.002, 1.120] \text{ GeV}^2/c^4$  bin of  $m^2(\ell\ell)$  [1026], and has also determined the branching fraction in the dilepton mass region  $[10, 1000] \text{ MeV}/c^2$  [1023].

- $B \rightarrow K^*\ell^-\ell^+$ : Belle has measured  $F_L, A_{FB}$ , isospin asymmetry in 6  $m^2(\ell\ell)$  bins [970] and  $P'_4, P'_5, P'_6, P'_8$  in 4  $m^2(\ell\ell)$  bins [1025]. BABAR has measured  $F_L, A_{FB}, P_2$  in 5  $m^2(\ell\ell)$  bins [1027].
- $B^0 \rightarrow K^{*0}\mu^-\mu^+$ : LHCb has measured  $F_L, A_{FB}, S_3 - S_9, A_3 - A_9, P_1 - P_3, P'_4 - P'_8$  in 8  $m^2(\ell\ell)$  bins [1028]. CMS has measured  $F_L$  and  $A_{FB}$  in 7  $m^2(\ell\ell)$  bins [1029].
- For  $B \rightarrow X_s\ell^-\ell^+$  ( $X_s$  is a hadronic system with an  $s$  quark), Belle has measured  $A_{FB}$  in bins of  $m^2(\ell\ell)$  with a sum of 10 exclusive final states [1030].
- $B^0 \rightarrow K^+\pi^-\mu^+\mu^-$ , with  $1330 < m(K^+\pi^-) < 1530 \text{ GeV}/c^2$ : LHCb has measured the partial branching fraction in bins of  $m^2(\mu^-\mu^+)$  in the range  $[0.1, 8.0] \text{ GeV}^2/c^4$ , and has also determined angular moments [1031].

### 7.6 Charge asymmetries in $b$ -hadron decays

This section contains, in Tables 242, 243, 244, 245, 246 247, compilations of  $CP$  asymmetries in decays of various  $b$ -hadrons:  $B^+, B^0$  mesons,  $B^\pm/B^0$  admixtures,  $B_s^0$  mesons and finally  $\Lambda_b^0$  baryons. Measurements of time-dependent  $CP$  asymmetries are not listed here but are discussed in Sect. 4.

Figure 188 shows a graphic representation of a selection of results given in this section. Footnote symbols indicate that the footnote in the corresponding table should be consulted.

List of other measurements that are not included in the tables:

- In the paper [1044], LHCb has measured the triple-product asymmetries for the decays  $\Lambda_b^0 \rightarrow p\pi^-\pi^+\pi^-$  and  $\Lambda_b^0 \rightarrow p\pi^-K^+K^-$ .

### 7.7 Polarization measurements in $b$ -hadron decays

In this section, compilations of polarization measurements in  $b$ -hadron decays are given. Tables 248 (249) details measurements of the longitudinal fraction,  $f_L$ , in  $B^+$  ( $B^0$ ) decays, and Tables 250 (251) the results of the full angular analyses of  $B^+$  ( $B^0$ )  $\rightarrow \phi K^*$  decays. Table 252 gives results of the full angular analysis of  $B^0 \rightarrow \phi K_2^{*0}(1430)$  decays. Tables 253, 254 and 255 detail quantities of  $B_s^0$  decays:  $f_L$  measurements, and observables from full angular analyses of decays to  $\phi\phi$  and  $\phi\bar{K}^{*0}$ .

Figures 189 and 190 show graphic representations of a selection of results shown in this section. Footnote symbols indicate that the footnote in the corresponding table should be consulted (Table 256).

### 7.8 Decays of $B_c^+$ mesons

Table 257 details branching fractions of  $B_c^+$  meson decays to charmless hadronic final states.

**Table 226** Branching fractions of charmless baryonic  $B^+$  decays in units of  $\times 10^{-6}$ . Upper limits are at 90% CL. Where values are shown in red (blue), this indicates that they are new published (preliminary) results since PDG2014

RPP#	Mode	PDG2014 Avg.	BABar	Belle	LHCb	Our Avg.
417	$p\bar{p}\pi^+$	$1.62 \pm 0.20$	$1.69 \pm 0.29 \pm 0.26^\dagger$	[666]	$1.60^{+0.22}_{-0.19} \pm 0.12$	[910]
417	$p\bar{p}\pi^+ \S$				<b><math>1.07 \pm 0.11 \pm 0.11</math></b>	[911]
420	$p\bar{p}K^+$	$5.9 \pm 0.5$	$6.7 \pm 0.5 \pm 0.4^\dagger$	[740]	$5.54^{+0.27}_{-0.25} \pm 0.36$	[910]
421	$\Theta^{++}\bar{p}^- \mathbf{1}$	$< 0.091$	$< 0.09$	[740]	$< 0.091$	[912]
422	$f_J(2221)K^+ \mathbf{2}$	$< 0.41$			$< 0.41$	[912]
423	$p\bar{\Lambda}(1520)$	$< 1.5$	$< 1.5$	[740]		
425	$p\bar{p}K^{*+}$	$3.6^{+0.8}_{-0.7}$	$5.3 \pm 1.5 \pm 1.3^\dagger$	[666]	$3.38^{+0.73}_{-0.60} \pm 0.39^\ddagger$	[913]
426	$f_J(2221)K^{*+} \mathbf{2}$	$< 0.77$	$< 0.77$	[666]		
427	$p\bar{\Lambda}$	$< 0.32$			$< 0.32$	[914]
429	$p\bar{\Lambda}\pi^0$	$3.00^{+0.7}_{-0.6}$	$3.00 \pm 0.7$		$3.00^{+0.61}_{-0.53} \pm 0.33$	[915]
430	$p\bar{\Sigma}(1385)^0$	$< 0.47$	$< 0.47$		$< 0.47$	[915]
431	$\Delta^+\bar{\Lambda}$	$< 0.82$			$< 0.82$	[915]
433	$p\bar{\Lambda}\pi^+\pi^- \text{ (NR)}$	$5.9 \pm 1.1$			$5.92^{+0.88}_{-0.84} \pm 0.69$	[916]
434	$p\bar{\Lambda}\rho^0$	$4.8 \pm 0.9$	$4.8 \pm 0.9$		$4.78^{+0.67}_{-0.64} \pm 0.60$	[916]
435	$p\bar{\Lambda}f_2(1270)$	$2.0 \pm 0.8$	$2.0 \pm 0.8$		$2.03^{+0.77}_{-0.72} \pm 0.27$	[916]
436	$\Lambda\bar{\Lambda}\pi^+$	$< 0.94$			$< 0.94 \S$	[627]
437	$\Lambda\bar{\Lambda}K^+$	$3.4 \pm 0.6$			$3.38^{+0.41}_{-0.36} \pm 0.41^\ddagger$	[627]
438	$\Lambda\bar{\Lambda}K^{*+}$	$2.2^{+1.2}_{-0.9}$			$2.19^{+1.13}_{-0.88} \pm 0.33 \S$	[627]
439	$\bar{\Delta}^0 p$	$< 1.38$			$< 1.38 \S$	[910]
440	$\Delta^{++}\bar{p}$	$< 0.14$			$< 0.14 \S$	[910]

Results for LHCb are relative BFs converted to absolute BFs.

<sup>†</sup> Charmonium decays to  $p\bar{p}$  have been statistically subtracted.

<sup>‡</sup> The charmonium mass region has been vetoed.

<sup>§</sup> Di-baryon mass is less than  $2.85 \text{ GeV}/c^2$ .

<sup>¶</sup> Includes contribution where  $p\bar{p}$  is produced in charmonia decays.

<sup>1</sup>  $\Theta(1540)^{++} \rightarrow K^+ p$  (pentaquark candidate).  
<sup>2</sup> In this product of BFs, all daughter BFs not shown are set to 100%.

**Table 227** Branching fractions of charmless baryonic  $B^0$  decays in units of  $\times 10^{-6}$ . Upper limits are at 90% CL. Where values are shown in red (blue), this indicates that they are new published (preliminary) results since PDG2014

RPP#	Mode	PDG2014 Avg.	BABAR	Belle	LHCb	Our Avg.
407	$p\bar{p}$	$0.015^{+0.007}_{-0.005}$	< 0.27	[917]	< 0.11	[918]
409	$p\bar{p}K^0$	$2.66 \pm 0.32$	$3.0 \pm 0.5 \pm 0.3^\dagger$	[666]	$2.51^{+0.35}_{-0.29} \pm 0.21^\ddagger$	$0.0147^{+0.0062 \pm 0.0035}_{-0.0051 \pm 0.0014}$
410	$\Theta^+\bar{p}^\pm$ §	< 0.05	< 0.05	[666]	< 0.23	$2.66^{+0.34}_{-0.32}$
411	$f_J(2221)K^0$ ¶	< 0.45	< 0.45	[666]		< 0.05
412	$p\bar{p}K^{*0}$	$1.24^{+0.28}_{-0.25}$	$1.47 \pm 0.45 \pm 0.40^\dagger$	[666]	$1.18^{+0.29}_{-0.25} \pm 0.11^\ddagger$	$1.24^{+0.28}_{-0.25}$
413	$f_J(2221)K^{*0}$ ¶	< 0.15	< 0.15	[666]		< 0.15
414	$p\bar{\Lambda}\pi^-$	$3.14 \pm 0.29$	$3.07 \pm 0.31 \pm 0.23$	[919]	$3.23^{+0.33}_{-0.29} \pm 0.29$	$3.14^{+0.29}_{-0.28}$
415	$p\bar{\Sigma}(1385)^-$	< 0.26				< 0.26
416	$\Delta^0\bar{\Lambda}$	< 0.93				< 0.93
417	$p\bar{\Lambda}K^-$	< 0.82				< 0.82
418	$p\bar{\Sigma}^0\pi^-$	< 3.8				< 3.8
419	$\bar{\Lambda}\Lambda$	< 0.32				< 0.32
420	$\bar{\Lambda}\Lambda K^0$	$4.8^{+1.0}_{-0.9}$				$4.76^{+0.84}_{-0.68} \pm 0.61^\ddagger$
421	$\bar{\Lambda}\Lambda K^{*0}$	$2.5^{+0.9}_{-0.8}$				$2.46^{+0.87}_{-0.72} \pm 0.34^\ddagger$

Results for LHCb are relative BFs converted to absolute BFs.

† Charmonium decays to  $p\bar{p}$  have been statistically subtracted.

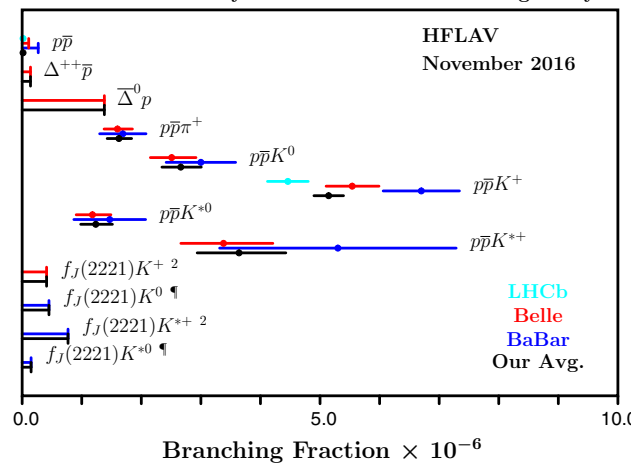
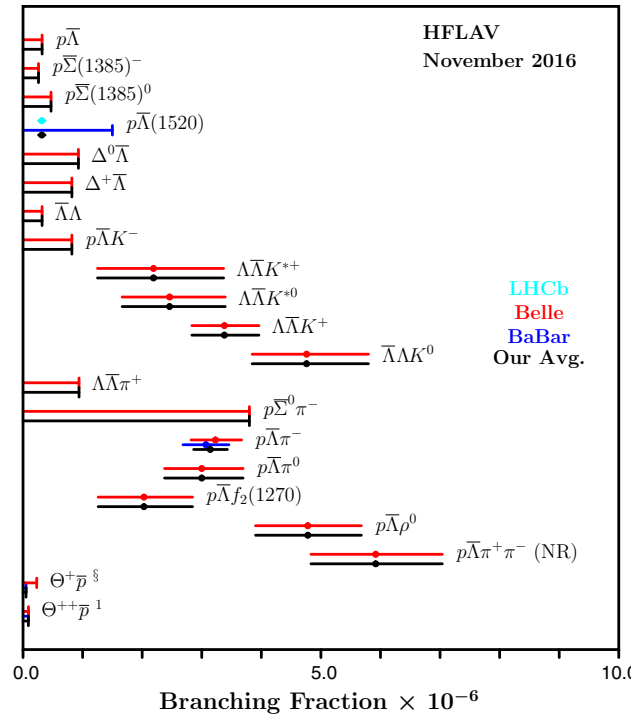
‡ The charmonium mass region has been vetoed.

§  $\Theta(1540)^+ \rightarrow pK^0$  (pentaquark candidate).

¶ In this product of BFs, all daughter BFs not shown are set to 100%.

**Table 228** Relative branching fractions of charmless baryonic  $B$  decays. Where values are shown in red (blue), this indicates that they are new published (preliminary) results since PDG2014

RPP#	Mode	PDG2014 Avg.	LHCb	Our Avg.
417	$\mathcal{B}(B^+ \rightarrow p\bar{p}\pi^+, m_{p\bar{p}} < 2.85 \text{ GeV}/c^2)/\mathcal{B}(B^+ \rightarrow J/\psi(\rightarrow p\bar{p})\pi^+)$	$12.0 \pm 1.2 \pm 0.3$	$12.0 \pm 1.2$	[911]
420	$\mathcal{B}(B^+ \rightarrow p\bar{p}K^+)/\mathcal{B}(B^+ \rightarrow J/\psi(\rightarrow p\bar{p})K^+)$	$4.91 \pm 0.19 \pm 0.14^\dagger$	$4.91 \pm 0.24$	[747]
420	$\mathcal{B}(B^+ \rightarrow p\bar{p}K^{*-})/\mathcal{B}(B^+ \rightarrow J/\psi K^+)$	$0.0104 \pm 0.0005 \pm 0.0001^{\ddagger}$	$0.0104 \pm 0.0005 \pm 0.0001^{\ddagger}$	[747]
423	$\mathcal{B}(B^+ \rightarrow \bar{\Lambda}(1520)(\rightarrow K^+\bar{p})p)/\mathcal{B}(B^+ \rightarrow J/\psi(\rightarrow p\bar{p})\pi^+)$	$0.033 \pm 0.005 \pm 0.007$	$0.033 \pm 0.009$	[911]

<sup>†</sup> Includes contribution where  $p\bar{p}$  is produced in charmonia decays.<sup>‡</sup> Original experimental relative BF multiplied by the best values (PDG2014) of certain reference BFs. The first error is experimental, and the second is from the reference BFs.**BFs of Charmless Baryonic Modes with Non-Strange Baryons****Fig. 177** Branching fractions of charmless baryonic modes with non-strange baryons**BFs of Charmless Baryonic Modes with Strange Baryons****Fig. 178** Branching fractions of charmless baryonic modes with strange baryons

**Table 229** Branching fractions of charmless  $\Lambda_b^0$  decays in units of  $\times 10^{-6}$ . Upper limits are at 90% CL. Where values are shown in red (blue), this indicates that they are new published (preliminary) results since PDG2014

RPP#	Mode	PDG2014 Avg.	CDF	LHCb	Our Avg.
19	$p\pi^-$	$3.5 \pm 0.8 \pm 0.6$	$3.5 \pm 0.8 \pm 0.6$	[921]	$3.5 \pm 1.0$
20	$pK^-$	$5.5 \pm 1.0 \pm 1.0$	$5.5 \pm 1.0 \pm 1.0$	[921]	$5.5 \pm 1.4$
21	$\Lambda\mu^+\mu^-$	$1.73 \pm 0.42 \pm 0.55$	$1.73 \pm 0.42 \pm 0.55$	[922]	$0.96 \pm 0.16 \pm 0.25$
	$\Lambda\eta$			$9.3^{+7.3}_{-5.3}$ ¶	[924] $9.3^{+7.3}_{-5.3}$
	$\Lambda\eta'$			$< 3.1$	[924] $< 3.1$
	$\Lambda\phi$			$5.18 \pm 1.04 \pm 0.35^{+0.67}_{-0.62}$ ‡	[925] $5.18^{+1.29}_{-1.26}$
	$\bar{K}^0 p\pi^-$			$1.26 \pm 0.19 \pm 0.09 \pm 0.34 \pm 0.05$ §	[926] $1.26 \pm 0.40$
	$K^0 pK^-$			$< 3.5$	[926] $< 3.5$
	$\Lambda\pi^+\pi^-$			$4.6 \pm 1.2 \pm 1.4 \pm 0.6$ †	[927] $4.6 \pm 1.9$
	$\Lambda K^+\pi^-$			$5.6 \pm 0.8 \pm 0.8 \pm 0.7$ †	[927] $5.6 \pm 1.3$
	$\Lambda K^+K^-$			$15.9 \pm 1.2 \pm 1.2 \pm 2.0$ †	[927] $15.9 \pm 2.6$

Results for CDF and LHCb are relative BFs converted to absolute BFs.

<sup>†</sup> Last quoted uncertainty is due to the precision with which the normalization channel branching fraction is known.

<sup>‡</sup> Third uncertainty is related to external inputs.

<sup>§</sup> Third uncertainty is from the ratio of fragmentation fractions  $f_{A_b^0}/f_d$ , and the fourth is due to the uncertainty on  $\mathcal{B}(B^0 \rightarrow K^0\pi^+\pi^-)$ .

¶ Result at 68% CL.

**Table 230** Partial branching fractions of  $A_0^0 \rightarrow \mu^+ \mu^-$  decays in intervals of  $q^2 = m^2(\mu^+ \mu^-)$  in units of  $\times 10^{-6}$ . Where values are shown in red (blue), this indicates that they are new published (preliminary) results since PDG2014

RPP#	Mode	$q^2$ [GeV $^2/c^4$ ] <sup>†</sup>	PDG2014 Avg.	CDF	LHCb		Our Avg.
21	$\Lambda\mu^+\mu^-$ <sup>‡</sup>	< 2.0	$0.15 \pm 2.01 \pm 0.05$	$0.15 \pm 2.01 \pm 0.05$	[922]	<b><math>0.56 \pm 0.76 \pm 0.80</math></b>	[923]
	$\Lambda\mu^+\mu^-$	[2.0, 4.3]	$1.8 \pm 1.7 \pm 0.6$	$1.8 \pm 1.7 \pm 0.6$		<b><math>0.71 \pm 0.60 \pm 0.10</math></b>	$0.91 \pm 0.55$
	$\Lambda\mu^+\mu^-$	[4.3, 8.68]	$-0.2 \pm 1.6 \pm 0.1$	$-0.2 \pm 1.6 \pm 0.1$		<b><math>0.66 \pm 0.72 \pm 0.16</math></b>	$0.40 \pm 0.62$
	$\Lambda\mu^+\mu^-$	[10.09, 12.86]	$3.0 \pm 1.5 \pm 1.0$	$3.0 \pm 1.5 \pm 1.0$		<b><math>1.55 \pm 0.58 \pm 0.55</math></b>	$1.96 \pm 0.68$
	$\Lambda\mu^+\mu^-$	[14.18, 16.00]	$1.0 \pm 0.7 \pm 0.3$	$1.0 \pm 0.7 \pm 0.3$		<b><math>1.44 \pm 0.44 \pm 0.42</math></b>	$1.19 \pm 0.40$
	$\Lambda\mu^+\mu^-$	> 16.00	$7.0 \pm 1.9 \pm 2.2$	$7.0 \pm 1.9 \pm 2.2$		<b><math>4.7 \pm 0.8 \pm 1.2</math></b>	$5.5 \pm 1.2$

Results for CDF and LHCb are relative BFs converted to absolute BFs.

<sup>†</sup> See the original paper for the exact  $m^2(\mu^+\mu^-)$  selection.

<sup>‡</sup> The LHCb measurement was superseded with a more accurate result in different  $m^2(\mu^+\mu^-)$  bins (see list of not-included results).

**Table 231** Branching fractions of charmless  $\Xi_b^0$  decays in units of  $\times 10^{-6}$ . Upper limits are at 90% CL. Where values are shown in red (blue), this indicates that they are new published (preliminary) results since PDG2014

RPP#	Mode	PDG2014 Avg.	LHCb	Our Avg.
	$\Lambda\pi^+\pi^-$		< 1.7	[927]
	$\Lambda K^+\pi^-$		< 0.8	[927]
	$\Lambda K^+K^-$		< 0.3	[927]
	$\bar{K}^0 p \pi^-$		< 1.6	[926]
	$\bar{K}^0 p K^-$		< 1.1	[926]

Results for LHCb are relative BFs converted to absolute BFs

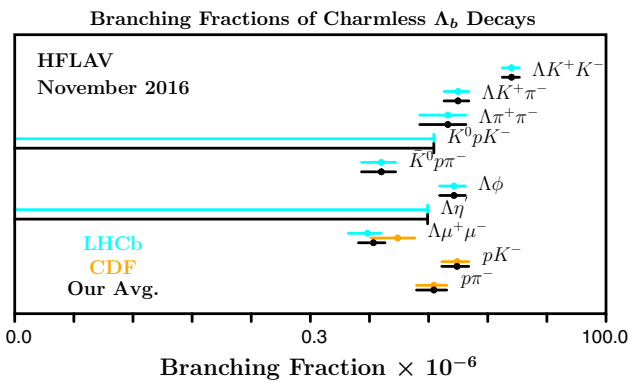


**Fig. 179** Branching fractions of charmless  $\Lambda_b^0$  decays

**Table 232** Branching fractions of charmless  $B_s^0$  decays in units of  $\times 10^{-6}$ . Upper limits are at 90% CL. Where values are shown in red (blue), this indicates that they are new published (preliminary) results since PDG2014

RPP#	Mode	PDG2014 Avg.	Belle	CDF	D0	LHCb	CMS	ATLAS	Our Avg.
45	$\pi^+\pi^-$	0.76±0.19	< 12	[931] 0.60±0.17±0.04 <sup>†</sup> [883]	<b>0.691±0.083±0.044<sup>‡</sup></b> [884]				0.671±0.083
51	$\phi\phi$	19.1±3.1		[931] 19.1±2.6±1.6 <sup>†</sup>	<b>18.4±0.5±1.8<sup>§</sup></b> [933]				18.6±1.6
52	$\pi^+K^-$	5.5±0.6	< 26	[931] 5.3±0.9±0.3 <sup>†</sup>	[921]	5.6±0.6±0.3 <sup>†</sup>	[898]		5.5±0.5
53	$K^+K^-$	24.9±1.7	38±10±7	[931] 25.9±2.2±1.7 <sup>†</sup>	[897]	23.7±1.6±1.5 <sup>†</sup>	[898]		24.8±1.7
54	$K^0\overline{K}^0$		< 66	<b>19.6±5.8<sup>¶</sup></b> ± 1.0 ± 2.0 <sup>†</sup> [934]					19.6 <sup>±6.2</sup> <sub>-5.6</sub>
55	$K^0\pi^+\pi^-$	19±5			19±5±2 <sup>†</sup>	[879]			19±5
56	$K^0K^-\pi^+\pi^-$	97±17			97±12±12 <sup>†</sup>	[879]			97±16
57	$K^0K^+K^-$	57	< 4		< 4 <sup>†</sup>	[879]			< 4 <sup>†</sup>
	$K^{*+}K^\mp$				<b>12.7±1.9±1.9</b>	[888]			12.7±2.7
	$K^{*-}\pi^+$				<b>3.3±1.1±0.5</b>	[888]			3.3±1.2
59	$K^{*0}\overline{K}^{*0}$	28.1±4.6±5.6			<b>10.8±1.4±1.5<sup>§</sup></b>	[935]			10.8±2.1
60	$\phi\overline{K}^{*0}$	1.13±0.3			1.13±0.29±0.06 <sup>†</sup>	[936]			1.13±0.30
61	$p\overline{p}$	0.028 <sup>+0.022</sup> <sub>-0.017</sub>			0.0284 <sup>+0.0203±0.0088</sup> <sub>-0.0168±0.0018</sub>	[918]			0.0280 <sup>+0.0220</sup> <sub>-0.0170</sub>
63	$\gamma\gamma$	< 8.7	< 3.1	[937]					< 3.1
64	$\phi\gamma$	36±4	<b>36±5±7</b>	[937]					35.2±3.4
65	$\mu^+\mu^-$	0.0031±0.0007			35.1±3.5±1.2 <sup>†</sup>	[938]			35.2±3.4
66	$e^+e^-$	< 0.28	< 0.28	[944]	0.0029 <sup>+0.0011±0.0003</sup> <sub>-0.0010±0.0001</sub>	[941]	0.0030 <sup>+0.0010±0.0009</sup> <sub>-0.0009±0.0009</sub>	< 0.28	0.0029 <sup>+0.0007</sup> <sub>-0.0006</sub>
67	$e^\pm\mu^\mp$	< 0.011	< 0.011	[944]	< 0.011	[945]			< 0.011
68	$\mu^+\mu^-\mu^+\mu^-$	< 0.012	< 0.012		< 0.012	[946]			< 0.012
70	$\phi\mu^+\mu^-$	0.76±0.15			< 3.2	[947]	<b>0.797<sup>+0.045±0.068</sup></b>	[948]	0.797 <sup>+0.082</sup> <sub>-0.080</sub>
	$\eta'\eta'$						<b>33.1±7.0±1.2<sup>†</sup></b>	[949]	33.1±7.1
	$\pi^+\pi^-\mu^+\mu^-$						<b>0.086±0.015±0.010</b> <sup>2</sup>	[933]	0.086±0.018
	$K^0\overline{K}^{*0}$ ¶						<b>16.4±3.4±2.3</b>	[887]	16.4±4.1
	$\phi\pi^+\pi^-$						<b>3.48±0.29±0.35</b> <sup>4</sup>	[909]	3.48±0.46
	$\phi f_0(980), f_0(980) \rightarrow \pi^+\pi^-$						<b>1.12±0.18±0.11</b>	[909]	1.12±0.21
	$\phi f_2(1270), f_2(1270) \rightarrow \pi^+\pi^-$						<b>0.61<sup>+0.18</sup><sub>-0.14</sub>±0.06</b>	[909]	0.61 <sup>+0.19</sup> <sub>-0.15</sub>
	$\phi\phi(770)$						<b>0.27±0.07±0.02</b>	[909]	0.27±0.07

Results for CDF, D0, LHCb, CMS and ATLAS are relative BFs converted to absolute BFs.

<sup>†</sup> The first error is experimental, and the second is from the reference BF.

<sup>‡</sup> Last error represents the uncertainty due to the total number of  $B_s^0\overline{B}_s^0$  pairs.

<sup>§</sup> Last error takes into account  $\mathcal{B}(B^0 \rightarrow \phi K^{*0})$  and  $f_d/f_s$ .

<sup>¶</sup> Includes two distinct decay processes:  $\mathcal{B}(B_s^0 \rightarrow f) + \mathcal{B}(B_s^0 \rightarrow \bar{f})$ .

<sup>1</sup> UL at 95% CL.

<sup>2</sup> Muon pairs do not originate from resonances and  $0.5 < m(\pi^+\pi^-) < 1.3 \text{ GeV}/c^2$ .

<sup>3</sup> The average is done between the combined LHCb and CMS result,  $0.0028_{-0.0006}^{+0.0007}$  (Ref. [950]) and CDF.  
<sup>4</sup> In the mass range  $400 < m(\pi^+\pi^-) < 1600 \text{ GeV}/c^2$ .

**Table 233** Relative branching fractions of charmless  $B_s^0$  decays. Upper limits are at 90% CL. Where values are shown in red (blue), this indicates that they are new published (preliminary) results since PDG2014

RPP#	Mode	PDG2014 Avg.	CDF	LHCb	Our Avg.
45	$f_s \mathcal{B}(B_s^0 \rightarrow \pi^+ \pi^-)/f_d \mathcal{B}(B^0 \rightarrow K^+ \pi^-)$	0.008±0.002±0.001	[883]	<b>0.00915±0.00071±0.00083</b>	[884]
45	$f_s \mathcal{B}(B_s^0 \rightarrow \pi^+ \pi^-)/f_d \mathcal{B}(B^0 \rightarrow \pi^+ \pi^-)$	0.0178±0.0014±0.0020	[932]	<b>0.050<sup>+0.011</sup><sub>-0.009</sub>±0.004</b>	[898]
51	$\mathcal{B}(B_s^0 \rightarrow \phi \phi)/\mathcal{B}(B_s^0 \rightarrow J/\psi \phi)$			<b>1.84±0.05±0.13</b>	0.0180±0.0020
	$\mathcal{B}(B_s^0 \rightarrow \phi \phi)/\mathcal{B}(B^0 \rightarrow \phi K^*)$				1.84±0.14
52	$f_s \mathcal{B}(B_s^0 \rightarrow K^+ \pi^-)/f_d \mathcal{B}(B_d^0 \rightarrow K^+ \pi^-)$	0.071±0.010±0.007	[921]	0.074±0.006±0.006	[898]
53	$f_s \mathcal{B}(B_s^0 \rightarrow K^+ K^-)/f_d \mathcal{B}(B_d^0 \rightarrow K^+ \pi^-)$	0.347±0.020±0.021	[897]	0.316±0.009±0.019	[898]
55	$\mathcal{B}(B_s^0 \rightarrow K^0 \pi^+ \pi^-)/\mathcal{B}(B^0 \rightarrow K^0 \pi^+ \pi^-)$			0.29±0.06±0.04	[879]
56	$\mathcal{B}(B_s^0 \rightarrow K^0 K^- \pi^+)/\mathcal{B}(B^0 \rightarrow K^0 K^- \pi^+)^\dagger$	1.48±0.12±0.14			[879]
57	$\mathcal{B}(B_s^0 \rightarrow K^0 K^+ K^-)/\mathcal{B}(B^0 \rightarrow K^0 K^+ K^-)$	< 0.068			[879]
	$\mathcal{B}(B_s^0 \rightarrow K^{*-} K^+)/\mathcal{B}(B^0 \rightarrow K^{*-} \pi^-)$			<b>1.49±0.22±0.18</b>	< 0.068
	$\mathcal{B}(B_s^0 \rightarrow K^{*-} K^+)/\mathcal{B}(B^0 \rightarrow K^{*-} \pi^-)$			<b>0.39±0.13±0.05</b>	[888]
	$\mathcal{B}(B_s^0 \rightarrow K^{*-} \pi^+)/\mathcal{B}(B^0 \rightarrow K^{*-} \pi^-)$			<b>1.11±0.22±0.13</b>	[888]
59	$\mathcal{B}(B_s^0 \rightarrow K^{*0} \bar{K}^{*0})/\mathcal{B}(B^0 \rightarrow K^{*0} \pi^-)$			<b>0.39±0.13±0.05</b>	[888]
60	$\mathcal{B}(B_s^0 \rightarrow \phi \bar{K}^{*0})/\mathcal{B}(B^0 \rightarrow \phi K^{*0})$			<b>0.113±0.024±0.016</b>	[935]
64	$\mathcal{B}(B_s^0 \rightarrow \phi \gamma)/\mathcal{B}(B^0 \rightarrow K^{*0} \gamma)$			<b>0.113±0.024±0.016</b>	[946]
70	$\mathcal{B}(B_s^0 \rightarrow \phi \mu^+ \mu^-)/\mathcal{B}(B_s^0 \rightarrow J/\psi \phi) \times 10^4$	7.1±1.3		<b>0.81±0.04±0.07</b>	[938]
	$\mathcal{B}(B_s^0 \rightarrow K_S^0 K^{*0})/\mathcal{B}(B^0 \rightarrow K_S^0 \pi^+ \pi^-)^\dagger$			<b>7.41<sup>+0.42</sup><sub>-0.40</sub>±0.29</b>	[948]
	$\mathcal{B}(B_s^0 \rightarrow K_S^0 K^{*0})/\mathcal{B}(B^0 \rightarrow K_S^0 \pi^+ \pi^-)^\dagger$			<b>0.33±0.07±0.04</b>	[887]

<sup>†</sup> Numerator includes two distinct decay processes:  $\mathcal{B}(B_s^0 \rightarrow f) + \mathcal{B}(B_s^0 \rightarrow \bar{f})$ .

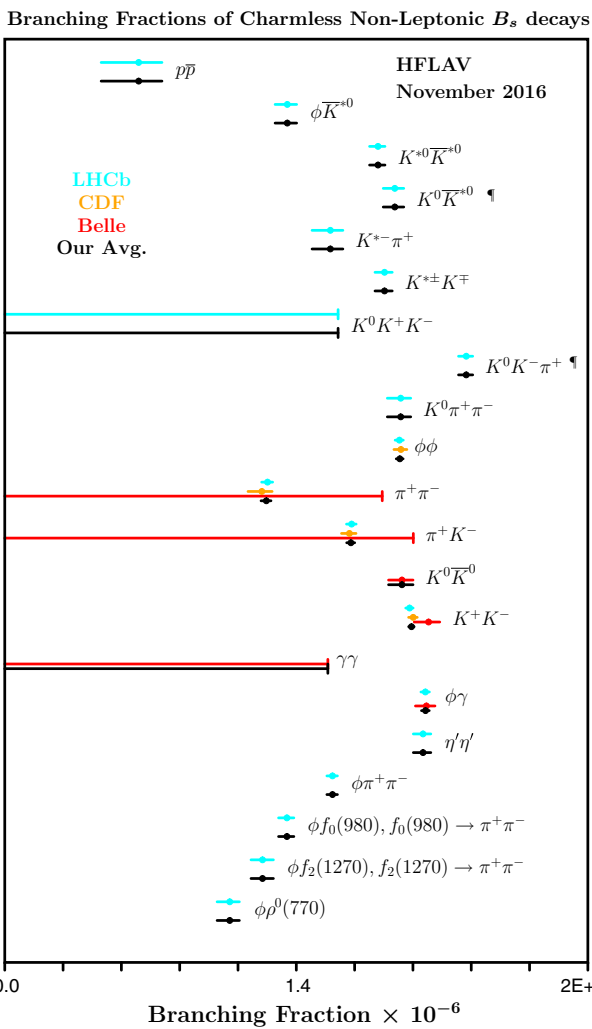


**Fig. 180** Branching fractions of charmless non-leptonic  $B_s^0$  decays

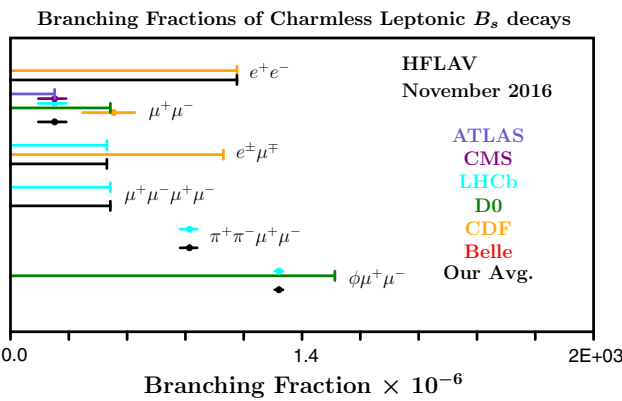


**Fig. 181** Branching fractions of charmless leptonic  $B_s^0$  decays

**Table 234** Branching fractions of charmless semileptonic and radiative  $B^+$  decays in units of  $\times 10^{-6}$ . Upper limits are at 90% CL. Where values are shown in red (blue), this indicates that they are new published (preliminary) results since PDG2014

RPP#	Mode	PDG2014 Avg.	BABAR	Belle	CLEO	LHCb	Our Avg.
363	$K^{*+}\gamma$	$42.1 \pm 1.8$	$42.2 \pm 1.4 \pm 1.6$	[951]	$42.5 \pm 3.1 \pm 2.4$	[952]	$37.6^{+8.9}_{-8.3} \pm 2.8$
364	$K_1^+(1270)\gamma$	$43 \pm 13$	$44.1^{+6.3}_{-4.4} \pm 5.8^\dagger$	[401]	$43 \pm 9 \pm 9$	[954]	$42.1 \pm 1.8$
365	$K^+\eta\gamma$	$7.9 \pm 0.9$	$7.7 \pm 1.0 \pm 0.4$	[405]	$8.4^{+1.5}_{-1.2} \pm 0.9$	[955]	$43.8^{+7.1}_{-6.3}$
366	$K^+\eta'\gamma$	$2.9^{+1.0}_{-0.9}$	$1.9^{+1.5}_{-1.2} \pm 0.1$	[956]	$3.6 \pm 1.2 \pm 0.4$	[957]	$7.9 \pm 0.9$
367	$K^+\phi\gamma$	$2.7 \pm 0.4$	$3.5 \pm 0.6 \pm 0.4$	[958]	$2.48 \pm 0.30 \pm 0.24$	[406]	$2.9^{+1.0}_{-0.9}$
368	$K^+\pi^-\pi^+\gamma$	$27.6 \pm 2.2$	$24.5 \pm 0.9 \pm 1.2^\dagger$	[401]	$25.0 \pm 1.8 \pm 2.2^\ddagger$	[954]	$2.71 \pm 0.34$
369	$K^{*0}\pi^+\gamma$ §	$20^{+7}_{-6}$	$23.4 \pm 0.9^{+0.8}_{-0.7} \pm 1$	[401]	$20^{+7}_{-6} \pm 2$	[959]	$24.6 \pm 1.3$
370	$K^+\rho^0\gamma$ §	$< 20$	$8.2 \pm 0.4 \pm 0.8^\dagger$	[401]	$< 20$	[959]	$23.3^{+1.2}_{-1.1}$
	$(K\pi)_0^*\pi^+\gamma$		$10.3^{+0.7+1.5}_{-0.8-2.0} \pm 1$	[401]			$8.2 \pm 0.9$
371	$K^+\pi^-\pi^+\gamma$ (N.R.) §	$< 9.2$	$9.9 \pm 0.7^{+1.5}_{-1.9} \pm 1$	[401]	$< 9.2$	[959]	$10.3^{+1.7}_{-2.2}$
	$K_0^*(1430)\pi^+\gamma$		$1.32^{+0.09+0.24}_{-0.10-0.30} \pm 1$	[401]			$9.9^{+1.7}_{-2.0}$
372	$K^0\pi^+\pi^0\gamma$	$46 \pm 5$	$45.6 \pm 4.2 \pm 3.1^\dagger$	[960]			$1.32^{+0.26}_{-0.32}$
373	$K_1^+(1400)\gamma$	$< 15$	$9.7^{+4.6+2.9}_{-2.9-2.4} \pm 1$	[401]	$< 15$	[954]	$45.6 \pm 5.2$
	$K^{*+}(1410)\gamma$		$27.1^{+5.4+5.9}_{-4.8-3.7} \pm 1$	[401]			$9.7^{+5.4}_{-3.8}$
374	$K_2^*(1430)^+\gamma$	$14 \pm 4$	$8.7^{+7.0+8.7}_{-5.3-10.4} \pm 1$	[401]			$27.1^{+8.0}_{-6.1}$
375	$K^{*+}(1680)\gamma$	$< 1900$	$66.7^{+9.3+14.4}_{-7.8-11.4} \pm 1$	[401]			$8.7^{+11.2}_{-11.7}$
376	$K_3^*(1780)^+\gamma$	$< 39$					$66.7^{+17.1}_{-13.8}$
378	$\rho^+\gamma$	$0.98 \pm 0.25$	$1.20^{+0.42}_{-0.37} \pm 0.20$	[961]	$0.87^{+0.29+0.09}_{-0.27-0.11}$	[955]	$< 39$
428	$p\overline{\Lambda}\gamma$		$2.4^{+0.5}_{-0.4}$		$2.45^{+0.44}_{-0.38} \pm 0.22$	[915]	$0.98^{+0.25}_{-0.24}$
432	$p\overline{\Sigma}^0\gamma$	$< 4.6$			$< 4.6$	[963]	$2.45^{+0.49}_{-0.44}$
467	$\pi^+\ell^+\ell^-$	$< 0.049$	$< 0.066$	[964]	$< 0.049$	[965]	$< 4.6$
468	$\pi^+e^+e^-$	$< 0.080$	$< 0.125$	[964]	$< 0.080$	[965]	$< 0.049$
469	$\pi^+\mu^+\mu^-$	$< 0.055$	$< 0.055$	[964]	$< 0.069$	[965]	$< 0.080$
470	$\pi^+\nu\bar{v}$	$< 98$	$< 100$	[967]	$< 98$	[968]	$0.55 \pm 0.07$
471	$K^+\ell^+\ell^-$	$0.451 \pm 0.023$	$0.48 \pm 0.09 \pm 0.02$	[969]	$0.53^{+0.06}_{-0.05} \pm 0.03$	[970]	$0.51 \pm 0.05$
472	$K^+e^+e^-$	$0.55 \pm 0.07$	$0.51^{+0.12}_{-0.11} \pm 0.02$	[969]	$0.57^{+0.09}_{-0.08} \pm 0.03$	[970]	$0.55 \pm 0.07$
473	$K^+\mu^+\mu^-$	$0.449 \pm 0.023$	$0.41^{+0.16}_{-0.15} \pm 0.02$	[969]	$0.53 \pm 0.08^{+0.07}_{-0.03}$	[970]	$0.429 \pm 0.007 \pm 0.021$
	$K^+\tau^+\tau^-$		$< 2250$	[972]			$< 2250$

Table 234 continued

RPP#	Mode	PDG2014 Avg.	BABAR	Belle	CLEO	LHCb	Our Avg.
476	$K^+\nu\bar{\nu}$	< 16	[973]	< 55	[968]		< 16
477	$\rho^+\nu\bar{\nu}$	< 213		< 213	[968]		< 213
478	$K^{*+}\ell^+\ell^-$	$1.29 \pm 0.21$	$1.40^{+0.40}_{-0.37} \pm 0.09$	[969]	$1.24^{+0.23}_{-0.21} \pm 0.13$	[970]	$1.29^{+0.22}_{-0.21}$
479	$K^{*+}e^+e^-$	$1.55^{+0.40}_{-0.31}$	$1.38^{+0.47}_{-0.42} \pm 0.08$	[969]	$1.73^{+0.50}_{-0.42} \pm 0.20$	[970]	$1.55^{+0.35}_{-0.32}$
480	$K^{*+}\mu^+\mu^-$	$1.12 \pm 0.15$	$1.46^{+0.79}_{-0.75} \pm 0.12$	[969]	$1.11^{+0.32}_{-0.27} \pm 0.10$	[970]	$0.958^{+0.107}_{-0.104}$
481	$K^{*+}\nu\bar{\nu}$	< 40		< 40	[968]		< 40
	$K^+\pi^+\pi^-\mu^+\mu^-$				$0.436^{+0.029}_{-0.027} \pm 0.028$ <sup>2</sup>	[975]	$0.436^{+0.040}_{-0.039}$
	$K^+\phi\mu^+\mu^-$				$0.082^{+0.019}_{-0.017} \pm 0.029$ <sup>2</sup>	[975]	$0.082^{+0.035}_{-0.032}$

Results for LHCb are relative BFs converted to absolute BFs.

CLEO upper limits that have been greatly superseded are not shown.

<sup>†</sup>  $M_{K\pi\pi} < 1.8 \text{ GeV}/c^2$ .

<sup>‡</sup>  $1.0 < M_{K\pi\pi} < 2.0 \text{ GeV}/c^2$ .

<sup>§</sup>  $M_{K\pi\pi} < 2.4 \text{ GeV}/c^2$ .

<sup>1</sup> PDG2014 cites only the measurement:  $\mathcal{B}(\pi^+\mu^+\mu^-)/\mathcal{B}(K^+\mu^+\mu^-) = 0.053 \pm 0.014 \pm 0.01$ .

<sup>2</sup> Differential BF in bins of  $m(\mu^+\mu^-)$  is also available.

**Table 235** Branching fractions of charmless semileptonic  $B^+$  decays to LFV and LNV final states in units of  $\times 10^{-6}$ . Upper limits are at 90% CL. Where values are shown in red (blue), this indicates that they are new published (preliminary) results since PDG2014

RPP#	Mode	PDG2014 Avg.	BABAR	LHCb	Our Avg.
484	$\pi^+ e^\pm \mu^\mp$	< 0.17	< 0.17	[976]	< 0.17
485	$\pi^+ e^+ \tau^-$	< 74	< 74	[977]	< 74
486	$\pi^+ e^- \tau^+$	< 20	< 20	[977]	< 20
487	$\pi^+ e^\pm \tau^\mp$	< 75	< 75	[977]	< 75
488	$\pi^+ \mu^+ \tau^-$	< 62	< 62	[977]	< 62
489	$\pi^+ \mu^- \tau^+$	< 45	< 45	[977]	< 45
490	$\pi^+ \mu^\pm \tau^\mp$	< 72	< 72	[977]	< 72
491	$K^+ e^+ \mu^-$	< 0.091	< 0.091	[978]	< 0.091
492	$K^+ e^- \mu^+$	< 0.13	< 0.13	[978]	< 0.13
493	$K^+ e^\pm \mu^\mp$	< 0.091	< 0.091	[978]	< 0.091
494	$K^+ e^+ \tau^-$	< 43	< 43	[977]	< 43
495	$K^+ e^- \tau^+$	< 15	< 15	[977]	< 15
496	$K^+ e^\pm \tau^\mp$	< 30	< 30	[977]	< 30
497	$K^+ \mu^+ \tau^-$	< 45	< 45	[977]	< 45
498	$K^+ \mu^- \tau^+$	< 28	< 28	[977]	< 28
499	$K^+ \mu^\pm \tau^\mp$	< 48	< 48	[977]	< 48
500	$K^{*+} e^+ \mu^-$	< 1.3	< 1.3	[978]	< 1.3
501	$K^{*+} e^- \mu^+$	< 0.99	< 0.99	[978]	< 0.99
502	$K^{*+} e^\pm \mu^\mp$	< 1.4	< 1.4	[978]	< 1.4
503	$\pi^- e^+ e^+$	< 0.023	< 0.023	[979]	< 0.023
504	$\pi^- \mu^+ \mu^+$	< 0.013	< 0.107	[979] < 0.004 <sup>†</sup>	[980] < 0.004
505	$\pi^- e^+ \mu^+$	< 0.15	< 0.15	[981]	< 0.15
506	$\rho^- e^+ e^+$	< 0.17	< 0.17	[981]	< 0.17
507	$\rho^- \mu^+ \mu^+$	< 0.42	< 0.42	[981]	< 0.42
508	$\rho^- e^+ \mu^+$	< 0.47	< 0.47	[981]	< 0.47
509	$K^- e^+ e^+$	< 0.03	< 0.03	[979]	< 0.03
510	$K^- \mu^+ \mu^+$	< 0.041	< 0.067	[979] < 0.041	[982] < 0.041
511	$K^- e^+ \mu^+$	< 0.16	< 0.16	[981]	< 0.16
512	$K^{*-} e^+ e^+$	< 0.40	< 0.40	[981]	< 0.40
513	$K^{*-} \mu^+ \mu^+$	< 0.59	< 0.59	[981]	< 0.59
514	$K^{*-} e^+ \mu^+$	< 0.30	< 0.30	[981]	< 0.30

Results for LHCb are relative BFs converted to absolute BFs.

CLEO upper limits that have been greatly superseded are not shown.

<sup>†</sup> UL at 95% CL.

**Table 236** Branching fractions of charmless semileptonic and radiative  $B^0$  decays in units of  $\times 10^{-6}$ . Upper limits are at 90% CL. Where values are shown in red (blue), this indicates that they are new published (preliminary) results since PDG2014

RPP#	Mode	PDC2014 Avg.	BABAR	Belle	CLEO	LHCb	Our Avg.
336	$K^0 \eta \gamma$	7.6±1.8	7.1 $^{+2.0}_{-2.0}$ ±0.4	[405]	8.7 $^{+3.1+1.9}_{-2.7-1.6}$	[955]	7.6 $^{+1.8}_{-1.7}$
337	$K^0 \eta' \gamma$	< 6.4	< 6.6	[956]	< 6.4	[957]	< 6.4
338	$K^0 \phi \gamma$	2.7±0.7	< 2.7	[558]	2.74±0.60±0.32	[406]	2.74±0.68
339	$K^+ \pi^- \gamma$ §	4.6±1.4			4.6 $^{+1.3+0.5}_{-1.2-0.7}$	[959]	4.6±1.4
340	$K^{*0} \gamma$	43.3±1.5	44.7±1.0±1.6	[951]	40.1±2.1±1.7	[952]	43.3±1.5
341	$K^*(1410)^0 \gamma$	< 130			< 130	[959]	< 130
342	$K^+ \pi^- \gamma$ (N.R.) §	< 2.6			< 2.6	[959]	< 2.6
344	$K^0 \pi^+ \pi^- \gamma$	19.5±2.2	18.5±2.1±1.2 †	[960]	24±4±3 ‡	[954]	19.5±2.2
345	$K^+ \pi^- \pi^0 \gamma$	41±4	40.7±2.2±3.1 †	[960]			40.7±3.8
346	$K_1^0(1270)\gamma$	< 58			< 58	[954]	< 58
347	$K_1^0(1400)\gamma$	< 12			< 12	[954]	< 12
348	$K_2^*(1430)^0 \gamma$	12.4±2.4	12.2±2.5±1.0	[983]	13±5±1	[959]	12.4±2.4
350	$K_3^*(1780)^0 \gamma$	< 83			< 83	[955]	< 83
352	$\rho^0 \gamma$	0.86±0.15	0.97 $^{+0.24}_{-0.22}$ ±0.06	[961]	0.78 $^{+0.17+0.09}_{-0.16-0.10}$	[962]	0.86 $^{+0.15}_{-0.14}$
354	$\omega \gamma$	0.44 $^{+0.18}_{-0.16}$	0.50 $^{+0.27}_{-0.23}$ ±0.09	[961]	0.40 $^{+0.19}_{-0.17}$ ±0.13	[962]	0.44 $^{+0.18}_{-0.16}$
355	$\phi \gamma$	< 0.85	< 0.85	[984]	< 0.1	[985]	< 0.1
	$p\bar{\Lambda}\pi^-\gamma$				< 0.65	[986]	< 0.65
465	$\pi^0 \ell^+ \ell^-$	< 0.053	< 0.053	[964]	< 0.154	[965]	< 0.053
466	$\pi^0 e^+ e^-$	< 0.084	< 0.084	[964]	< 0.227	[965]	< 0.084
467	$\pi^0 \mu^+ \mu^-$	< 0.069	< 0.069	[964]	< 0.184	[965]	< 0.069
468	$\eta \ell^+ \ell^-$	< 0.064	< 0.064	[964]			< 0.064
469	$\eta e^+ e^-$	< 0.108	< 0.108	[964]			< 0.108
470	$\eta \mu^+ \mu^-$	< 0.112	< 0.112	[964]			< 0.112
471	$\pi^0 \nu \bar{\nu}$	< 69			< 69	[968]	< 69
472	$K^0 \ell^+ \ell^-$	0.31 $^{+0.08}_{-0.07}$	0.21 $^{+0.15}_{-0.13}$ ±0.02	[969]	0.34 $^{+0.09}_{-0.08}$ ±0.02	[970]	0.31 $^{+0.08}_{-0.07}$
473	$K^0 e^+ e^-$	0.16 $^{+0.10}_{-0.08}$	0.08 $^{+0.15}_{-0.12}$ ±0.01	[969]	0.20 $^{+0.14}_{-0.10}$ ±0.01	[970]	0.16 $^{+0.10}_{-0.08}$
474	$K^0 \mu^+ \mu^-$	0.34±0.05	0.49 $^{+0.29}_{-0.25}$ ±0.03	[969]	0.44 $^{+0.13}_{-0.10}$ ±0.03	[970]	0.343 $^{+0.036}_{-0.035}$
475	$K^0 \nu \bar{\nu}$	< 49	< 49	[973]	< 194	[968]	< 49
476	$\rho^0 \nu \bar{\nu}$	< 208			< 208	[968]	< 208
477	$K^{*0} \ell^+ \ell^-$	0.99 $^{+0.12}_{-0.11}$	1.03 $^{+0.22}_{-0.21}$ ±0.07	[969]	0.97 $^{+0.13}_{-0.11}$ ±0.07	[970]	0.99 $^{+0.13}_{-0.11}$
478	$K^{*0} e^+ e^-$	1.03 $^{+0.19}_{-0.17}$	0.86 $^{+0.26}_{-0.24}$ ±0.05	[969]	1.18 $^{+0.27}_{-0.22}$ ±0.09	[970]	1.03 $^{+0.19}_{-0.17}$
479	$K^{*0} \mu^+ \mu^-$	1.05±0.10	1.35 $^{+0.40}_{-0.37}$ ±0.10	[969]	1.06 $^{+0.19}_{-0.14}$ ±0.07	[970]	1.049 $^{+0.067}_{-0.065}$
480	$K^{*0} \nu \bar{\nu}$	< 55	< 120	[973]	< 55	[968]	< 55

**Table 236** continued

RPP#	Mode	PDG2014 Avg.	BABAR	Belle	CLEO	LHCb	Our Avg.
481	$\phi\nu\nu$	< 127	< 127 [968]	< 127 [968]	<b>0.0211±0.0051±0.0022</b> <sup>1</sup>	[933]	< 127
	$\pi^+\pi^-\mu^+\mu^-$						$0.0210\pm 0.0060$
483	$\pi^0e^\pm\mu^\mp$	< 0.14	< 0.14 [976]	< 0.14 [976]			< 0.14
484	$K^0e^\pm\mu^\mp$	< 0.27	< 0.27 [978]	< 0.27 [978]			< 0.27
485	$K^{*0}e^\pm\mu^\mp$	< 0.53	< 0.53 [978]	< 0.53 [978]			< 0.53

Results for LHCb are relative BFs converted to absolute BFs.

CLEO upper limits that have been greatly superseded are not shown.

<sup>†</sup>  $M_{K\pi\pi} < 1.8 \text{ GeV}/c^2$ .

<sup>‡</sup>  $1.0 < M_{K^*\pi\pi} < 2.0 \text{ GeV}/c^2$ .

<sup>§</sup>  $1.25 < M_{K\pi} < 1.60 \text{ GeV}/c^2$ .

<sup>¶</sup> This result takes into account the S-wave fraction in the  $K\pi$  system.  
<sup>1</sup> Muon pairs do not originate from resonances and  $0.5 < m(\pi^+\pi^-) < 1.3 \text{ GeV}/c^2$ .

**Table 237** Branching fractions of charmless semileptonic and radiative decays of  $B^\pm/B^0$  admixture in units of  $\times 10^{-6}$ . Upper limits are at 90% CL. Where values are shown in red (blue), this indicates that they are new published (preliminary) results since PDG2014

RPP#	Mode	PDG2014 Avg.	BABAR	Belle	CLEO	CDF	Our Avg.
66	$K\eta\gamma$	$8.5^{+1.8}_{-1.6}$		$8.5^{+1.3}_{-1.2}\pm 0.9$	[955]	$17\pm 6\pm 1$	[953]
68	$K_2^*(1430)\gamma$	$17^{+6}_{-5}$		$< 2.8^{\dagger}$	[955]		$17\pm 6$
70	$K_3^*(1780)\gamma$	$< 37$		[988–990]	$328^{+20}_{-16}{}^{\dagger}$	$329\pm 44\pm 29$	[519]
77	$s\gamma^\pm$	$340\pm 21$	$341\pm 28{}^{\dagger}$	[988–990]	$305\pm 16{}^{\dagger}$	[991,992]	$332\pm 15$
77	$s\gamma^2$		$9.2\pm 3.0$	$9.2\pm 2.0\pm 2.3$	[993]		$306\pm 13$
78	$d\gamma$	$1.39\pm 0.25$		$1.73^{+0.34}_{-0.32}\pm 0.17$	[961]	$1.21^{+0.24}_{-0.22}\pm 0.12$	$9.2\pm 3.0$
84	$\rho\gamma$			$1.63^{+0.30}_{-0.28}\pm 0.16$	[961]	$1.14\pm 0.20^{+0.10}_{-0.12}$	$1.39^{+0.22}_{-0.21}$
85	$\rho/\omega\gamma$	$1.30\pm 0.23$		$7.69^{+0.82\pm 0.71}_{-0.77\pm 0.60}$	[994]		$1.30^{+0.18}_{-0.19}$
119	$se^+e^-{}^{\ddagger}$	$4.7\pm 1.3$		$4.41^{+1.31\pm 0.63}_{-1.17\pm 0.50}$	[994]		$7.69^{+0.08}_{-0.98}$
120	$s\mu^+\mu^-{}^{\ddagger}$	$4.3\pm 1.2$		$6.73^{+0.70\pm 0.60}_{-0.64\pm 0.56}$	[994]		$4.41^{+1.45}_{-1.27}$
121	$s\ell^+\ell^-{}^{\ddagger}$	$4.5\pm 1.0$		$< 0.059$	[964]	$< 0.062$	$6.73^{+0.92}_{-0.85}$
122	$\pi\ell^+\ell^-$	$< 0.059$		$< 0.110$	[964]		$< 0.059$
123	$\pi e^+e^-$			$< 0.050$	[964]		$< 0.110$
124	$\pi\mu^+\mu^-$			$0.39^{+0.09}_{-0.08}\pm 0.02$	[969]	$0.48^{+0.08}_{-0.07}\pm 0.03$	$< 0.050$
125	$Ke^+e^-$	$0.44\pm 0.06$		$0.99^{+0.23}_{-0.21}\pm 0.06$	[969]	$1.39^{+0.23}_{-0.20}\pm 0.12$	$0.44\pm 0.06$
126	$K^*e^+e^-$	$1.19\pm 0.20$		$0.41^{+0.13}_{-0.12}\pm 0.02$	[969]	$0.50\pm 0.06\pm 0.03$	$1.19^{+0.17}_{-0.16}$
127	$K\mu^+\mu^-$	$0.44\pm 0.04$		$1.35^{+0.35}_{-0.33}\pm 0.10$	[969]	$1.10^{+0.16}_{-0.14}\pm 0.08$	$0.42\pm 0.04\pm 0.02$
128	$K^*\mu^+\mu^-$	$1.06\pm 0.09$		$0.47\pm 0.06\pm 0.02$	[995]	$0.48^{+0.05}_{-0.04}\pm 0.03$	$1.01\pm 0.10\pm 0.05$
129	$K\ell^+\ell^-$	$0.48\pm 0.04$		$1.05\pm 0.10$	[995]	$1.07^{+0.11}_{-0.10}\pm 0.09$	$1.01\pm 0.10\pm 0.05$
130	$K^*\ell^+\ell^-$			$< 17$	[973]		$1.05\pm 0.10$
131	$Kv\bar{v}$			$< 76$	[973]		$< 17$
132	$K^*v\bar{v}$			$< 0.092$	[976]		$< 76$
134	$\pi e^\pm\mu^\mp$			$< 3.2$			$< 0.092$
135	$\rho e^\pm\mu^\mp$			$< 0.038$	[978]		$< 3.2$
136	$Ke^\pm\mu^\mp$			$< 0.51$	[978]		$< 0.038$
137	$K^*e^\pm\mu^\mp$					$< 3.2$	$< 0.51$

Results for CDF are relative BF<sub>S</sub> converted to absolute BF<sub>S</sub>.

CLEO upper limits that have been greatly superseded are not shown.

<sup>†</sup> Results extrapolated to  $E_\gamma > 1.6$  GeV, using the method of Ref. [997].

<sup>‡</sup> Belle:  $m(\ell^+\ell^-) > 0.2$  GeV/ $c^2$ , BABar:  $m^2(\ell^+\ell^-) > 0.1$  GeV $^2/c^4$ .

<sup>§</sup> The value quoted is  $\mathcal{B}(B \rightarrow K_3^*\gamma) \times \mathcal{B}(K_3^* \rightarrow K\eta)$ . PDG gives the BF assuming  $\mathcal{B}(K_3^* \rightarrow K\eta) = 11^{+5}_{-4}\%$ .

<sup>1</sup> Average of several results, obtained with different methods.

<sup>2</sup> Only results originally measured in the interval  $E_\gamma > 1.9$  GeV (also taken into account in the previous line).

**Table 238** Branching fractions of leptonic and radiative-leptonic  $B^+$  and  $B^0$  decays in units of  $\times 10^{-6}$ . Upper limits are at 90% CL. Where values are shown in red (blue), this indicates that they are new published (preliminary) results since PDG2014

RPP#	Mode	PDG2014 Avg.	BABAR	Belle	CDF	LHCb	CMS	ATLAS	Our Avg.
29	$e^+\nu$	< 0.98	< 1.9	[998]	< 0.98 <sup>†</sup>	[999]			< 0.98 <sup>†</sup>
30	$\mu^+\nu$	< 1.0	< 1.0	[998]	< 1.7 <sup>†</sup>	[999]			< 1.0
31	$\tau^+\nu$	114±27	179±48 <sup>‡</sup>	[1000]	<b>91±19±11<sup>‡</sup></b>	[1001]			106±19
32	$\ell^+\nu_\ell\gamma$	< 15.6	< 15.6	[1002]	< 3.5	[1003]			< 3.5
33	$e^+\nu_e\gamma$	< 17	< 17	[1002]	<b>&lt; 6.1</b>	[1003]			< 6.1
34	$\mu^+\nu_\mu\gamma$	< 24	< 24	[1002]	<b>&lt; 3.4</b>	[1003]			< 3.4
457	$\gamma\gamma$	< 0.32	< 0.32	[1004]	< 0.62	[1005]			< 0.32
458	$e^+e^-$	< 0.083	< 0.113	[1006]	< 0.19	[1007]	< 0.083	[944]	< 0.083
459	$e^+e^-\gamma$	< 0.12	< 0.12	[1008]					< 0.12
460	$\mu^+\mu^-$	< 0.00063	< 0.052	[1006]	< 0.16	[1007]	< 0.0038	[939]	< 0.00042 <sup>¶</sup>
461	$\mu^+\mu^-\gamma$	< 0.16	< 0.16	[1008]					[943]
462	$\mu^+\mu^-\mu^+\mu^-$	< 0.0053					< 0.0053	[946]	$0.00039^{+0.00016}_{-0.00014}$ <sup>§</sup>
464	$\tau^+\tau^-$	< 4100	< 4100	[1009]					< 0.16
482	$e^\pm\mu^\mp$	< 0.0028	< 0.092	[1006]	< 0.17	[1007]	< 0.064	[944]	< 0.0028
488	$e^\pm\tau^\mp$	< 28	< 28	[1010]					< 28
489	$\mu^\pm\tau^\mp$	< 22	< 22	[1010]					< 22
490	$\nu\bar{\nu}$	< 24	< 24	[1011]	< 130	[1012]			< 24
491	$\nu\bar{\nu}\gamma$	< 17	< 17	[1011]					< 17

Results for CDF, LHCb, CMS and ATLAS are relative BFs converted to absolute BFs.

<sup>†</sup> More recent results exist, with hadronic tagging [013], which do not improve the limits ( $< 3.5$  and  $< 2.7$ ) for  $e^+\nu$  and  $\mu^+\nu$ , respectively).

<sup>‡</sup> The authors make the average with their previous results, derived from statistically independent samples [1014, 1015].

<sup>¶</sup> This is the combined result obtained by the LHCb and CMS collaborations [950].

<sup>§</sup> UL at 95% CL.

**Table 239** Relative branching fractions of semileptonic and radiative  $B^+$  decays. Where values are shown in red (blue), this indicates that they are new published (preliminary) results since PDG2014

RPP#	Mode	PDG2014 AVG.	Belle	$B_{ABAR}$	LHCb	Our Avg.
	$10^4 \times \mathcal{B}(K^+ \pi^+ \pi^- \mu^+ \mu^-) / \mathcal{B}(\psi(2S) K^+)$			<b>6.95<sup>+0.46</sup><sub>-0.43</sub>±0.34</b>	[975]	<b>6.95<sup>+0.57</sup><sub>-0.55</sub></b>
	$10^4 \times \mathcal{B}(K^+ \phi \mu^+ \mu^-) / \mathcal{B}(\psi(2S) K^+)$			<b>1.58<sup>+0.36</sup><sub>-0.32</sub><sup>+0.19</sup><sub>-0.07</sub></b>	[975]	<b>1.58<sup>+0.41</sup><sub>-0.33</sub></b>
469	$\mathcal{B}(\pi^+ \mu^+ \mu^-) / \mathcal{B}(K^+ \mu^+ \mu^-)^\dagger$	$0.053 \pm 0.014 \pm 0.01$		<b>0.038 ± 0.009 ± 0.001</b>	[966]	<b>0.038 ± 0.009</b>
473	$\mathcal{B}(K^+ \mu^+ \mu^-) / \mathcal{B}(K^+ e^+ e^-)^\ddagger$			<b>0.745<sup>+0.090</sup><sub>-0.074</sub>±0.036</b>	[1016]	<b>0.745<sup>+0.097</sup><sub>-0.082</sub></b>
473	$\mathcal{B}(K^+ \mu^+ \mu^-) / \mathcal{B}(K^+ e^+ e^-)^\S$	$1.03 \pm 0.19 \pm 0.06$	[970]			$1.03 \pm 0.20$
473	$\mathcal{B}(K^+ \mu^+ \mu^-) / \mathcal{B}(K^+ e^+ e^-)^\P$	$0.83 \pm 0.17 \pm 0.08$	[970]	$1.00+0.31-0.25±0.07$	[995]	$1.00+0.32-0.26$
	$\mathcal{B}(K^* \mu^+ \mu^-) / \mathcal{B}(K^* e^+ e^-)^\S$			$1.013+0.34-0.26±0.010$	[995]	$0.83 \pm 0.19$
	$\mathcal{B}(K^* \mu^+ \mu^-) / \mathcal{B}(K^* e^+ e^-)^\P$					$1.013+0.340-0.260$

<sup>†</sup> For  $0.1 < m^2(\ell^+ \ell^-) < 6.0 \text{ GeV}^2/c^4$ .

<sup>‡</sup> For  $1.0 < m^2(\ell^+ \ell^-) < 6.0 \text{ GeV}^2/c^4$ .

<sup>§</sup> For the full  $m^2(\ell^+ \ell^-)$  range.

<sup>¶</sup> For  $0.10 < m^2(\ell^+ \ell^-) < 8.12 \text{ GeV}^2/c^4$  and  $m^2(\ell^+ \ell^-) > 10.11 \text{ GeV}^2/c^4$ .

**Table 240** Branching fractions of  $B^+ / B^0 \rightarrow \bar{q}$  gluon decays in units of  $\times 10^{-6}$ . Upper limits are at 90% CL. Where values are shown in red (blue), this indicates that they are new published (preliminary) results since PDG2014

RPP#	Mode	PDG2014 Avg.	BABAR	Belle	CLEO	Our Avg.
80	$\eta X$	$260^{+50}_{-80}$	$390 \pm 80 \pm 90^\dagger$	[1019]	$261 \pm 30^{+44}_{-74} \S$	[1018]
81	$\eta' X$	$420 \pm 90$	$< 187^\ddagger$	[1021]	$460 \pm 110 \pm 60^\dagger$	[1020]
82	$K^+ X$	$< 187$	$195^{+51}_{-67} \pm 50^\ddagger$	[1021]	$< 187$	$195^{+71}_{-67}$
83	$K^0 X$	$195^{+71}_{-67}$	$372^{+50}_{-47} \pm 59 \S$	[1021]	$372^{+77}_{-75}$	
94	$\pi^+ X$	$370 \pm 80$				

$\dagger 2.0 < p^*(\eta) < 2.7 \text{ GeV}/c$ .

$\ddagger m_X < 1.69 \text{ GeV}/c^2$ .

$\S 0.4 < m_X < 2.6 \text{ GeV}/c^2$ .

$\S m_X < 1.71 \text{ GeV}/c^2$ .

**Table 241** Isospin asymmetry in radiative and semileptonic  $B$  meson decays. The notations are those adopted by the PDG. Where values are shown in red (blue), this indicates that they are new published (preliminary) results since PDG2014

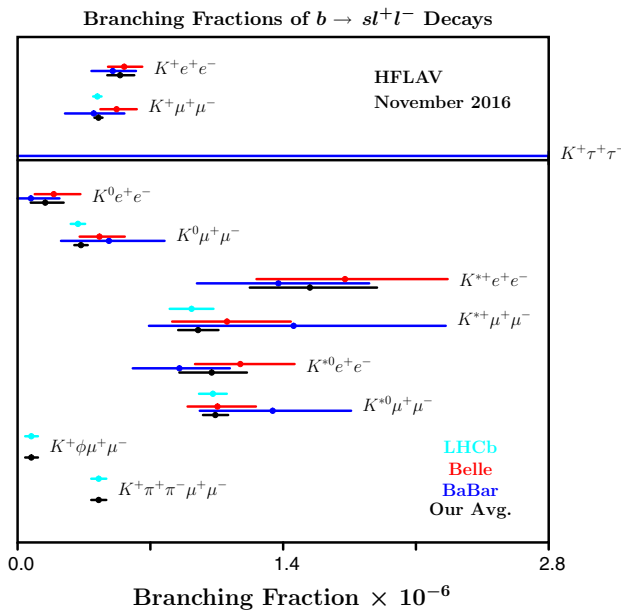
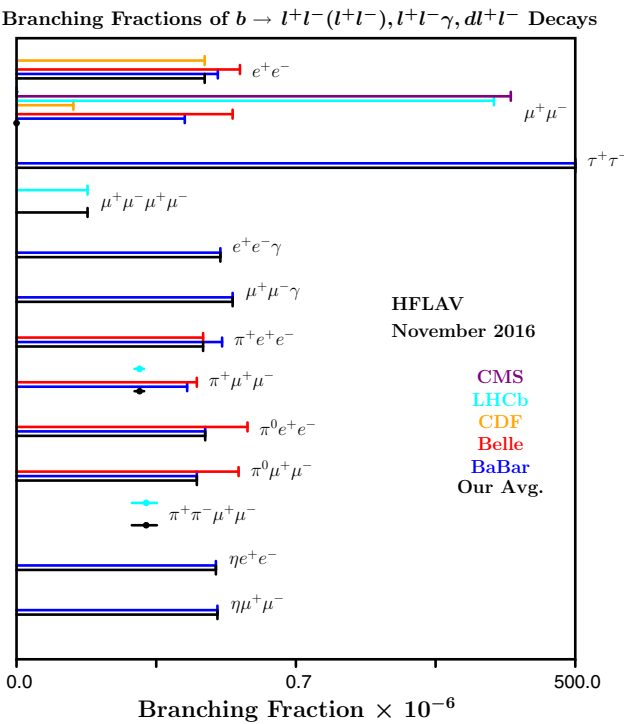
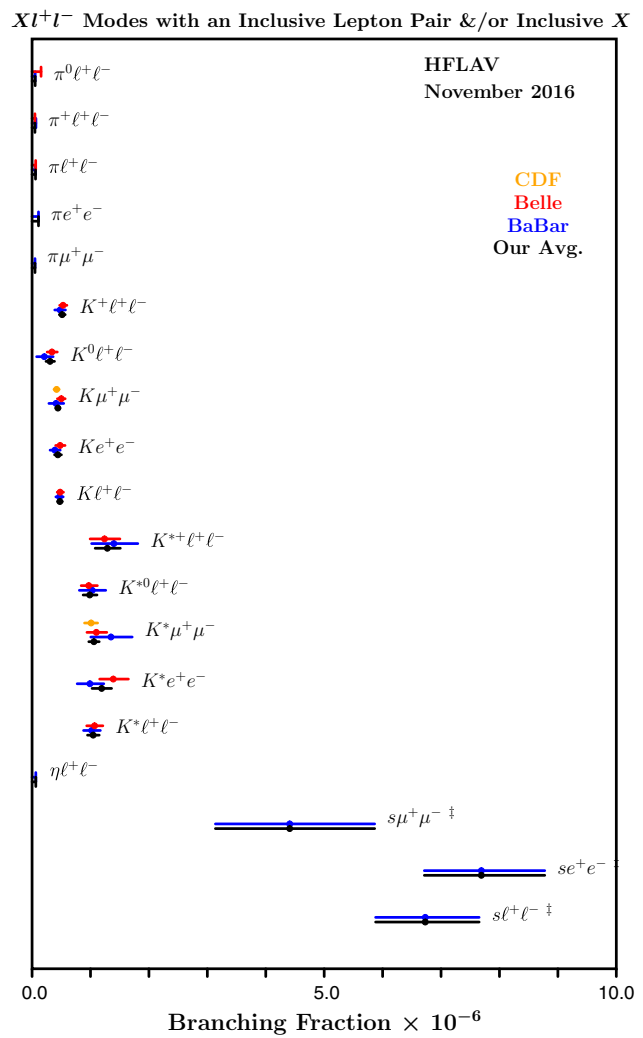
Parameter	PDG2014 Avg.	BABAR	Belle	LHCb	Our Avg.
$\Delta_{0^-}(X_s \gamma)$	$-0.01 \pm 0.06$	$-0.01 \pm 0.06^\ddagger$	[516, 988]		$-0.01 \pm 0.06$
$\Delta_{0^+}(K^* \gamma)$	$0.052 \pm 0.026$	$0.066 \pm 0.021 \pm 0.022$	[951]	$0.012 \pm 0.044 \pm 0.026$	$0.052 \pm 0.026$
$\Delta_{\rho\gamma}$	$-0.46 \pm 0.17$	$-0.43^{+0.25}_{-0.22} \pm 0.10$	[961]	$-0.48^{+0.21}_{-0.19} \pm 0.08$	$-0.46^{+0.17}_{-0.16}$
$\Delta_0 - (K \ell \ell)^\dagger$	$-0.37 \pm 0.13$	$-0.41 \pm 0.25 \pm 0.01$	[995]	$-0.41^{+0.25}_{-0.20} \pm 0.07$	$-0.16 \pm 0.08$
$\Delta_0 - (K^* \ell \ell)^\dagger$	$-0.22 \pm 0.10$	$-0.20^{+0.30}_{-0.23} \pm 0.03$	[995]	$0.33^{+0.37}_{-0.43} \pm 0.08$	$0.00^{+0.12}_{-0.10} \pm 0.02 \S$
			[970]	[974]	[974]

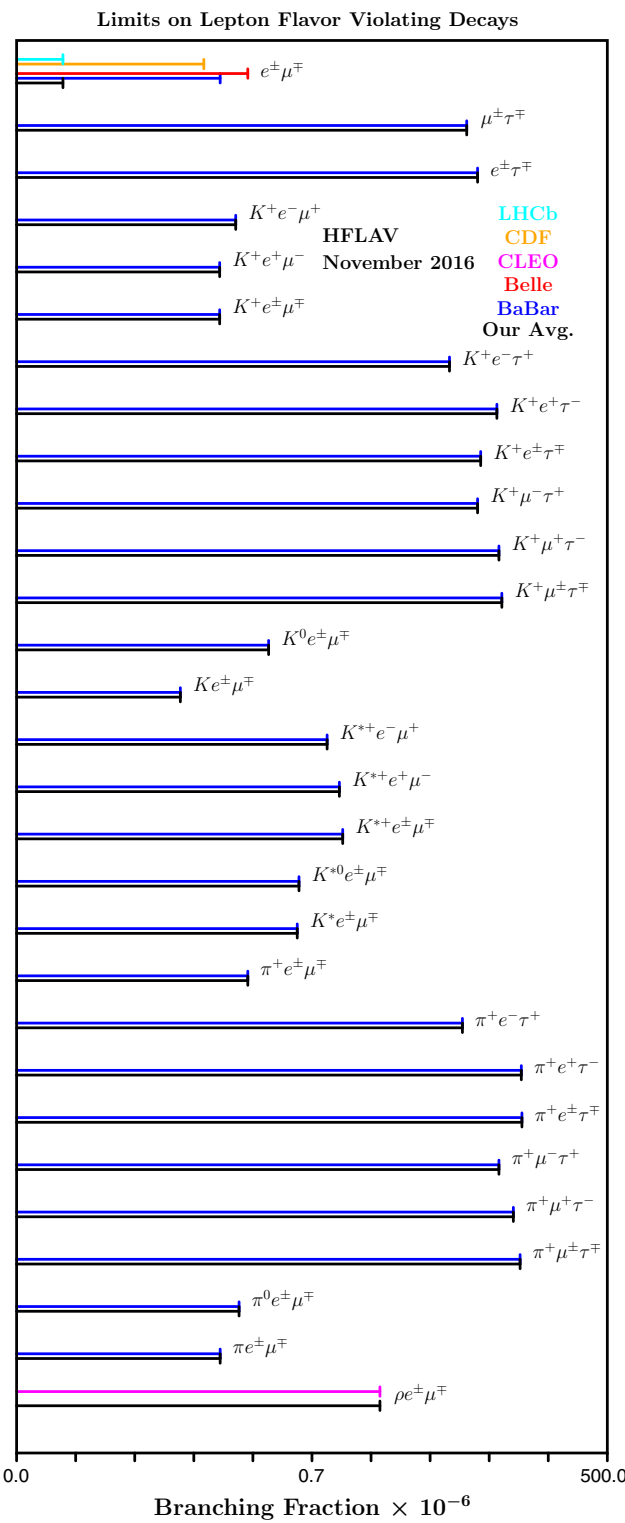
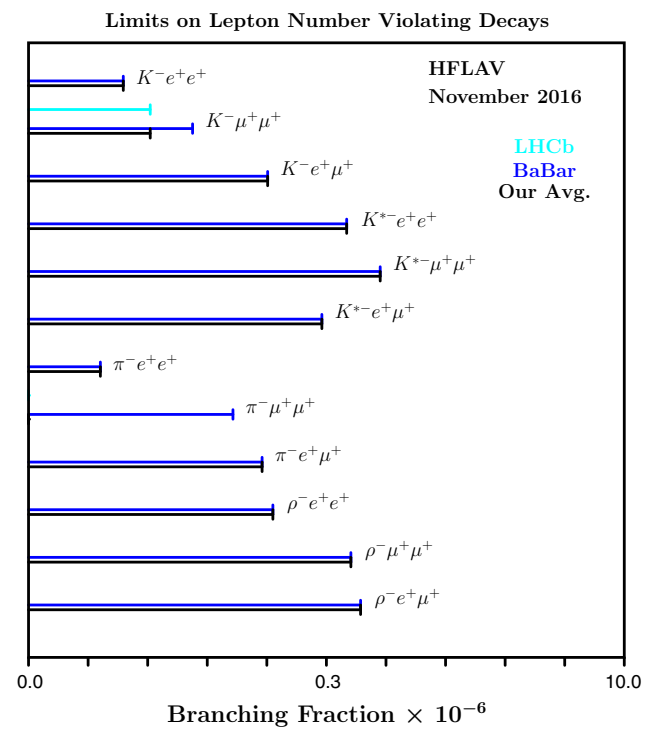
In some of the  $B$ -factory results it is assumed that  $\mathcal{B}(T(4S) \rightarrow B^+ B^-) = \mathcal{B}(T(4S) \rightarrow B^0 \bar{B}^0)$ , and in others a measured value of the ratio of branching fractions is used. See original papers for details. The averages quoted above are computed naively and should be treated with caution.

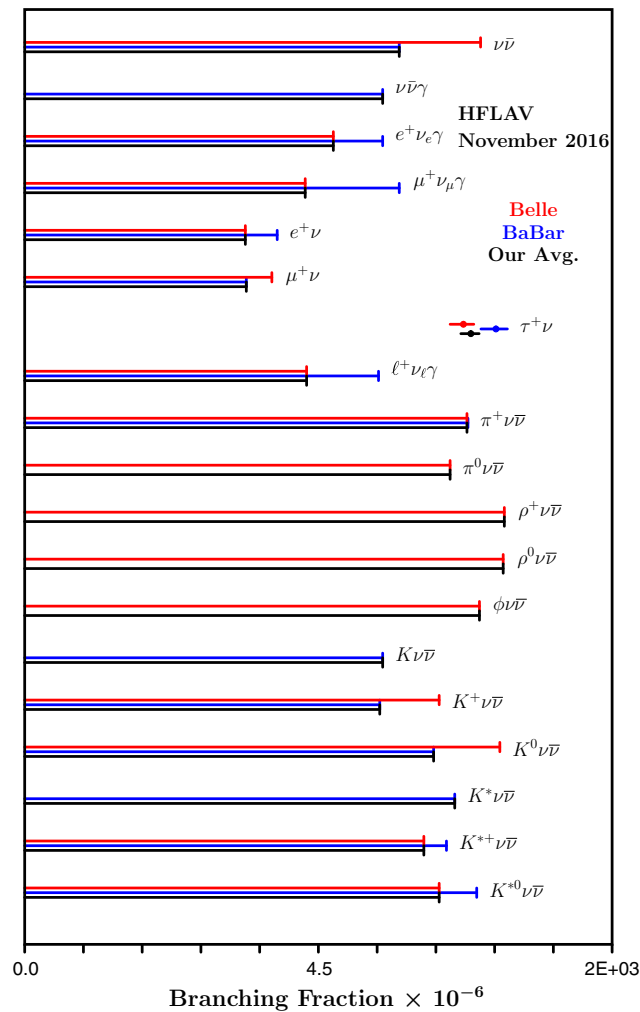
$\dagger$  Results given for the bin  $1 < m^2(\ell^+ \ell^-) < 6 \text{ GeV}^2/c^4$ , see references for the other bins.

$\ddagger$  Average of two independent measurements from BABAR.

$\S$  Only muons are used

**Fig. 182** Branching fractions of  $b \rightarrow sl^+l^-$  decays**Fig. 183** Branching fractions of  $b \rightarrow l^+l^-(l^+l^-)$ ,  $l^+l^-\gamma$  and  $b \rightarrow dl^+l^-$  decays**Fig. 184**  $Xl^+l^-$  modes with an inclusive lepton pair and/or inclusive  $X$

**Fig. 185** Limits on lepton-flavor-violating decays**Fig. 186** Limits on lepton-number-violating decays

Branching Fractions of Charmless  $B$  Decays with Neutrinos**Fig. 187** Branching fractions of charmless  $B$  decays with neutrinos

**Table 242**  $CP$  asymmetries of charmless hadronic  $B^+$  decays (part 1). Where values are shown in red (blue), this indicates that they are new published (preliminary) results since PDG2014

RPP#	Mode	PDG2014 Avg.	BaBar	Belle	CDF	LHCb	Our Avg.
262	$K^0\pi^+$	-0.017±0.016	-0.029±0.039±0.010	[398]	-0.011±0.021±0.006	[808]	-0.022±0.025±0.010
263	$K^+\pi^0$	0.037±0.021 $^\ddagger$	0.030±0.039±0.010	[810]	0.043±0.024±0.002	[808]	0.040±0.021
264	$\eta'K^+$	0.013±0.017	0.008 $^{+0.017}_{-0.018}$ ±0.009	[811]	0.028±0.028±0.021	[812]	0.013±0.017
265	$\eta'K^{*+}$	-0.26±0.27	-0.26±0.27±0.02	[813]			-0.26±0.27
266	$\eta'K_0^*(1430)^+$	0.06±0.20	0.06±0.20±0.02	[813]			0.06±0.20
267	$\eta'K_2^*(1430)^+$	0.15±0.13	0.15±0.13±0.02	[813]			0.15±0.13
268	$\eta K^+$	-0.37±0.08	-0.36±0.11±0.03	[811]	-0.38±0.11±0.01	[815]	-0.37±0.08
269	$\eta K^{*+}$	0.02±0.06	0.01±0.08±0.02	[817]	0.03±0.10±0.01	[818]	0.02±0.06
270	$\eta K_0^*(1430)^+$	0.05±0.13±0.02	0.05±0.13±0.02	[817]			0.05±0.13
271	$\eta K_2^*(1430)^+$	-0.45±0.30±0.02	-0.45±0.30±0.02	[817]			-0.45±0.30
281	$\omega K^+$	0.02±0.05	-0.01±0.07±0.01	[820]			-0.02±0.04
282	$\omega K^{*+}$	0.29±0.35	0.29±0.35±0.02	[822]			0.29±0.35
284	$\omega K_0^*(1430)^+$	-0.10±0.09	-0.10±0.09±0.02	[822]			-0.10±0.09
285	$\omega K_2^*(1430)^+$	0.14±0.15	0.14±0.15±0.02	[822]			0.14±0.15
288	$K^{*0}\pi^+$	-0.04±0.09	0.032±0.052 $^{+0.016}_{-0.013}$	[278]	-0.149±0.064±0.022	[276]	-0.038±0.042
289	$K^{*+}\pi^0$	-0.06±0.24	-0.06±0.24±0.04	[824]			-0.06±0.24
290	$K^+\pi^-\pi^-$	0.033±0.010	0.028±0.020±0.023	[278]	0.049±0.026±0.020	[276]	0.027±0.008
293	$f_0(980)K^+$	-0.08±0.09 $^\dagger$	-0.106±0.050 $^{+0.036}_{-0.015}$	[278]	-0.077±0.065 $^{+0.046}_{-0.026}$	[276]	-0.095 $^{+0.049}_{-0.042}$
294	$f_2(1270)K^+$	-0.68 $^{+0.19}_{-0.017}$	-0.85±0.22 $^{+0.26}_{-0.13}$	[278]	-0.59±0.22±0.04	[276]	-0.68 $^{+0.20}_{-0.18}$
295	$f_0(1370)K^+$	0.28 $^{+0.30}_{-0.29}$	0.28±0.26 $^{+0.15}_{-0.14}$	[278]			0.28 $^{+0.30}_{-0.29}$
298	$\rho^0K^+$	0.37±0.10	0.44±0.10 $^{+0.06}_{-0.14}$	[278]	0.30±0.11 $^{+0.11}_{-0.05}$	[276]	0.37±0.11
299	$K_0^*(1430)^0\pi^+$	0.055±0.033	0.032±0.035 $^{+0.034}_{-0.015}$	[278]	0.076±0.038 $^{+0.028}_{-0.022}$	[276]	0.055 $^{+0.034}_{-0.032}$
300	$K_2^*(1430)^0\pi^+$	0.05 $^{+0.29}_{-0.24}$	0.05±0.23 $^{+0.18}_{-0.08}$	[278]			0.05 $^{+0.29}_{-0.24}$
303	$K^+\pi^0\pi^0$	-0.06±0.07	-0.06±0.06±0.04	[824]			-0.06±0.07
310	$\rho^+K^0$	-0.12±0.17	-0.12±0.17±0.02	[830]			-0.12±0.17
311	$K^{*+}\pi^+\pi^-$	0.07±0.08	0.07±0.07±0.04	[831]			0.07±0.08
312	$K^{*+}\rho^0$	0.31±0.13	0.31±0.13±0.03	[832]			0.31±0.13
313	$f_0(980)K^{*+}$	-0.15±0.12	-0.15±0.12±0.03	[832]			-0.15±0.12
314	$a_1^+K^0$	0.12±0.11	0.12±0.11±0.02	[833]			0.12±0.11
315	$b_1^+K^0$	-0.03±0.15	-0.03±0.15±0.02	[834]			-0.03±0.15
312	$K^{*0}\rho^+$	-0.01±0.16	-0.01±0.16±0.02	[1034]			-0.01±0.16
319	$b_1^0K^+$	-0.46±0.20	-0.46±0.20±0.02	[836]			-0.46±0.20

**Table 242** continued

RPP#	Mode	PDG2014 Avg.	BaBar	Belle	CDF	LHCb	Our Avg.
322	$K^+\bar{K}^0$	0.04±0.14	0.10±0.26±0.03	[398]	0.014±0.168±0.002	[808]	-0.21±0.14±0.01
324	$K^+K_SK_S$	0.04 <sup>+0.04</sup> <sub>-0.05</sub>	0.04 <sup>+0.04</sup> <sub>-0.05</sub> ±0.02	[271]			0.04 <sup>+0.04</sup> <sub>-0.05</sub>
329	$K^+K^-\pi^+$	-0.12±0.05	0.00±0.10±0.03	[840]			-0.118±0.022
340	$K^+K^-K^+$	-0.036±0.012	-0.017 <sup>+0.019</sup> <sub>-0.014</sub> ±0.014	[271]			-0.033±0.007
341	$\phi K^+$	0.04±0.04	0.128±0.044±0.013	[271]	0.01±0.12±0.05	[849]	-0.07±0.17 <sup>+0.03</sup> <sub>-0.02</sub>
						[846]	0.022±0.021±0.009
						[866]	0.041±0.020

<sup>†</sup> PDG takes the value from the BaBar amplitude analysis of  $B^+ \rightarrow K^+K^-K^+$ , while our numbers are from amplitude analyses of  $B^+ \rightarrow K^+\pi^-\pi^+$

<sup>‡</sup> PDG uses also a result from CLEO

**Table 243**  $CP$  asymmetries of charmless hadronic  $B^+$  decays (part 2). Where values are shown in red (blue), this indicates that they are new published (preliminary) results since PDG2014

RPP#	Mode	PDG2014 Avg.	BABAR	Belle	CDF	LHCb	Our Avg.
348	$K^{*+} K^+ K^-$	0.11±0.09	0.11±0.08±0.03	[831]	-0.02±0.14±0.03	[1035]	0.11±0.09
349	$\phi K^{*+}$	-0.01±0.08	0.00±0.09±0.04	[848]	-0.02±0.14±0.03		-0.01±0.08
351	$\phi K_1(1270)^+$	0.15±0.20	0.15±0.19±0.05	[850]	-0.23±0.20		0.15±0.20
354	$\phi K_0^*(1430)^+$	0.04±0.15	0.04±0.15±0.04	[850]	-0.23±0.19±0.06		0.04±0.15
355	$\phi K_2^*(1430)^+$	-0.23±0.20	-0.10±0.08	[850]	-0.10±0.08		-0.23±0.20
359	$\phi\phi K^+$	-0.10±0.08	-0.10±0.08	[852]	-0.10±0.08		-0.10±0.08
363	$K^{*+}\gamma$	0.18±0.29	0.18±0.28±0.07	[952]	0.007±0.074±0.017		0.018±0.073
365	$K^+\eta\gamma$	-0.12±0.07	-0.09±0.10±0.01	[405]	-0.16±0.09±0.06	[955]	-0.12±0.07
367	$K^+\phi\gamma$	-0.13±0.11	-0.26±0.14±0.05	[958]	-0.03±0.11±0.08	[406]	-0.13±0.10
378	$\rho^+\gamma$	-0.11±0.33	-0.11±0.32±0.09	[962]	-0.11±0.32±0.09		-0.11±0.33
379	$\pi^+\pi^0$	0.03±0.04	0.03±0.08±0.01	[810]	0.025±0.043±0.007	[808]	0.026±0.039
380	$\pi^+\pi^-\pi^+$	0.105±0.029	0.032±0.044±0.040	[855]	0.058±0.008±0.011	[1033]	0.057±0.014
381	$\rho^0\pi^+$	0.18±0.09	0.18±0.07±0.05	[855]	0.18±0.09		0.18±0.09
383	$f_2(1270)\pi^+$	0.41±0.31	0.41±0.25±0.18	[855]	0.41±0.31		0.41±0.31
384	$\rho(1450)^0\pi^+$	-0.06±0.36	-0.06±0.28±0.23	[855]	-0.06±0.36		-0.06±0.36
385	$f_0(1370)\pi^+$	0.72±0.22	0.72±0.15±0.16	[855]	0.72±0.22		0.72±0.22
387	$\pi^+\pi^-\pi^+(NR)$	-0.14±0.23	-0.14±0.14±0.18	[855]	-0.14±0.23		-0.14±0.23
389	$\rho^+\pi^0$	0.02±0.11	-0.01±0.13±0.02	[858]	0.06±0.17±0.04	[859]	0.02±0.11
391	$\rho^+\rho^0$	-0.05±0.05	-0.054±0.055±0.010	[860]	0.00±0.22±0.03	[860]	-0.051±0.054
397	$\eta\pi^+$	-0.14±0.07	-0.03±0.09±0.03	[811]	-0.19±0.06±0.01	[815]	-0.14±0.05
398	$\eta o^+$	0.11±0.11	0.13±0.11±0.02	[863]	-0.04±0.34±0.01	[818]	0.11±0.11
399	$\eta'\pi^+$	0.06±0.16	0.03±0.17±0.02	[811]	0.20±0.37±0.04	[812]	0.06±0.15
400	$\eta\rho^+$	0.26±0.17	0.26±0.17±0.02	[813]	0.26±0.17		0.26±0.17
401	$\omega\pi^+$	-0.04±0.06 <sup>†</sup>	-0.02±0.08±0.01	[820]	-0.02±0.09±0.01	[862]	-0.02±0.06
402	$\omega\rho^+$	-0.20±0.09	-0.20±0.09±0.02	[822]	-0.20±0.09±0.02		-0.20±0.09
408	$b_1^0\pi^+$	0.05±0.16	0.05±0.16±0.02	[836]	-0.17±0.10±0.02 <sup>‡</sup>	[910]	0.05±0.16
417	$p\bar{p}\pi^+$	0.00±0.04	0.04±0.07±0.04	[666]	-0.17±0.10±0.02 <sup>‡</sup>	[910]	-0.04±0.06
420	$p\bar{p}K^+$	-0.08±0.04	-0.16±0.08±0.04	[740]	-0.02±0.05±0.02 <sup>‡</sup>	[910]	-0.051±0.029
425	$p\bar{p}K^{*+}$	0.21±0.16	0.32±0.13±0.05	[666]	-0.01±0.19±0.02	[913]	0.21±0.11
428	$p\bar{\Lambda}\gamma$	0.17±0.17	0.17±0.16±0.05	[915]	0.17±0.16±0.05		0.17±0.17
429	$p\bar{\Lambda}\pi^0$	0.01±0.17	0.01±0.17±0.04	[915]	0.01±0.17±0.04		0.01±0.17

Table 243 continued

RPP#	Mode	PDG2014 Avg.	BABAR	Belle	CDF	LHCb	Our Avg.
471	$K^+\ell\ell$	-0.02±0.08	-0.03±0.14±0.01 §	[995]	0.04±0.10±0.02 [970]		0.02±0.08
472	$K^+e^+e^-$	0.14±0.14			0.14±0.14±0.03 [970]		0.14±0.14
473	$K^+\mu^+\mu^-$	-0.003±0.033			-0.05±0.13±0.03 [970]		0.011±0.017
478	$K^{*+}\ell\ell$	-0.09±0.14	0.01 <sup>+0.26</sup> <sub>-0.24</sub> ±0.02 [969]		-0.13 <sup>+0.17</sup> <sub>-0.16</sub> ±0.01 [970]		-0.09 <sup>+0.14</sup> <sub>-0.13</sub>
479	$K^{*+}e^+e^-$	-0.14 <sup>+0.23</sup> <sub>-0.22</sub>			-0.14 <sup>+0.23</sup> <sub>-0.22</sub> ±0.02 [970]		-0.14 <sup>+0.23</sup> <sub>-0.22</sub>
480	$K^{*+}\mu^+\mu^-$	-0.12±0.24			-0.12±0.24±0.02 [970]		-0.036±0.024±0.003 ¶
480	$\pi^+\mu^+\mu^-$					-0.11±0.12±0.01 [966]	-0.11±0.12

† PDG uses also a result from CLEO.

‡ PDG swaps the Belle results corresponding to  $A_{CP}(p\bar{p}\pi^+)$  and  $A_{CP}(p\bar{p}K^+)$ .

§ PDG uses also a previous result from BABAR (1999).

¶ LHCb also quotes results in bins of  $m(\ell^+\ell^-)^2$ .

**Table 244**  $CP$  asymmetries of charmless hadronic  $B^0$  decays. Where values are shown in red (blue), this indicates that they are new published (preliminary) results since PDG2014

RPP#	Mode	PDG2014 Avg.	BABAR	Belle	CDF	LHCb	Our Avg.
227	$K^+\pi^-$	-0.082±0.006 <sup>†</sup>	-0.107±0.016 <sup>+0.006</sup> <sub>-0.004</sub>	[416] -0.069±0.014±0.007	[808] -0.083±0.013±0.004	[1038] -0.080±0.007±0.003	[1039] -0.082±0.006
230	$\eta' K^{*0}$	0.02±0.23	0.02±0.23±0.02	[813] -0.22±0.29±0.07	[871]		-0.07±0.18
231	$\eta' K_0^*(1430)^0$	-0.19±0.17	-0.19±0.17±0.02	[813]			-0.19±0.17
232	$\eta' K_2^*(1430)^0$	0.14±0.18	0.14±0.18±0.02	[813]			0.14±0.18
234	$\eta K^{*0}$	0.19±0.05	0.21±0.06±0.02	[817]	0.17±0.08±0.01	[818]	0.19±0.05
235	$\eta K_0^*(1430)^0$	0.06±0.13	0.06±0.13±0.02	[817]			0.06±0.13
236	$\eta K_2^*(1430)^0$	-0.07±0.19	-0.07±0.19±0.02	[817]			-0.07±0.19
241	$b_1^- K^+$	-0.07±0.12	-0.07±0.12±0.02	[836]			-0.07±0.12
246	$\omega K^{*0}$	0.45±0.25	0.45±0.25±0.02	[822]			0.45±0.25
248	$\omega K_0^*(1430)^0$	-0.07±0.09	-0.07±0.09±0.02	[822]			-0.07±0.09
249	$\omega K_2^*(1430)^0$	-0.37±0.17	-0.37±0.17±0.02	[822]			-0.37±0.17
251	$K^+\pi^-\pi^0$	0.00±0.06	-0.030 <sup>+0.045</sup> <sub>-0.051</sub> ±0.055	[877]	0.07±0.11±0.01	[876]	0.000 <sup>+0.059</sup> <sub>-0.061</sub>
252	$\rho^- K^+$	0.20±0.11	0.20±0.09±0.08	[875]	0.22 <sup>+0.22±0.06</sup> <sub>-0.23±0.02</sub>	[876]	0.20±0.11
253	$\rho(1450)^-K^+$	-0.10±0.33	-0.10±0.32±0.09	[875]			-0.10±0.33
254	$\rho(1700)^-K^+$	-0.36±0.61	-0.36±0.57±0.23	[875]			-0.36±0.61
255	$K^+\pi^-\pi^0(NR)$	0.10±0.18	0.10±0.16±0.08	[875]			0.10±0.18
257	$K_0^*(1430)^0\pi^0$	-0.15±0.11	-0.15±0.10±0.04	[875]			-0.15±0.11
261	$K^0\pi^+\pi^-$	-0.01±0.05	-0.01±0.05±0.01	[274]			-0.01±0.05
264	$K^{*+}\pi^-$	-0.22±0.06 <sup>†</sup>	-0.24±0.07±0.02 <sup>‡</sup>	[875]	-0.21±0.11±0.07	[275]	-0.23±0.06
265	$K_0^*(1430)^+\pi^-$	0.09±0.07	0.09±0.07±0.03	[274]			0.09±0.08
271	$K^{*0}\pi^0$	-0.15±0.13	-0.15±0.12±0.04	[875]			-0.15±0.13
278	$K^{*0}\pi^+\pi^-$	0.07±0.05	0.07±0.04±0.03	[881]			0.07±0.05
279	$K^{*0}\rho^0$	-0.06±0.09	-0.06±0.09±0.02	[882]			-0.06±0.09
280	$f_0(980)K^{*0}$	0.07±0.10	0.07±0.10±0.02	[882]			0.07±0.10
283	$a_1^- K^+$	-0.16±0.12	-0.16±0.12±0.01	[833]			-0.16±0.12
284	$K^{*+}\rho^-$	0.21±0.15	0.21±0.15±0.02	[882]			0.21±0.15
311	$K^{*0}K^+K^-$	0.01±0.05	0.01±0.05±0.02	[881]			0.01±0.05
312	$\phi K^{*0}$	0.00±0.04	0.01±0.06±0.03	[391]	-0.007±0.048±0.021	[892]	-0.0032±0.10 <sup>¶</sup>
314	$K^{*0}\pi^+K^-$	0.22±0.39	0.22±0.33±0.20	[881]			0.22±0.39
326	$\phi K_0^*(1430)^0$	0.12±0.08	0.20±0.14±0.06	[391]	0.093±0.094±0.017	[892]	0.124±0.081
333	$\phi K_2^*(1430)^0$	-0.11±0.10	-0.08±0.12±0.05	[391]	-0.155 <sup>+0.152</sup> <sub>-0.133</sub> ±0.033	[892]	-0.113 <sup>+0.102</sup> <sub>-0.096</sub>
340	$K^{*0}\gamma$	-0.002±0.015	-0.016±0.022±0.007	[951]	-0.030±0.055±0.014	[952]	0.008±0.017±0.009
357	$\pi^0\pi^0$	0.43±0.14	0.43±0.26±0.05	[416]	0.44 <sup>+0.52</sup> <sub>-0.53</sub> ±0.17	[899]	0.43±0.24
391	$a_1^\mp\pi^\pm$	-0.07±0.06	-0.07±0.07±0.02	[836]	-0.06±0.05±0.07	[418]	-0.07±0.06

**Table 244** continued

RPP#	Mode	PDG2014 Avg.	BABAR	Belle	CDF	LHCb	Our Avg.
400	$b_1^\mp \pi^\pm$	-0.05±0.10	-0.05±0.10±0.02	[836]			-0.05±0.10
412	$p\bar{p}K^{*0}$	0.05±0.12	0.11±0.13±0.06	[666]	-0.08±0.20±0.02	[913]	0.05±0.12
414	$p\bar{\Lambda}\pi^-$	0.04±0.07	-0.10±0.10±0.02	§	-0.02±0.10±0.03	[915]	-0.06±0.07
477	$K^{*0}\ell\ell$	-0.05±0.10	0.02±0.20±0.02	[969]	-0.08±0.12±0.02	[970]	-0.05±0.10
478	$K^{*0}e^+e^-$	-0.21±0.19	-0.21±0.19±0.02	[970]	-0.21±0.19±0.02	[970]	-0.21±0.19
479	$K^{*0}\mu^+\mu^-$	-0.07±0.04	0.00±0.15±0.03	[970]	-0.035±0.024±0.003	◊	-0.034±0.024

Measurements of time-dependent  $CP$  asymmetries are listed in Sec. 4.

† PDG uses also a result from CLEO.

‡ Average of  $BaBar$  results from  $B^0 \rightarrow K^+\pi^-\pi^0$  and  $B^0 \rightarrow K^0\pi^+\pi^-$ .

§ PDG quotes the opposite asymmetry.

¶ Extracted from measured  $\Delta A_{CP} = A_{CP}(\phi K^{*0}) - A_{CP}(J/\psi K^{*0}) = 0.015 \pm 0.032 \pm 0.005$ .

◊ LHCb also quotes results in bins of  $m(\ell^+\ell^-)^2$ .

**Table 245**  $CP$  asymmetries of charmless hadronic decays of  $B^\pm/B^0$  admixture. Where values are shown in red (blue), this indicates that they are new published (preliminary) results since PDG2014

RPP#	Mode	PDG2014 Avg.	BABAR	Belle		Our Avg.	
65	$K^*\gamma$	$-0.003 \pm 0.017^\dagger$	$-0.003 \pm 0.017 \pm 0.007$	[951]	$-0.015 \pm 0.044 \pm 0.012$	[952]	$-0.005 \pm 0.017$
77	$s\gamma$	$-0.008 \pm 0.029$	$0.017 \pm 0.019 \pm 0.010^\ddagger$	[1041]	$0.002 \pm 0.050 \pm 0.030$	[1042]	$0.015 \pm 0.020$
	$(s+d)\gamma$	$-0.01 \pm 0.05$	$0.057 \pm 0.060 \pm 0.018^\S$	[989]	$0.022 \pm 0.039 \pm 0.009^\diamond$	[1032]	$0.032 \pm 0.034$
80	$s\eta$	$-0.13^{+0.04}_{-0.05}$			$-0.13 \pm 0.04^{+0.02}_{-0.03}$	[1017]	$-0.13^{+0.04}_{-0.05}$
86	$\pi^+X$	$0.10 \pm 0.17$	$0.10 \pm 0.16 \pm 0.05$	[1021]			$0.10 \pm 0.17$
121	$s\ell\ell$	$-0.22 \pm 0.26$	$0.04 \pm 0.11 \pm 0.01$	[994]			$0.04 \pm 0.11$
126	$K^*e^+e^-$	$-0.18 \pm 0.15$			$-0.18 \pm 0.15 \pm 0.01$	[970]	$-0.18 \pm 0.15$
128	$K^*\mu^+\mu^-$	$-0.03 \pm 0.13$			$-0.03 \pm 0.13 \pm 0.02$	[970]	$-0.03 \pm 0.13$
129	$K\ell\ell$		$-0.03 \pm 0.14 \pm 0.01$	[995]			$-0.03 \pm 0.14$
130	$K^*\ell\ell$	$-0.04 \pm 0.07$	$0.03 \pm 0.13 \pm 0.01^\¶$	[995]	$-0.10 \pm 0.10 \pm 0.01$	[970]	$-0.05 \pm 0.08$

<sup>†</sup> PDG includes also a result from CLEO.<sup>‡</sup> BABAR also measures the difference in direct  $CP$  asymmetry for charged and neutral  $B$  mesons:  $\Delta A_{CP} = +(5.0 \pm 3.9 \pm 1.5)\%$ .<sup>§</sup> There is another BABAR result using the recoil method [988], and a CLEO result [1043] that are used in the PDG average.<sup>¶</sup> Previous BABAR result is also included in the PDG Average.<sup>◊</sup> Requires  $E_\gamma > 2.1$  GeV.**Table 246**  $CP$  asymmetries of charmless hadronic  $B_s^0$  decays. Where values are shown in red (blue), this indicates that they are new published (preliminary) results since PDG2014

RPP#	Mode	PDG2014 Avg.	CDF	LHCb	Our Avg.
52	$\pi^+K^-$	$0.28 \pm 0.04$	$0.22 \pm 0.07 \pm 0.02$	[1038]	$0.27 \pm 0.04 \pm 0.01$
				[1039]	$0.26 \pm 0.04$

**Table 247**  $CP$  asymmetries of charmless hadronic  $\Lambda_b^0$  decays. Where values are shown in red (blue), this indicates that they are new published (preliminary) results since PDG2014

RPP#	Mode	PDG2014 Avg.	CDF	LHCb	Our Avg.
21	$p\pi^-$	$0.03 \pm 0.18$	$0.06 \pm 0.07 \pm 0.03$	[1038]	$0.06 \pm 0.08$
22	$pK^-$	$0.37 \pm 0.17$	$-0.10 \pm 0.08 \pm 0.04$	[1038]	$-0.10 \pm 0.09$
	$\bar{K}^0 p\pi^-$				$0.22 \pm 0.13 \pm 0.03$
	$\Lambda K^+\pi^-$				$-0.53 \pm 0.23 \pm 0.11$
	$\Lambda K^+K^-$				$-0.28 \pm 0.10 \pm 0.07$
				[926]	$0.22 \pm 0.13$
				[927]	$-0.53 \pm 0.26$
				[927]	$-0.28 \pm 0.12$

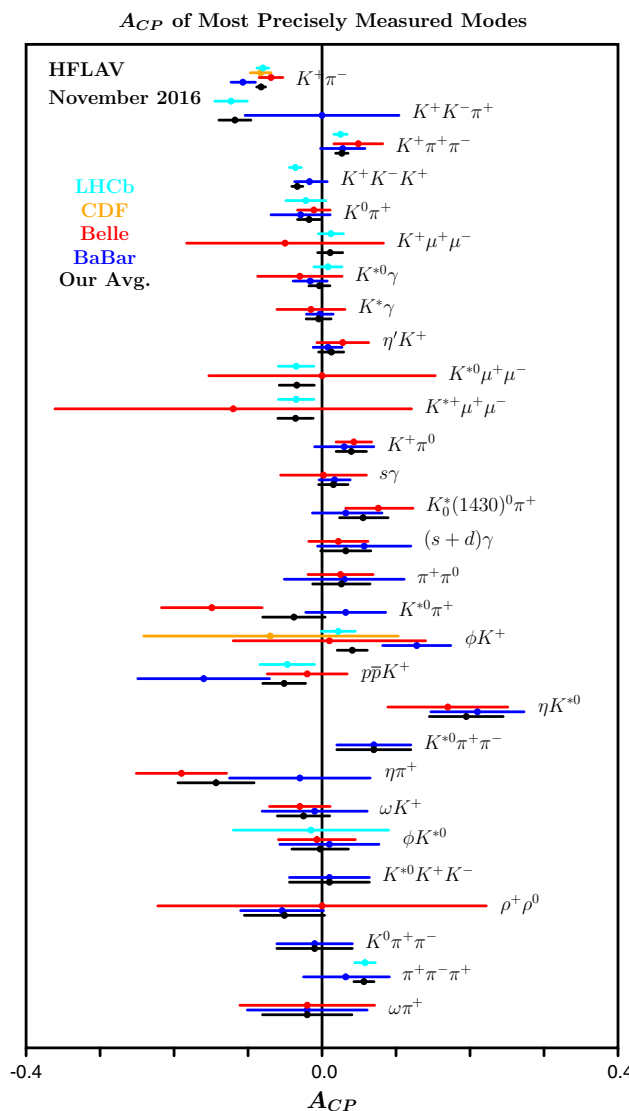


**Fig. 188**  $A_{CP}$  of most precisely measured modes

**Table 248** Longitudinal polarization fraction  $f_L$  for  $B^+$  decays. Where values are shown in red (blue), this indicates that they are new published (preliminary) results since PDG2014

RPP#	Mode	PDG2014 Avg.	BABAR	Belle	Our Avg.
282	$\omega K^{*+}$	$0.41 \pm 0.18 \pm 0.05$	$0.41 \pm 0.18 \pm 0.05$	[822]	$0.41 \pm 0.19$
285	$\omega K_2^*(1430)^+$	$0.56 \pm 0.10 \pm 0.04$	$0.56 \pm 0.10 \pm 0.04$	[822]	$0.56 \pm 0.11$
312	$K^{*+}\rho^0$	$0.78 \pm 0.12 \pm 0.03$	$0.78 \pm 0.12 \pm 0.03$	[832]	$0.78 \pm 0.12$
316	$K^{*0}\rho^+$	$0.48 \pm 0.08$	$0.52 \pm 0.10 \pm 0.04$	[1034]	$0.43 \pm 0.11^{+0.05}_{-0.02}$
338	$K^{*+}\bar{K}^{*0}$	$0.75^{+0.16}_{-0.26} \pm 0.03$	$0.75^{+0.16}_{-0.26} \pm 0.03$	[843]	$0.75^{+0.16}_{-0.26}$
349	$\phi K^{*+}$	$0.50 \pm 0.05$	$0.49 \pm 0.05 \pm 0.03$	[848]	$0.52 \pm 0.08 \pm 0.03$
351	$\phi K_1(1270)^+$	$0.46^{+0.12+0.06}_{-0.13-0.07}$	$0.46^{+0.12+0.06}_{-0.13-0.07}$	[850]	$0.46^{+0.13}_{-0.15}$
355	$\phi K_2^*(1430)^+$	$0.80^{+0.09}_{-0.10} \pm 0.03$	$0.80^{+0.09}_{-0.10} \pm 0.03$	[850]	$0.80 \pm 0.10$
391	$\rho^+\rho^0$	$0.950 \pm 0.016$	$0.950 \pm 0.015 \pm 0.006$	[421]	$0.95 \pm 0.11 \pm 0.02$
396	$\omega\rho^+$	$0.90 \pm 0.05 \pm 0.03$	$0.90 \pm 0.05 \pm 0.03$	[822]	$0.90 \pm 0.06$

**Table 249** Longitudinal polarization fraction  $f_L$  for  $B^0$  decays. Where values are shown in red (blue), this indicates that they are new published (preliminary) results since PDG2014

RPP#	Mode	PDG2014 Avg.	BABAR	Belle	LHCb	Our Avg.
246	$\omega K^{*0}$	0.69±0.13	0.72±0.14±0.02	[822]	0.56±0.29 <sup>+0.18</sup> <sub>-0.08</sub>	[874]
249	$\omega K_2^*(1430)^0$	0.45±0.12±0.02	0.45±0.12±0.02	[822]		0.45±0.12
279	$K^{*0}\rho^0$	0.40±0.08±0.11	0.40±0.08±0.11	[882]		0.40±0.14
284	$K^{*+}\rho^-$	0.38±0.13±0.03	0.38±0.13±0.03	[882]		0.38±0.13
312	$\phi K^{*0}$	0.497±0.025	0.494±0.034±0.013	[391]	0.499±0.030±0.018	[892]
315	$K^{*0}\bar{K}^{*0}$	0.80 <sup>+0.10</sup> <sub>-0.12</sub> ±0.06	0.80 <sup>+0.10</sup> <sub>-0.12</sub> ±0.06	[894]		0.80 <sup>+0.12</sup> <sub>-0.13</sub>
333	$\phi K_2^*(1430)^0$	0.901 <sup>+0.046</sup> <sub>-0.058</sub> ±0.037	0.901 <sup>+0.046</sup> <sub>-0.058</sub> ±0.037	[391]		0.901 <sup>+0.059</sup> <sub>-0.069</sub>
386	$\rho^0\rho^0$	0.75 <sup>+0.11</sup> <sub>-0.14</sub> ±0.05	0.75 <sup>+0.11</sup> <sub>-0.14</sub> ±0.05	[411]	<b>0.21<sup>+0.18</sup><sub>-0.22</sub>±0.15</b>	[412]
394	$\rho^+\rho^-$	0.977 <sup>+0.028</sup> <sub>-0.024</sub>	0.992±0.024 <sup>+0.026</sup> <sub>-0.013</sub>	[409]	0.941 <sup>+0.034</sup> <sub>-0.040</sub> ±0.030	[906]
405	$a_1^\pm a_1^\mp$	0.31±0.22±0.10	0.31±0.22±0.10	[908]		0.31±0.24

**Table 250** Results of the full angular analyses of  $B^+ \rightarrow \phi K^{*+}$  decays. Where values are shown in red (blue), this indicates that they are new published (preliminary) results since PDG2014

Parameter	PDG2014 Avg.	BABAR	Belle	LHCb	Our Avg.
$f_\perp = A_{\perp\perp}$	0.20±0.05	0.21±0.05±0.02	[848]	0.19±0.08±0.02	[1035]
$\phi_\parallel$	2.34±0.18	2.47±0.20±0.07		2.10±0.28±0.04	2.34±0.17
$\phi_\perp$	2.58±0.17	2.69±0.20±0.03		2.31±0.30±0.07	2.58±0.17
$\delta_0$	3.07±0.18±0.06	3.07±0.18±0.06			3.07±0.19
$A_{CP}^0$	0.17±0.11±0.02	0.17±0.11±0.02			0.17±0.11
$A_{CP}^\perp$	0.22±0.24±0.08	0.22±0.24±0.08			0.22±0.25
$\Delta\phi_\parallel$	0.07±0.20±0.05	0.07±0.20±0.05			0.07±0.21
$\Delta\phi_\perp$	0.19±0.20±0.07	0.19±0.20±0.07			0.19±0.21
$\Delta\delta_0$	0.20±0.18±0.03	0.20±0.18±0.03			0.20±0.18

Angles ( $\phi, \delta$ ) are in radians. BF,  $f_L$  and  $A_{CP}$  are tabulated separately

**Table 251** Results of the full angular analyses of  $B^0 \rightarrow \phi K^{*0}$  decays. Where values are shown in red (blue), this indicates that they are new published (preliminary) results since PDG2014

Parameter	PDG2014 Avg.	BABAR	Belle	LHCb	Our Avg.
$f_{\perp} = A_{\perp\perp}$	0.228±0.021	0.212±0.032±0.013	[391]	0.238±0.026±0.008	[892] 0.221±0.016±0.013 [1040] 0.225±0.015
$f_S(K\pi)$					0.143±0.013±0.012 0.143±0.018
$f_S(KK)$	2.28±0.08	2.40±0.13±0.08		2.23±0.10±0.02	0.122±0.013±0.008
$\phi_{\parallel}$	2.36±0.09	2.35±0.13±0.09		2.37±0.10±0.04	2.562±0.069±0.040
$\phi_{\perp}$					2.430±0.058
$\delta_0$	2.88±0.10	2.82±0.15±0.09		2.91±0.10±0.08	2.633±0.062±0.037
$\phi_S(K\pi)^{\dagger}$					2.527±0.056
$\phi_S(KK)^{\dagger}$	-0.01±0.05	0.01±0.07±0.02		-0.03±0.06±0.01	2.88±0.10
$A_{CP}^0$	-0.11±0.09	-0.04±0.15±0.06		-0.14±0.11±0.01	2.222±0.063±0.081
$A_{CP}^{\perp}$					2.481±0.072±0.048
$A_{CP}^{\perp}$					2.481±0.087
$A_{CP}^S(K\pi)$					-0.007±0.030
$A_{CP}^S(KK)$					-0.014±0.057
$\Delta\phi_{\parallel}$	0.06±0.11	0.22±0.12±0.08		-0.02±0.10±0.01	0.073±0.091±0.035
$\Delta\phi_{\perp}$	0.10±0.08	0.21±0.13±0.08		0.05±0.10±0.02	0.073±0.097
$\Delta\delta_0$	0.13±0.09	0.27±0.14±0.08		0.08±0.10±0.01	-0.209±0.105±0.012
$\Delta\phi_S(K\pi)^{\dagger}$					0.045±0.068±0.015
$\Delta\phi_S(KK)^{\dagger}$					0.062±0.062±0.022
					0.022±0.072±0.004
					0.022±0.072±0.072

Angles  $(\phi, \delta)$  are in radians. BF,  $f_L$  and  $A_{CP}$  are tabulated separately  
<sup>†</sup> Original LHCb notation adapted to match similar existing quantities

**Table 252** Results of the full angular analyses of  $B^0 \rightarrow \phi K_2^{*0}(1430)$  decays. Where values are shown in red (blue), this indicates that they are new published (preliminary) results since PDG2014

Parameter	PDG2014 Avg.	BABAR		Belle		Our Avg.
$f_{\perp} = A_{\perp\perp}$	$0.027^{+0.031}_{-0.025}$	$0.002^{+0.018}_{-0.002} \pm 0.031$	[391]	$0.056^{+0.050}_{-0.035} \pm 0.009$	[892]	$0.027^{+0.027}_{-0.024}$
$\phi_{\parallel}$	$4.0 \pm 0.4$	$3.96 \pm 0.38 \pm 0.06$		$3.76 \pm 2.88 \pm 1.32$		$3.96 \pm 0.38$
$\phi_{\perp}$	$4.5 \pm 0.4$			$4.45^{+0.43}_{-0.38} \pm 0.13$		$4.45^{+0.45}_{-0.40}$
$\delta_0$	$3.46 \pm 0.14$	$3.41 \pm 0.13 \pm 0.13$		$3.53 \pm 0.11 \pm 0.19$		$3.46 \pm 0.14$
$A_{CP}^0$	$-0.03 \pm 0.04$	$-0.05 \pm 0.06 \pm 0.01$		$-0.016^{+0.066}_{-0.051} \pm 0.008$		$-0.032^{+0.043}_{-0.038}$
$A_{CP}^{\perp}$	$0.0^{+0.9}_{-0.7}$			$-0.01^{+0.85}_{-0.67} \pm 0.09$		$-0.01^{+0.85}_{-0.68}$
$\Delta\phi_{\parallel}$	$-0.9 \pm 0.4$	$-1.00 \pm 0.38 \pm 0.09$		$-0.02 \pm 1.08 \pm 1.01$		$-0.94 \pm 0.38$
$\Delta\phi_{\perp}$	$-0.2 \pm 0.4$			$-0.19 \pm 0.42 \pm 0.11$		$-0.19 \pm 0.43$
$\Delta\delta_0$	$0.08 \pm 0.09$	$0.11 \pm 0.13 \pm 0.06$		$0.06 \pm 0.11 \pm 0.02$		$0.08 \pm 0.09$

Angles ( $\phi, \delta$ ) are in radians. BF,  $f_L$  and  $A_{CP}$  are tabulated separately

**Table 253** Longitudinal polarization fraction  $f_L$  for  $B_s^0$  decays. Where values are shown in red (blue), this indicates that they are new published (preliminary) results since PDG2014

RPP#	Mode	PDG2014 Avg.	CDF		LHCb		Our Avg.
51	$\phi\phi$	$0.361 \pm 0.022$	$0.348 \pm 0.041 \pm 0.021$	[932]	$0.365 \pm 0.022 \pm 0.012$	[1046]	$0.361 \pm 0.022$
59	$K^{*0}\bar{K}^{*0}$	$0.31 \pm 0.13$			$0.201 \pm 0.057 \pm 0.040$	[935]	$0.201 \pm 0.070$
60	$\phi\bar{K}^{*0}$	$0.51 \pm 0.17$			$0.51 \pm 0.15 \pm 0.07$	[936]	$0.51 \pm 0.17$

**Table 254** Results of the full angular analyses of  $B_s^0 \rightarrow \phi\phi$  decays. Where values are shown in red (blue), this indicates that they are new published (preliminary) results since PDG2014

Parameter	PDG2014 Avg.	CDF		LHCb		Our Avg.
$f_{\perp} = A_{\perp\perp}$	$0.306 \pm 0.030$	$0.365 \pm 0.044 \pm 0.027$	[932]	$0.291 \pm 0.024 \pm 0.010$	[1046]	$0.306 \pm 0.023$
$\phi_{\parallel}$	$2.59 \pm 0.15$	$2.71^{+0.31}_{-0.36} \pm 0.22$		$2.57 \pm 0.15 \pm 0.06$		$2.59 \pm 0.15$

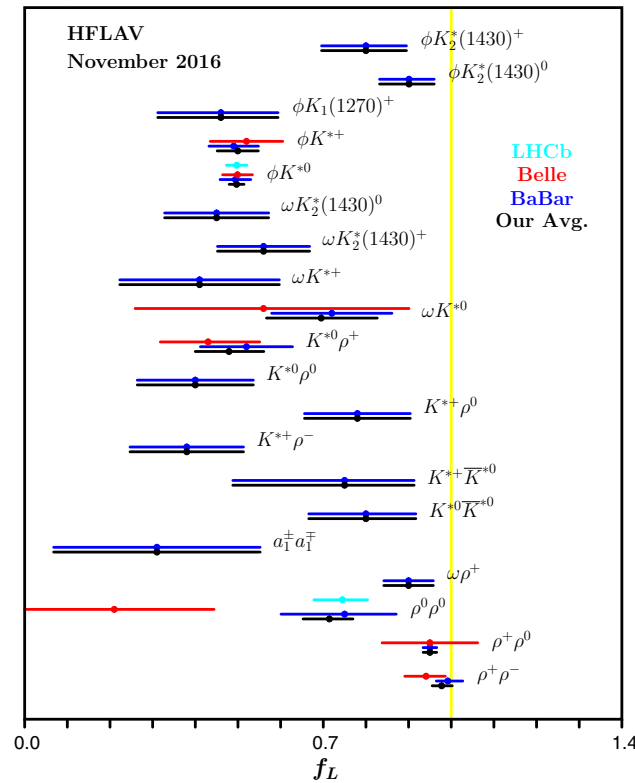
The parameter  $\phi$  is in radians. BF,  $f_L$  and  $A_{CP}$  are tabulated separately

**Table 255** Results of the full angular analyses of  $B_s^0 \rightarrow \phi\bar{K}^{*0}$  decays. Where values are shown in red (blue), this indicates that they are new published (preliminary) results since PDG2014

Parameter	PDG2014 Avg.	LHCb	Our Avg.
$f_{\perp} = A_{\perp\perp}$		$0.28 \pm 0.12 \pm 0.03$	[936]
$f_0$		$0.51 \pm 0.15 \pm 0.07$	
$f_{\parallel}$	$0.21 \pm 0.11$	$0.21 \pm 0.11 \pm 0.02$	
$\phi_{\parallel}^{\dagger}$	$1.75 \pm 0.53 \pm 0.29$	$1.75^{+0.59+0.38}_{-0.53-0.30}$	$1.75^{+0.70}_{-0.61}$

The parameter  $\phi$  is in radians. BF,  $f_L$  and  $A_{CP}$  are tabulated separately.

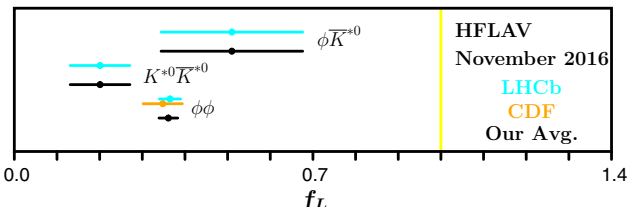
<sup>†</sup> Converted from the measurement of  $\cos(\phi_{\parallel})$ . PDG takes the smallest resulting asymmetric error as parabolic

Longitudinal Polarization Fraction in Charmless  $B$  Decays**Fig. 189** Longitudinal polarization fraction in charmless  $B$  decays**Table 256** Results of the full angular analyses of  $B_s^0 \rightarrow K^{*0} \bar{K}^{*0}$  decays. Where values are shown in red (blue), this indicates that they are new published (preliminary) results since PDG2014

Parameter	PDG2014 Avg.	LHCb	Our Avg.
$f_L$	$0.31 \pm 0.12 \pm 0.04$	$0.201 \pm 0.057 \pm 0.040$	[935] $0.201 \pm 0.070$
$f_{\parallel}$		$0.215 \pm 0.046 \pm 0.015$	$0.215 \pm 0.048$
$ A_s^+ ^2$		$0.114 \pm 0.037 \pm 0.023$	$0.114 \pm 0.044$
$ A_s^- ^2$		$0.485 \pm 0.051 \pm 0.019$	$0.485 \pm 0.054$
$ A_{ss} ^2$		$0.066 \pm 0.022 \pm 0.007$	$0.066 \pm 0.023$
$\delta_{\parallel}$		$5.31 \pm 0.24 \pm 0.14$	$5.31 \pm 0.28$
$\delta_{\perp} - \delta_s^+$		$1.95 \pm 0.21 \pm 0.04$	$1.95 \pm 0.21$
$\delta_s^-$		$1.79 \pm 0.19 \pm 0.19$	$1.79 \pm 0.27$
$\delta_{ss}$		$1.06 \pm 0.27 \pm 0.23$	$1.06 \pm 0.35$

**Table 257** Relative branching fractions of  $B_c^+$  decays. Where values are shown in red (blue), this indicates that they are new published (preliminary) results since PDG2014

RPP#	Mode	PDG2014 AVG.	LHCb	Our Avg.
	$f_c \mathcal{B}(B_c^+ \rightarrow K^+ K^0) / f_u \mathcal{B}(B_c^+ \rightarrow K_s^0 \pi^+)$	‡	$< 5.8 \times 10^{-2}$	[838] $< 5.8 \times 10^{-2}$
	$f_c \mathcal{B}(B_c^+ \rightarrow p \bar{p} \pi^+) / f_u$		$< 2.8 \times 10^{-8}$	[1047] $< 2.8 \times 10^{-8}$
	$\sigma(B_c^+) \mathcal{B}(B_c^+ \rightarrow K^+ K^- \pi^+) / \sigma(B_c^+) \dagger$		$< 15 \times 10^{-8}$	[795] $< 15 \times 10^{-8}$

† Measured in the annihilation region  $m(K^- \pi^+) < 1.834 \text{ GeV}/c^2$ .‡ PDG converts the LHCb result to  $f_c \mathcal{B}(B_c^+ \rightarrow K^+ K^0) < 4.6 \times 10^{-7}$ Longitudinal Polarization Fraction in Charmless  $B_s$  Decays**Fig. 190** Longitudinal polarization fraction in charmless  $B_s^0$  decays

## 8 Charm physics

### 8.1 $D^0$ - $\bar{D}^0$ mixing and $CP$ violation

#### 8.1.1 Introduction

In 2007 Belle [1048] and BABAR [1049] obtained the first evidence of  $D^0$ - $\bar{D}^0$  mixing, for which experiments had searched for more than two decades. These results were later confirmed by CDF [1050] and more recently by LHCb [1051]. There are now numerous measurements of  $D^0$ - $\bar{D}^0$  mixing with various levels of sensitivity. All measurements are input into a global fit to determine world average values of mixing parameters,  $CP$ -violation ( $CPV$ ) parameters, and strong phase differences.

Our notation is as follows. The mass eigenstates are denoted

$$D_1 = p|D^0\rangle - q|\bar{D}^0\rangle \quad (221)$$

$$D_2 = p|D^0\rangle + q|\bar{D}^0\rangle, \quad (222)$$

where we use the convention [1052]  $CP|D^0\rangle = -|\bar{D}^0\rangle$  and  $CP|\bar{D}^0\rangle = -|D^0\rangle$ . Thus in the absence of  $CP$  violation,  $D_1$  is  $CP$ -even and  $D_2$  is  $CP$ -odd. The weak phase  $\phi$  is defined as  $\text{Arg}(q/p)$ . The mixing parameters are defined as  $x \equiv (m_1 - m_2)/\Gamma$  and  $y \equiv (\Gamma_1 - \Gamma_2)/(2\Gamma)$ , where  $m_1$ ,  $m_2$  and  $\Gamma_1$ ,  $\Gamma_2$  are the masses and decay widths for the mass eigenstates, and  $\Gamma \equiv (\Gamma_1 + \Gamma_2)/2$ .

The global fit determines central values and errors for ten underlying parameters. These consist of the mixing parameters  $x$  and  $y$ ; indirect  $CPV$  parameters  $|q/p|$  and  $\phi$ ; the ratio of decay rates  $R_D \equiv [\Gamma(D^0 \rightarrow K^+\pi^-) + \Gamma(\bar{D}^0 \rightarrow K^-\pi^+)]/[\Gamma(D^0 \rightarrow K^-\pi^+) + \Gamma(\bar{D}^0 \rightarrow K^+\pi^-)]$ ; direct  $CPV$  asymmetries  $A_D$ ,  $A_K$ , and  $A_\pi$  in  $D^0 \rightarrow K^+\pi^-$ ,  $K^+K^-$ , and  $\pi^+\pi^-$  decays, respectively; the strong phase difference  $\delta$  between  $\bar{D}^0 \rightarrow K^-\pi^+$  and  $D^0 \rightarrow K^-\pi^+$  amplitudes; and the strong phase difference  $\delta_{K\pi\pi}$  between  $\bar{D}^0 \rightarrow K^-\rho^+$  and  $D^0 \rightarrow K^-\rho^+$  amplitudes.

The fit uses 50 observables from measurements of  $D^0 \rightarrow K^+\ell^-\bar{\nu}$ ,  $D^0 \rightarrow K^+K^-$ ,  $D^0 \rightarrow \pi^+\pi^-$ ,  $D^0 \rightarrow K^+\pi^-$ ,  $D^0 \rightarrow K^+\pi^-\pi^0$ ,  $D^0 \rightarrow K_S^0\pi^+\pi^-$ ,  $D^0 \rightarrow \pi^0\pi^+\pi^-$ ,  $D^0 \rightarrow K_S^0K^+K^-$ , and  $D^0 \rightarrow K^+\pi^-\pi^+\pi^-$  decays,<sup>37</sup> and from double-tagged branching fractions measured at the  $\psi(3770)$  resonance. The relationships between the measured observables and the fitted parameters are given in Table 258. Correlations among observables are accounted for by using covariance matrices provided by the experimental collaborations. Errors are assumed to be Gaussian, and systematic errors among different experiments are assumed to be uncorrelated unless specific correlations have been identified. We have checked this method with a second method that adds

together three-dimensional log-likelihood functions for  $x$ ,  $y$ , and  $\delta$  obtained from several analyses; this combination accounts for non-Gaussian errors. When both methods are applied to the same set of measurements, equivalent results are obtained.

Mixing in the  $D^0$ ,  $B^0$ , and  $B_s^0$  heavy flavor systems is governed by a short-distance box diagram. In the  $D^0$  system, this diagram is doubly-Cabibbo-suppressed *relative to amplitudes dominating the decay width*. In addition, because the  $d$  and  $s$  quark masses are sufficiently close, this diagram is also GIM-suppressed. Thus the short-distance mixing rate is extremely small, and  $D^0$ - $\bar{D}^0$  mixing is expected to be dominated by long-distance processes. These are difficult to calculate, and theoretical estimates for  $x$  and  $y$  range over three orders of magnitude (up to the percent level) [1053–1056].

Almost all methods besides that of the  $\psi(3770) \rightarrow \bar{D}\bar{D}$  measurements [1057] identify the flavor of the  $D^0$  or  $\bar{D}^0$  when produced by reconstructing the decay  $D^{*+} \rightarrow D^0\pi^+$  or  $D^{*-} \rightarrow \bar{D}^0\pi^-$ . The charge of the pion, which has low momentum relative to that of the  $D^0$  and is often referred to as the “soft” pion, identifies the  $D$  flavor. For this decay  $M_{D^*} - M_{D^0} - M_{\pi^+} = Q \approx 6$  MeV, which is close to the kinematic threshold; thus analyses typically require that the reconstructed  $Q$  be small to suppress backgrounds. An LHCb measurement [1058] of the difference between time-integrated  $CP$  asymmetries  $A_{CP}(K^+K^-) - A_{CP}(\pi^+\pi^-)$  identifies the flavor of the  $D^0$  by partially reconstructing  $\bar{B} \rightarrow D^0\mu^-\chi$  decays (and charge-conjugates); in this case the charge of the muon originating from the  $B$  decay identifies the flavor of the  $D^0$ .

For time-dependent measurements, the  $D^0$  decay time is calculated as  $M_{D^0} \times (\vec{d} \cdot \vec{p})/(cp^2)$ , where  $\vec{d}$  is the displacement vector between the  $D^*$  and  $D^0$  decay vertices,  $\vec{p}$  is the reconstructed  $D^0$  momentum, and  $p$  and  $M_{D^0}$  are in GeV. The  $D^*$  vertex position is taken to be the intersection of the  $D^0$  momentum vector with the beamspot profile for  $e^+e^-$  experiments, and at the primary interaction vertex for  $\bar{p}p$  and  $pp$  experiments [1050, 1051].

#### 8.1.2 Input observables

The global fit determines central values and errors for ten underlying parameters using a  $\chi^2$  statistic. The fitted parameters are  $x$ ,  $y$ ,  $R_D$ ,  $A_D$ ,  $|q/p|$ ,  $\phi$ ,  $\delta$ ,  $\delta_{K\pi\pi}$ ,  $A_K$ , and  $A_\pi$ . In the  $D \rightarrow K^+\pi^-\pi^0$  Dalitz plot analysis [1059], the phases of intermediate resonances in the  $\bar{D}^0 \rightarrow K^+\pi^-\pi^0$  decay amplitude are determined relative to the phase for  $\mathcal{A}(\bar{D}^0 \rightarrow K^+\rho^-)$ , and the phases of intermediate resonances for  $D^0 \rightarrow K^+\pi^-\pi^0$  are determined relative to the phase for  $\mathcal{A}(D^0 \rightarrow K^+\rho^-)$ . As the  $\bar{D}^0$  and  $D^0$  Dalitz plots are fitted independently, the phase difference  $\delta_{K\pi\pi}$  between the

<sup>37</sup> Charge-conjugate modes are implicitly included.

**Table 258** Left: decay modes used to determine fitted parameters  $x$ ,  $y$ ,  $\delta$ ,  $\delta_{K\pi\pi}$ ,  $R_D$ ,  $A_D$ ,  $A_K$ ,  $A_\pi$ ,  $|q/p|$ , and  $\phi$ . Middle: the observables measured for each decay mode. Right: the relationships between

Decay Mode	Observables	Relationship
$D^0 \rightarrow K^+ K^- / \pi^+ \pi^-$	$y_{CP} A_\Gamma$	$2y_{CP} = \left(  q/p  +  p/q  \right) y \cos \phi - \left(  q/p  -  p/q  \right) x \sin \phi$
$D^0 \rightarrow K_S^0 \pi^+ \pi^-$	$x$ $y$ $ q/p $ $\phi$	$2A_\Gamma = \left(  q/p  -  p/q  \right) y \cos \phi - \left(  q/p  +  p/q  \right) x \sin \phi$
$D^0 \rightarrow K^+ \ell^- \nu$	$R_M$	$R_M = (x^2 + y^2)/2$
$D^0 \rightarrow K^+ \pi^- \pi^0$ (Dalitz plot analysis)	$x''$ $y''$	$x'' = x \cos \delta_{K\pi\pi} + y \sin \delta_{K\pi\pi}$ $y'' = y \cos \delta_{K\pi\pi} - x \sin \delta_{K\pi\pi}$
“Double-tagged” branching fractions measured in $\psi(3770) \rightarrow D D$ decays	$R_M$ $y$ $R_D$ $\sqrt{R_D} \cos \delta$	$R_M = (x^2 + y^2)/2$
$D^0 \rightarrow K^+ \pi^-$	$x'^2, y'$ $x'^2+, x'^2-$ $y'^+, y'^-$	$x' = x \cos \delta + y \sin \delta$ $y' = y \cos \delta - x \sin \delta$ $A_M \equiv ( q/p ^4 - 1)/( q/p ^4 + 1)$ $x'^{\pm} = [(1 \pm A_M)/(1 \mp A_M)]^{1/4} \times (x' \cos \phi \pm y' \sin \phi)$ $y'^{\pm} = [(1 \pm A_M)/(1 \mp A_M)]^{1/4} \times (y' \cos \phi \mp x' \sin \phi)$
$D^0 \rightarrow K^+ \pi^- / K^- \pi^+$ (time-integrated)	$\frac{\Gamma(D^0 \rightarrow K^+ \pi^-) + \Gamma(\bar{D}^0 \rightarrow K^- \pi^+)}{\Gamma(D^0 \rightarrow K^- \pi^+) + \Gamma(\bar{D}^0 \rightarrow K^+ \pi^-)}$	$R_D$
$D^0 \rightarrow K^+ K^- / \pi^+ \pi^-$ (time-integrated)	$\frac{\Gamma(D^0 \rightarrow K^+ \pi^-) - \Gamma(\bar{D}^0 \rightarrow K^- \pi^+)}{\Gamma(D^0 \rightarrow K^+ \pi^-) + \Gamma(\bar{D}^0 \rightarrow K^- \pi^+)}$ $\frac{\Gamma(D^0 \rightarrow K^+ K^-) - \Gamma(\bar{D}^0 \rightarrow K^+ K^-)}{\Gamma(D^0 \rightarrow K^+ K^-) + \Gamma(\bar{D}^0 \rightarrow K^+ K^-)}$ $\frac{\Gamma(D^0 \rightarrow \pi^+ \pi^-) - \Gamma(\bar{D}^0 \rightarrow \pi^+ \pi^-)}{\Gamma(D^0 \rightarrow \pi^+ \pi^-) + \Gamma(\bar{D}^0 \rightarrow \pi^+ \pi^-)}$	$A_D$ $A_K + \frac{\langle t \rangle}{\tau_D} \mathcal{A}_{CP}^{\text{indirect}} \quad (\mathcal{A}_{CP}^{\text{indirect}} \approx -A_\Gamma)$ $A_\pi + \frac{\langle t \rangle}{\tau_D} \mathcal{A}_{CP}^{\text{indirect}} \quad (\mathcal{A}_{CP}^{\text{indirect}} \approx -A_\Gamma)$

two reference amplitudes cannot be determined from these fits. However, the phase difference can be constrained in the global fit and thus is included as a fitted parameter.

All input measurements are listed in Tables 259, 260 and 261. The observable  $R_M = (x^2 + y^2)/2$  is measured in both  $D^0 \rightarrow K^+ \pi^- \pi^+ \pi^-$  [1061] and  $D^0 \rightarrow K^+ \ell^- \nu$  decays. In the case of the latter, the HFLAV world average [1060] is used in the global fit. The inputs used for this average [1062–1065] are plotted in Fig. 191. The observables

$$y_{CP} = \frac{1}{2} \left( \left| \frac{q}{p} \right| + \left| \frac{p}{q} \right| \right) y \cos \phi - \frac{1}{2} \left( \left| \frac{q}{p} \right| - \left| \frac{p}{q} \right| \right) x \sin \phi \quad (223)$$

$$A_\Gamma = \frac{1}{2} \left( \left| \frac{q}{p} \right| - \left| \frac{p}{q} \right| \right) y \cos \phi - \frac{1}{2} \left( \left| \frac{q}{p} \right| + \left| \frac{p}{q} \right| \right) x \sin \phi \quad (224)$$

are also HFLAV world average values [1060]; the inputs used for these averages are plotted in Figs. 192 and 193,

the observables measured and the fitted parameters.  $\langle t \rangle$  is the mean reconstructed decay time for  $D^0 \rightarrow K^+ K^-$  or  $D^0 \rightarrow \pi^+ \pi^-$  decays

respectively. The  $D^0 \rightarrow K^+ \pi^-$  measurements used are from Belle [1066, 1067], BABAR [1049], CDF [1068], and more recently LHCb [1051, 1069]; earlier measurements have much less precision and are not used. The observables from  $D^0 \rightarrow K_S^0 \pi^+ \pi^-$  decays are measured in two ways: assuming  $CP$  conservation ( $D^0$  and  $\bar{D}^0$  decays combined), and allowing for  $CP$  violation ( $D^0$  and  $\bar{D}^0$  decays fitted separately). The no- $CPV$  measurements are from Belle [1070], BABAR [1071], and LHCb [1072], but for the  $CPV$ -allowed case only Belle measurements [1070] are available. The  $D^0 \rightarrow K^+ \pi^- \pi^0$ ,  $D^0 \rightarrow K_S^0 K^+ K^-$ , and  $D^0 \rightarrow \pi^0 \pi^+ \pi^-$  results are from BABAR [1059, 1073], the  $D^0 \rightarrow K^+ \pi^- \pi^+ \pi^-$  results are from LHCb [1061], and the  $\psi(3770) \rightarrow \bar{D} D$  results are from CLEOc [1057].

The relationships between the observables and the fitted parameters are listed in Table 258. For each set of correlated observables we construct a difference vector  $\vec{V}$  between measured values and those calculated from fitted parame-

**Table 259** Observables used in the global fit except those from time-dependent  $D^0 \rightarrow K^+ \pi^-$  measurements, and those from direct CPV measurements. The  $D^0 \rightarrow K^+ \pi^- \pi^0$  observables are  $x'' \equiv x \cos \delta_{K\pi\pi} + y \sin \delta_{K\pi\pi}$  and  $y'' \equiv -x \sin \delta_{K\pi\pi} + y \cos \delta_{K\pi\pi}$ 

Mode	Observable	Values	Correlation coefficients
$D^0 \rightarrow K^+ K^- / \pi^+ \pi^-$ , $\phi K_S^0$ [1060]	$y_{CP}$	$(0.835 \pm 0.155)\%$	
	$A_\Gamma$	$(-0.032 \pm 0.026)\%$	
$D^0 \rightarrow K_S^0 \pi^+ \pi^-$ [1070] (Belle: no CPV)	$x$	$(0.56 \pm 0.19^{+0.067}_{-0.127})\%$	
	$y$	$(0.30 \pm 0.15^{+0.050}_{-0.078})\%$	+0.012
$D^0 \rightarrow K_S^0 \pi^+ \pi^-$ [1070] (Belle: no direct CPV)	$ q/p $	$0.90^{+0.16+0.078}_{-0.15-0.064}$	
	$\phi$	$(-6 \pm 11^{+4.2}_{-5.0})$ degrees	
$D^0 \rightarrow K_S^0 \pi^+ \pi^-$ [1070] (Belle: direct CPV allowed)	$x$	$(0.58 \pm 0.19^{+0.0734}_{-0.1177})\%$	$\begin{Bmatrix} 1 & 0.054 & -0.074 & -0.031 \\ 0.054 & 1 & 0.034 & -0.019 \\ -0.074 & 0.034 & 1 & 0.044 \\ -0.031 & -0.019 & 0.044 & 1 \end{Bmatrix}$
	$y$	$(0.27 \pm 0.16^{+0.0546}_{-0.0854})\%$	
	$ q/p $	$0.82^{+0.20+0.0807}_{-0.18-0.0645}$	
	$\phi$	$(-13^{+12+4.15}_{-13-4.77})$ degrees	
$D^0 \rightarrow K_S^0 \pi^+ \pi^-$ [1072] (LHCb: no CPV)	$x$	$(-0.86 \pm 0.53 \pm 0.17)\%$	+0.37
	$y$	$(0.03 \pm 0.46 \pm 0.13)\%$	
$D^0 \rightarrow K_S^0 \pi^+ \pi^-$ [1071] $K_S^0 K^+ K^-$ (BABAR: no CPV)	$x$	$(0.16 \pm 0.23 \pm 0.12 \pm 0.08)\%$	+0.0615
	$y$	$(0.57 \pm 0.20 \pm 0.13 \pm 0.07)\%$	
$D^0 \rightarrow \pi^0 \pi^+ \pi^-$ [1073] (BABAR: no CPV)	$x$	$(1.5 \pm 1.2 \pm 0.6)\%$	-0.006
	$y$	$(0.2 \pm 0.9 \pm 0.5)\%$	
$D^0 \rightarrow K^+ \ell^- \nu$ [1060]	$R_M = (x^2 + y^2)/2$	$(0.0130 \pm 0.0269)\%$	
$D^0 \rightarrow K^+ \pi^- \pi^0$ [1059]	$x''$	$(2.61^{+0.57}_{-0.68} \pm 0.39)\%$	-0.75
	$y''$	$(-0.06^{+0.55}_{-0.64} \pm 0.34)\%$	
$D^0 \rightarrow K^+ \pi^- \pi^+ \pi^-$ [1061]	$R_M/2$	$(4.8 \pm 1.8) \times 10^{-5}$	
	$R_D$	$(0.533 \pm 0.107 \pm 0.045)\%$	$\begin{Bmatrix} 1 & 0 & -0.42 & 0.01 \\ 1 & -0.73 & 0.39 & 0.02 \\ & 1 & -0.53 & -0.03 \\ & & 1 & 0.04 \\ & & & 1 \end{Bmatrix}$
$\psi(3770) \rightarrow \bar{D}D$ [1057] (CLEOc)	$x^2$	$(0.06 \pm 0.23 \pm 0.11)\%$	
	$y$	$(4.2 \pm 2.0 \pm 1.0)\%$	
	$\cos \delta$	$0.81^{+0.22+0.07}_{-0.18-0.05}$	
	$\sin \delta$	$-0.01 \pm 0.41 \pm 0.04$	

ters using these relations; e.g., for  $D^0 \rightarrow K_S^0 \pi^+ \pi^-$  decays,  $\vec{V} = (\Delta x, \Delta y, \Delta |q/p|, \Delta \phi)$ . The contribution of a set of observables to the fit  $\chi^2$  is calculated as  $\vec{V} \cdot (M^{-1}) \cdot \vec{V}^T$ , where  $M^{-1}$  is the inverse of the covariance matrix for the measurement. Covariance matrices are constructed from the correlation coefficients among the measured observables. These correlation coefficients are also listed in Tables 259, 260 and 261.

### 8.1.3 Fit results

The global fit uses MINUIT with the MIGRAD minimizer, and all errors are obtained from MINOS [1090]. Four separate fits are performed:

1. assuming  $CP$  conservation, i.e., fixing  $A_D = 0$ ,  $A_K = 0$ ,  $A_\pi = 0$ ,  $\phi = 0$ , and  $|q/p| = 1$ ;

2. assuming no direct CPV in doubly Cabibbo-suppressed (DCS) decays ( $A_D = 0$ ) and fitting for parameters  $(x, y, |q/p|)$  or  $(x, y, \phi)$ ;
3. assuming no direct CPV in DCS decays and fitting for alternative parameters [1091, 1092]  $x_{12} = 2|M_{12}|/\Gamma$ ,  $y_{12} = |\Gamma_{12}|/\Gamma$ , and  $\phi_{12} = \text{Arg}(M_{12}/\Gamma_{12})$ , where  $M_{12}$  and  $\Gamma_{12}$  are the off-diagonal elements of the  $D^0$ - $\bar{D}^0$  mass and decay matrices, respectively. The parameter  $\phi_{12}$  is a weak phase that is responsible for  $CP$  violation in mixing.
4. allowing full CPV (floating all parameters).

For fits (2) and (3) assuming no direct CPV in DCS decays, in addition to  $A_D = 0$  we impose other constraints that reduce four independent parameters to three.<sup>38</sup> For fit (2) we impose

<sup>38</sup> One can also use Eq. (15) of Ref. [1091] to reduce four parameters to three.

**Table 260** Time-dependent  $D^0 \rightarrow K^+ \pi^-$  observables used for the global fit. The observables  $R_D^+$  and  $R_D^-$  are related to parameters  $R_D$  and  $A_D$  via  $R_D^\pm = R_D(1 \pm A_D)$ 

Mode	Observable	Values	Correlation coefficients
$D^0 \rightarrow K^+ \pi^-$ [1049] (BABAR 384 fb $^{-1}$ )	$R_D$	(0.303 $\pm$ 0.0189)%	$\begin{Bmatrix} 1 & 0.77 & -0.87 \\ 0.77 & 1 & -0.94 \\ -0.87 & -0.94 & 1 \end{Bmatrix}$
	$x'^{2+}$	(−0.024 $\pm$ 0.052)%	
	$y'^+$	(0.98 $\pm$ 0.78)%	
$\bar{D}^0 \rightarrow K^- \pi^+$ [1049] (BABAR 384 fb $^{-1}$ )	$A_D$	(−2.1 $\pm$ 5.4)%	Same as above
	$x'^{2-}$	(−0.020 $\pm$ 0.050)%	
	$y'^-$	(0.96 $\pm$ 0.75)%	
$D^0 \rightarrow K^+ \pi^-$ [1067] (Belle 976 fb $^{-1}$ No CPV)	$R_D$	(0.353 $\pm$ 0.013)%	$\begin{Bmatrix} 1 & 0.737 & -0.865 \\ 0.737 & 1 & -0.948 \\ -0.865 & -0.948 & 1 \end{Bmatrix}$
	$x'^2$	(0.009 $\pm$ 0.022)%	
	$y'$	(0.46 $\pm$ 0.34)%	
$D^0 \rightarrow K^+ \pi^-$ [1066] (Belle 400 fb $^{-1}$ CPV-allowed)	$R_D$	(0.364 $\pm$ 0.018)%	$\begin{Bmatrix} 1 & 0.655 & -0.834 \\ 0.655 & 1 & -0.909 \\ -0.834 & -0.909 & 1 \end{Bmatrix}$
	$x'^{2+}$	(0.032 $\pm$ 0.037)%	
	$y'^+$	(−0.12 $\pm$ 0.58)%	
$\bar{D}^0 \rightarrow K^- \pi^+$ [1066] (Belle 400 fb $^{-1}$ CPV-allowed)	$A_D$	(+2.3 $\pm$ 4.7)%	Same as above
	$x'^{2-}$	(0.006 $\pm$ 0.034)%	
	$y'^-$	(0.20 $\pm$ 0.54)%	
$D^0 \rightarrow K^+ \pi^-$ [1068] (CDF 9.6 fb $^{-1}$ No CPV)	$R_D$	(0.351 $\pm$ 0.035)%	$\begin{Bmatrix} 1 & 0.90 & -0.97 \\ 0.90 & 1 & -0.98 \\ -0.97 & -0.98 & 1 \end{Bmatrix}$
	$x'^2$	(0.008 $\pm$ 0.018)%	
	$y'$	(0.43 $\pm$ 0.43)%	
$D^0 \rightarrow K^+ \pi^-$ [1069] (LHCb 3.0 fb $^{-1}$ CPV-allowed)	$R_D^+$	(0.3474 $\pm$ 0.0081)%	$\begin{Bmatrix} 1 & 0.823 & -0.920 \\ 0.823 & 1 & -0.962 \\ -0.920 & -0.962 & 1 \end{Bmatrix}$
	$x'^{2+}$	(0.0011 $\pm$ 0.0065)%	
	$y'^+$	(0.597 $\pm$ 0.125)%	
$\bar{D}^0 \rightarrow K^- \pi^+$ [1069] (LHCb 3.0 fb $^{-1}$ CPV-allowed)	$R_D^-$	(0.3591 $\pm$ 0.0081)%	$\begin{Bmatrix} 1 & 0.812 & -0.918 \\ 0.812 & 1 & -0.956 \\ -0.918 & -0.956 & 1 \end{Bmatrix}$
	$x'^{2-}$	(0.0061 $\pm$ 0.0061)%	
	$y'^-$	(0.450 $\pm$ 0.121)%	

the relation [1092, 1093]  $\tan \phi = (1 - |q/p|^2)/(1 + |q/p|^2) \times (x/y)$  in two ways: first we float parameters  $x$ ,  $y$ , and  $\phi$  and from these derive  $|q/p|$ ; we then repeat the fit floating  $x$ ,  $y$ , and  $|q/p|$  and from these derive  $\phi$ . The central values returned by the two fits are identical, but the first fit yields MINOS errors for  $\phi$ , while the second fit yields MINOS errors for  $|q/p|$ . For no-direct-CPV fit (3), we fit for underlying parameters  $x_{12}$ ,  $y_{12}$ , and  $\phi_{12}$ , and from these calculate  $x$ ,  $y$ ,  $|q/p|$ , and  $\phi$  to which measured observables are compared. All fit results are listed in Table 262. For the CPV-allowed fit, individual contributions to the  $\chi^2$  are listed in

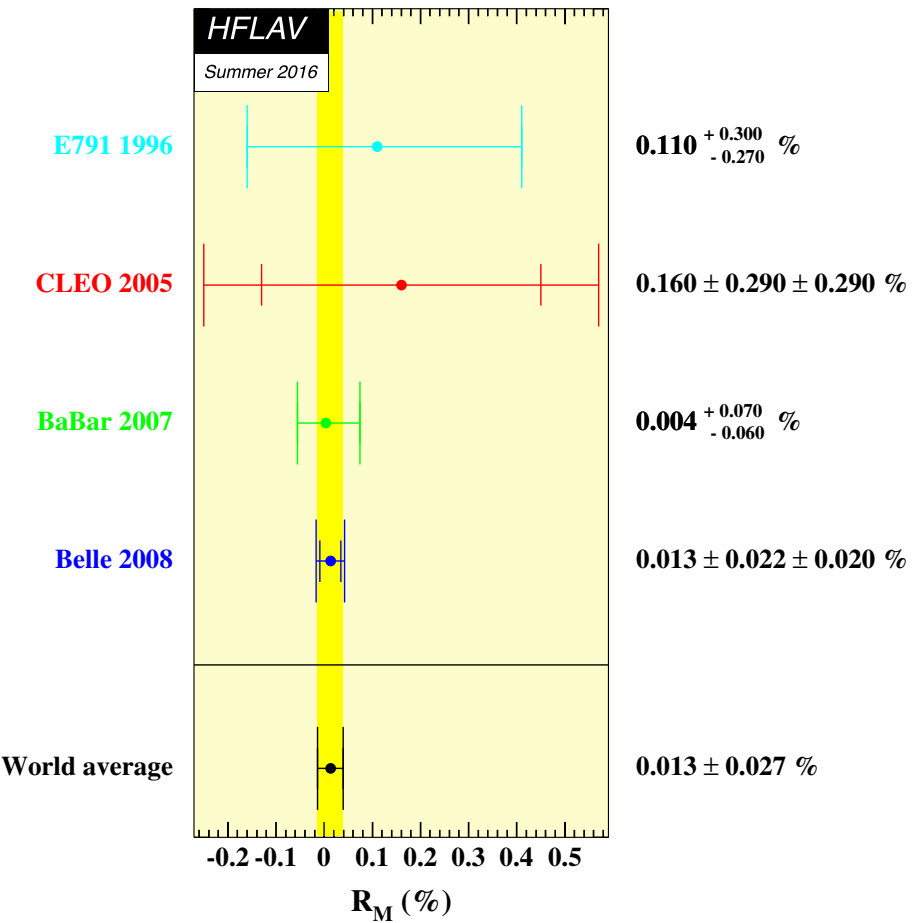
Table 263. The total  $\chi^2$  is 76.8 for  $50 - 10 = 40$  degrees of freedom.

Confidence contours in the two dimensions  $(x, y)$  or  $(|q/p|, \phi)$  are obtained by allowing, for any point in the two-dimensional plane, all other fitted parameters to take their preferred values. The resulting  $1\sigma - 5\sigma$  contours are shown in Fig. 194 for the CP-conserving case, in Fig. 195 for the no-direct-CPV case, and in Fig. 196 for the CPV-allowed case. The contours are determined from the increase of the  $\chi^2$  above the minimum value. One observes that the  $(x, y)$  contours for the no-CPV fit are very similar to those for the

**Table 261** Measurements of time-integrated  $CP$  asymmetries. The observable  $A_{CP}(f) \equiv [\Gamma(D^0 \rightarrow f) - \Gamma(\bar{D}^0 \rightarrow f)]/[\Gamma(D^0 \rightarrow$ 

$f) + \Gamma(\bar{D}^0 \rightarrow f)]$ , and  $\Delta\langle t \rangle$  is the difference between the mean reconstructed decay times for  $D^0 \rightarrow K^+ K^-$  and  $D^0 \rightarrow \pi^+ \pi^-$  decays (due to different trigger and reconstruction efficiencies)

Mode	Observable	Values	$\Delta\langle t \rangle/\tau_D$
$D^0 \rightarrow h^+ h^-$ [1074] (BABAR 386 fb $^{-1}$ )	$A_{CP}(K^+ K^-)$	( $+0.00 \pm 0.34 \pm 0.13$ )%	
	$A_{CP}(\pi^+ \pi^-)$	( $-0.24 \pm 0.52 \pm 0.22$ )% 0	
$D^0 \rightarrow h^+ h^-$ [1075] (Belle 976 fb $^{-1}$ )	$A_{CP}(K^+ K^-)$	( $-0.32 \pm 0.21 \pm 0.09$ )%	
	$A_{CP}(\pi^+ \pi^-)$	( $+0.55 \pm 0.36 \pm 0.09$ )% 0	
$D^0 \rightarrow h^+ h^-$ [1076, 1077] (CDF 9.7 fb $^{-1}$ )	$A_{CP}(K^+ K^-) - A_{CP}(\pi^+ \pi^-)$	( $-0.62 \pm 0.21 \pm 0.10$ )%	
	$A_{CP}(K^+ K^-)$	( $-0.32 \pm 0.21$ )%	
	$A_{CP}(\pi^+ \pi^-)$	( $+0.31 \pm 0.22$ )% 0.27 ± 0.01	
$D^0 \rightarrow h^+ h^-$ [1078] (LHCb 3.0 fb $^{-1}$ , $D^{*+} \rightarrow D^0 \pi^+$ tag)	$A_{CP}(K^+ K^-) - A_{CP}(\pi^+ \pi^-)$	( $-0.10 \pm 0.08 \pm 0.03$ )% 0.1153 ± 0.0007 ± 0.0018	
	$A_{CP}(K^+ K^-) - A_{CP}(\pi^+ \pi^-)$	( $+0.14 \pm 0.16 \pm 0.08$ )% 0.014 ± 0.004	

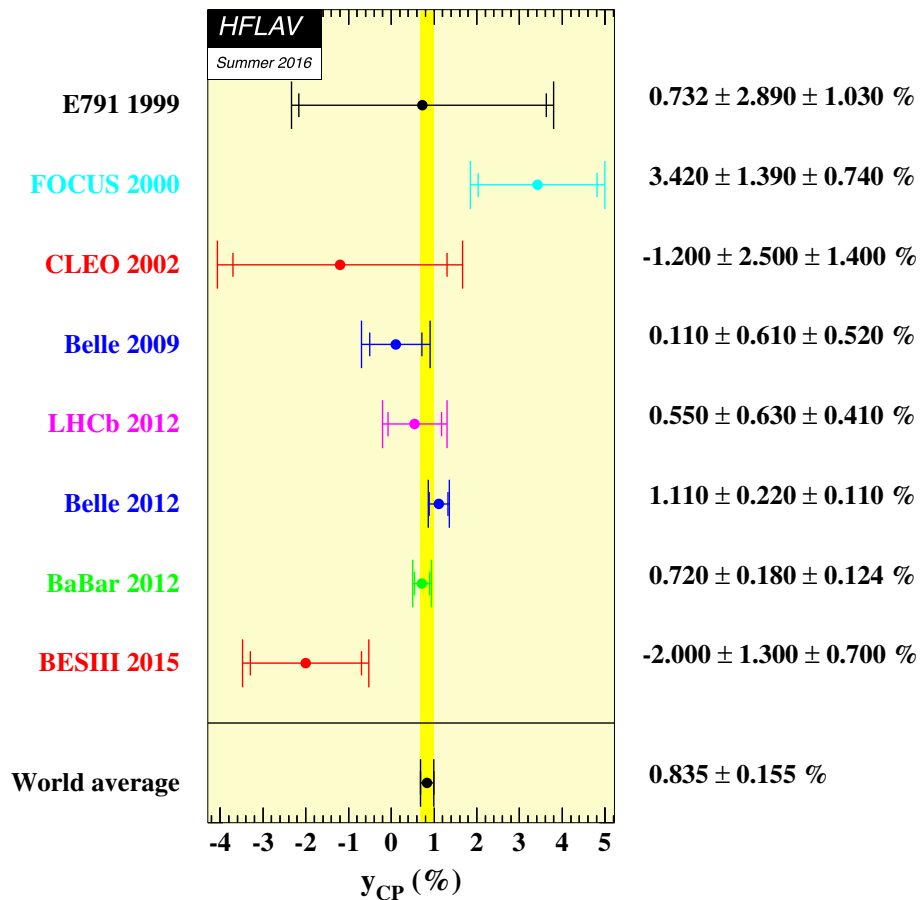
**Fig. 191** World average value of  $R_M = (x^2 + y^2)/2$  from Ref. [1060], as calculated from  $D^0 \rightarrow K^+ \ell^- \bar{\nu}$  measurements [1062–1065]

$CPV$ -allowed fit. In the latter fit, the  $\chi^2$  at the no-mixing point  $(x, y) = (0, 0)$  is 450 units above the minimum value, which, for two degrees of freedom, corresponds to a confi-

dence level<sup>39</sup> (C.L.)  $> 11.5\sigma$ . Thus, no mixing is excluded at this high level. In the  $(|q/p|, \phi)$  plot, the no- $CPV$  point  $(1, 0)$

<sup>39</sup> This is the limit of the CERNLIB PROB routine [1094] used for this calculation.

**Fig. 192** World average value of  $y_{CP}$  from Ref. [1060], as calculated from  $D^0 \rightarrow K^+ K^-$ ,  $\pi^+ \pi^-$  measurements [1079–1086]



is within the  $1\sigma$  contour; thus the data is consistent with  $CP$  conservation.

One-dimensional likelihood curves for individual parameters are obtained by allowing, for a fixed value of a selected parameter, all other fitted parameters to take their preferred values. The resulting functions  $\Delta\chi^2 = \chi^2 - \chi^2_{\min}$  ( $\chi^2_{\min}$  is the minimum value) are shown in Fig. 197. The points where  $\Delta\chi^2 = 3.84$  determine 95% C.L. intervals for the parameters. These intervals are listed in Table 262.

#### 8.1.4 Conclusions

From the fit results listed in Table 262 and shown in Figs. 196 and 197, we conclude that:

- the experimental data consistently indicate that  $D^0$  mesons mix. The no-mixing point  $x = y = 0$  is excluded at  $> 11.5\sigma$ . The parameter  $x$  differs from zero by  $1.9\sigma$ , and  $y$  differs from zero by  $9.4\sigma$ . This mixing is presumably dominated by long-distance processes, which are difficult to calculate. Thus unless it turns out that  $|x| \gg |y|$  [1053], which is not indicated, it will be difficult to identify new physics from  $(x, y)$  alone.

- Since  $y_{CP}$  is positive, the  $CP$ -even state is shorter-lived as in the  $K^0-\bar{K}^0$  system. However, since  $x$  also appears to be positive, the  $CP$ -even state is heavier, unlike in the  $K^0-\bar{K}^0$  system.
- There is no evidence for  $CPV$  arising from  $D^0-\bar{D}^0$  mixing ( $|q/p| \neq 1$ ) or from a phase difference between the mixing amplitude and a direct decay amplitude ( $\phi \neq 0$ ). The CDF experiment (and initially LHCb) measured a time-integrated asymmetry in  $D^0 \rightarrow K^+ K^-$ ,  $\pi^+ \pi^-$  decays that hints at direct  $CPV$  (see Table 261); however, recent measurements from LHCb with higher statistics disfavor this hypothesis and are consistent with zero.

#### 8.2 $CP$ asymmetries

One way  $CP$  violation manifests itself is if the decay rate for a particle differs from that of its  $CP$ -conjugate [1095]. Such phenomena can be classified into two broad categories, termed *direct CP* violation and *indirect CP* violation [1096]. Direct  $CP$  violation refers to charm changing,  $\Delta C = 1$ , processes and can occur in both charged and neutral charm hadron decays. It results from interference between two different decay amplitudes (e.g., a penguin and tree amplitude)

**Fig. 193** World average value of  $A_\Gamma$  from Ref. [1060], as calculated from  $D^0 \rightarrow K^+ K^-$ ,  $\pi^+ \pi^-$  measurements [1084, 1085, 1087–1089]

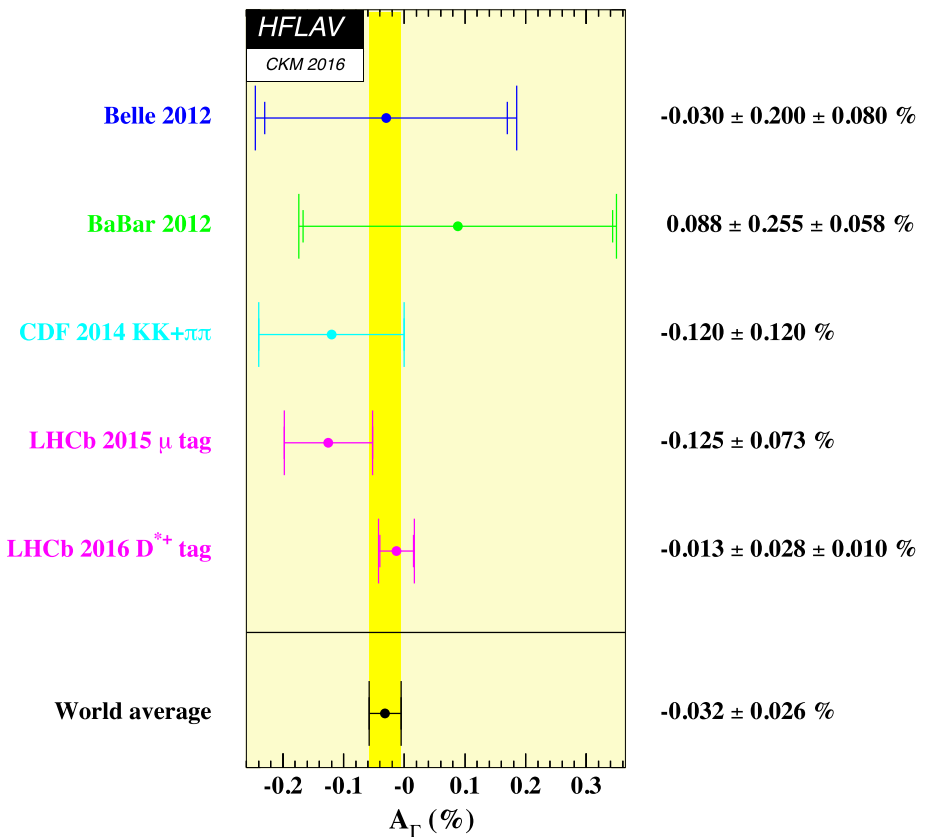


**Table 262** Results of the global fit for different assumptions concerning  $CPV$

Parameter	No $CPV$	No direct $CPV$ in DCS decays	$CPV$ -allowed	$CPV$ -allowed 95% C.L. interval
$x$ (%)	$0.46^{+0.14}_{-0.15}$	$0.41^{+0.14}_{-0.15}$	$0.32 \pm 0.14$	[0.04, 0.62]
$y$ (%)	$0.62 \pm 0.08$	$0.61 \pm 0.07$	$0.69^{+0.06}_{-0.07}$	[0.50, 0.80]
$\delta_{K\pi}$ (°)	$8.0^{+9.7}_{-11.2}$	$4.8^{+10.4}_{-12.3}$	$15.2^{+7.6}_{-10.0}$	[-16.8, 30.1]
$R_D$ (%)	$0.348^{+0.004}_{-0.003}$	$0.347^{+0.004}_{-0.003}$	$0.349^{+0.004}_{-0.003}$	[0.342, 0.356]
$A_D$ (%)	—	—	$-0.88 \pm 0.99$	[-2.8, 1.0]
$ q/p $	—	$0.999 \pm 0.014$	$0.89^{+0.08}_{-0.07}$	[0.77, 1.12]
$\phi$ (°)	—	$0.05^{+0.54}_{-0.53}$	$-12.9^{+9.9}_{-8.7}$	[-30.2, 10.6]
$\delta_{K\pi\pi}$ (°)	$20.4^{+23.3}_{-23.8}$	$22.6^{+24.1}_{-24.4}$	$31.7^{+23.5}_{-24.2}$	[-16.4, 77.7]
$A_\pi$ (%)	—	$+0.02 \pm 0.13$	$+0.01 \pm 0.14$	[-0.25, 0.28]
$A_K$ (%)	—	$-0.11 \pm 0.13$	$-0.11 \pm 0.13$	[-0.37, 0.14]
$x_{12}$ (%)	—	$0.41^{+0.14}_{-0.15}$		[0.10, 0.67]
$y_{12}$ (%)	—	$0.61 \pm 0.07$		[0.47, 0.75]
$\phi_{12}$ (°)	—	$-0.17 \pm 1.8$		[-5.3, 4.4]

that have different weak (CKM) and strong phases.<sup>40</sup> In the Standard Model a difference in strong phases may arise for example due to final-state interactions (FSI)[1097], different

isospin amplitudes, intermediate resonance contributions, or different partial waves. A difference in weak phases arises from different CKM vertex couplings, as is often the case for tree and penguin diagrams. Within the SM direct  $CP$  violation is expected only in Singly Cabibbo Suppressed (SCS) charm decays, as only these decays receive a contribution from the penguin amplitude. This type of  $CP$  violation depends on the decay mode, the SM asymmetries may reach

<sup>40</sup> The weak phase difference will have opposite signs for  $D \rightarrow f$  and  $\bar{D} \rightarrow \bar{f}$  decays, while the strong phase difference will have the same sign. As a result, squaring the total amplitudes to obtain the decay rates gives interference terms having opposite sign, i.e., non-identical decay rates.

**Table 263** Individual contributions to the  $\chi^2$  for the  $CPV$ -allowed fit

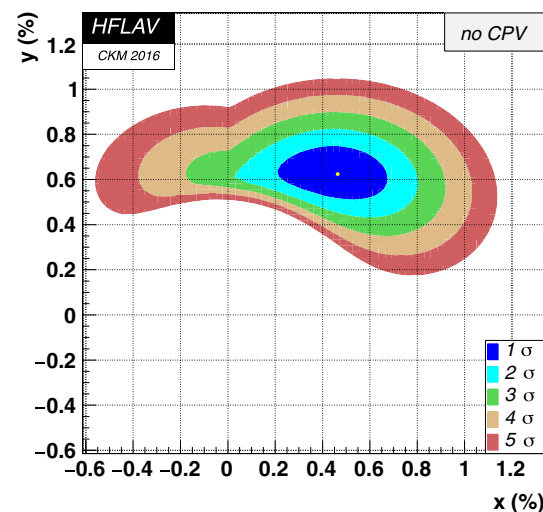
Observable	$\chi^2$	$\sum \chi^2$
$y_{CP}$	1.19	1.19
$A_\Gamma$	0.83	2.01
$x_{K_S^0\pi^+\pi^-}$ Belle	1.33	3.35
$y_{K_S^0\pi^+\pi^-}$ Belle	5.30	8.64
$ q/p _{K_S^0\pi^+\pi^-}$ Belle	0.10	8.74
$\phi_{K_S^0\pi^+\pi^-}$ Belle	0.23	8.97
$x_{K_S^0\pi^+\pi^-}$ LHCb	4.51	13.48
$y_{K_S^0\pi^+\pi^-}$ LHCb	0.40	13.88
$x_{K_S^0h^+h^-}$ BABAR	0.36	14.24
$y_{K_S^0h^+h^-}$ BABAR	0.19	14.43
$x_{\pi^0\pi^+\pi^-}$ BABAR	0.77	15.20
$y_{\pi^0\pi^+\pi^-}$ BABAR	0.22	15.42
$(x^2 + y^2)_{K^+\ell^-\nu}$	0.14	15.56
$x_{K^+\pi^-\pi^0}$ BABAR	7.10	22.67
$y_{K^+\pi^-\pi^0}$ BABAR	3.92	26.58
CLEOc ( $x/y/R_D/\cos\delta/\sin\delta$ )	10.53	37.12
$R_D^+/x'^{2+}/y'^+$ BABAR	11.13	48.25
$R_D^-/x'^{2-}/y'^-$ BABAR	6.04	54.29
$R_D^+/x'^{2+}/y'^+$ Belle	2.08	56.36
$R_D^-/x'^{2-}/y'^-$ Belle	3.22	59.58
$R_D/x'^2/y'$ CDF	1.29	60.87
$R_D^+/x'^{2+}/y'^+$ LHCb	0.58	61.46
$R_D^-/x'^{2-}/y'^-$ LHCb	1.65	63.11
$A_{KK}/A_{\pi\pi}$ BABAR	0.30	63.41
$A_{KK}/A_{\pi\pi}$ Belle	2.89	66.30
$A_{KK}/A_{\pi\pi}$ CDF	4.63	70.94
$A_{KK} - A_{\pi\pi}$ LHCb ( $D^{*+} \rightarrow D^0\pi^+$ tag)	0.12	71.05
$A_{KK} - A_{\pi\pi}$ LHCb ( $\bar{B} \rightarrow D^0\mu^-X$ tag)	2.24	73.30
$(x^2 + y^2)_{K^+\pi^-\pi^+\pi^-}$ LHCb	3.48	76.78

a percent level. Indirect  $CP$  violation refers to  $\Delta C = 2$  processes and arises in  $D^0$  decays due to  $D^0 - \bar{D}^0$  mixing. It can occur as an asymmetry in the mixing itself, or it can result from interference between a decay amplitude following mixing and a non-mixed amplitude. Within the SM charm indirect  $CP$  asymmetry is expected to be universal.

The  $CP$  asymmetry is defined as the difference between  $D$  and  $\bar{D}$  partial widths divided by their sum:

$$A_{CP} = \frac{\Gamma(D) - \Gamma(\bar{D})}{\Gamma(D) + \Gamma(\bar{D})}. \quad (225)$$

In the case of  $D^+$  and  $D_s^+$  decays,  $A_{CP}$  measures direct  $CP$  violation; in the case of  $D^0$  decays,  $A_{CP}$  measures direct and indirect  $CP$  violation combined (see also Sect. 8.4).

**Fig. 194** Two-dimensional contours for mixing parameters ( $x$ ,  $y$ ), for no  $CPV$ 

In each experiment, care must be taken to correct for production and detection asymmetries. To take into account differences in production rates between  $D$  and  $\bar{D}$  (which would affect the number of respective decays observed), some experiments (like FOCUS and E791) normalize to a Cabibbo-favored mode. In this case there is the additional benefit that most corrections due to reconstruction inefficiencies cancel out, reducing systematic uncertainties. An implicit assumption is that there is no measurable  $CP$  violation in the Cabibbo-favored normalizing mode. The  $CP$  asymmetry is calculated as

$$A_{CP} = \frac{\eta(D) - \eta(\bar{D})}{\eta(D) + \eta(\bar{D})}, \quad (226)$$

where (considering, for example,  $D^0 \rightarrow K^-K^+$ )

$$\eta(D) = \frac{N(D^0 \rightarrow K^-K^+)}{N(D^0 \rightarrow K^-\pi^+)}, \quad (227)$$

$$\eta(\bar{D}) = \frac{N(\bar{D}^0 \rightarrow K^-K^+)}{N(\bar{D}^0 \rightarrow K^+\pi^-)}. \quad (228)$$

Other experiments (like LHCb) determine  $A_{CP}$  through the relation:

$$A_{\text{meas}} = A_{CP} + A_{\text{prod}} + A_{\text{det}}, \quad (229)$$

where  $A_{\text{meas}}$  is the measured asymmetry,  $A_{\text{prod}}$  is the asymmetry in the charm meson production, and  $A_{\text{det}}$  is due to difference in detection efficiencies between positively and negatively charged hadrons.

Values of  $A_{CP}$  for  $D^+$ ,  $D^0$  and  $D_s^+$  decays are listed in Tables 264, 265, 266, 267 and 268 respectively. In these tables we report asymmetries for the actual final state, i.e., resonant substructure is implicitly included but not considered separately. The high accuracy of these measurements

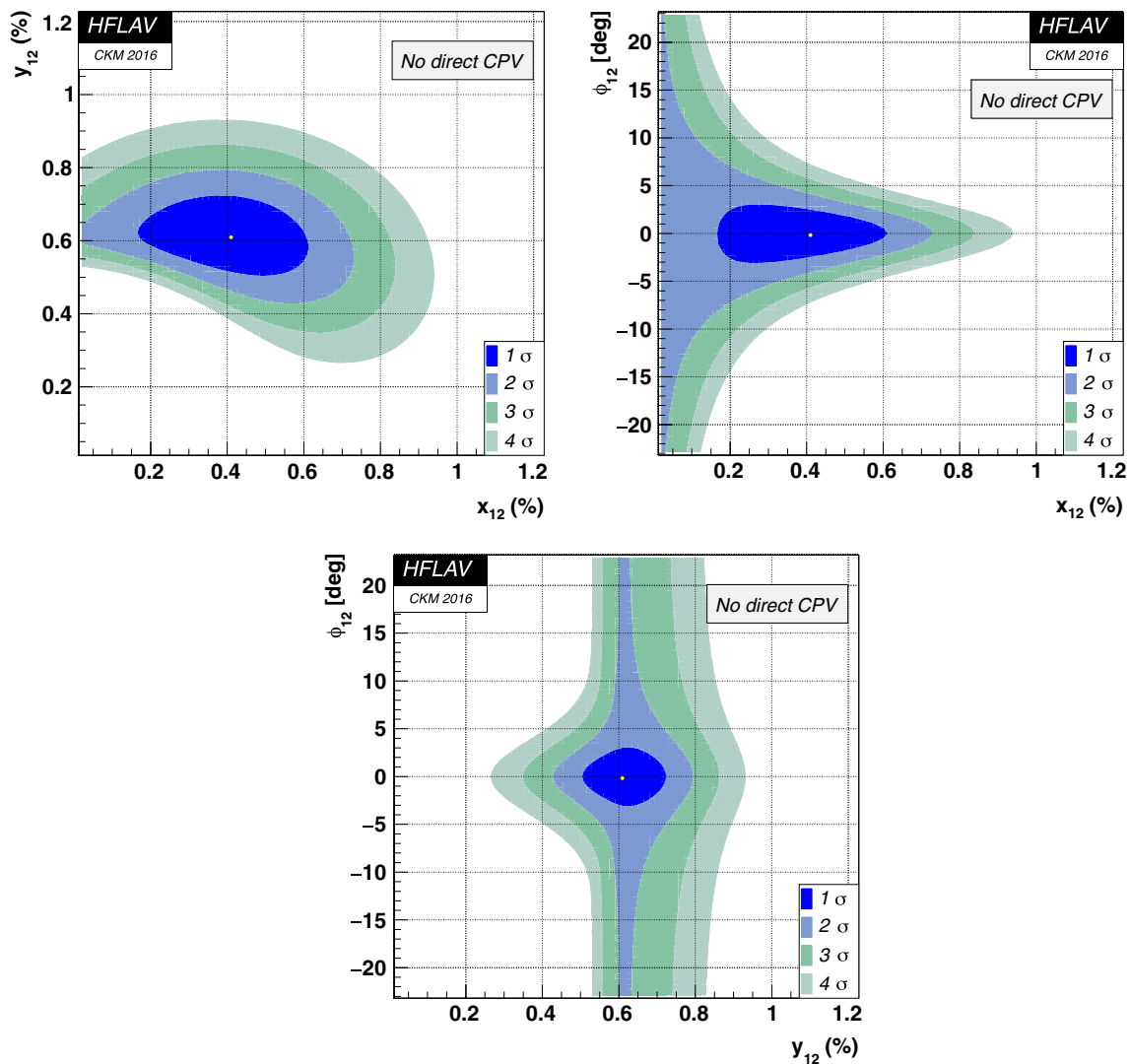


**Fig. 195** Two-dimensional contours for theoretical parameters ( $x_{12}, y_{12}$ ) (top left), ( $x_{12}, \phi_{12}$ ) (top right), and ( $y_{12}, \phi_{12}$ ) (bottom), for no direct CPV in DCS decays

allows one to see and correct for  $CP$  violation due to the CPV in  $K^0$ - $\bar{K}^0$  mixing [1098]. For example, the decay modes  $D^+ \rightarrow (\bar{K}^0/K^0)K^+$  and  $D_s^+ \rightarrow (\bar{K}^0/K^0)\pi^+$  (shown in Tables 264 and 268, respectively) are the modes  $D^+ \rightarrow K_s^0 K^+$  and  $D_s^+ \rightarrow K_s^0 \pi^+$  after subtracting for this effect. For multi-body decays some experiments use model independent techniques to reveal local  $CP$  asymmetry. The first technique (Miranda method) [1099] uses a binned  $\chi^2$  approach to compare the relative density in a bin of phase space of a decay with that of its  $CP$  conjugate. In the Energy Test technique [1100] two event samples are compared and a test statistic variable ( $T$ ) is used to determine the average distances of events in phase space. If the distributions of events in both samples are identical,  $T$  will randomly fluctuate around a value close to zero.

Overall,  $CP$  asymmetry measurements have been carried out for 49 charm decay modes, and in several modes the sensitivity is well below  $5 \times 10^{-3}$ . There is currently no evidence for  $CP$  violation in the charm meson sector. The  $CP$  asymmetry observed in the mode  $D^+ \rightarrow K_s^0 \pi^+$  is consistent with what expected from the  $K^0 - \bar{K}^0$  system [1098], and thus it is not attributed to charm.

Neither in the charm baryon sector there is evidence of  $CP$  asymmetry. These are just two measurements on  $\Lambda_C^+$ , with limited sensitivity, done by FOCUS [1101] and by CLEO [1102].

Taken together, the limits obtained for  $CP$  asymmetries in the charm sector pose tight constraints on new physics models.

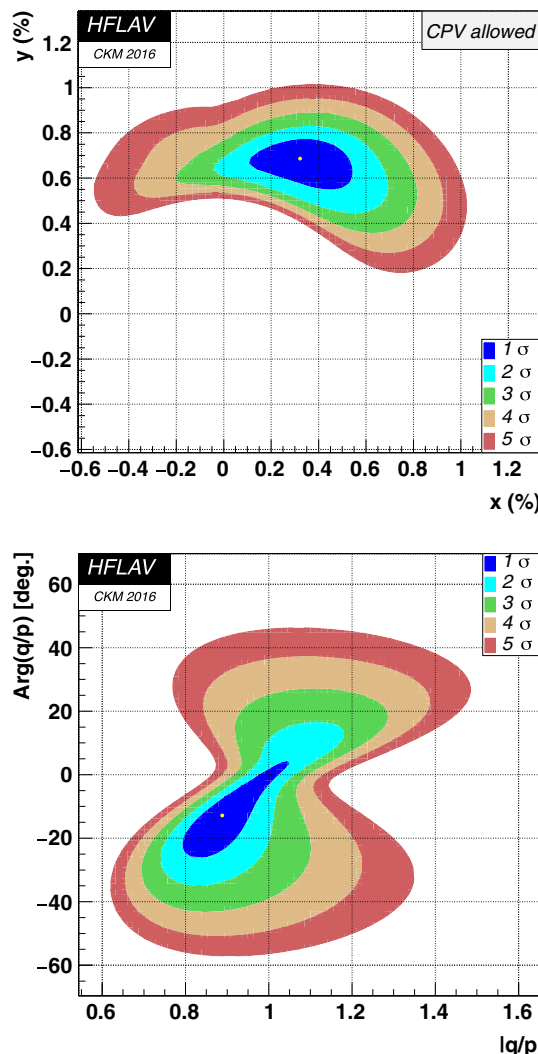


**Fig. 196** Two-dimensional contours for parameters  $(x, y)$  (top) and  $(|q/p|, \phi)$  (bottom), allowing for  $CPV$

### 8.3 $T$ -odd asymmetries

Measuring  $T$ -odd asymmetries provides an alternative way to search for  $CP$  violation in the charm sector, due to  $CPT$  invariance.  $T$ -odd asymmetries are measured using triple-product correlations of the form  $\vec{a} \cdot (\vec{b} \times \vec{c})$ , where  $a, b$ , and  $c$  are spins or momenta; this combination is odd under time reversal ( $T$ ). If the triple-product is formed using *both* spin and momenta, i.e.,

$$\vec{s}_1 \cdot (\vec{p}_2 \times \vec{p}_3), \quad (230)$$

then it is even for  $P$ -conjugation. However, if only momenta are used, then it is odd for  $P$ -conjugation. In this case the asymmetry allows one to probe  $CP$  violation occurring via  $P$ -violation. This may arise in  $P$ -odd amplitudes, which are allowed in decays to final states with 4 spinless particles.

Taking as an example the decay mode  $D^0 \rightarrow K^+ K^- \pi^+ \pi^-$ , one forms the triple-product correlation using the momenta of the final state particles. We note that when using only momenta, at least four daughter particles are required to give a nonzero correlation (as three daughters decay in a plane). Defining for  $D^0$  the  $T$ -odd correlation

$$C_T \equiv \vec{p}_{K^+} \cdot (\vec{p}_{\pi^+} \times \vec{p}_{\pi^-}), \quad (231)$$

and the corresponding quantity for  $\bar{D}^0$

$$\bar{C}_T \equiv \vec{p}_{K^-} \cdot (\vec{p}_{\pi^-} \times \vec{p}_{\pi^+}), \quad (232)$$

one constructs the asymmetry

$$A_T = \frac{\Gamma(C_T > 0) - \Gamma(C_T < 0)}{\Gamma(C_T > 0) + \Gamma(C_T < 0)} \quad (233)$$

for  $D^0$  decays and

$$\bar{A}_T = \frac{\Gamma(-\bar{C}_T > 0) - \Gamma(-\bar{C}_T < 0)}{\Gamma(-\bar{C}_T > 0) + \Gamma(-\bar{C}_T < 0)} \quad (234)$$

for  $\bar{D}^0$  decays. In these expressions,  $\Gamma$  represents a partial width. The asymmetries  $A_T$  and  $\bar{A}_T$  depend on the angular distribution of the daughter particles and may be nonzero due to final state interactions or  $P$ -violation in weak decays.

Since  $P(C_T) = -C_T$  and  $C(\bar{C}_T) = \bar{C}_T$ ,  $CP(A_T) = \bar{A}_T$ . One can thus construct the  $CP$ -odd (and  $P$ -odd,  $T$ -odd) quantity

$$\mathcal{A}_T \equiv \frac{A_T - \bar{A}_T}{2}; \quad (235)$$

a nonzero value indicates  $CP$  violation (see Refs. [1140–1145]).

Recently, this topic has been revisited (see Refs. [1146, 1147]) with the suggestion to use other asymmetries constructed from triple products in multi-body decays to probe  $C$ ,  $P$ , and  $CP$  symmetries. Up until now, experiments have measured only the asymmetry  $\mathcal{A}_T$  defined in Eq. (235). (Note that this asymmetry is referred to in the literature by several names:  $A_{T\text{ viol}}$ ,  $a_{CP}^P$ , and  $a_{CP}^{T\text{-odd}}$ .)

Values of  $\mathcal{A}_T$  for  $D^+$ ,  $D_s^+$ , and  $D^0$  decay modes are listed in Table 269. The first measurements were made by FOCUS, and subsequent BABAR measurements reached a sensitivity of  $\sim 1\%$ . Currently the best sensitivity is from LHCb.

However, despite relatively high precision ( $< 1\%$ ), there is no evidence for  $CP$  violation.

### 8.4 Interplay of direct and indirect $CP$ violation

In decays of  $D^0$  mesons,  $CP$  asymmetry measurements have contributions from both direct and indirect  $CP$  violation as discussed in Sect. 8.1. The contribution from indirect  $CP$  violation depends on the decay-time distribution of the data

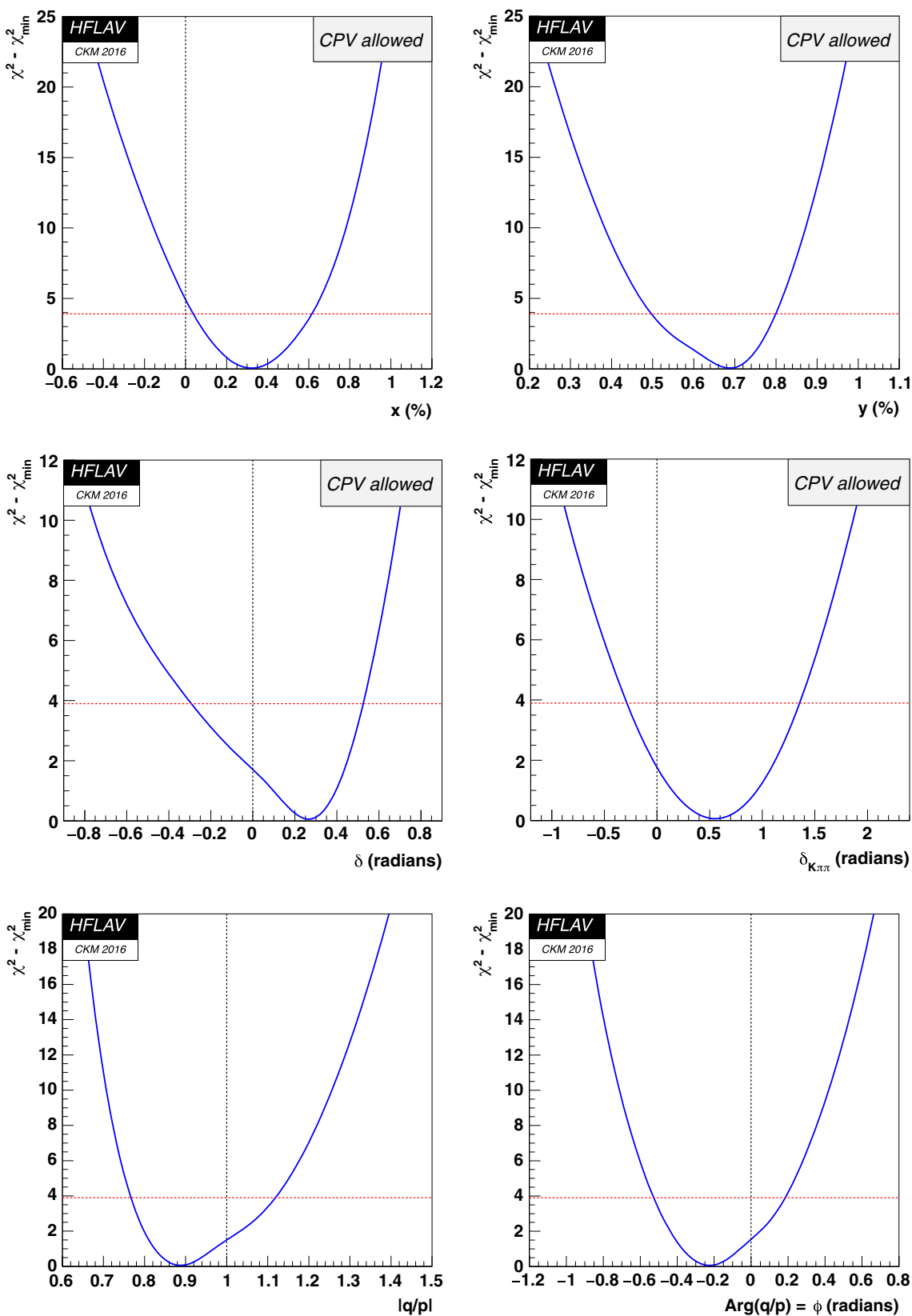


**Fig. 197** The function  $\Delta\chi^2 = \chi^2 - \chi_{\min}^2$  for fitted parameters  $x$ ,  $y$ ,  $\delta$ ,  $\delta_{K\pi\pi}$ ,  $|q/p|$ , and  $\phi$ . The points where  $\Delta\chi^2 = 3.84$  (denoted by dashed horizontal lines) determine 95% C.L. intervals

**Table 264**  $CP$  asymmetries  $A_{CP} = [\Gamma(D^+) - \Gamma(D^-)]/[\Gamma(D^+) + \Gamma(D^-)]$  for two-body  $D^\pm$  decays

Mode	Year	Collaboration	$A_{CP}$
$D^+ \rightarrow \mu^+ \nu$	2008	CLEO [1103]	$+0.08 \pm 0.08$
$D^+ \rightarrow \pi^+ \pi^0$	2010	CLEO [1104]	$+0.029 \pm 0.029 \pm 0.003$
$D^+ \rightarrow \pi^+ \eta$	2011	Belle [1105]	$+0.0174 \pm 0.0113 \pm 0.0019$
	2010	CLEO [1104]	$-0.020 \pm 0.023 \pm 0.003$
		HFLAV average	$+0.010 \pm 0.010$
$D^+ \rightarrow \pi^+ \eta'$	2011	Belle [1105]	$-0.0012 \pm 0.0112 \pm 0.0017$
	2010	CLEO [1104]	$-0.040 \pm 0.034 \pm 0.003$
		HFLAV average	$-0.005 \pm 0.011$
$D^+ \rightarrow K^+ \pi^0$	2010	CLEO [1104]	$-0.035 \pm 0.107 \pm 0.009$
$D^+ \rightarrow K_s^0 \pi^+$	2014	CLEO [1106]	$-0.011 \pm 0.006 \pm 0.002$
	2012	Belle [1107]	$-0.00363 \pm 0.00094 \pm 0.00067$
	2011	BABAR [1108]	$-0.0044 \pm 0.0013 \pm 0.0010$
	2002	FOCUS [1109]	$-0.016 \pm 0.015 \pm 0.009$
		HFLAV average	$-0.0041 \pm 0.0009$
$D^+ \rightarrow K_s^0 K^+$	2013	BABAR [1110]	$+0.0013 \pm 0.0036 \pm 0.0025$
	2013	Belle [1111]	$-0.0025 \pm 0.0028 \pm 0.0014$
	2010	CLEO [1104]	$-0.002 \pm 0.015 \pm 0.009$
	2002	FOCUS [1109]	$+0.071 \pm 0.061 \pm 0.012$
		HFLAV average	$-0.0011 \pm 0.0025$
$D^+ \rightarrow (\bar{K}^0/K^0) K^+$	2014	LHCb [1112]	$+0.0003 \pm 0.0017 \pm 0.0014$
	2013	BABAR [1110]	$+0.0046 \pm 0.0036 \pm 0.0025$
	2013	Belle [1111]	$-0.0008 \pm 0.0028 \pm 0.0014$
		HFLAV average	$+0.0011 \pm 0.0017$

**Table 265**  $CP$  asymmetries  $A_{CP} = [\Gamma(D^+) - \Gamma(D^-)]/[\Gamma(D^+) + \Gamma(D^-)]$  for three- and four-body  $D^\pm$  decays

Mode	Year	Collaboration	$A_{CP}$
$D^+ \rightarrow \pi^+ \pi^- \pi^+$	2014	LHCb [1113]	Model independent technique, no evidence for $CP$ violation
	1997	E791 [1114]	$-0.017 \pm 0.042$ (stat.)
$D^+ \rightarrow K^- \pi^+ \pi^+$	2014	D0 [1115]	$-0.0016 \pm 0.0015 \pm 0.0009$
	2014	CLEO [1106]	$-0.003 \pm 0.002 \pm 0.004$
		HFLAV average	$-0.0018 \pm 0.0016$
$D^+ \rightarrow K_s^0 \pi^+ \pi^0$	2014	CLEO [1106]	$-0.001 \pm 0.007 \pm 0.002$
$D^+ \rightarrow K^+ K^- \pi^+$	2014	CLEO [1106]	$-0.001 \pm 0.009 \pm 0.004$
	2013	BABAR [1116]	$+0.0037 \pm 0.0030 \pm 0.0015$
	2008	CLEO [1117]	Dalitz plot analysis, no evidence for $CP$ violation
	2000	FOCUS [1118]	$+0.006 \pm 0.011 \pm 0.005$
	1997	E791 [1114]	$-0.014 \pm 0.029$ (stat.)
		HFLAV average	$+0.0032 \pm 0.0031$
$D^+ \rightarrow K^- \pi^+ \pi^+ \pi^0$	2014	CLEO [1106]	$-0.003 \pm 0.006 \pm 0.004$
$D^+ \rightarrow K_s^0 \pi^+ \pi^+ \pi^-$	2014	CLEO [1106]	$+0.000 \pm 0.012 \pm 0.003$
$D^+ \rightarrow K_s^0 K^+ \pi^+ \pi^-$	2005	FOCUS [1119]	$-0.042 \pm 0.064 \pm 0.022$

**Table 266**  $CP$  asymmetries  $A_{CP} = [\Gamma(D^0) - \Gamma(\bar{D}^0)]/[\Gamma(D^0) + \Gamma(\bar{D}^0)]$  for two-body  $D^0, \bar{D}^0$  decays

Mode	Year	Collaboration	$A_{CP}$
$D^0 \rightarrow \pi^+ \pi^-$	2014	LHCb [1058]	$-0.0020 \pm 0.0019 \pm 0.0010$
	2012	CDF [1120]	$+0.0022 \pm 0.0024 \pm 0.0011$
	2008	BABAR [1074]	$-0.0024 \pm 0.0052 \pm 0.0022$
	2012	Belle [1121]	$+0.0043 \pm 0.0052 \pm 0.0012$
	2002	CLEO [1081]	$+0.019 \pm 0.032 \pm 0.008$
	2000	FOCUS [1118]	$+0.048 \pm 0.039 \pm 0.025$
	1998	E791 [1122]	$-0.049 \pm 0.078 \pm 0.030$
HFLAV average			
$D^0 \rightarrow \pi^0 \pi^0$			
$D^0 \rightarrow K_s^0 \pi^0$	2014	Belle [1123]	$-0.0003 \pm 0.0064 \pm 0.0010$
	2001	CLEO [1124]	$+0.001 \pm 0.048 \text{ (stat. and syst. combined)}$
	HFLAV average		
$D^0 \rightarrow K_s^0 \eta$	2014	Belle [1123]	$-0.0021 \pm 0.0016 \pm 0.0007$
	2001	CLEO [1124]	$+0.001 \pm 0.013 \text{ (stat. and syst. combined)}$
	HFLAV average		
$D^0 \rightarrow K_s^0 \eta'$	2011	Belle [1125]	$+0.0054 \pm 0.0051 \pm 0.0016$
	2011	Belle [1125]	$+0.0098 \pm 0.0067 \pm 0.0014$
$D^0 \rightarrow K_s^0 K_s^0$	2015	LHCb [1126]	$-0.029 \pm 0.052 \pm 0.022$
	2001	CLEO [1124]	$-0.23 \pm 0.19 \text{ (stat. and syst. combined)}$
	HFLAV average		
$D^0 \rightarrow K^- \pi^+$	2014	CLEO [1106]	$+0.003 \pm 0.003 \pm 0.006$
	2014	LHCb [1058]	$-0.0006 \pm 0.0015 \pm 0.0010$
$D^0 \rightarrow K^+ K^-$	2012	CDF [1120]	$-0.0024 \pm 0.0022 \pm 0.0009$
	2008	BABAR [1074]	$+0.0000 \pm 0.0034 \pm 0.0013$
	2012	Belle [1121]	$-0.0043 \pm 0.0030 \pm 0.0011$
	2002	CLEO [1081]	$+0.000 \pm 0.022 \pm 0.008$
	2000	FOCUS [1118]	$-0.001 \pm 0.022 \pm 0.015$
	1998	E791 [1122]	$-0.010 \pm 0.049 \pm 0.012$
	HFLAV average		

**Table 267**  $CP$  asymmetries  $A_{CP} = [\Gamma(D^0) - \Gamma(\bar{D}^0)]/[\Gamma(D^0) + \Gamma(\bar{D}^0)]$  for three- and four-body  $D^0, \bar{D}^0$  decays

Mode	Year	Collaboration	$A_{CP}$
$D^0 \rightarrow \pi^+ \pi^- \pi^0$	2015	LHCb [1127]	Model independent technique, no evidence for $CP$ violation
	2008	BABAR [1128]	$+0.0031 \pm 0.0041 \pm 0.0017$
	2008	Belle [1129]	$+0.0043 \pm 0.0130 \text{ (stat. and syst. combined)}$
	2005	CLEO [1130]	$+0.01^{+0.09}_{-0.07} \pm 0.05$
	HFLAV average		
	$D^0 \rightarrow K^- \pi^+ \pi^0$		
	2014	CLEO [1106]	$+0.001 \pm 0.003 \pm 0.004$
$D^0 \rightarrow K^+ \pi^- \pi^0$	2005	Belle [1131]	$-0.006 \pm 0.053 \text{ (stat.)}$
	2001	CLEO [1132]	$+0.09^{+0.25}_{-0.22} \text{ (stat.)}$
	HFLAV average		
$D^0 \rightarrow K_s^0 \pi^+ \pi^-$	2012	CDF [1133]	$-0.0005 \pm 0.0057 \pm 0.0054$
	2004	CLEO [1134]	$-0.009 \pm 0.021^{+0.016}_{-0.057}$
	HFLAV average		
$D^0 \rightarrow K_s^0 + K^- \pi^+$	2016	LHCb [473]	Amplitude analysis, no evidence for $CP$ violation
	2016	LHCb [473]	Amplitude analysis, no evidence for $CP$ violation

**Table 267** continued

Mode	Year	Collaboration	$A_{CP}$
$D^0 \rightarrow K^+ K^- \pi^0$	2008	BABAR [1128]	$-0.0100 \pm 0.0167 \pm 0.0025$
$D^0 \rightarrow \pi^- \pi^- \pi^+ \pi^+$	2013	LHCb [1135]	Model independent technique, no evidence for $CP$ violation
$D^0 \rightarrow K^- \pi^+ \pi^+ \pi^-$	2014	CLEO [1106]	$+0.002 \pm 0.003 \pm 0.004$
$D^0 \rightarrow K^+ \pi^- \pi^+ \pi^-$	2005	Belle [1131]	$-0.018 \pm 0.044$ (stat.)
$D^0 \rightarrow K^+ K^- \pi^+ \pi^-$	2013	LHCb [1135]	Model independent technique, no evidence for $CP$ violation
	2012	CLEO [1136]	Amplitude analysis, no evidence for $CP$ violation
	2005	FOCUS [1119]	$-0.082 \pm 0.056 \pm 0.047$

**Table 268**  $CP$  asymmetries  $A_{CP} = [\Gamma(D_s^+) - \Gamma(D_s^-)]/[\Gamma(D_s^+) + \Gamma(D_s^-)]$  for  $D_s^\pm$  decays

Mode	Year	Collaboration	$A_{CP}$
$D_s^+ \rightarrow \mu^+ \nu$	2009	CLEO [1137]	$+0.048 \pm 0.061$
$D_s^+ \rightarrow \pi^+ \eta$	2013	CLEO [1138]	$+0.011 \pm 0.030 \pm 0.008$
$D_s^+ \rightarrow \pi^+ \eta'$	2013	CLEO [1138]	$-0.022 \pm 0.022 \pm 0.006$
$D_s^+ \rightarrow K_s^0 \pi^+$	2013	BABAR [1110]	$+0.006 \pm 0.020 \pm 0.003$
	2010	Belle [1139]	$+0.0545 \pm 0.0250 \pm 0.0033$
	2010	CLEO [1104]	$+0.163 \pm 0.073 \pm 0.003$
		HFLAV average	$+0.0311 \pm 0.0154$
$D_s^+ \rightarrow (\bar{K}^0/K^0)\pi^+$	2014	LHCb [1112]	$+0.0038 \pm 0.0046 \pm 0.0017$
	2013	BABAR [1110]	$+0.003 \pm 0.020 \pm 0.003$
		HFLAV average	$+0.0038 \pm 0.0048$
$D_s^+ \rightarrow K_s^0 K^+$	2013	CLEO [1138]	$+0.026 \pm 0.015 \pm 0.006$
	2013	BABAR [1110]	$-0.0005 \pm 0.0023 \pm 0.0024$
	2010	Belle [1139]	$+0.0012 \pm 0.0036 \pm 0.0022$
		HFLAV average	$+0.0008 \pm 0.0026$
$D_s^+ \rightarrow K^+ \pi^0$	2010	CLEO [1104]	$+0.266 \pm 0.228 \pm 0.009$
$D_s^+ \rightarrow K^+ \eta$	2010	CLEO [1104]	$+0.093 \pm 0.152 \pm 0.009$
$D_s^+ \rightarrow K^+ \eta'$	2010	CLEO [1104]	$+0.060 \pm 0.189 \pm 0.009$
$D_s^+ \rightarrow \pi^+ \pi^+ \pi^-$	2013	CLEO [1138]	$-0.007 \pm 0.030 \pm 0.006$
$D_s^+ \rightarrow \pi^+ \pi^0 \eta$	2013	CLEO [1138]	$-0.005 \pm 0.039 \pm 0.020$
$D_s^+ \rightarrow \pi^+ \pi^0 \eta'$	2013	CLEO [1138]	$-0.004 \pm 0.074 \pm 0.019$
$D_s^+ \rightarrow K_s^0 K^+ \pi^0$	2013	CLEO [1138]	$-0.016 \pm 0.060 \pm 0.011$
$D_s^+ \rightarrow K_s^0 K_s^0 \pi^+$	2013	CLEO [1138]	$+0.031 \pm 0.052 \pm 0.006$
$D_s^+ \rightarrow K^+ \pi^+ \pi^-$	2013	CLEO [1138]	$+0.045 \pm 0.048 \pm 0.006$
$D_s^+ \rightarrow K^+ K^- \pi^+$	2013	CLEO [1138]	$-0.005 \pm 0.008 \pm 0.004$
$D_s^+ \rightarrow K_s^0 K^- \pi^+ \pi^+$	2013	CLEO [1138]	$+0.041 \pm 0.027 \pm 0.009$
$D_s^+ \rightarrow K_s^0 K^+ \pi^+ \pi^-$	2013	CLEO [1138]	$-0.057 \pm 0.053 \pm 0.009$
$D_s^+ \rightarrow K^+ K^- \pi^+ \pi^0$	2013	CLEO [1138]	$+0.000 \pm 0.027 \pm 0.012$

sample [1092]. This section describes a combination of measurements that allows the extraction of the individual contributions of the two types of  $CP$  violation. At the same time, the level of agreement for a no- $CP$ -violation hypothesis is tested. The observables are:

$$A_\Gamma \equiv \frac{\tau(\bar{D}^0 \rightarrow h^+ h^-) - \tau(D^0 \rightarrow h^+ h^-)}{\tau(\bar{D}^0 \rightarrow h^+ h^-) + \tau(D^0 \rightarrow h^+ h^-)}, \quad (236)$$

where  $h^+ h^-$  can be  $K^+ K^-$  or  $\pi^+ \pi^-$ , and

$$\Delta A_{CP} \equiv A_{CP}(K^+ K^-) - A_{CP}(\pi^+ \pi^-), \quad (237)$$

where  $A_{CP}$  are time-integrated  $CP$  asymmetries. The underlying theoretical parameters are:

$$a_{CP}^{\text{dir}} \equiv \frac{|\mathcal{A}_{D^0 \rightarrow f}|^2 - |\mathcal{A}_{\bar{D}^0 \rightarrow f}|^2}{|\mathcal{A}_{D^0 \rightarrow f}|^2 + |\mathcal{A}_{\bar{D}^0 \rightarrow f}|^2},$$

**Table 269** Measurements of the  $T$ -odd asymmetry  $\mathcal{A}_T = (A_T - \bar{A}_T)/2$ 

Mode	Year	Collaboration	$\mathcal{A}_T$
$D^0 \rightarrow K^+ K^- \pi^+ \pi^-$	2014	LHCb [1148]	$+0.0018 \pm 0.0029 \pm 0.0004$
	2010	BABAR [1149]	$+0.0010 \pm 0.0051 \pm 0.0044$
	2005	FOCUS [1119]	$+0.010 \pm 0.057 \pm 0.037$
		HFLAV average	$+0.0017 \pm 0.0027$
$D^+ \rightarrow K_s^0 K^+ \pi^+ \pi^-$	2011	BABAR [1150]	$-0.0120 \pm 0.0100 \pm 0.0046$
	2005	FOCUS [1119]	$+0.023 \pm 0.062 \pm 0.022$
		HFLAV average	$-0.0110 \pm 0.0109$
$D_s^+ \rightarrow K_s^0 K^+ \pi^+ \pi^-$	2011	BABAR [1150]	$-0.0136 \pm 0.0077 \pm 0.0034$
	2005	FOCUS [1119]	$-0.036 \pm 0.067 \pm 0.023$
		HFLAV average	$-0.0139 \pm 0.0084$

**Table 270** Inputs to the fit for direct and indirect  $CP$  violation. The first uncertainty listed is statistical, and the second is systematic

Year	Experiment	Results	$\Delta\langle t \rangle/\tau$	$\langle t \rangle/\tau$	References
2012	BABAR	$A_\Gamma = (+0.09 \pm 0.26 \pm 0.06)\%$	–	–	[1085]
2016	LHCb prompt	$A_\Gamma(KK) = (-0.030 \pm 0.032 \pm 0.010)\%$	–	–	[1089]
		$A_\Gamma(\pi\pi) = (+0.046 \pm 0.058 \pm 0.012)\%$	–	–	
2014	CDF	$A_\Gamma = (-0.12 \pm 0.12)\%$	–	–	[1087]
2015	LHCb SL	$A_\Gamma = (-0.125 \pm 0.073)\%$	–	–	[1088]
2015	Belle	$A_\Gamma = (-0.03 \pm 0.20 \pm 0.07)\%$	–	–	[1084]
2008	BABAR	$A_{CP}(KK) = (+0.00 \pm 0.34 \pm 0.13)\%$			
		$A_{CP}(\pi\pi) = (-0.24 \pm 0.52 \pm 0.22)\%$	0.00	1.00	[1074]
2012	Belle prel.	$\Delta A_{CP} = (-0.87 \pm 0.41 \pm 0.06)\%$	0.00	1.00	[1153]
2012	CDF	$\Delta A_{CP} = (-0.62 \pm 0.21 \pm 0.10)\%$	0.25	2.58	[1077]
2014	LHCb SL	$\Delta A_{CP} = (+0.14 \pm 0.16 \pm 0.08)\%$	0.01	1.07	[1058]
2016	LHCb prompt	$\Delta A_{CP} = (-0.10 \pm 0.08 \pm 0.03)\%$	0.12	2.10	[1078]

$$a_{CP}^{\text{ind}} \equiv \frac{1}{2} \left[ \left( \left| \frac{q}{p} \right| + \left| \frac{p}{q} \right| \right) x \sin \phi - \left( \left| \frac{q}{p} \right| - \left| \frac{p}{q} \right| \right) y \cos \phi \right], \quad (238)$$

where  $\mathcal{A}_{D \rightarrow f}$  is the amplitude for  $D \rightarrow f$  [1151]. We use the following relations between the observables and the underlying parameters [1152]:

$$A_\Gamma = -a_{CP}^{\text{ind}} - a_{CP}^{\text{dir}} y_{CP}, \quad (239)$$

$$\begin{aligned} \Delta A_{CP} &= \Delta a_{CP}^{\text{dir}} \left( 1 + y_{CP} \frac{\langle t \rangle}{\tau} \right) + a_{CP}^{\text{ind}} \frac{\Delta \langle t \rangle}{\tau} + \overline{a_{CP}^{\text{dir}}} y_{CP} \frac{\Delta \langle t \rangle}{\tau}, \\ &\approx \Delta a_{CP}^{\text{dir}} \left( 1 + y_{CP} \frac{\langle t \rangle}{\tau} \right) + a_{CP}^{\text{ind}} \frac{\Delta \langle t \rangle}{\tau}. \end{aligned} \quad (240)$$

Equation (239) constrains mostly indirect  $CP$  violation, and the direct  $CP$  violation contribution can differ for different final states. In Eq. (240),  $\langle t \rangle/\tau$  denotes the mean decay time in units of the  $D^0$  lifetime;  $\Delta X$  denotes the difference in quantity  $X$  between  $K^+ K^-$  and  $\pi^+ \pi^-$  final states; and  $\overline{X}$  denotes the average for quantity  $X$ . We neglect the last term in this relation as all three factors are  $\mathcal{O}(10^{-2})$

or smaller, and thus this term is negligible with respect to the other two terms. Note that  $\Delta\langle t \rangle/\tau \ll \langle t \rangle/\tau$ , and it is expected that  $|a_{CP}^{\text{dir}}| < |\Delta a_{CP}^{\text{dir}}|$  because  $a_{CP}^{\text{dir}}(K^+ K^-)$  and  $a_{CP}^{\text{dir}}(\pi^+ \pi^-)$  are expected to have opposite signs in the Standard Model [1151].

A  $\chi^2$  fit is performed in the plane  $\Delta a_{CP}^{\text{dir}}$  vs.  $a_{CP}^{\text{ind}}$ . For the BABAR result the difference of the quoted values for  $A_{CP}(K^+ K^-)$  and  $A_{CP}(\pi^+ \pi^-)$  is calculated, adding all uncertainties in quadrature. This may overestimate the systematic uncertainty for the difference as it neglects correlated errors; however, the result is conservative and the effect is small as all measurements are statistically limited. For all measurements, statistical and systematic uncertainties are added in quadrature when calculating the  $\chi^2$ . We use the current world average value  $y_{CP} = (0.835 \pm 0.155)\%$  (see Sect. 8.1) and the measurements listed in Table 270.

In this fit,  $A_\Gamma(KK)$  and  $A_\Gamma(\pi\pi)$  are assumed to be identical. This assumption (expected to hold in the Standard Model) is supported by all measurements to date. A sig-

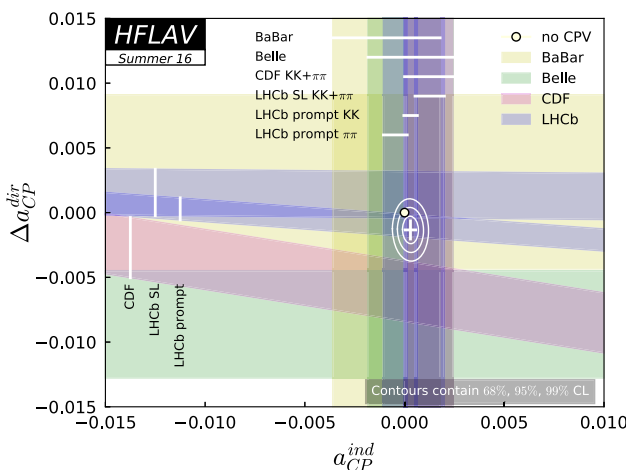


**Fig. 198** Plot of all data and the fit result. Individual measurements are plotted as bands showing their  $\pm 1\sigma$  range. The no-CPV point (0,0) is shown as a filled circle, and the best fit value is indicated by a cross showing the one-dimensional uncertainties. Two-dimensional 68% C.L., 95% C.L., and 99.7% C.L. regions are plotted as ellipses

nificant relative shift due to final-state dependent  $A_\Gamma$  values between  $\Delta A_{CP}$  measurements with different mean decay times is excluded by these measurements.

The combination plot (see Fig. 198) shows the measurements listed in Table 270 for  $\Delta A_{CP}$  and  $A_\Gamma$ .

From the fit, the change in  $\chi^2$  from the minimum value for the no-CPV point (0,0) is 4.7, which corresponds to a C.L. of  $9.3 \times 10^{-2}$  for two degrees of freedom. Thus the data are consistent with the no-CP-violation hypothesis at 9.3% C.L. This  $p$ -value corresponds to  $1.7\sigma$ . The central values and  $\pm 1\sigma$  uncertainties for the individual parameters are

$$\begin{aligned} a_{CP}^{\text{ind}} &= (+0.030 \pm 0.026)\% \\ \Delta a_{CP}^{\text{dir}} &= (-0.134 \pm 0.070)\%. \end{aligned} \quad (241)$$

Compared to the previous average, the tension in the difference between direct  $CP$  violation in the two final states is reduced, while the common indirect  $CP$  violation moved away from the no- $CP$ -violation point by about one standard deviation.

## 8.5 Semileptonic decays

### 8.5.1 Introduction

Semileptonic decays of  $D$  mesons involve the interaction of a leptonic current with a hadronic current. The latter is non-perturbative and cannot be calculated from first principles; thus it is usually parameterized in terms of form factors. The transition matrix element is written

$$\mathcal{M} = -i \frac{G_F}{\sqrt{2}} V_{cq} L^\mu H_\mu, \quad (242)$$

where  $G_F$  is the Fermi constant and  $V_{cq}$  is a CKM matrix element. The leptonic current  $L^\mu$  is evaluated directly from the lepton spinors and has a simple structure; this allows one to extract information about the form factors (in  $H_\mu$ ) from data on semileptonic decays [1154]. Conversely, because there are no strong final-state interactions between the leptonic and hadronic systems, semileptonic decays for which the form factors can be calculated allow one to determine  $V_{cq}$  [2].

### 8.5.2 $D \rightarrow P \bar{\ell} v_\ell$ decays

When the final state hadron is a pseudoscalar, the hadronic current is given by

$$\begin{aligned} H_\mu &= \langle P(p)|\bar{q}_\mu c|D(p')\rangle \\ &= f_+(q^2) \times \left[ (p' + p)_\mu - \frac{m_D^2 - m_P^2}{q^2} q_\mu \right] \\ &\quad + f_0(q^2) \frac{m_D^2 - m_P^2}{q^2} q_\mu, \end{aligned} \quad (243)$$

where  $m_D$  and  $p'$  are the mass and four momentum of the parent  $D$  meson,  $m_P$  and  $p$  are those of the daughter meson,  $f_+(q^2)$  and  $f_0(q^2)$  are form factors, and  $q = p' - p$ . Kinematics require that  $f_+(0) = f_0(0)$ . The contraction  $q_\mu L^\mu$  results in terms proportional to  $m_\ell$  [1155], and thus for  $\ell = e$  the terms proportional to  $q_\mu$  in Eq. (243) are negligible. For light leptons only the  $f_+(q^2)$  vector form factor is relevant and the differential partial width is

$$\frac{d\Gamma(D \rightarrow P \bar{\ell} v_\ell)}{dq^2 d \cos \theta_\ell} = \frac{G_F^2 |V_{cq}|^2}{32\pi^3} p^*{}^3 |f_+(q^2)|^2 \sin \theta_\ell^2, \quad (244)$$

where  $p^*$  is the magnitude of the momentum of the final state hadron in the  $D$  rest frame, and  $\theta_\ell$  is the angle of the lepton in the  $\ell v$  rest frame with respect to the direction of the pseudoscalar meson in the  $D$  rest frame.

### 8.5.3 Form factor parameterizations

The form factor is traditionally parameterized with an explicit pole and a sum of effective poles:

$$\begin{aligned} f_+(q^2) &= \frac{f_+(0)}{(1-\alpha)} \left[ \left( \frac{1}{1-q^2/m_{\text{pole}}^2} \right) \right. \\ &\quad \left. + \sum_{k=1}^N \frac{\rho_k}{1-q^2/(\gamma_k m_{\text{pole}}^2)} \right], \end{aligned} \quad (245)$$

where  $\rho_k$  and  $\gamma_k$  are expansion parameters and  $\alpha$  is a parameter that normalizes the form factor at  $q^2 = 0$ ,  $f_+(0)$ . The parameter  $m_{\text{pole}}$  is the mass of the lowest-lying  $c\bar{q}$  resonance with the vector quantum numbers; this is expected to provide the largest contribution to the form factor for the  $c \rightarrow q$  transition. The sum over  $N$  gives the contribution

**Table 271** Results for  $m_{\text{pole}}$  and  $\alpha_{\text{BK}}$  from various experiments for  $D^0 \rightarrow K^-\ell^+\nu$  and  $D^+ \rightarrow \bar{K}^0\ell^+\nu$  decays

$D \rightarrow K\ell\nu_\ell$ Expt.	Mode	Refs.	$m_{\text{pole}} (\text{GeV}/c^2)$	$\alpha_{\text{BK}}$
CLEO III	( $D^0; \ell = e, \mu$ )	[1175]	$1.89 \pm 0.05^{+0.04}_{-0.03}$	$0.36 \pm 0.10^{+0.03}_{-0.07}$
FOCUS	( $D^0; \ell = \mu$ )	[1176]	$1.93 \pm 0.05 \pm 0.03$	$0.28 \pm 0.08 \pm 0.07$
Belle	( $D^0; \ell = e, \mu$ )	[1171]	$1.82 \pm 0.04 \pm 0.03$	$0.52 \pm 0.08 \pm 0.06$
BABAR	( $D^0; \ell = e$ )	[1172]	$1.889 \pm 0.012 \pm 0.015$	$0.366 \pm 0.023 \pm 0.029$
CLEO-c (tagged)	( $D^0, D^+; \ell = e$ )	[1173]	$1.93 \pm 0.02 \pm 0.01$	$0.30 \pm 0.03 \pm 0.01$
CLEO-c (untagged)	( $D^0; \ell = e$ )	[1174]	$1.97 \pm 0.03 \pm 0.01$	$0.21 \pm 0.05 \pm 0.03$
CLEO-c (untagged)	( $D^+; \ell = e$ )	[1174]	$1.96 \pm 0.04 \pm 0.02$	$0.22 \pm 0.08 \pm 0.03$
BESIII	( $D^0; \ell = e$ )	[1169]	$1.921 \pm 0.010 \pm 0.007$	$0.309 \pm 0.020 \pm 0.013$
BESIII	( $D^+; \ell = e$ )	[1170]	$1.953 \pm 0.044 \pm 0.036$	$0.239 \pm 0.077 \pm 0.065$

**Table 272** Results for  $m_{\text{pole}}$  and  $\alpha_{\text{BK}}$  from various experiments for  $D^0 \rightarrow \pi^-\ell^+\nu$  and  $D^+ \rightarrow \pi^0\ell^+\nu$  decays

$D \rightarrow \pi\ell\nu_\ell$ Expt.	Mode	Refs.	$m_{\text{pole}} (\text{GeV}/c^2)$	$\alpha_{\text{BK}}$
CLEO III	( $D^0; \ell = e, \mu$ )	[1175]	$1.86^{+0.10+0.07}_{-0.06-0.03}$	$0.37^{+0.20}_{-0.31} \pm 0.15$
FOCUS	( $D^0; \ell = \mu$ )	[1176]	$1.91^{+0.30}_{-0.15} \pm 0.07$	–
Belle	( $D^0; \ell = e, \mu$ )	[1171]	$1.97 \pm 0.08 \pm 0.04$	$0.10 \pm 0.21 \pm 0.10$
CLEO-c (tagged)	( $D^0, D^+; \ell = e$ )	[1173]	$1.91 \pm 0.02 \pm 0.01$	$0.21 \pm 0.07 \pm 0.02$
CLEO-c (untagged)	( $D^0; \ell = e$ )	[1174]	$1.87 \pm 0.03 \pm 0.01$	$0.37 \pm 0.08 \pm 0.03$
CLEO-c (untagged)	( $D^+; \ell = e$ )	[1174]	$1.97 \pm 0.07 \pm 0.02$	$0.14 \pm 0.16 \pm 0.04$
BES III	( $D^0; \ell = e$ )	[1169]	$1.911 \pm 0.012 \pm 0.004$	$0.279 \pm 0.035 \pm 0.011$
BABAR	( $D^0; \ell = e$ )	[1168]	$1.906 \pm 0.029 \pm 0.023$	$0.268 \pm 0.074 \pm 0.059$

of higher mass states. For example, for  $D \rightarrow \pi$  transitions the dominant resonance is expected to be  $D^*(2010)$ , and thus  $m_{\text{pole}} = m_{D^*(2010)}$ . For  $D \rightarrow K$  transitions, the dominant contribution is expected from  $D_s^*(2112)$ , with  $m_{\text{pole}} = m_{D_s^*(2112)}$ .

#### 8.5.4 Simple pole

Equation (245) can be simplified by neglecting the sum over effective poles, leaving only the explicit vector meson pole. This approximation is referred to as “nearest pole dominance” or “vector-meson dominance.” The resulting parameterization is

$$f_+(q^2) = \frac{f_+(0)}{(1 - q^2/m_{\text{pole}}^2)}. \quad (246)$$

However, values of  $m_{\text{pole}}$  that give a good fit to the data do not agree with the expected vector meson masses [1156]. To address this problem, the “modified pole” or Becirevic–Kaidalov (BK) parameterization [1157] was introduced.  $m_{\text{pole}}/\sqrt{\alpha_{\text{BK}}}$  is interpreted as the mass of an effective pole, higher than  $m_{\text{pole}}$ , thus it is expected that  $\alpha_{\text{BK}} < 1$ .

The parameterization takes the form

$$f_+(q^2) = \frac{f_+(0)}{(1 - q^2/m_{\text{pole}}^2)} \frac{1}{\left(1 - \alpha_{\text{BK}} \frac{q^2}{m_{\text{pole}}^2}\right)}. \quad (247)$$

These parameterizations are used by several experiments to determine form factor parameters. Measured values of  $m_{\text{pole}}$  and  $\alpha_{\text{BK}}$  are listed in Tables 271 and 272 for  $D \rightarrow K\ell\nu_\ell$  and  $D \rightarrow \pi\ell\nu_\ell$  decays, respectively.

#### 8.5.5 $z$ expansion

An alternative series expansion around some value  $q^2 = t_0$  to parameterize  $f_+(q^2)$  can be used [1154, 1158–1160]. This parameterization is model independent and satisfies general QCD constraints, being suitable for fitting experimental data. The expansion is given in terms of a complex parameter  $z$ , which is the analytic continuation of  $q^2$  into the complex plane:

$$z(q^2, t_0) = \frac{\sqrt{t_+ - q^2} - \sqrt{t_+ - t_0}}{\sqrt{t_+ - q^2} + \sqrt{t_+ - t_0}}, \quad (248)$$

where  $t_{\pm} \equiv (m_D \pm m_P)^2$  and  $t_0$  is the (arbitrary)  $q^2$  value corresponding to  $z = 0$ . The physical region corresponds

to  $\pm |z|_{max} = \pm 0.051$  for  $D \rightarrow K\ell\nu_\ell$  and  $= \pm 0.17$  for  $D \rightarrow \pi\ell\nu_\ell$ , using  $t_0 = t_+(1 - \sqrt{1 - t_-/t_+})$ .

The form factor is expressed as

$$f_+(q^2) = \frac{1}{P(q^2)\phi(q^2, t_0)} \sum_{k=0}^{\infty} a_k(t_0)[z(q^2, t_0)]^k, \quad (249)$$

where the  $P(q^2)$  factor accommodates sub-threshold resonances via

$$P(q^2) \equiv \begin{cases} 1 & (D \rightarrow \pi) \\ z(q^2, M_{D_s^*}^2) & (D \rightarrow K). \end{cases} \quad (250)$$

The “outer” function  $\phi(t, t_0)$  can be any analytic function, but a preferred choice (see, e.g. Refs. [1158, 1159, 1161]) obtained from the Operator Product Expansion (OPE) is

$$\phi(q^2, t_0) = \alpha \left( \sqrt{t_+ - q^2} + \sqrt{t_+ - t_0} \right) \times \frac{t_+ - q^2}{(t_+ - t_0)^{1/4}} \frac{\left( \sqrt{t_+ - q^2} + \sqrt{t_+ - t_-} \right)^{3/2}}{\left( \sqrt{t_+ - q^2} + \sqrt{t_+} \right)^5}, \quad (251)$$

with  $\alpha = \sqrt{\pi m_c^2/3}$ . The OPE analysis provides a constraint upon the expansion coefficients,  $\sum_{k=0}^N a_k^2 \leq 1$ . These coefficients receive  $1/M_D$  corrections, and thus the constraint is only approximate. However, the expansion is expected to converge rapidly since  $|z| < 0.051$  (0.17) for  $D \rightarrow K$  ( $D \rightarrow \pi$ ) over the entire physical  $q^2$  range, and Eq. (249) remains a useful parameterization. The main disadvantage as compared to phenomenological approaches is that there is no physical interpretation of the fitted coefficients  $a_K$ .

### 8.5.6 Three-pole formalism

An update of the vector pole dominance model has been developed for the  $D \rightarrow \pi\ell\nu_\ell$  channel [1162]. It uses information of the residues of the semileptonic form factor at its first two poles, the  $D^*(2010)$  and  $D^{*'}(2600)$  resonances. The form factor is expressed as an infinite sum of residues from  $J^P = 1^-$  states with masses  $m_{D_n^*}$ :

$$f_+(q^2) = \sum_{n=0}^{\infty} \frac{\text{Res}_{q^2=m_{D_n^*}^2} f_+(q^2)}{m_{D_n^*}^2 - q^2}, \quad (252)$$

with the residues given by

$$\text{Res}_{q^2=m_{D_n^*}^2} f_+(q^2) = \frac{1}{2} m_{D_n^*} f_{D_n^*} g_{D_n^* D\pi}. \quad (253)$$

Values of the  $f_{D^*}$  and  $f_{D^{*']}$  decay constants have been obtained by lattice QCD calculations, relative to  $f_D$ , with 2% and 28% precision, respectively [1162]. The couplings to the

$D\pi$  state,  $g_{D^* D\pi}$  and  $g_{D^{*'} D\pi}$ , are extracted from measurements of the  $D^*(2010)$  and  $D^{*'}(2600)$  widths by BABAR and LHCb experiments [1163–1165]. Thus the contribution from the first pole is known with a 3% accuracy. The contribution from the  $D^{*'}(2600)$  is determined with poorer accuracy, ~30%, mainly due to lattice uncertainties. A *superconvergence* condition [1166] is applied:

$$\sum_{n=0}^{\infty} \text{Res}_{q^2=m_{D_n^*}^2} f_+(q^2) = 0, \quad (254)$$

protecting the form factor behavior at large  $q^2$ . Within this model the first two poles are not sufficient to describe the data, and a third effective pole needs to be included.

One of the advantages of this phenomenological model is that it can be extrapolated outside the charm physical region, providing a method to extract the CKM matrix element  $V_{ub}$  using the ratio of the form factors of the  $D \rightarrow \pi\ell\nu$  and  $B \rightarrow \pi\ell\nu$  decay channels. It will be used once lattice calculations provide the form factor ratio  $f_{B\pi}^+(q^2)/f_{D\pi}^+(q^2)$  at the same pion energy.

This form factor description can be extended to the  $D \rightarrow K\ell\nu$  decay channel, considering the contribution of several  $c\bar{s}$  resonances with  $J^P = 1^-$ . The first two pole masses contributing to the form factor correspond to the  $D_s^*(2112)$  and  $D_{s1}^*(2700)$  resonant states [327]. A constraint on the first residue can be obtained using information of the  $f_K$  decay constant [327] and the  $g$  coupling extracted from the  $D^{*+}$  width [1163]. The contribution from the second pole can be evaluated using the decay constants from [1167], the measured total width and the ratio of  $D^*K$  and  $DK$  decay branching fractions [327].

### 8.5.7 Experimental techniques and results

Different techniques by several experiments are used to measure  $D$  meson semileptonic decays having a pseudoscalar particle in the final state. The most recent results are provided by the BABAR [1168] and BES III [1169, 1170] collaborations. Belle [1171], BABAR [1172], and CLEO-c [1173, 1174] have all previously reported results. Belle fully reconstructs  $e^+e^- \rightarrow D\bar{D}X$  events from the continuum under the  $\Upsilon(4S)$  resonance, achieving very good  $q^2$  resolution (15 MeV $^2$ ) and a low background level but with a low efficiency. Using 282 fb $^{-1}$  of data, about 1300 and 115 signal semileptonic decays are isolated for both lepton channels together ( $e + \mu$ ), for the Cabibbo-favored and Cabibbo-suppressed modes, respectively. The BABAR experiment uses a partial reconstruction technique in which the semileptonic decays are tagged via  $D^{*+} \rightarrow D^0\pi^+$  decays. The  $D$  direction and neutrino energy are obtained using information from the rest of the event. With 75 fb $^{-1}$  of data, 74,000 signal events in the  $D^0 \rightarrow K^-e^+\nu$  mode are obtained. This

**Table 273** Results for  $r_1$  and  $r_2$  from various experiments for the  $D \rightarrow K\ell\nu_\ell$  decay channel. The correlation coefficient between these parameters is larger than 0.9

Expt. $D \rightarrow K\ell\nu_\ell$	Mode	Refs.	$r_1$	$r_2$
BABAR	$(D^0; \ell = e)$	[1172]	$-2.5 \pm 0.2 \pm 0.2$	$0.6 \pm 6.0 \pm 5.0$
CLEO-c (tagged)	$(D^0; \ell = e)$	[1173]	$-2.65 \pm 0.34 \pm 0.08$	$13 \pm 9 \pm 1$
CLEO-c (tagged)	$(D^+; \ell = e)$	[1173]	$-1.66 \pm 0.44 \pm 0.10$	$-14 \pm 11 \pm 1$
CLEO-c (untagged)	$(D^0; \ell = e)$	[1174]	$-2.4 \pm 0.4 \pm 0.1$	$21 \pm 11 \pm 2$
CLEO-c (untagged)	$(D^+; \ell = e)$	[1174]	$-2.8 \pm 6 \pm 2$	$32 \pm 18 \pm 4$
BES III	$(D^0; \ell = e)$	[1169]	$-2.334 \pm 0.159 \pm 0.080$	$3.42 \pm 3.91 \pm 2.41$
BES III	$(D^+; \ell = e)$	[1170]	$-2.23 \pm 0.42 \pm 0.53$	$11.3 \pm 8.5 \pm 8.7$

**Table 274** Results for  $r_1$  and  $r_2$  from various experiments, for  $D \rightarrow \pi\ell\nu_\ell$ . The correlation coefficient between these parameters is larger than 0.9

Expt. $D \rightarrow \pi\ell\nu_\ell$	Mode	Refs.	$r_1$	$r_2$
CLEO-c (tagged)	$(D^0; \ell = e)$	[1173]	$-2.80 \pm 0.49 \pm 0.04$	$6 \pm 3 \pm 0$
CLEO-c (tagged)	$(D^+; \ell = e)$	[1173]	$-1.37 \pm 0.88 \pm 0.24$	$-4 \pm 5 \pm 1$
CLEO-c (untagged)	$(D^0; \ell = e)$	[1174]	$-2.1 \pm 0.7 \pm 0.3$	$-1.2 \pm 4.8 \pm 1.7$
CLEO-c (untagged)	$(D^+; \ell = e)$	[1174]	$-0.2 \pm 1.5 \pm 0.4$	$-9.8 \pm 9.1 \pm 2.1$
BES III	$(D^0; \ell = e)$	[1169]	$-1.85 \pm 0.22 \pm 0.07$	$-1.4 \pm 1.5 \pm 0.5$
BABAR	$(D^0; \ell = e)$	[1168]	$-1.31 \pm 0.70 \pm 0.43$	$-4.2 \pm 4.0 \pm 1.9$

technique provides a large signal yield but also a high background level and a poor  $q^2$  resolution (ranging from 66 to 219 MeV $^2$ ). In this case the measurement of the branching fraction is obtained by normalizing to the  $D^0 \rightarrow K^-\pi^+$  decay channel; thus the measurement would benefit from future improvements in the determination of this reference channel. The Cabibbo-suppressed mode has been recently measured using the same technique and 350 fb $^{-1}$  data. For this measurement, 5000  $D^0 \rightarrow \pi^-e^+\nu$  signal events were reconstructed [1168].

The CLEO-c experiment uses two different methods to measure charm semileptonic decays. Tagged analyses [1173] rely on the full reconstruction of  $\Psi(3770) \rightarrow D\bar{D}$  events. One of the  $D$  mesons is reconstructed in a hadronic decay mode, the other in the semileptonic channel. The only missing particle is the neutrino so the  $q^2$  resolution is very good and the background level very low. With the entire CLEO-c data sample, 818 pb $^{-1}$ , 14,123 and 1374 signal events are reconstructed for the  $D^0 \rightarrow K^-e^+\nu$  and  $D^0 \rightarrow \pi^-e^+\nu$  channels, and 8467 and 838 for the  $D^+ \rightarrow \bar{K}^0e^+\nu$  and  $D^+ \rightarrow \pi^0e^+\nu$  decays, respectively. Another technique without tagging the  $D$  meson in a hadronic mode (“untagged” in the following) has been also used by CLEO-c [1174]. In this method, the entire missing energy and momentum in an event are associated with the neutrino four momentum, with the penalty of larger background as compared to the tagged method. Using the “tagged” method the BES III experiment measures the  $D^0 \rightarrow K^-e^+\nu$  and  $D^0 \rightarrow \pi^-e^+\nu$  decay channels. With 2.9 fb $^{-1}$  they fully reconstruct 70,700 and 6300 signal events for each channel, respectively [1169]. In a sep-

arated analysis the BES III experiment measures also the  $D^+$  decay mode into  $D^+ \rightarrow K_L^0e^+\nu$  [1170]. Using several tagged hadronic events they reconstruct 20,100 semileptonic candidates.

Previous measurements were also performed by several experiments. Events registered at the  $\Upsilon(4S)$  energy corresponding to an integrated luminosity of 7 fb $^{-1}$  were analyzed by CLEO III [1175]. Fixed target photo-production experiments performed also measurements of the normalized form factor distribution (FOCUS [1176]) and total decay rates (Mark-III [1177], E653 [1178, 1179], E687 [1180, 1181], E691 [1182], BES II [1183, 1184], CLEO II [1185]). In the FOCUS fixed target photo-production experiment,  $D^0$  semimuonic events were obtained from the decay of a  $D^{*+}$ , with a kaon or a pion detected.

Results of the hadronic form factor parameters,  $m_{pole}$  and  $\alpha_{BK}$ , obtained from the measurements discussed above, are given in Tables 271 and 272.

The  $z$ -expansion formalism has been used by BABAR [1168, 1172], BES III [1186] and CLEO-c [1173], [1174]. Their fits use the first three terms of the expansion, and the results for the ratios  $r_1 \equiv a_1/a_0$  and  $r_2 \equiv a_2/a_0$  are listed in Tables 273 and 274.

### 8.5.8 Combined results for the $D \rightarrow K\ell\nu_\ell$ channel

The  $q^2$  distribution provided by each individual measurement is used to determine a combined result by performing a fit to the  $z$ -expansion formalism at second order. Results for the form factor normalization  $f_+^K(0)|V_{cs}|$  and the shape param-

**Table 275** Results of the fits to  $D \rightarrow K\ell\nu_\ell$  measurements from several experiments, using the  $z$ -expansion. External inputs have been updated to PDG [327]. The correlation coefficients listed in the last column refer to  $\rho_{12} \equiv \rho_{|V_{cs}|f_+^K(0),r_1}$ ,  $\rho_{13} \equiv \rho_{|V_{cs}|f_+^K(0),r_2}$ , and  $\rho_{23} \equiv \rho_{r_1,r_2}$  and are for the total uncertainties (statistical  $\oplus$  systematic). The

Expt. $D \rightarrow K\ell\nu_\ell$	Mode	$ V_{cs} f_+^K(0)$	$r_1$	$r_2$	$\rho_{12}/\rho_{13}/\rho_{23}$
BES III (tagged) [1169]	( $D^0$ )	0.7195(35)(43)	-2.33(16)(8)	3.4(4.0)(2.5)	-0.21/0.58/-0.81
CLEO-c (tagged) [1173]	( $D^0, D^+$ )	0.7189(64)(48)	-2.29(28)(27)	3.0(7.0)(1.0)	-0.19/0.58/-0.81
CLEO-c (un>tagged) [1174]	( $D^0, D^+$ )	0.7436(76)(79)	-2.57(33)(18)	23.9(8.9)(4.3)	-0.34/0.66/-0.84
BABAR [1172]	( $D^0$ )	0.7241(64)(60)	-2.45(20)(18)	-0.6(6.0)(3.8)	-0.36/0.59/-0.82
Belle [1171]	( $D^0$ )	0.700(19)	-3.06(71)	-3.3(17.9)	-0.20/0.66/-0.81
FOCUS [1176] and others		0.724(29)	-2.54(75)	7.0(12.8)	-0.02/0.02/-0.97
Combined	( $D^0, D^+$ )	0.7226(22)(26)	-2.38(11)(6)	4.7(2.6)(1.4)	-0.19/0.51/-0.84

**Table 276** Results for the  $D^0 \rightarrow K^-\ell^+\nu_\ell$  and  $D^+ \rightarrow \bar{K}^0\ell^+\nu_\ell$  decay channels using the  $z$ -expansion formalism at second order

Fit value	$D^0 \rightarrow K^-\ell^+\nu_\ell$	$D^+ \rightarrow \bar{K}^0\ell^+\nu_\ell$
$ V_{cs} f_+^K(0)$	$0.7219 \pm 0.0024 \pm 0.0027$	$0.726 \pm 0.005 \pm 0.007$
$r_1$	$-2.41 \pm 0.11 \pm 0.07$	$-2.07 \pm 0.38 \pm 0.10$
$r_2$	$4.7 \pm 2.7 \pm 1.4$	$5.4 \pm 8.2 \pm 4.6$
$\rho_{12}/\rho_{13}/\rho_{23}$	$-0.19/0.51/-0.84$	$-0.10/0.39/-0.84$

eters  $r_1$  and  $r_2$  for each individual measurement and for the combination are presented in Table 275. Measurements have been corrected with respect to the original ones using recent values from PDG [327]. This includes updated branching fractions of normalization channels, corrected CKM matrix elements and the  $D$  meson lifetime. The BABAR measurement has been corrected accounting for final-state radiation. The result for the  $D^+ \rightarrow K_L^0 e^+ \nu_e$  decay channel from BES III [1170] is included as a constraint in the combined result since correlation matrices are not provided. Correlation coefficients of the parameters are quoted in the last column of Table 275. The  $\chi^2$  per degree of freedom is 114.7/101. Results are shown in Fig. 201.

In the combination of the electron and muon channels, the measurements with muons are corrected for the reduction of phase space and for the  $f_0(q^2)$  contribution [1187]. Channels with a  $D^0$  or a  $D^+$  are combined assuming isospin invariance and using physical meson and lepton masses. These combined results are noted as  $D \rightarrow K\ell\nu_\ell$  in the following. Hadronic form factors are assumed to be the same for charged and neutral  $D$  mesons. Separate results for the  $D^0 \rightarrow K^-\ell^+\nu_\ell$  and  $D^+ \rightarrow \bar{K}^0\ell^+\nu_\ell$  decay channels are shown in Table 276 and Fig. 200. Using the fitted parameters and integrating over the full  $q^2$  range, the combined semileptonic branching fraction, expressed in terms of the  $D^0$  decay channel gives:

$$\mathcal{B}(D^0 \rightarrow K^-\ell^+\nu_\ell) = (3.490 \pm 0.011 \pm 0.020)\% \quad (255)$$

result for the  $D^+ \rightarrow K_L^0 e^+ \nu_e$  decay channel from BES III [1170] is included in the combined results as a constraint on the normalization,  $|V_{cs}|f_+^K(0)$ . The entry *others* refers to total decay rates measured by Mark-III [1177], E653 [1178, 1179], E687 [1180, 1181], E691 [1182], BES II [1183, 1184] and CLEO II [1185]

**Table 277** Results of the three-pole model form factors obtained from a fit to all measurements. Fitted parameters are the first two residues  $\gamma_0^K$  and  $\gamma_1^K$ , which are constrained using present measurements of masses and widths of the  $D_s^*$  and  $D_{s1}^*$  mesons, and lattice computations of decay constants, and the effective mass,  $m_{D_s^{*''}}$ , accounting for higher mass hadronic contributions

Parameter	Combined result ( $D \rightarrow K\ell\nu_\ell$ )
$\gamma_0^K$	$4.85 \pm 0.08 \text{ GeV}^2$
$\gamma_1^K$	$-1.2 \pm 0.30 \text{ GeV}^2$
$m_{D_s^{*''}}$	$4.46 \pm 0.26 \text{ GeV}$

Data from the different experiments are also fitted within the three-pole form factor formalism. Constraints on the first and second poles are imposed using information of the  $D_s^*(2112)$  and  $D_{s1}^*(2700)$  resonances. Results are presented in Table 277. Fitted parameters are the first two residues  $\gamma_0^K = \operatorname{Res}_{q^2=m_{D_s^*(2112)}^2} f_+^K(q^2)$  and  $\gamma_1^K = \operatorname{Res}_{q^2=m_{D_{s1}^*(2700)}^2} f_+^K(q^2)$  and an effective mass,  $m_{D_s^{*''}}$ , accounting for higher mass hadronic contributions. It is found that the fitted effective third pole mass is larger than the mass of the second radial excitation, around  $3.2 \text{ GeV}/c^2$ , as expected. The contribution to the form factor by only the  $D_s^*$  resonance is disfavoured by the data. Figure 199 (left) shows the result of the fitted form factors for the  $z$ -expansion and three-pole parametrizations (Figs. 200, 201).

**Fig. 199** Form factors as function of  $q^2$  for the  $D \rightarrow K \ell \nu_\ell$  (left) and  $D \rightarrow \pi \ell \nu_\ell$  (right) channels, obtained from a fit to all experimental data. Central values (*central lines*) and uncertainties (one  $\sigma$  deviation) are shown for the z-expansion and the 3-pole parameterization

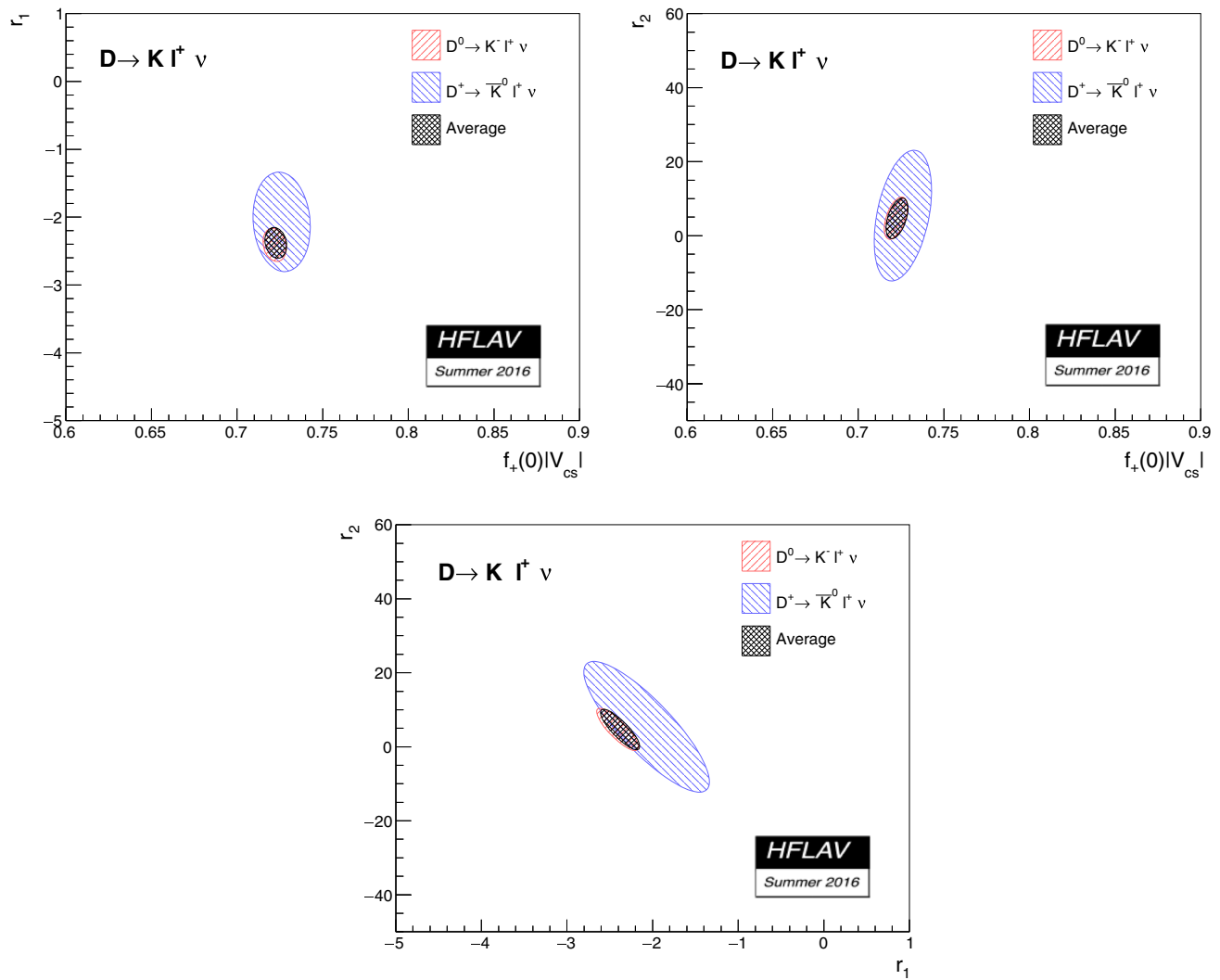
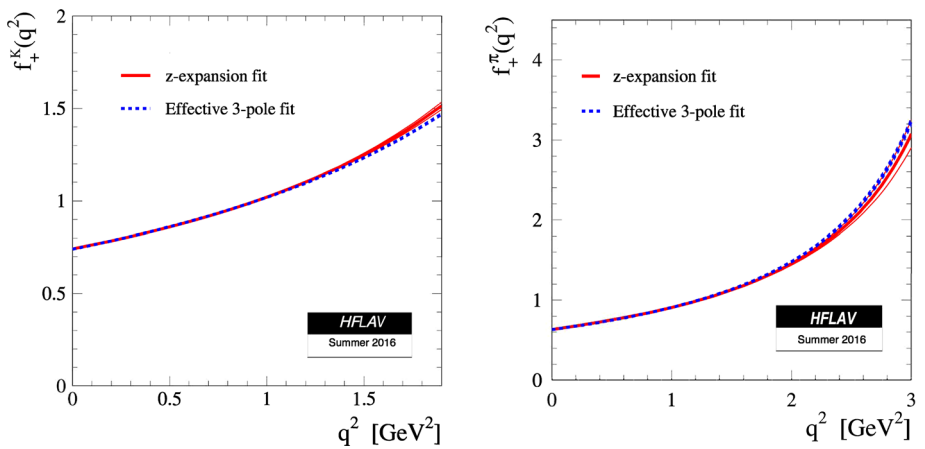


**Fig. 200** Results of the combined fit shown separately for the  $D^0 \rightarrow K^- \ell^+ \nu$  and  $D^+ \rightarrow \bar{K}^0 \ell^+ \nu$  decay channels. Ellipses are shown for 68% C.L.

#### 8.5.9 Combined results for the $D \rightarrow \pi \ell \nu_\ell$ channel

The combined result for the  $D \rightarrow \pi \ell \nu_\ell$  decay channel is obtained from a fit to BABAR, Belle, BES III, and CLEO-c

data, with updated input values from [327]. The available measurements are fitted in bins of  $q^2$  to the  $z$ -expansion model at second order. Results of the individual fits for each experiment and the combined result are shown in

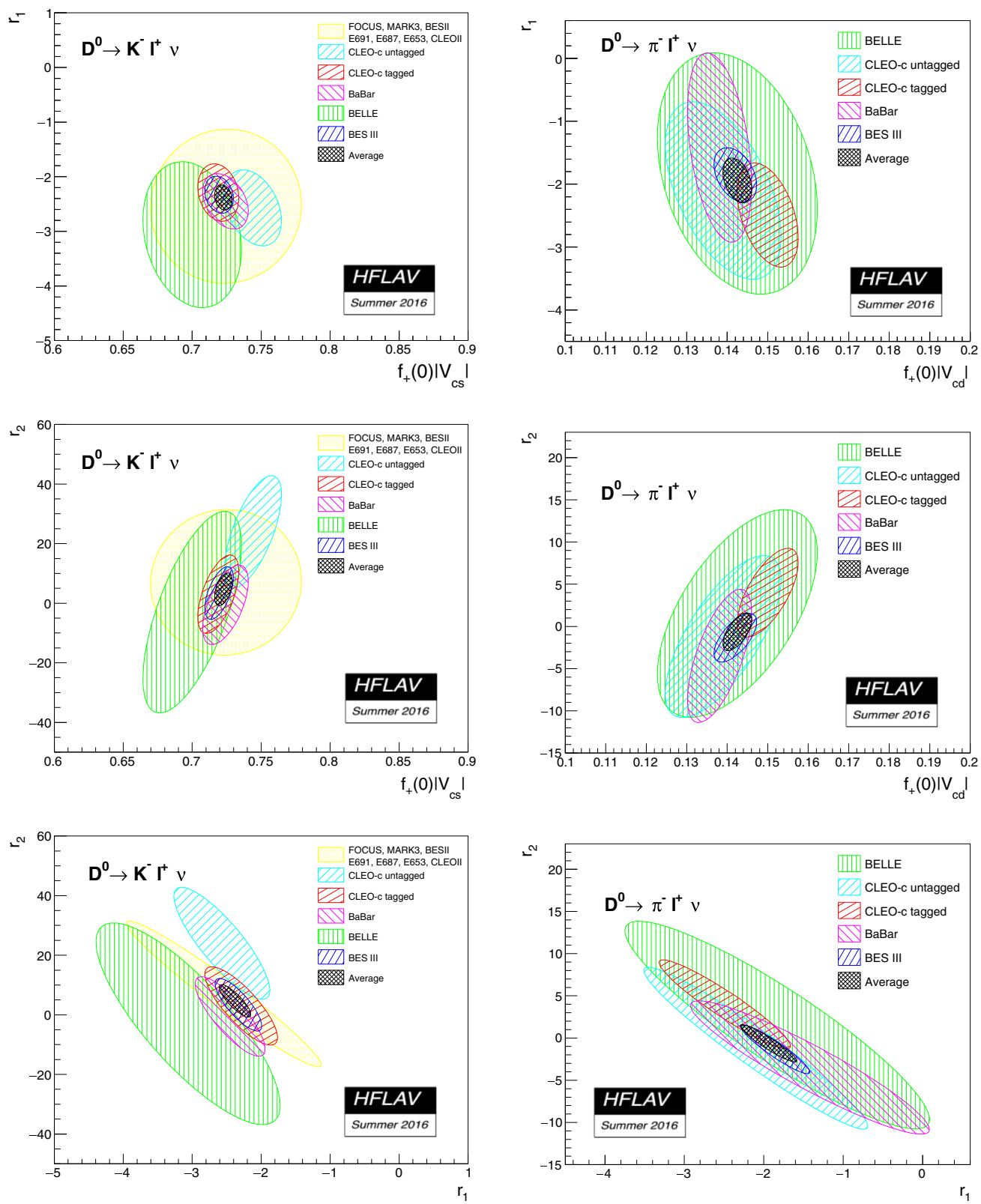


**Fig. 201** The  $D^0 \rightarrow K^-\ell^+\nu$  (left) and  $D^0 \rightarrow \pi^-\ell^+\nu$  (right) 68% C.L. error ellipses from the average fit of the 3-parameter  $z$ -expansion results

**Table 278** Results of the fits to  $D \rightarrow \pi \ell v_\ell$  measurements from several experiments, using the  $z$ -expansion. External inputs are updated to PDG [327]. The correlation coefficients listed in the last column refer

Expt. $D \rightarrow \pi \ell v_\ell$	mode	$ V_{cd} f_+^\pi(0)$	$r_1$	$r_2$	$\rho_{12}/\rho_{13}/\rho_{23}$
BES III (tagged) [1169]	( $D^0$ )	0.1422(25)(10)	-1.86(23)(7)	-1.24(1.51)(47)	-0.37/0.64/-0.93
CLEO-c (tagged) [1173]	( $D^0, D^+$ )	0.1507(42)(11)	-2.45(43)(9)	3.8(2.8)(6)	-0.43/0.67/-0.94
CLEO-c (untagged) [1174]	( $D^0, D^+$ )	0.1394(58)(25)	-1.71(62)(25)	-2.8(4.0)(1.6)	-0.50/0.69/-0.96
BABAR [1172]	( $D^0$ )	0.1381(36)(22)	-1.42(66)(45)	-3.5(3.7)(2.0)	-0.40/0.57/-0.97
Belle [1171]	( $D^0$ )	0.142(11)	-1.83(1.00)	1.5(6.5)	-0.30/0.59/-0.91
Combined	( $D^0, D^+$ )	0.1426(17)(8)	-1.95(18)(1)	-0.52(1.17)(32)	-0.37/0.63/-0.94

**Table 279** Results of the three-pole model to BABAR, Belle, BES III and CLEO-c (tagged and untagged) data. Fitted parameters are the first two residues  $\gamma_0^\pi$  and  $\gamma_1^\pi$ , which are constrained using present measurements of masses and widths of the  $D^*$  and  $D^{*'} mesons, and lattice computations of decay constants, and the effective mass,  $m_{D_{\text{eff}}^{*''}}$ , accounting for higher mass hadronic contributions$ 

Parameter	Combined result ( $D \rightarrow \pi \ell v_\ell$ )
$\gamma_0^\pi$	$3.881 \pm 0.093 \text{ GeV}^2$
$\gamma_1^\pi$	$-1.18 \pm 0.30 \text{ GeV}^2$
$m_{D_{\text{eff}}^{*''}}$	$4.17 \pm 0.42 \text{ GeV}$

Table 278. The  $\chi^2$  per degree of freedom of the combined fit is 51/55.

Using the fitted parameters and integrating over the full  $q^2$  range, the combined semileptonic branching fraction, expressed in terms of the  $D^0$  decay channel gives:

$$\mathcal{B}(D^0 \rightarrow \pi^- \ell^+ v_\ell) = (2.891 \pm 0.030 \pm 0.022) \times 10^{-3} \quad (256)$$

Results of the three-pole model to the  $D \rightarrow \pi \ell v_\ell$  data are shown in Table 279. Fitted parameters are the first two residues  $\gamma_0^\pi = \text{Res}_{q^2=m_{D^*}^2} f_+^\pi(q^2)$  and  $\gamma_1^\pi = \text{Res}_{q^2=m_{D^{*'}}^2} f_+^\pi(q^2)$

(which are constrained using present measurements of masses and widths of the  $D^*(2010)$  and  $D^{*'}(2600)$  mesons, and lattice computations of decay constants, following [1162]), and an effective mass,  $m_{D_{\text{eff}}^{*''}}$ , accounting for higher mass hadronic contributions. The  $V_{cd}$  value entering in the fit is given in Eq. (257). The  $\chi^2$  per degree of freedom of the combined fit is 57.5/57.

The effective mass  $m_{D_{\text{eff}}^{*''}}$  is larger than the predicted mass of the second radially excited state with  $J^P = 1^-$  (~3.11 GeV), indicating that more contributions are needed to explain the form factor. Figure 199 (right) shows the result of the combined form factor for the  $z$ -expansion and three-pole parameterizations.

to  $\rho_{12} \equiv \rho_{|V_{cd}|f_+^\pi(0), r_1}$ ,  $\rho_{13} \equiv \rho_{|V_{cd}|f_+^\pi(0), r_2}$ , and  $\rho_{23} \equiv \rho_{r_1, r_2}$  and are for the total uncertainties (statistical  $\oplus$  systematic)

### 8.5.10 $V_{cs}$ and $V_{cd}$ determination

Assuming unitarity of the CKM matrix, the values of the CKM matrix elements entering in charm semileptonic decays are evaluated from the  $V_{ud}$ ,  $V_{td}$  and  $V_{cb}$  elements [327]:

$$|V_{cs}| = 0.97343 \pm 0.00015, \quad |V_{cd}| = 0.22521 \pm 0.00061. \quad (257)$$

Using the combined values of  $f_+^K(0)|V_{cs}|$  and  $f_+^\pi(0)|V_{cd}|$  in Tables 275 and 278, leads to the form factor values:

$$f_+^K(0) = 0.7423 \pm 0.0035, \\ f_+^\pi(0) = 0.6327 \pm 0.0086,$$

which are in agreement with present lattice QCD computations [222]:  $f_+^K(0) = 0.747 \pm 0.019$  and  $f_+^\pi(0) = 0.666 \pm 0.029$ . The experimental accuracy is at present higher than the one from lattice calculations. If instead one assumes the lattice QCD form factor values, one obtains for the CKM matrix elements using the combined results in Tables 275 and 278:

$$|V_{cs}| = 0.967 \pm 0.025, \\ |V_{cd}| = 0.2140 \pm 0.0097,$$

still compatible with unitarity of the CKM matrix.

### 8.5.11 $D \rightarrow V \bar{\ell} v_\ell$ decays

When the final state hadron is a vector meson, the decay can proceed through both vector and axial vector currents, and four form factors are needed. The hadronic current is  $H_\mu = V_\mu + A_\mu$ , where [1155]

$$V_\mu = \langle V(p, \varepsilon) | \bar{q} \gamma_\mu c | D(p') \rangle \\ = \frac{2V(q^2)}{m_D + m_V} \varepsilon_{\mu\nu\rho\sigma} \varepsilon^{*\nu} p'^\rho p^\sigma \quad (258)$$

$$A_\mu = \langle V(p, \varepsilon) | -\bar{q} \gamma_\mu \gamma_5 c | D(p') \rangle \\ = -i(m_D + m_V) A_1(q^2) \varepsilon_\mu^*$$

$$\begin{aligned}
& + i \frac{A_2(q^2)}{m_D + m_V} (\varepsilon^* \cdot q)(p' + p)_\mu \\
& + i \frac{2m_V}{q^2} \left( A_3(q^2) - A_0(q^2) \right) [\varepsilon^* \cdot (p' + p)] q_\mu.
\end{aligned} \tag{259}$$

In this expression,  $m_V$  is the daughter meson mass and

$$A_3(q^2) = \frac{m_D + m_V}{2m_V} A_1(q^2) - \frac{m_D - m_V}{2m_V} A_2(q^2). \tag{260}$$

Kinematics require that  $A_3(0) = A_0(0)$ . Terms proportional to  $q_\mu$  are only important for the case of  $\tau$  leptons. Thus, only three form factors are relevant in the decays involving  $\mu$  or  $e$ :  $A_1(q^2)$ ,  $A_2(q^2)$  and  $V(q^2)$ . The differential partial width is

$$\begin{aligned}
\frac{d\Gamma(D \rightarrow V\bar{\ell}v_\ell)}{dq^2 d\cos\theta_\ell} &= \frac{G_F^2 |V_{cq}|^2}{128\pi^3 m_D^2} p^* q^2 \times \left[ \frac{(1-\cos\theta_\ell)^2}{2} |H_-|^2 \right. \\
&\quad \left. + \frac{(1+\cos\theta_\ell)^2}{2} |H_+|^2 + \sin^2\theta_\ell |H_0|^2 \right], \tag{261}
\end{aligned}$$

where  $H_\pm$  and  $H_0$  are helicity amplitudes, corresponding to helicities of the  $V$  meson or virtual  $W$ , given by

$$H_\pm = \frac{1}{m_D + m_V} \left[ (m_D + m_V)^2 A_1(q^2) \mp 2m_D p^* V(q^2) \right] \tag{262}$$

$$\begin{aligned}
H_0 &= \frac{1}{|q|} \frac{m_D^2}{2m_V(m_D + m_V)} \times \left[ \left( 1 - \frac{m_V^2 - q^2}{m_D^2} \right) \right. \\
&\quad \left. \times (m_D + m_V)^2 A_1(q^2) - 4p^{*2} A_2(q^2) \right]. \tag{263}
\end{aligned}$$

$p^*$  is the magnitude of the three-momentum of the  $V$  system, measured in the  $D$  rest frame, and  $\theta_\ell$  is the angle of the lepton momentum, in the  $W$  rest frame, with respect to the opposite direction of the  $D$  meson [see Fig. 202 for the electron case ( $\theta_e$ )]. The left-handed nature of the quark current manifests itself as  $|H_-| > |H_+|$ . The differential decay rate for  $D \rightarrow V\ell v$  followed by the vector meson decaying into two pseudoscalars is

$$\begin{aligned}
& \frac{d\Gamma(D \rightarrow V\bar{\ell}v, V \rightarrow P_1 P_2)}{dq^2 d\cos\theta_V d\cos\theta_\ell d\chi} \\
&= \frac{3G_F^2}{2048\pi^4} |V_{cq}|^2 \frac{p^*(q^2) q^2}{m_D^2} \mathcal{B}(V \rightarrow P_1 P_2) \\
&\quad \times \left\{ (1 + \cos\theta_\ell)^2 \sin^2\theta_V |H_+(q^2)|^2 \right. \\
&\quad + (1 - \cos\theta_\ell)^2 \sin^2\theta_V |H_-(q^2)|^2 \\
&\quad + 4 \sin^2\theta_\ell \cos^2\theta_V |H_0(q^2)|^2 \\
&\quad - 4 \sin\theta_\ell (1 + \cos\theta_\ell) \\
&\quad \times \sin\theta_V \cos\theta_V \cos\chi H_+(q^2) H_0(q^2)
\end{aligned}$$

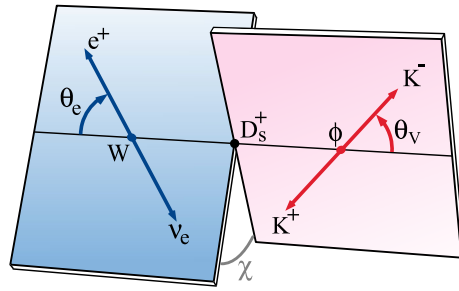


**Fig. 202** Decay angles  $\theta_V$ ,  $\theta_\ell$  and  $\chi$ . Note that the angle  $\chi$  between the decay planes is defined in the  $D$ -meson reference frame, whereas the angles  $\theta_V$  and  $\theta_\ell$  are defined in the  $V$  meson and  $W$  reference frames, respectively

$$\begin{aligned}
& + 4 \sin\theta_\ell (1 - \cos\theta_\ell) \\
& \times \sin\theta_V \cos\theta_V \cos\chi H_-(q^2) H_0(q^2) \\
& \left. - 2 \sin^2\theta_\ell \sin^2\theta_V \cos 2\chi H_+(q^2) H_-(q^2) \right\}, \tag{264}
\end{aligned}$$

where the helicity angles  $\theta_\ell$ ,  $\theta_V$ , and acoplanarity angle  $\chi$  are defined in Fig. 202.

Ratios between the values of the hadronic form factors expressed at  $q^2 = 0$  are usually introduced:

$$r_V \equiv V(0)/A_1(0), \quad r_2 \equiv A_2(0)/A_1(0). \tag{265}$$

### 8.5.12 Form factor measurements

In 2002 FOCUS reported [1188] an asymmetry in the observed  $\cos(\theta_V)$  distribution in  $D^+ \rightarrow K^-\pi^+\mu^+\nu$  decays. This is interpreted as evidence for an  $S$ -wave  $K^-\pi^+$  component in the decay amplitude. Since  $H_0$  typically dominates over  $H_\pm$ , the distribution given by Eq. (264) is, after integration over  $\chi$ , roughly proportional to  $\cos^2\theta_V$ . Inclusion of a constant  $S$ -wave amplitude of the form  $A e^{i\delta}$  leads to an interference term proportional to  $|AH_0 \sin\theta_\ell \cos\theta_V|$ ; this term causes an asymmetry in  $\cos(\theta_V)$ . When FOCUS fit their data including this  $S$ -wave amplitude, they obtained  $A = 0.330 \pm 0.022 \pm 0.015 \text{ GeV}^{-1}$  and  $\delta = 0.68 \pm 0.07 \pm 0.05$  [1189]. Both BABAR [1190] and CLEO-c [1191] have also found evidence for an  $f_0 \rightarrow K^+K^-$  component in semileptonic  $D_s$  decays.

The CLEO-c collaboration extracted the form factors  $H_+(q^2)$ ,  $H_-(q^2)$ , and  $H_0(q^2)$  from 11000  $D^+ \rightarrow K^-\pi^+\ell^+\nu_\ell$  events in a model-independent fashion directly as functions of  $q^2$  [1192]. They also determined the  $S$ -wave form factor  $h_0(q^2)$  via the interference term, despite the fact that the  $K\pi$  mass distribution appears dominated by the vector  $K^*(892)$  state. It is observed that  $H_0(q^2)$  dominates over a wide range of  $q^2$ , especially at low  $q^2$ . The transverse form factor  $H_t(q^2)$ , which can be related to  $A_3(q^2)$ , is small compared to lattice gauge theory calculations and suggests that the form factor ratio  $r_3 \equiv A_3(0)/A_1(0)$  is large and negative.

BABAR [1193] selected a large sample of  $244 \times 10^3$   $D^+ \rightarrow K^-\pi^+e^+\nu_e$  candidates with a ratio  $S/B \sim 2.3$  from an analyzed integrated luminosity of  $347 \text{ fb}^{-1}$ . With four particles emitted in the final state, the differential decay rate depends on five variables. In addition to the four variables defined in previous sections there is also  $m^2$ , the mass squared of the  $K\pi$  system. To analyze the  $D^+ \rightarrow K^-\pi^+e^+\nu_e$  decay channel it is assumed that all form factors have a  $q^2$  variation given by the simple pole model and the effective pole mass value,  $m_A = (2.63 \pm 0.10 \pm 0.13) \text{ GeV}/c^2$ , is fitted for the axial vector form factors. This value is compatible with expectations when comparing with the mass of  $J^P = 1^+$

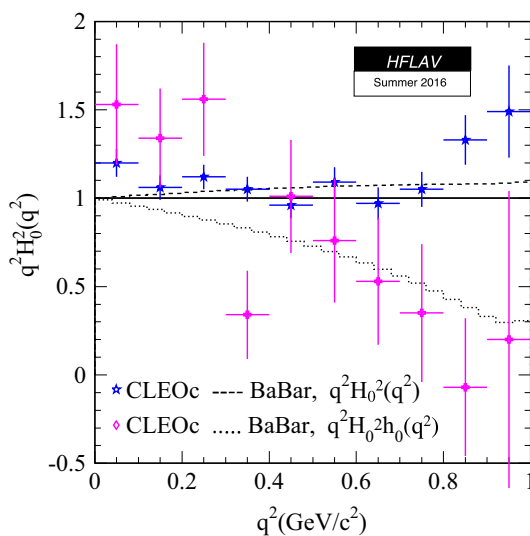


**Fig. 203** Comparison between CLEO-c and BABAR results for the quantities  $q^2 H_0^2(q^2)$  and  $q^2 h_0(q^2) H_0(q^2)$

**Table 280** Results for  $r_V$  and  $r_2$  from various experiments

Experiment	Refs.	$r_V$	$r_2$
$D^+ \rightarrow \bar{K}^{*0} l^+ \nu$			
E691	[1195]	$2.0 \pm 0.6 \pm 0.3$	$0.0 \pm 0.5 \pm 0.2$
E653	[1196]	$2.00 \pm 0.33 \pm 0.16$	$0.82 \pm 0.22 \pm 0.11$
E687	[1197]	$1.74 \pm 0.27 \pm 0.28$	$0.78 \pm 0.18 \pm 0.11$
E791 (e)	[1198]	$1.90 \pm 0.11 \pm 0.09$	$0.71 \pm 0.08 \pm 0.09$
E791 ( $\mu$ )	[1199]	$1.84 \pm 0.11 \pm 0.09$	$0.75 \pm 0.08 \pm 0.09$
Beatrice	[1200]	$1.45 \pm 0.23 \pm 0.07$	$1.00 \pm 0.15 \pm 0.03$
FOCUS	[1189]	$1.504 \pm 0.057 \pm 0.039$	$0.875 \pm 0.049 \pm 0.064$
$D^0 \rightarrow \bar{K}^0 \pi^- \mu^+ \nu$			
FOCUS	[1201]	$1.706 \pm 0.677 \pm 0.342$	$0.912 \pm 0.370 \pm 0.104$
BABAR	[1193]	$1.493 \pm 0.014 \pm 0.021$	$0.775 \pm 0.011 \pm 0.011$
$D_s^+ \rightarrow \phi e^+ \nu$			
BABAR	[1190]	$1.849 \pm 0.060 \pm 0.095$	$0.763 \pm 0.071 \pm 0.065$
$D^0, D^+ \rightarrow \rho e \nu$			
CLEO	[1202]	$1.40 \pm 0.25 \pm 0.03$	$0.57 \pm 0.18 \pm 0.06$

charm mesons. For the mass dependence of the form factors, a Breit–Wigner with a mass dependent width and a Blatt–Weisskopf damping factor is used. For the S-wave amplitude, considering what was measured in  $D^+ \rightarrow K^-\pi^+\pi^+$  decays, a polynomial variation below the  $\bar{K}_0^*(1430)$  and a Breit–Wigner distribution, above are assumed. For the polynomial part, a linear term is sufficient to fit data. It is verified that the variation of the S-wave phase is compatible with expectations from elastic  $K\pi$  [343, 1194] (after correcting for  $\delta^{3/2}$ ) according to the Watson theorem. At variance with elastic scattering, a negative relative sign between the S- and P-waves is measured; this is compatible with the previous theorem. Contributions from other spin-1 and spin-2 resonances decaying into  $K^-\pi^+$  are considered.

In Fig. 203, measured values from CLEO-c of the products  $q^2 H_0^2(q^2)$  and  $q^2 h_0(q^2) H_0(q^2)$  are compared with corresponding results from BABAR illustrating the difference in behavior of the scalar  $h_0$  component and the  $H_0$  form factor. For this comparison, the plotted values from BABAR for the two distributions are fixed to 1 at  $q^2 = 0$ . The different behavior of  $h_0(q^2)$  and  $H_0(q^2)$  can be explained by their different dependence in the  $p^*$  variable.

Table 280 lists measurements of  $r_V$  and  $r_2$  from several experiments. Most of the measurements assume that the  $q^2$  dependence of hadronic form factors is given by the simple pole ansatz. Some of these measurements do not consider a S-wave contribution and it is included in the measured values. The measurements are plotted in Fig. 204, which shows that they are all consistent.

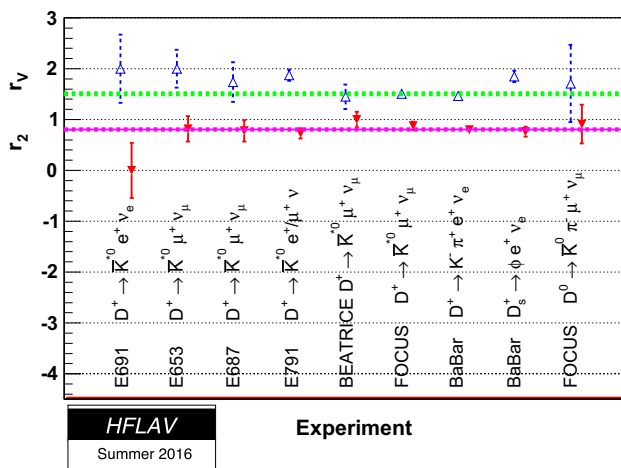


**Fig. 204** A comparison of  $r_2$  (filled inverted triangles) and  $r_V$  (open triangles) values from various experiments. The first seven measurements are for  $D^+ \rightarrow K^-\pi^+\ell^+\nu_\ell$  decays. Also shown as a line with  $1-\sigma$  limits is the average of these. The last two points are  $D_s^+$  and  $D^0$  decays

## 8.6 Leptonic decays

Purely leptonic decays of  $D^+$  and  $D_s^+$  mesons are among the simplest and theoretically cleanest probes of  $c \rightarrow d$  and  $c \rightarrow s$  quark flavor-changing transitions. The branching fraction of leptonic decays that proceed via the annihilation of the initial quark-antiquark pair ( $c\bar{d}$  or  $c\bar{s}$ ) into a virtual  $W^+$  that finally materializes as an antilepton-neutrino pair ( $\ell^+\nu_\ell$ ). Their Standard Model branching fraction is given by

$$\mathcal{B}(D_q^+ \rightarrow \ell^+\nu_\ell) = \frac{G_F^2}{8\pi} \tau_{D_q} f_{D_q}^2 |V_{cq}|^2 m_{D_q} m_\ell^2 \left(1 - \frac{m_\ell^2}{m_{D_q}^2}\right)^2. \quad (266)$$

Here,  $m_{D_q}$  is the  $D_q$  meson mass,  $\tau_{D_q}$  is its lifetime,  $m_\ell$  is the charged lepton mass,  $|V_{cq}|$  is the magnitude of the relevant CKM matrix element, and  $G_F$  is the Fermi coupling constant. The parameter  $f_{D_q}$  is the  $D_q$  meson decay constant and is related to the wave-function overlap of the meson's constituent quark and anti-quark. The decay constants have been predicted using several methods, the most accurate and robust being the lattice gauge theory (LQCD) calculations. The Flavor Lattice Averaging Group [222] combines all LQCD calculations and provides averaged values for  $f_D$  and  $f_{D_s}$  (see Table 281) that are used within this section to extract the magnitudes of the  $V_{cd}$  and  $V_{cs}$  CKM matrix elements from experimentally measured branching fractions of  $D^+ \rightarrow \ell^+\nu_\ell$  and  $D_s^+ \rightarrow \ell^+\nu_\ell$  decays, respectively.

The leptonic decays of pseudoscalar mesons are helicity-suppressed and their decay rates are thus proportional to the square of the charged lepton mass. Leptonic decays into electrons, with expected  $\mathcal{B} \lesssim 10^{-7}$ , are not experimentally observable yet, whereas decays to taus are favored over

**Table 281** The LQCD average for  $D$  and  $D_s$  meson decay constants and their ratio from the Flavor Lattice Averaging Group [222]

Quantity	Value
$f_D$	$212.15 \pm 1.45$ MeV
$f_{D_s}$	$248.83 \pm 1.27$ MeV
$f_{D_s}/f_D$	$1.1716 \pm 0.0032$

decays to muons. In particular, the ratio of the latter decays is equal to  $R_{\tau/\mu}^{D_q} \equiv \mathcal{B}(D_q^+ \rightarrow \tau^+\nu_\tau)/\mathcal{B}(D_q^+ \rightarrow \mu^+\nu_\mu) = m_\tau^2/m_\mu^2 \cdot (1 - m_\tau^2/m_{D_q}^2)^2/(1 - m_\mu^2/m_{D_q}^2)^2$ , and amounts to  $9.76 \pm 0.03$  in the case of  $D_s^+$  decays and to  $2.67 \pm 0.01$  in the case of  $D^+$  decays based on the world average values of masses of the muon, tau and  $D_q$  meson given in Ref. [6]. Any deviation from this expectation could only be interpreted as violation of lepton universality in charged currents and would hence point to NP effects [1203].

Averages presented within this subsection are weighted averages, in which correlations between measurements and dependencies on input parameters are taken into account. There is only one new experimental result on leptonic charm decays since our last report from 2014 – the measurements of  $\mathcal{B}(D_s^+ \rightarrow \mu^+\nu_\mu)$  and  $\mathcal{B}(D_s^+ \rightarrow \tau^+\nu_\tau)$  by BESIII collaboration [1204]. The Lattice QCD calculations of the  $D$  and  $D_s$  meson decay constants have improved significantly since our last report and we use the latest averages of  $N_f = 2 + 1 + 1$  calculations provided by the Flavour Lattice Averaging Group [222] in our determinations of the CKM matrix elements  $|V_{cd}|$  and  $|V_{cs}|$ .

### 8.6.1 $D^+ \rightarrow \ell^+\nu_\ell$ decays and $|V_{cd}|$

We use measurements of the branching fraction  $\mathcal{B}(D^+ \rightarrow \mu^+\nu_\mu)$  from CLEO-c [1103] and BESIII [1205] to calculate the world average (WA) value. We obtain

$$\mathcal{B}^{\text{WA}}(D^+ \rightarrow \mu^+\nu_\mu) = (3.74 \pm 0.17) \times 10^{-4}, \quad (267)$$

from which we determine the product of the decay constant and the CKM matrix element to be

$$f_D |V_{cd}| = (45.9 \pm 1.1) \text{ MeV}, \quad (268)$$

where the uncertainty includes the uncertainty on  $\mathcal{B}^{\text{WA}}(D^+ \rightarrow \mu^+\nu_\mu)$  and external inputs<sup>41</sup> needed to extract  $f_D |V_{cd}|$  from the measured branching fraction using Eq. (266). Using the LQCD value for  $f_D$  from Table 281 we finally obtain the CKM matrix element  $V_{cd}$  to be

$$|V_{cd}| = 0.2164 \pm 0.0050(\text{exp.}) \pm 0.0015(\text{LQCD}), \quad (269)$$

<sup>41</sup> These values (taken from the PDG 2014 edition [327]) are  $m_\mu = (0.1056583715 \pm 0.0000000035)$  GeV/ $c^2$ ,  $m_D = (1.86961 \pm 0.00009)$  GeV/ $c^2$  and  $\tau_D = (1040 \pm 7) \times 10^{-15}$  s.